OPTIMUM DESIGN OF REINFORCED CONCRETE BUILDINGS

Phd thesis

by

Nikolaos P. Bakas

Supervisor

Manolis Papadrakakis

National Technical University of Athens

December 2011

Table of Contents

1 ΠΕΡΙΛΗΨΗ ΔΙΔΑΚΤΟΡΙΚΗΣ ΔΙΑΤΡΙΒΗΣ

με τίτλο

'*Βέλτιστος Σχεδιασμός Κτηρίων από Οπλισμένο Σκυρόδεμα*'

Νικολάου Π. Μπάκα

1.1 Αντικείμενο της Διδακτορικής Διατριβής

Ο κύριος στόχος της Διατριβής είναι η διατύπωση ενός ποσοτικού κριτιρίου αποτίμησης της στρεπτικής κανονικότητας κτηριακών κατασκευών, το οποίο να εχει γενική εφαρμογή τόσο σε ελαστική όσο και σε ανελαστική συμπεριφορά, για πολυώροφα κτήρια και η τεκμηρίωση αυτού μέσω αλγορίθμων βέλτιστου σχεδιασμού κατασκευών. Αυτός ο καθολικός στόχος της Διατριβής επετεύχθη μέσω των ακόλουθων βημάτων:

(i) Στο πρώτο μέρος της Διατριβής πραγματοποιήθηκε η βέλτιστη σχεδίαση τριδιάστατων κτηρίων από οπλισμένο σκυρόδεμα όσον αφορά τις αποκρίσεις τους σε σεισμική φόρτιση. Αυτός ο στόχος επετεύχθει, λαμβάνοντας υπόψη την ελαχιστοποίηση της εκκεντρότητας μεταξύ του κέντρου μάζας και του κέντρου ακαμψιών σε κάθε όροφο με στόχο τον σχεδιασμό στρεπτικά μη ευαίσθητων κατασκευών. Το πρόβλημα αυτό διατυπώθηκε ως ένα συνδυασμένο πρόβλημα βελτιστοποίησης τοπολογίας και διατομών. Η θέση και το μέγεθος των υποστυλωμάτων και των τοιχωμάτων του κάθε ορόφου αποτελούν τις μεταβλητές σχεδιασμού. Εκτός από τους περιορισμούς που επιβάλλονται από τον κανονισμό οπλισμένου σκυροδέματος και τον αντισεισμικό κανονισμό, λαμβάνονται επίσης υπόψη και οι αρχιτεκτονικά περιορισμοί. Οι αριθμητικές αναλύσεις κατέδειξαν ότι επιτυγχάνεται μείωση του κατασκευαστικού κόστους του κτηρίου με την ελαχιστοποίηση της εκκεντρότητας μεταξύ του κέντρου μάζας και του κέντρου ακαμψίας του κάθε ορόφου. Για την επίλυση του προβλήματος αυτού εφαρμόστηκαν εξελικτικοί αλγόριθμοι βελτιστοποίησης ειδικά διαμορφωμένοι, βασισμένοι στις Στρατηγικές Εξέλιξης.

(ii) Στο δεύτερο μέρος της Διατριβής διατυπώνονται διάφορες προσεγγίσεις σχεδιασμού τριδιάστατων κτηρίων οπλισμένου σκυροδέματος (ΟΣ) ως προβλήματα βέλτιστου δομοστατικού σχεδιασμού και αποτιμώνται με βάση την επίδοση τους σε σεισμική καταπόνηση. Λαμβάνεται επίσης υπόψη το κόστος κύκλου ζωής ως μέτρο αποτίμησης των σχεδιασμών που προκύπτουν. Τρεις προσεγγίσεις σχεδιασμού κτηρίων από ΟΣ διερευνούνται σε αυτό το μέρος της Διδακτορικής Διατριβής. Στην πρώτη το αρχικό κατασκευαστικό κόστος θεωρείται ως αντικειμενική συνάρτηση ελαχιστοποίησης. Με τη δεύτερη θεώρηση η στρεπτική απόκριση διατυπώνεται ως πρόβλημα ελαχιστοποίησης, ενώ στην τρίτη θεώρηση σχεδιασμού εξετάζεται μια συνδυασμένη διατύπωση των δύο προηγούμενων διατυπώσεων. Στη δεύτερη

θεώρηση εξετάζονται δύο διακριτές διατυπώσεις. Σύμφωνα με την πρώτη, η στρεπτική μετατόπιση μειώνεται μέσω της ελαχιστοποίησης της απόστασης του κέντρου μάζας από το κέντρο ελαστικής στροφής, ενώ στη δεύτερη διατύπωση αυτό επιτυγχάνεται ελαχιστοποιώντας την εκκεντρότητα μεταξύ του κέντρου αντοχών και του κέντρου μάζας. Γίνεται φανερό ότι οι σχεδιασμοί που λαμβάνονται σύμφωνα με την ελαχιστοποίηση της εκκεντρότητας του κέντρου ελαστικής στροφής συμπεριφέρονται ικανοποιητικά σε συχνούς σεισμούς (50/50 επίπεδο επικινδυνότητας) και σε συνήθεις σεισμούς (10/50 επίπεδο επικινδυνότητας), ενώ οι σχεδιασμοί που λαμβάνονται σύμφωνα με την ελαχιστοποίηση της εκκεντρότητας του κέντρου αντοχής επιδεικνύουν καλή συμπεριφορά στα σπάνια σεισμικά γεγονότα (2/50 επίπεδο επικινδυνότητας). Σχεδιασμοί βασισμένοι στην τρίτη θεώρηση, δείχνουν καλή συμπεριφορά και στα τρία επίπεδα επικινδυνότητας που εξετάστηκαν.

(iii) Επόμενο βήμα της Διατριβής αποτέλεσε η διατύπωση ενός νέου κριτηρίου σχεδιασμού κατασκευών έναντι στρέψης. Η επίδραση της στρέψης σε κτήρια από οπλισμένο σκυρόδεμα αποτέλεσε αντικείμενο εντατικής έρευνας από πολλούς ερευνητές. Ο λόγος είναι ότι πολλά κτήρια υφίστανται εκτεταμένες ζημιές, μετά από ισχυρές σεισμικές καταγραφές, λόγω της έκκεντρης διάταξης στην κάτοψη των κατακόρυφων στοιχείων αντίστασης. Παρά τις πολλές προσπάθειες να προταθεί κατά το παρελθόν ένα αξιόπιστο κριτήριο σχεδιασμού ευρέως αποδεκτό για την αντιμετώπιση των επιπτώσεων της στρέψης πολυωρόφων κτηρίων, τόσο στην ελαστική όσο και την ανελαστική περιοχή, δεν κατέστη αυτό δυνατό σύμφωνα με τα δεδομένα της διεθνούς βιβλιογραφίας. Σε αυτή τη Διδακτορική Διατριβή, αφού διερευνήθηκε η απόκριση των κτηρίων που παρουσιάζουν στρεπτικά φαινόμενα, προτείνεται ένα κριτήριο το οποίο μπορεί να αποτελέσει ένα χρήσιμο εργαλείο για την αξιολόγηση και τον σχεδιασμό κτηριακών κατασκευών έναντι στρέψης. Τα αριθμητικά αποτελέσματα δείχνουν ότι οι κατασκευές με τις μικρές τιμές του προτεινόμενου κριτηρίου αναπτύσσουν χαμηλές τιμές της στρεπτικής ροπής βάσης, καθώς και των μεταφορικών και στροφικών μετατοπίσεων των διαφραγμάτων.

1.2 Βέλτιστος Σχεδιασμός Κατασκευών

1.2.1 Εισαγωγή

Ένα πλήθος εργασιών έχουν παρουσιαστεί στο παρελθόν όπου αντιμετωπίζεται το πρόβλημα του βέλτιστου σχεδιασμού των κτηρίων από οπλισμένο σκυρόδεμα, σε αυτές το αρχικό κόστος αποτελεί την προς ελαχιστοποίηση αντικειμενική συνάρτηση . Βέλτιστος σχεδιασμός βασισμένος στην επίδοση είναι μία νέα σχετικά προσέγγιση, όπου τα κριτήρια συμπεριφοράς εφαρμόζονται σαν περιορισμοί οι οποίοι επιδρούν το αρχικό κόστος κατασκευής το προς ελαχιστοποίηση. Βασισμένοι σε αυτή την προσέγγιση οι Ganzerli et al. πρότειναν μια μεθοδολογία βελτιστοποίησης σχεδιασμού λαμβάνοντας υπόψη περιορισμούς συμπεριφοράς. Οι Fragiadakis et al. παρουσίασαν μια μεθοδολογία βέλτιστου σχεδιασμού βασισμένη στη συμπεριφορά για μη κανονικά κτήρια από οπλισμένο σκυρόδεμα, ενώ οι Chan και Zou [4] παρουσίασαν μια αποτελεσματική τεχνική για ελαστικό και ανελαστικό σχεδιασμό βασισμένο στη γωνιακή παραμόρφωση ορόφου για κτήρια οπλισμένου σκυροδέματος υπό φασματική φόρτιση και υπερωθητική ανάλυση. Σε μια επακόλουθη δουλειά των Zou και Chan αποδείχτηκε ότι ο οπλισμός χάλυβα συγκρινόμενος με το σκυρόδεμα φαίνεται να είναι πιο οικονομικά αποτελεσματικό υλικό το οποίο μπορεί αποτελεσματικά να χρησιμοποιηθεί για να ελεγχθούν οι γωνιακές παραμορφώσεις ορόφου.

Τα κατακόρυφα φέροντα στοιχεία (υποστυλώματα και τοιχώματα), σε συνεργασία με τις δοκούς και τις πλάκες σε ένα κτήριο οπλισμένου σκυροδέματος αποτελούν το στατικό σύστημα που έχει να αντισταθεί στη σεισμική δράση. Η απόκριση και η συμπεριφορά ενός τέτοιου συστήματος υπό σεισμικές δράσεις εξαρτάται κυρίως από τις διαστάσεις και την τοπολογία των υποστυλωμάτων και των τοιχωμάτων. Ένα υψηλό ποσοστό βλαβών ή ακόμη και καταρρεύσεων σε κτήρια έχουν αποδοθεί στην εσφαλμένη τοποθέτηση των υποστυλωμάτων και των τοιχίων, τα οποία δημιουργούν στρεπτικές ταλαντώσεις στην κατασκευή [6-8]. Οι Duan και Chandler [9] έχουν προτείνει μια διαδικασία βελτιστοποίησης για στρεπτικά ευαίσθητες κατασκευές υποκείμενες σε σεισμικά φορτία, λαμβάνοντας υπόψη τόσο την οριακή κατάσταση αστοχίας, όσο και λειτουργικότητας. Ενώ, οι Lagaros et al. [10] έχουν προτείνει μια αυτοματοποιημένη διαδικασία ελαχιστοποίησης της εκκεντρότητας μεταξύ του κέντρου μάζας και του κέντρου ελαστικής στροφής.

Σε ένα πλήθος μελετών [11-13] φαίνεται ότι το ελαστικό κέντρο έχει νόημα μόνο όταν η κατασκευή συμπεριφέρεται ελαστικά. Όταν η απόκριση του συστήματος περνά στην

ανελαστική περιοχή, η ακαμψία των στοιχείων δεν επηρεάζει σημαντικά. Σε αυτή την περίπτωση, είναι το κέντρο αντοχών που παίζει κυρίαρχο ρόλο στις παραμορφώσεις της κατασκευής. Στα πλαίσια της παρούσας εργασίας, τρείς φιλοσοφίες σχεδιασμού έχουν εξεταστεί. Σύμφωνα με την πρώτη το αρχικό κόστος κατασκευής θεωρείται ως το κύριο αντικείμενο, κριτήρια επιτελεστικότητας εφαρμόζονται στο δεύτερο, ενώ η εκκεντρότητα μεταξύ του κέντρου μάζας και των κέντρων ελαστικής στροφής και αντοχών ελαχιστοποιείται, ενώ στην τρίτη κριτήρια επιτελεστικότητας και ελάχιστου κόστους χρησιμοποιούνται από κοινού. Και οι τρεις διαδικασίες σχεδιασμού θεωρούνται σας πεπλεγμένα τοπολογίας και διαστάσεων. Η θέση και οι διαστάσεις των στύλων και των τοιχίων του κάθε ορόφου της κατασκευής αποτελούν τις μεταβλητές σχεδιασμού. Πέρα από τους περιορισμούς που επιβάλουν οι κανονισμοί, έχουν ληφθεί υπόψη και περιορισμοί συμπεριφοράς. Το αντικείμενο της παρούσας εργασίας είναι η σύγκριση αυτών των σχεδιασμών με βάση την επίδοσή τους κατά τη σεισμική φόρτιση. Οι τελικοί σχεδιασμοί συγκρίνονται με κριτήριο το κόστος κύκλου ζωής το οποίο είναι το άθροισμα του αρχικού κόστους και του κόστους επισκευών. Το κόστος επισκευών όπως αυτό θεωρείται στην παρούσα μελέτη αναπαριστά τις νομισματικά ισοδύναμες απώλειες εξαιτίας των σεισμικών συμβάντων οι οποίες αναμένεται να συμβούν κατά τη διάρκεια ζωής της κατασκευής. Ο στόχος είναι να προταθεί μια μεθοδολογία που θα βελτιώνει τη φιλοσοφία σχεδιασμού τρισδιάστατων κτηρίων από οπλισμένο σκυρόδεμα με βάση την επίδοσή τους σε σεισμικές δράσεις σύμφωνα με τις απαιτήσεις των κανονισμών [14].

1.2.2 Προβλήματα βελτιστοποίησης χωρίς περιορισμούς

Στα προβλήματα βελτιστοποίησης χωρίς περιορισμούς, πρέπει να ελαχιστοποιηθεί μια αντικειμενική συνάρτηση F, που είναι συνάρτηση πραγματικών μεταβλητών σχεδιασμού. Η μαθηματική διατύπωση ενός προβλήματος βελτιστοποίησης χωρίς περιορισμούς, δίνεται από τη σχέση:

$$\min \ F\ \mathbf{x}$$

όπου $\mathbf{x} \in \mathbb{R}^n$ είναι το διάνυσμα των μεταβλητών σχεδιασμού και $F : \mathbb{R}^n \rightarrow \mathbb{R}$ είναι η αντικειμενική συνάρτηση.

Ο στόχος σε ένα πρόβλημα βελτιστοποίησης, είναι η εύρεση του ολικού ελαχίστου της αντικειμενικής συνάρτησης. Ένας σχεδιασμός $\mathbf{x}^*$ αποτελεί *ολικό ελάχιστο* της αντικειμενικής συνάρτησης F, όταν ισχύει η σχέση:

$$F\ \mathbf{x}^*\ \leq F\ \mathbf{x}\ , \quad \forall \mathbf{x} \in \mathbb{R}^n$$

Η εύρεση του ολικού ελαχίστου είναι συνήθως πολύ δύσκολη. Οι περισσότεροι αλγόριθμοι βρίσκουν συνήθως ένα τοπικό ελάχιστο της αντικειμενικής συνάρτησης. Ένας σχεδιασμός $\mathbf{x}^*$ αποτελεί *τοπικό ελάχιστο* της αντικειμενικής συνάρτησης F όταν ισχύει η σχέση:

$$F\ \mathbf{x}^*\ \leq F\ \mathbf{x}\ , \quad \forall \mathbf{x} \in N$$

όπου N είναι μια περιοχή γύρω από το σχεδιασμό $\mathbf{x}^*$ και η οποία περιέχει το σχεδιασμό $\mathbf{x}^*$.

Για μια ομαλή και δύο φορές παραγωγίσιμη αντικειμενική συνάρτηση F, είναι δυνατόν να εξαχθεί ένα συμπέρασμα για τον αν ο σχεδιασμός $\mathbf{x}^*$ είναι τοπικό ελάχιστο από την κλίση $\nabla F\ \mathbf{x}^*$ και την εσσιανή $\nabla^2 F\ \mathbf{x}^*$. Ισχύουν τα παρακάτω θεωρήματα:

Θεώρημα 1: *Έστω F μια παραγωγίσιμη αντικειμενική συνάρτηση στην περιοχή του σχεδιασμού $\mathbf{x}^*$ η οποία συμπεριλαμβάνει το σχεδιασμό $\mathbf{x}^*$. Αν ο σχεδιασμός $\mathbf{x}^*$ είναι τοπικό ελάχιστο της συνάρτησης F, τότε ισχύει:*

$$\nabla F\ \mathbf{x}^*\ = 0$$

Θεώρημα 2: *Αν ο σχεδιασμός $\mathbf{x}^*$ είναι τοπικό ελάχιστο της αντικειμενικής συνάρτησης F και οι δεύτερες παράγωγοι της F είναι συνεχείς στην περιοχή του σχεδιασμού $\mathbf{x}^*$, τότε $\nabla F\ \mathbf{x}^*\ = 0$ και $\nabla^2 F\ \mathbf{x}^*$ θετικά ημιορισμένο μητρώο.*

Θεώρημα 3: *Αν η αντικειμενική συνάρτηση F έχει συνεχείς δεύτερες παραγώγους, $\nabla F\ \mathbf{x}^*\ = 0$ και $\nabla^2 F\ \mathbf{x}^*$ θετικά ορισμένο μητρώο, τότε ο σχεδιασμός $\mathbf{x}^*$ αποτελεί τοπικό ελάχιστο της συνάρτησης F.*

Θεώρημα 4: *Αν η αντικειμενική συνάρτηση F είναι κυρτή, τότε κάθε σχεδιασμός $\mathbf{x}^*$ που είναι τοπικό ελάχιστο της F, είναι και ολικό ελάχιστο της αντικειμενικής συνάρτησης F.*

Οι περισσότεροι αλγόριθμοι βελτιστοποίησης αναζητούν συνήθως ένα τοπικό ελάχιστο της αντικειμενικής συνάρτησης, επομένως δεν βρίσκουν πάντα τον καλύτερο σχεδιασμό, δηλαδή το ολικό ελάχιστο της αντικειμενικής συνάρτησης. Τα ολικά ελάχιστα, αν και επιθυμητά στα περισσότερα προβλήματα, είναι πολύ δύσκολο να βρεθούν. Μια ειδική περίπτωση, είναι οι κυρτές αντικειμενικές συναρτήσεις για τις οποίες κάθε τοπικό ελάχιστο είναι ταυτόχρονα και ολικό ελάχιστο.

Μια συνάρτηση ονομάζεται *κυρτή* αν για κάθε δύο σημεία του πεδίου ορισμού της, η γραφική της παράσταση βρίσκεται κάτω από την ευθεία που ενώνει αυτά τα δύο σημεία, δηλαδή:

$$F\ a\mathbf{x} + \ 1-a\ \mathbf{y}\ \leq aF\ \mathbf{x}\ +\ 1-a\ F\ \mathbf{y} \qquad \forall a \in 0,1$$

όπου $\mathbf{x}, \mathbf{y}$ είναι δύο σημεία-σχεδιασμοί και a παράμετρος που μπορεί να πάρει τιμές στο διάστημα $0,1$. Αν η αντικειμενική συνάρτηση είναι κυρτή, ο αλγόριθμος βελτιστοποίησης θα συγκλίνει πάντα σε ολικό βέλτιστο.

Στα προβλήματα του γραμμικού προγραμματισμού η αντικειμενική συνάρτηση είναι κυρτή. Γενικά όμως, τα μή-γραμμικά προβλήματα, όπως αυτό του βέλτιστου σχεδιασμού των

κατασκευών, είναι μή-κυρτά και συνήθως έχουν πολλά τοπικά ελάχιστα τα οποία δεν είναι ολικά ελάχιστα.

1.2.3 Κλασσικές μέθοδοι αντιμετώπισης προβλημάτων χωρίς περιορισμούς

Οι πλέον γνωστές μέθοδοι επίλυσης προβλημάτων χωρίς περιορισμούς, είναι οι μέθοδοι της μέγιστης καθόδου, των συζυγών κλίσεων και οι μέθοδοι Newton και quasi-Newton. Οι αλγόριθμοι αυτοί ακολουθούν ένα επαναληπτικό σχήμα της μορφής:

$$\mathbf{x}^{g} = \mathbf{x}^{g-1} + a^{g}\mathbf{s}^{g}$$

όπου a είναι μια παράμετρος που ονομάζεται μήκος βήματος, $\mathbf{s}$ είναι η διεύθυνση στην οποία γίνεται η έρευνα για το βέλτιστο στην επανάληψη g και $\mathbf{x}^{g-1}, \mathbf{x}^{g}$ είναι η προσέγγιση της βέλτιστου σχεδιασμού κατά την επανάληψη $g-1$ και g αντίστοιχα.

Καθένας από αυτούς τους αλγόριθμους καθορίζει με κάποια μεθοδολογία το μήκος βήματος a και τη διεύθυνση έρευνας $\mathbf{s}$. Για να γίνει αυτό, πρέπει προηγουμένως να υπολογιστεί ή να εκτιμηθεί το διάνυσμα κλίσης της αντικειμενικής συνάρτησης $\nabla F\ \mathbf{x}$ και το εσσιανό μητρώο $\nabla^2 F\ \mathbf{x}$.

1.2.4 Η μέθοδος της μέγιστης καθόδου (Steepest Descent)

Η μέθοδος της μέγιστης καθόδου ανήκει στις μεθόδους πρώτης τάξης, αφού χρησιμοποιεί ως πληροφορία το διάνυσμα κλίσης της αντικειμενικής συνάρτησης. Η διεύθυνση $\mathbf{s}^{g}$ της έρευνας (βλ. σχέση **Error! Reference source not found.**) υπολογίζεται από τη σχέση:

$$\mathbf{s}^{g} = -\nabla F\ \mathbf{x}^{g-1} \qquad (0.1)$$

Η ροή του αλγόριθμου απεικονίζεται συνοπτικά στο Σχήμα 2.1.

Algorithm: Steepest Descent

1 Choose initial $\mathbf{x}^{(0)}$
2 **repeat**
3 g=g+1
3 $\mathbf{s}^{(g)} = -\nabla F\left(\mathbf{x}^{(g-1)}\right)$
4 **choose** a **to minimize** $F\left(\mathbf{x}^{(g-1)} + a\mathbf{s}^{(g)}\right)$
5 $\mathbf{x}^{(g)} = \mathbf{x}^{(g-1)} + a^{(g)}\mathbf{s}^{(g)}$
6 **until** termination_criterion

Σχήμα 1.1: Ο αλγόριθμος Steepest Descent

Η παράμετρος a συνήθως υπολογίζεται με κάποια μέθοδο έρευνας γραμμής (line search), όπως η μέθοδος της χρυσής τομής (golden section).

Ο αλγόριθμος της μέγιστης καθόδου δεν χρησιμοποιεί πληροφορία προηγούμενων επαναλήψεων και γενικά συγκλίνει πολύ αργά στην τελική λύση.

1.2.5 Οι μέθοδοι Newton και Quasi-Newton

Η μέθοδος Newton ανήκει στις μεθόδους δεύτερης τάξης, οι οποίες κάνουν χρήση του εσσιανού μητρώου **H**. Η διεύθυνση $\mathbf{s}$ της έρευνας υπολογίζεται από τη σχέση:

$$\mathbf{s} = -\mathbf{H}\ \mathbf{x}\ ^{-1} \nabla F\ \mathbf{x}$$

όπου **H** είναι ο Hessian πίνακας της αντικειμενικής συνάρτησης.

Αν η αντικειμενική συνάρτηση είναι τετραγωνικής μορφής, τότε η μέθοδος Newton συγκλίνει σε μια επανάληψη. Δυστυχώς απαιτείται ο υπολογισμός του Hessian πίνακα, κάτι που είναι χρονοβόρο για πολλές μεταβλητές σχεδιασμού. Επίσης, αν κάποια μεταβλητή σχεδιασμού είναι γραμμικά εξαρτημένη από κάποια άλλη, τότε ενδέχεται να μην υπάρχει ο αντίστροφος του Hessian πίνακα.

Αντίθετα με τη μέθοδο Newton, στις μεθόδους quasi-Newton δεν είναι αναγκαίο να υπολογίζεται ο Hessian πίνακας σε κάθε επανάληψη. Η διεύθυνση $\mathbf{s}^{\,g}$ της έρευνας (βλ. σχέση **Error! Reference source not found.**) υπολογίζεται από τη σχέση:

$$\mathbf{s}^{\,g} = -\mathbf{A}^{\,g} \nabla F\ \mathbf{x}^{\,g-1}$$

όπου $\mathbf{A}^{\,g}$ είναι ένας $n \times n$ πίνακας συμμετρικός και θετικά ορισμένος. που προσεγγίζει τον αντίστροφο του Hessian πίνακα $\mathbf{H}^{-1}$. Ο πίνακας $\mathbf{A}^{\,g}$ αρχικά τίθεται ίσος με τον μοναδιαίο πίνακα **I**, επομένως η πρώτη διεύθυνση υπολογίζεται όπως στη μέθοδο της μέγιστης καθόδου. Στις επόμενες επαναλήψεις υπολογίζεται από τη σχέση:

$$\mathbf{A}^{\,g+1} = \mathbf{A}^{\,g} + \mathbf{D}^{\,g}$$

όπου $\mathbf{D}^{\,g}$ είναι ένας συμμετρικός $n \times n$ πίνακας που δίνεται από μια σχέση της μορφής:

$$\mathbf{D}^{\,g} = function\ \mathbf{x}^{\,g} - \mathbf{x}^{\,g-1}, \nabla F\ \mathbf{x}^{\,g} - \nabla F\ \mathbf{x}^{\,g-1}, \mathbf{A}^{\,g}$$

Υπάρχουν διάφορες μέθοδοι υπολογισμού του πίνακα $\mathbf{D}^{\,g}$. Η πιο γνωστές από αυτές είναι η μέθοδος DFP (Davidon-Fletcher-Powell) και η BFGS (Broydon-Fletcher-Goldfarb-Shanno) η οποία θεωρείται και η καλύτερη.

1.2.6 Προβλήματα βελτιστοποίησης με περιορισμούς

Η μαθηματική διατύπωση ενός προβλήματος βελτιστοποίησης με ανισοτικούς και ισοτικούς περιορισμούς, δίνεται από τη σχέση:

$$\text{minimize } F(\mathbf{x}) = F(x_1, x_2, \ldots, x_n)$$

$$\text{subject to: } h_j(\mathbf{x}) \equiv h_j(x_1, x_2, \ldots, x_n) = 0,\ j = 1, \ldots, p$$

$$g_i(\mathbf{x}) \equiv g_i(x_1, x_2, \ldots, x_n) \leq 0,\ i = 1, \ldots, m$$

$$x_i^L \leq x_i \leq x_i^U,\ i = 1, \ldots, n$$

όπου *F* είναι η αντικειμενική συνάρτηση, **x** είναι το διάνυσμα μεταβλητών σχεδιασμού, $h_j(\mathbf{x})$ είναι η *j* συνάρτηση ισοτικών περιορισμών, $g_i(\mathbf{x})$ είναι η *i* συνάρτηση ανισοτικών περιορισμών, και x_i^L, x_i^U είναι το κάτω και άνω όριο της *i* μεταβλητής σχεδιασμού αντίστοιχα.

Ορίζεται επίσης ο χώρος S των εφικτών σχεδιασμών, τέτοιος ώστε:

$$S = \{\mathbf{x} \in \mathbb{R}^n \mid \mathbf{g}(\mathbf{x}) \leq 0, \mathbf{h}(\mathbf{x}) = 0, \mathbf{x}^L \leq \mathbf{x} \leq \mathbf{x}^U\}$$

Επομένως, το πρόβλημα με περιορισμούς μπορεί να διατυπωθεί ως εξής:

$$\min F(\mathbf{x}) \quad \mathbf{x} \in S$$

Ο χώρος S αποτελεί την εφικτή περιοχή του προβλήματος, στην οποία όλοι οι περιορισμοί ικανοποιούνται. Σε πολλά προβλήματα, ο βέλτιστος σχεδιασμός βρίσκεται στο όριο μεταξύ της περιοχής των εφικτών σχεδιασμών, και της μή-επιτρεπόμενης περιοχής, στην οποία τουλάχιστον ένας περιορισμός παραβιάζεται.

1.2.7 Κλασσικές μέθοδοι αντιμετώπισης προβλημάτων με περιορισμούς

Οι κλασσικές μεθοδολογίες επίλυσης ενός προβλήματος βελτιστοποίησης με περιορισμούς, χωρίζονται στις λεγόμενες «άμεσες» (direct) μεθόδους, οι οποίες προσπαθούν να επιλύσουν το πρόβλημα κινούμενες μεταξύ των ορίων που θέτουν οι περιορισμοί, και στις «έμμεσες» (indirect) μεθόδους, οι οποίες μετατρέπουν το πρόβλημα με περιορισμούς σε ένα πρόβλημα χωρίς περιορισμούς.

Το πρόβλημα βελτιστοποίησης με περιορισμούς, όπως διατυπώνεται από τη σχέση **Error! Reference source not found.** μπορεί να μετατραπεί σε ένα πρόβλημα βελτιστοποίησης χωρίς περιορισμούς, από τη σχέση:

$$L(\mathbf{x}, \lambda) = F(\mathbf{x}) + \sum_{j=1}^{p} \lambda_j h_j(\mathbf{x}) + \sum_{i=1}^{m} \lambda_i g_i(\mathbf{x})$$

όπου $L(\mathbf{x}, \lambda)$ είναι η λανγκραζιανή της F, και λ_i, λ_j είναι οι συντελεστές Lagrange.

Μία αναγκαία συνθήκη αλλά όχι ικανή, για να είναι ένας σχεδιασμός $\mathbf{x}^*$ ελάχιστο (τοπικό ή ολικό), είναι:

$$\nabla L\ \mathbf{x}^*,\lambda\ = \nabla F\ \mathbf{x}^*\ + \sum_{j=1}^{p} \lambda_j \nabla \mathrm{h}_j\ \mathbf{x}^*\ + \sum_{i=1}^{m} \lambda_i \nabla \mathrm{g}_i\ \mathbf{x}^*\ = 0$$

με $\lambda_j \in \mathbb{R}_+$ και $\lambda_i \in \mathbb{R}$.

Αν ο σχεδιασμός $\mathbf{x}^*$ είναι τοπικό βέλτιστο της αντικειμενικής συνάρτησης, τότε ισχύουν οι παρακάτω συνθήκες:

1. Ο σχεδιασμός $\mathbf{x}^*$ είναι εφικτός.
2. $\lambda_i \nabla \mathrm{g}_i\ \mathbf{x}^*\ = 0,\ i = 1,\ldots,m$ και $\lambda_i \geq 0$.
3. $\nabla F\ \mathbf{x}^*\ + \sum_{j=1}^{p} \lambda_j \nabla \mathrm{h}_j\ \mathbf{x}^*\ + \sum_{i=1}^{m} \lambda_i \nabla \mathrm{g}_i\ \mathbf{x}^*\ = 0$ με $\lambda_i \geq 0$. Οι τιμές των συντελεστών Lagrange λ_j μπορούν να πάρουν οποιεσδήποτε τιμές.

Η πρώτη συνθήκη, σημαίνει πως η βέλτιστη λύση ικανοποιεί τους περιορισμούς. Η δεύτερη συνθήκη σημαίνει πως αν ένας περιορισμός δεν ικανοποιείται πλήρως, τότε ο αντίστοιχος συντελεστής Lagrange είναι μηδενικός. Τέλος, η τρίτη συνθήκη σημαίνει πως το διάνυσμα κλίσης της λανγκραζιανής είναι μηδενικό στο βέλτιστο σημείο.

Οι παραπάνω συνθήκες ονομάζονται συνθήκες *Kuhn-Tucker*, και είναι αναγκαίες συνθήκες για βέλτιστο. Στην περίπτωση που ο εφικτός χώρος που ορίζεται από την αντικειμενική συνάρτηση και τους περιορισμούς, είναι κυρτός, οι συνθήκες *Kuhn-Tucker* είναι και ικανές. Αν και τα περισσότερα προβλήματα βελτιστοποίησης δεν είναι κυρτά, η θεωρία των κυρτών προβλημάτων είναι σημαντική καθώς πολλές φορές τα μή-κυρτά προβλήματα προσεγγίζονται από μια σειρά κυρτών προβλημάτων.

1.2.8 Η μέθοδος των συναρτήσεων ποινής (Penalty Functions)

Οι μέθοδοι των συναρτήσεων ποινής διακρίνονται στις μεθόδους των εξωτερικών και των εσωτερικών συναρτήσεων ποινής. Στις μεθόδους των εξωτερικών συναρτήσεων ποινής, το πρόβλημα βελτιστοποίησης με περιορισμούς μπορεί να διατυπωθεί από τη σχέση:

$$\min R\ \mathbf{x}\ , \quad R\ \mathbf{x}\ = F\ \mathbf{x}\ + \sum a_i \mathrm{G}\ \left|\mathrm{g}_i\ \mathbf{x}\ \right|^- + \sum b_j \mathrm{H}\ \left|\mathrm{h}_j\ \mathbf{x}\ \right| \qquad (0.2)$$

όπου $R\ \mathbf{x}$ είναι η σύνθετη αντικειμενική συνάρτηση, G,H είναι συναρτήσεις των ανισοτικών και ισοτικών περιορισμών και a_i, b_j πραγματικοί αριθμοί με $a_i, b_j \geq 0$. Για τη συνάρτηση $\left|\mathrm{g}_i\ \mathbf{x}\ \right|^-$, ισχύει:

$$\left|\mathrm{g}_i\ \mathbf{x}\ \right|^- = \begin{cases} \left|\mathrm{g}_i\ \mathbf{x}\ \right|, & if\ \mathrm{g}_i\ \mathbf{x}\ < 0 \\ 0, & otherwise \end{cases}$$

Η σχέση (0.2) αντικαθιστά την αντικειμενική συνάρτηση και τους περιορισμούς σε όλο το πεδίο των τιμών (δυνατή και μή-δυνατή περιοχή). Οι διαμόρφωση της μή-δυνατής περιοχής

εξαρτάται από τις παραμέτρους a_i, b_j και από τις συναρτήσεις G, H. Για γραμμικές συναρτήσεις G, H, η σύνθετη αντικειμενικής συνάρτηση δίνεται από τη σχέση:

$$R(\mathbf{x}) = F(\mathbf{x}) + \sum a_i \left|\mathrm{g}_i(\mathbf{x})\right| + \sum b_j \left|\mathrm{h}_j(\mathbf{x})\right| \quad (0.3)$$

Για τετραγωνικές συναρτήσεις G, H, η σύνθετη συνάρτηση δίνεται από τη σχέση:

$$R(\mathbf{x}) = F(\mathbf{x}) + \sum a_i \left|\mathrm{g}_i(\mathbf{x})\right|^2 + \sum_j b_j \left|\mathrm{h}_j(\mathbf{x})\right|^2 \quad (0.4)$$

Η σχέση (0.4) μπορεί να γραφεί και ως:

$$R(\mathbf{x}) = F(\mathbf{x}) + r\left(\sum \left|\mathrm{g}_i(\mathbf{x})\right|^2 + \sum \left|\mathrm{h}_j(\mathbf{x})\right|^2\right) \quad (0.5)$$

όπου οι παράμετροι a_i, b_j έχουν αντικατασταθεί από μια παράμετρο r. Το ελάχιστο της σύνθετης αντικειμενικής συνάρτησης εξαρτάται από την παράμετρο r και αυτό είναι ένα μειονέκτημα των μεθόδων των συναρτήσεων ποινής.

Στην περίπτωση που το πρόβλημα βελτιστοποίησης διέπεται από ανισοτικές συναρτήσεις περιορισμών, τότε μια σύνθετη συνάρτηση που μετατρέπει το πρόβλημα σε ένα πρόβλημα χωρίς περιορισμούς, μπορεί να διατυπωθεί από τις σχέσεις:

$$R(\mathbf{x}) = F(\mathbf{x}) + \sum_i a_i \frac{1}{\mathrm{g}_i(\mathbf{x})}$$

$$R(\mathbf{x}) = F(\mathbf{x}) + r\sum_i \frac{1}{g_i(\mathbf{x})} \quad (0.6)$$

$$R(\mathbf{x}) = F(\mathbf{x}) + \sum_i \log\left(\frac{1}{\mathrm{g}_i(\mathbf{x})}\right)$$

Η σύνθετη συνάρτηση $R(\mathbf{x})$ όπως ορίζεται από την παραπάνω σχέση, ορίζεται μόνο στην εφικτή περιοχή του προβλήματος. Για την εφαρμογή των εσωτερικών συναρτήσεων ποινής, πρέπει να είναι γνωστή αρχική μια εφικτή λύση, διαφορετικά οι σύνθετες συναρτήσεις όπως διατυπώνονται από την σχέση (0.6), απειρίζονται. Η απόδοση της μεθόδου με συνδυασμό εξωτερικών και εσωτερικών συναρτήσεων ποινής δεν αλλάζει σημαντικά.

1.2.9 Αλγόριθμοι βελτιστοποίησης

Οι αλγόριθμοι βελτιστοποίησης είναι επαναληπτικοί. Συνήθως, ξεκινούν από μια αρχική εκτίμηση των βέλτιστων σχεδιασμού και στη συνέχεια δημιουργούν μια αλληλουχία βελτιωμένων σχεδιασμών μέχρι να καταλήξουν στο βέλτιστο. Η στρατηγική μέσω της οποίας από μια επανάληψη προκύπτει η επόμενη, κατηγοριοποιεί και τον αλγόριθμο βελτιστοποίησης.

Κάθε αλγόριθμος βελτιστοποίησης πρέπει να έχει τις παρακάτω ιδιότητες:

- *Σθεναρότητα (Robustness)*: Ένας αλγόριθμος πρέπει να μπορεί να αντιμετωπίσει μια πληθώρα προβλημάτων.
- *Απόδοση (Efficiency):* Ο αλγόριθμος δεν θα πρέπει να απαιτεί πολύ μεγάλη υπολογιστική ισχύ ή χρόνο, ώστε να βρει τη βέλτιστη λύση.
- *Ακρίβεια (Accuracy) :* Ένας αλγόριθμος βελτιστοποίησης θα πρέπει να μπορεί να αναγνωρίζει μια λύση με ακρίβεια, χωρίς να είναι υπερευαίσθητος σε αριθμητικής ακρίβειας σφάλματα.

Οι παραπάνω απαιτήσεις είναι αλληλοσυγκρουόμενες. Για παράδειγμα, ένας πολύ γρήγορος (στη σύγκλιση) αλγόριθμος μπορεί να απαιτεί υπερβολικά μεγάλο αποθηκευτικό χώρο ή μνήμη για προβλήματα με πολλές μεταβλητές σχεδιασμού. Αντίθετα, ένας αλγόριθμος με μεγάλη σθεναρότητα (Robustness) μπορεί να απαιτεί πολλές επαναλήψεις και μεγάλο υπολογιστικό χρόνο ώστε να βρεί το βέλτιστο σχεδιασμό.

Μερικοί αλγόριθμοι διατηρούν ένα ποσοστό της πληροφορίας από τους σχεδιασμούς των προηγούμενων σχεδιασμών, ενώ άλλοι χρησιμοποιούν μόνο πληροφορία του τρέχοντος σχεδιασμού. Οι αλγόριθμοι, σχετικά με το είδος της πληροφορίας, διακρίνονται στους αλγόριθμους *μηδενικής*, *πρώτης* και *δεύτερης* τάξης. Οι αλγόριθμοι μηδενικής τάξης χρησιμοποιούν μόνο την τιμή της αντικειμενικής συνάρτησης στην έρευνα για το βέλτιστο, οι αλγόριθμοι πρώτης τάξης χρησιμοποιούν και την πρώτη παράγωγο της αντικειμενικής συνάρτησης, ενώ οι αλγόριθμοι δεύτερης τάξης χρησιμοποιούν και τη δεύτερη παράγωγο, εκτός από την τιμή της αντικειμενικής συνάρτησης και την πρώτη της παράγωγο.

Οι αλγόριθμοι μηδενικής τάξης διακρίνονται σε *αιτιοκρατικούς* και *στοχαστικούς* αλγόριθμους, ανάλογα με τον τρόπο που σχηματίζονται οι νέοι σχεδιασμοί. Οι αιτιοκρατικοί αλγόριθμοι προσεγγίζουν επαναληπτικά το βέλτιστο σχεδιασμό πολύ γρήγορα. Το βασικό τους μειονέκτημα είναι πως εγκλωβίζονται εύκολα σε τοπικά ελάχιστα. Οι στοχαστικοί αλγόριθμοι αναζητούν με έναν τυχηματικό τρόπο νέους σχεδιασμούς καλύτερους από τους υπάρχοντες ώστε να οδηγηθούν στο βέλτιστο. Δεν εγκλωβίζονται τόσο εύκολα σε τοπικά ελάχιστα όπως οι αιτιοκρατικοί αλγόριθμοι, αλλά απαιτούν μεγαλύτερη υπολογιστική ισχύ και χρόνο από αυτούς για να συγκλίνουν στο βέλτιστο.

Οι αλγόριθμοι βελτιστοποίησης μπορούν να διαχωριστούν σε αλγόριθμους που διαχειρίζονται έναν σχεδιασμό τη φορά, και σε αυτούς που διαχειρίζονται έναν πληθυσμό από σχεδιασμούς ταυτόχρονα. Όλοι οι αιτιοκρατικοί αλγόριθμοι διαχειρίζονται έναν σχεδιασμό τη φορά. Από τους στοχαστικούς αλγόριθμους, ο γνωστότερος αλγόριθμος που χρησιμοποιεί έναν σχεδιασμό τη φορά, είναι ο αλγόριθμος της Προσομειούμενης Ανόπτησης (Simulated Annealing).

Οι στοχαστικοί αλγόριθμοι βελτιστοποίησης που διαχειρίζονται έναν πληθυσμό σχεδιασμών είναι γνωστοί και ως εξελικτικοί αλγόριθμοι. Οι εξελικτικοί αλγόριθμοι μοντελοποιούν συνήθως ένα φαινόμενο, φυσικό, κοινωνικό ή βιολογικό. Η λειτουργία τους είναι συνήθως παράλληλη, δηλαδή δημιουργούνται πολλοί σχεδιασμοί-λύσεις ταυτόχρονα. Οι εξελικτικοί αλγόριθμοι χαρακτηρίζονται από σθεναρότητα (robustness) και έχουν την ικανότητα να εντοπίζουν την περιοχή του ολικά βέλτιστου σχεδιασμού μετά από ένα μεγάλο αριθμό εκτιμήσεων της αντικειμενικής συνάρτησης. Η γνωστότερη στοχαστική μέθοδος που χρησιμοποιεί πληθυσμό σχεδιασμών, είναι οι Γενετικοί Αλγόριθμοι (Genetic Algorithms). Πληθυσμό σχεδιασμών επίσης χρησιμοποιούν οι Αποικίες Μυρμηγκιών (Ant Colonies) και οι Στρατηγικές Εξέλιξης (Evolution Strategies). Τα τελευταία χρόνια οι εξελικτικοί αλγόριθμοι έχουν εφαρμοστεί σε ερευνητικό επίπεδο, στο πεδίο του βέλτιστου σχεδιασμού των κατασκευών, και έχουν αποδειχθεί από τις πλέον αξιόπιστες μεθόδους.

1.2.10 Στρατηγικές εξέλιξης

Οι στρατηγικές εξέλιξης ανήκους στις επονομαζόμενες Δαρβίνειες μεθόδους, επειδή προσομοιάζουν τη διαδικασία εξέλιξης των ειδών, όπως την παρουσίασε πρώτος ο Δαρβίνος. Οι στρατηγικές εξέλιξης, σε αντίθεση με τους αιτιοκρατικούς αλγόριθμους, διαχειρίζονται έναν πληθυσμό από σχεδιασμούς-λύσεις ταυτόχρονα. Οι λύσεις αυτές είναι ανεξάρτητες η μία από την άλλη, επομένως είναι δυνατή η υλοποίηση των στρατηγικών εξέλιξης σε παράλληλο υπολογιστικό περιβάλλον. Αφού δημιουργηθεί ένας αρχικός πληθυσμός λύσεων με τυχαίο τρόπο, στη συνέχεια θα δράσουν σε αυτόν οι τελεστές *μετάλλαξης*, *ανασυνδυασμού* και *επιλογής* ώστε να εξελιχθεί ο πληθυσμός και να πετύχει τον εντοπισμό της βέλτιστης λύσης.

Το βασικό πλεονέκτημα των στρατηγικών εξέλιξης, είναι πως λόγο του τυχηματικού χαρακτήρα τους δεν εγκλωβίζονται εύκολα σε τοπικά ελάχιστα, κατά τη διάρκεια της έρευνας για τη βέλτιστη λύση, επομένως έχουν μεγαλύτερες πιθανότητες να εντοπίζουν την περιοχή της ολικά βέλτιστης λύσης. Σε προβλήματα με πάρα πολλές μεταβλητές σχεδιασμού, ή και πολλές αντικειμενικές συναρτήσεις, οι εξελικτικοί αλγόριθμοι είναι οι μόνοι που μπορούν να δώσουν αποδεκτή λύση. Το βασικό μειονέκτημα των στρατηγικών εξέλιξης, όπως και των περισσότερων εξελικτικών αλγόριθμων, είναι πως απαιτείται μεγάλος αριθμός υπολογισμών της αντικειμενικής συνάρτησης, για τον εντοπισμό της βέλτιστης λύσης.

Ο στόχος των στρατηγικής εξέλιξης, όπως και κάθε αλγόριθμου βελτιστοποίησης, σε ένα πρόβλημα βελτιστοποίησης με μια αντικειμενική συνάρτηση, είναι η βελτιστοποίηση μιας αντικειμενικής συνάρτησης *F* ως προς το διάνυσμα των παραμέτρων της $\mathbf{y} = \ y_1, y_2, \ldots, y_n \ ^T$, το οποίο ονομάζεται διάνυσμα σχεδιασμού. Ο στόχος δηλαδή, είναι η εύρεση ενός διανύσματος $\mathbf{y}$ τέτοιο ώστε:

$$F\ \mathbf{y}\ \rightarrow \text{optimum}, \mathbf{y} \in \mathrm{Y} \qquad (0.7)$$

Ο χώρος Y μπορεί να είναι ο *n*-διάστατος χώρος των πραγματικών αριθμών $\mathbf{R}^n$, ο *n*-διάστατος χώρος των ακέραιων αριθμών $\mathbf{Z}^n$, ο χώρος των δυαδικών αριθμών $\mathbf{B}^n$ ή και οποιοσδήποτε συνδυασμός τους.
Οι στρατηγικές εξέλιξης, όπως προαναφέρθηκε, δρουν σε άτομα που αποτελούν ένα πλυθυσμό. Ο πλυθυσμός συνήθως συμβολίζεται με $\mathbf{B}$ ενώ τα άτομα με a. Το *k* άτομο ενός πλυθυσμού, συμβολίζεται με a_k και αποτελείται από το διάνυσμα σχεδιασμού $\mathbf{y}_k$, την την τιμή της αντικειμενικής συνάρτησης $F_k = F\ \mathbf{y}_k$ και συνήθως από ένα σετ ενδογενών παραμέτρων $\mathbf{s}_k$, που ονομάζονται ενδογενείς παράμετροι στρατηγικής, έτσι ώστε:

$$a_k = \ \mathbf{y}_k, \mathbf{s}_k, F_k \qquad (0.8)$$

Οι ενδογενείς παράμετροι στρατηγικής ελέγχουν διάφορους τελεστές των στρατηγικών εξέλιξης, όπως για παράδειγμα τον τελεστή της *μετάλλαξης* και του *ανασυνδυασμού*, και μπορούν να προσαρμόζονται κατά τη διάρκεια της εξελιξης. Η μορφή των παραμέτρων στρατηγικής δεν είναι η ίδια σε όλους τους αλγόριθμους στρατηγικής εξέλιξης, αλλά διαφοροποιείται από αλγόριθμο σε αλγόριθμο, όπως θα δειχθεί στο τρίτο κεφάλαιο.

Γενικά, κατά τη διάρκεια μιας γενιάς στρατηγικής εξέλιξης, δημιουργούνται λ άτομα απογόνων από ένα πλυθυσμό μ γονέων. Οι παράμετροι μ, λ καθώς και μία ακόμη παράμετρος, που συμβολίζεται με ρ και ελέγχει τον τελεστή ανασυνδυασμού για τον οποίο θα γίνει αναφορά στη συνέχεια, ονομάζονται *εξωγενείς παράμετροι στρατηγικής*, και διατηρούνται σταθερές κατά τη διάρκεια της εξέλιξης. Ο τρόπος με τον οποίο δημιουργούνται οι απόγονοι από τον πληθυσμό των γονέων συμβολίζεται συνοπτικά με $\mu / \rho \overset{+}{,} \lambda$. Η παράμετρος ανασυνδυασμού ρ δηλώνει τον αριθμό των γονέων που θα συνδιαστούν για τη δημιουργία ενός απογόνου πριν δράσει σε αυτόν ο τελεστής μετάλλαξης. Προφανώς, πρέπει να ισχύει $\rho \leq \mu$. Ο συμβολισμός $\overset{+}{,}$ περιγράφει τον τρόπο με τον οποίο θα δράσει ο τελεστής επιλογής στον πληθυσμό. Στην περίπτωση του «+», η επιλογή των ατόμων που θα συνεχίσουν στην επόμενη γενιά γίνεται από ολόκληρο τον πληθυσμό, δηλαδή θα επιλεγούν τα μ άτομα από το συνολικό πληθυσμό $\mu + \lambda$ των γονέων και των απογόνων. Στην περίπτωση του «,» η επιλογή θα γίνει μόνο από τον πληθυσμό των απογόνων, δηλαδή θα επιλεγούν τα μ καλύτερα άτομα από τους λ απόγονους, χωρίς να ληφθεί υπόψην ο πληθυσμός των γονέων. Σε αυτήν την περίπτωση θα πρέπει προφανώς να ισχύει $\mu < \lambda$.

Στο επόμενο κεφάλαιο περιγράφονται οι αλγόριθμοι στρατηγικής εξέλιξης που χρησιμοποιήθηκαν στα πλαίσια της διπλωματικής εργασίας, και θα δίνεται μια πλήρης περιγραφή του τρόπου λειτουργίας των τελεστών μετάλλαξης, ανασυνδυασμού και επιλογής σε αυτούς τους αλγόριθμους.

1.2.11 Βέλτιστος σχεδιασμός κτηρίων από ΟΣ

Τα προβλήματα βελτιστοποίησης κατασκευών, χαρακτηρίζονται από διάφορες αντικειμενικές και περιορισμών συναρτήσεις οι οποίες γενικά είναι μη γραμμικές συναρτήσεις των μεταβλητών σχεδιασμού. Αυτές οι συναρτήσει είναι συχνά ασυνεχείς και μη κυρτές. Η μαθηματική διατύπωση των προβλημάτων βελτιστοποίησης σε κατασκευές, σε σχέση με τις μεταβλητές σχεδιασμού, την αντικειμενική συνάρτηση και τους περιορισμούς εξαρτάται από τον τύπο της εφαρμογής. Όμως, τα περισσότερα προβλήματα βελτιστοποίησης μπορούν να διατυπωθούν με συγκεκριμένους μαθηματικούς όρους σαν ένα πρόβλημα μη γραμμικού προγραμματισμού ως ακολούθως:

$$\begin{aligned} &\min && F(\mathbf{s}) \\ &\text{subject to} && g_j(\mathbf{s}) \leq 0 \quad j=1,\ldots,m \\ &&& s_i \in R^d, \quad i=1,\ldots,n \end{aligned} \tag{1}$$

όπου *F(s)* και $g_j(s)$ είναι η αντικειμενική συνάρτηση και οι συναρτήσεις περιορισμών αντίστοιχα, R^d είναι ένα δοσμένο σετ σχεδιασμού, ενώ οι μεταβλητές σχεδιασμού s_i (i=1,...,n) παίρνουν τιμές μόνο από αυτό το σύνολο.

1.2.12 Ορισμοί

Υπάρχουν κάποιοι ορισμοί που πρέπει να δοθούν για να περιγραφεί το πρόβλημα και η διαχείριση του από τον αλγόριθμο βελτιστοποίησης της παρούσας εργασίας.

Στρεπτικά ισορροπημένο: Ένα δομικό σύστημα προσδιορίζεται ως στρεπτικά ισορροπημένο όταν σε κάθε όροφο της κατασκευής, το κέντρο μάζας συμπίπτει με το κέντρο ελαστικής στροφής.

Κέντρο Αντοχών ή Αντιστάσεως (CV): Το σημείο αυτό προσδιορίζεται ως ακολούθως:

$$x_{CV} = \frac{\sum_i x_i V_{n,i}}{\sum_i V_{n,i}} \quad (2)$$

Όπου x_{CV} είναι η τετμημένη του CV, $V_{n,i}$ είναι η οριζόντια αντοχή του i-στού στοιχείου και xi είναι η απόσταση του i-στού στοιχείου από το κέντρο μάζας. Για κάθε στύλο και τοιχίο προσδιορίζονται δύο αρχιτεκτονικοί περιορισμοί:

Αρχιτεκτονικός περιορισμός 1: Ο πρώτος αρχιτεκτονικός περιορισμός (AC1) είναι σχετικός με τα όρια της κάτοψης όπου ένας στύλος ή ένα τοιχίο μπορεί να κινηθεί και τελικά τοποθετηθεί. Έχει υλοποιηθεί ως ένα ορθογώνιο διαστάσεων AC1x × AC1y. Ένας σχεδιασμός θεωρείται εφικτός σε σχέση με τον αρχιτεκτονικό περιορισμό AC1 όταν η εγκάρσια διατομή των στύλων και των τοιχίων εμπεριέχονται στα αντίστοιχα ορθογώνια.

Αρχιτεκτονικός περιορισμός 2: Ο δεύτερος αρχιτεκτονικός περιορισμός (AC2) σχετίζεται με την τοπολογία των δοκών σε συνδυασμό με τους στύλους ή τα τοιχία πάνω στα οποία στηρίζονται. Αυτός ο περιορισμός εφαρμόζεται σαν ένα σημείο μέσα στο ορθογώνιο AC2 είναι απαραίτητο στην διαδικασία βελτιστοποίησης για να καλύψουμε τον περιορισμό που θέτουν οι θέσεις των δοκών. Σε κάθε εφικτό σχεδιασμό το σημείο AC2 θα αντιστοιχεί σε ένα κόμβο δοκού - στύλου.

Τύπος στύλου: Δύο τύποι στύλων/τοιχίων εξετάζονται. Ο τύπος Ι είναι εκείνος όπου το σταθερό σημείο αντιστοιχεί σε μία από τις γωνίες του AC1· ενώ στον τύπο ΙΙ το σημείο AC2 είναι εντός του ορθογωνίου AC1.

1.2.13 Βελτιστοποίηση αρχικού κόστους

Σε όλες τις διατυπώσεις που θα περιγραφούν σε αυτή την εργασία, οι μεταβλητές σχεδιασμού χωρίζονται σε δύο κατηγορίες: (i) μεταβλητές τοπολογίας, που σχετίζονται με τη θέση των κατακόρυφων φερόντων στοιχείων και (ii) μεταβλητές μεγέθους που αντιστοιχούν στις διαστάσεις της εγκάρσιας διατομής. Η μαθηματική διατύπωση αυτού του προβλήματος βελτιστοποίησης για κτήρια από ΟΣ μπορεί να γίνει ως ακολούθως:

$$\begin{aligned} &\min && C_{IN}(s) = C_b(s) + C_{sl}(s) + C_{cl}(s) \\ &\text{subject to} && g_k(s) \le 0,\ k=1,2,...,m \text{ (behavioral)} \\ &&& \left.\begin{aligned} t^i_{lb,j} \le r^i_j \le t^i_{ub,j},\ j=1,2,...,n_{columns} \\ s^i_{lb,j} \le h^i_j \le s^i_{ub,j},\ j=1,2,...,n_{columns} \end{aligned}\right\} \text{(architectural)} \end{aligned} \tag{3}$$

όπου $C_{IN}(s)$ αναφέρεται στο συνολικό αρχικό κατασκευαστικό κόστος για την κατασκευή συνολικά, όπου $C_b(s)$, $C_{sl}(s)$ και $C_{cl}(s)$ αναφέρονται στο αρχικό κόστος των δοκών των πλακών και των στύλων αντίστοιχα. Ο όρος αρχικό κόστος μια νέας κατασκευής αναφέρεται στο κόστος κατά τη διάρκεια κατασκευής. Το αρχικό κόστος σχετίζεται με το κόστος των υλικών και του εργοταξίου για την κατασκευή του κτηρίου, το οποίο περιλαμβάνει σκυρόδεμα, χαλύβδινο οπλισμό κόστος εργοταξίου για την τοποθέτηση και κόστος μη δομικών στοιχείων. $g_k(s)$ είναι οι περιορισμοί συμπεριφοράς που επιβάλλονται από τους κανονισμούς, r^i_j είναι η απόσταση του αντιστοίχου στοιχείου του *j* στύλου ή τοιχίου στην *i* ομάδα ορόφων από το αντίστοιχο σημείο AC2. $t^i_{lb,j}, t^i_{ub,j}$ είναι τα κατώτατα και ανώτερα όρια των μεταβλητών τοπολογίας που επιβάλλονται από τους αρχιτεκτονικούς περιορισμούς. h^i_j είναι η μέγιστη διάσταση του *j* στύλου/τοιχείου στην *i* ομάδα ορόφων, που αντιστοιχεί στις μεταβλητές μεγέθους. $s^i_{lb,j}, s^i_{ub,j}$ είναι τα ανώτερα και κατώτερα όρια των διατομών μεγέθους που επιβάλλονται από τους αρχιτεκτονικούς περιορισμούς. Όπως θα φανεί και στη συνέχεια, στην περιγραφή του προβλήματος υπάρχει μια σχέση μεταξύ των δύο ειδών μεταβλητών σχεδιασμού – τοπολογίας και μεγέθους – όπως και των ορίων τους.

1.2.14 Πρόβλημα βελτιστοποίησης απόκρισης σε στρέψη

Σε αυτό το πρόβλημα ο βασικός στόχος είναι να διατυπώσουμε μια διαδικασία βελτιστοποίησης η οποία θα μπορούσε να οδηγήσει σε σχεδιασμούς με βελτιωμένη σεισμική συμπεριφορά και συγκεκριμένα, να παράγουμε σχεδιασμούς με ελάχιστη στρεπτική απόκριση. Σε αυτή τη δουλειά δύο διακριτές διατυπώσεις αυτού του προβλήματος εφαρμόστηκαν, στην πρώτη διατυπώνεται σαν πρόβλημα ελαχιστοποίησης της απόστασης e_{CM-CR} μεταξύ του κέντρου μάζας (CM) και του κέντρου ελαστικής στροφής (CR) του κάθε ορόφου, ενώ η δεύτερη διατύπωση εφαρμόζεται σαν πρόβλημα ελαχιστοποίησης της εκκεντρότητας e_{CM-CV} μεταξύ του κέντρου μάζας και του κέντρου αντοχών (CV). Και οι δύο διατυπώσεις υπόκεινται σε περιορισμούς συμπεριφοράς που επιβάλλονται από τη νομοθεσία όπως και σε αρχιτεκτονικούς περιορισμούς. Οι δύο μαθηματικές διατυπώσεις, μπορούν να εφαρμοστούν ως ακολούθως:

$$\begin{aligned} &\min && e_{CM-CR} = \sqrt{(x^i_{CM} - x^i_{CR})^2 + (y^i_{CM} - y^i_{CR})^2},\ i=1,2,...,n\_g_{storeys} \\ &\text{subject to} && g_k(\mathbf{s}) \le 0,\ k=1,2,...,m \text{ (behavioral)} \\ &&& \left.\begin{aligned} t^i_{lb,j} \le r^i_j \le t^i_{ub,j},\ j=1,2,...,n_{columns} \\ s^i_{lb,j} \le h^i_j \le s^i_{ub,j},\ j=1,2,...,n_{columns} \end{aligned}\right\} \text{(architectural)} \end{aligned} \tag{4a}$$

$$\begin{aligned} &\min && e_{CM-CV} = \sqrt{(x^i_{CM} - x^i_{CV})^2 + (y^i_{CM} - y^i_{CV})^2},\ i=1,2,...,n_{storeys} \\ &\text{subject to} && g_k(\mathbf{s}) \le 0,\ k=1,2,...,m \text{ (behavioral)} \\ &&& \left.\begin{aligned} t^i_{lb,j} \le r^i_j \le t^i_{ub,j},\ j=1,2,...,n_{columns} \\ s^i_{lb,j} \le h^i_j \le s^i_{ub,j},\ j=1,2,...,n_{columns} \end{aligned}\right\} \text{(architectural)} \end{aligned} \tag{4b}$$

όπου (x^i_{CM}, y^i_{CM}), (x^i_{CR}, y^i_{CR}) and (x^i_{CV}, y^i_{CV}) είναι οι συντεταγμένες του κέντρου μάζας, του κέντρου ελαστικής στροφής και του κέντρου αντοχών αντίστοιχα. Πρέπει να σημειωθεί ότι το κέντρο *CR* είναι το ίδιο για κάθε ομάδα ορόφων, ενώ το κέντρο *CV* προσδιορίζεται για κάθε όροφο. *n_gstoreys* είναι ο συνολικός αριθμός ορόφων που έχουν την ίδια κάτοψη ενώ *nstoreys* είναι ο συνολικός αριθμός των ορόφων.

1.2.15 Πεπλεγμένο πρόβλημα βελτιστοποίησης

Στην Τρίτη φιλοσοφία σχεδιασμού που εφαρμόστηκε στην παρούσα μελέτη και τα δύο αντικείμενα ελήφθησαν υπόψη σαν σταθμισμένο βάρος. Η μαθηματική διατύπωση αυτού του σύνθετου προβλήματος βελτιστοποίησης μπορεί να διατυπωθεί ως ακολούθως:

$$
\begin{aligned}
&\min && F(\mathbf{s}) = w \cdot C_{IN}^{*} + (1-w) \cdot \max(e_{CM-CR}^{*}, e_{CM-CV}^{*}) \\
&\text{subject to} && g_k(\mathbf{s}) \le 0,\ k=1,2,...,m \text{ (behavioral)} \\
& && \left.\begin{aligned} t_{lb,j}^{i} \le r_j^{i} \le t_{ub,j}^{i},\ j=1,2,...,n_{columns} \\ s_{lb,j}^{i} \le h_j^{i} \le s_{ub,j}^{i},\ j=1,2,...,n_{columns} \end{aligned}\right\} \text{(architectural)}
\end{aligned}
\tag{5}
$$

όπου C_{IN}^{*}, e_{CM-CR}^{*} and e_{CM-CV}^{*} είναι οι κανονικοποιημένες τιμές του αρχικού κόστους και οι δύο εκκεντρότητες, ενώ w είναι ο συντελεστής βάρους.

1.3 Περιορισμοί συμπεριφοράς

Πέρα από τους αρχιτεκτονικούς περιορισμούς, περιορισμοί συμπεριφοράς, που επιβάλλονται από τους κανονισμούς, πρέπει να ικανοποιηθούν με στόχο να αποδεχθούμε ένα σχεδιασμό ως εφικτό. Αυτοί οι έλεγχοι συμπεριφοράς εφαρμόζονται ακολουθώντας μια δομοστατική ανάλυση όπου τα εντατικά και παραμορφωσιακά μεγέθη ελέγχονται σύμφωνα με τους EC2 [15] και EC8 [14] κανονισμούς σχεδιασμού. Για κάθε σχεδιασμό, η δυναμική φασματική ανάλυση εφαρμόζεται στο τελευταίο στάδιο ύστερα από τη σύγκλιση του προβλήματος βελτιστοποίησης και βασίζεται στη πολυιδιομορφική ανάλυση χρησιμοποιώντας το πλήρες μοντέλο για το κτήριο. Η mMRS ανάλυση είναι μια απλοποίηση της μεθόδου υπέρθεσης των ιδιομορφών που επιβάλλει ο Ευρωκώδικας 8 [14] και χρησιμοποιείται αντί της ανάλυσης χρονοιστορίας.

Η πλειονότητα των κανονισμών σχεδιασμού ανήκουν στην κατηγορία των περιγραφικών κανονισμών, οι οποίοι περιλαμβάνουν: επιλογή τοποθεσίας και εφαρμογή και ανάπτυξη προσχέδιου, προμελέτης και τελικού σχεδιασμού. Σύμφωνα με ένα περιγραφικό κανονισμό σχεδιασμού η αντοχή της κατασκευής αποτιμάται σε μια οριακή κατάσταση μεταξύ της κατάστασης προστασίας της ζωής (life-safety) και πριν την κατάρρευση (near collapse) χρησιμοποιώντας ένα φάσμα απόκρισης που αντιστοιχεί σε ένα σεισμό σχεδιασμού [14]. Επιπρόσθετα, η οριακή κατάσταση λειτουργικότητας συχνά ελέγχεται με σκοπό να εκλεχθεί εάν η κατασκευή θα παραμορφώνεται ή ταλαντώνεται υπερβολικά κατά τη χρήση της.

Σύμφωνα με τον Ευρωκώδικα διάφοροι έλεγχοι πρέπει να θεωρηθούν προκειμένου να εξασφαλιστεί ότι η κατασκευή θα καλύψει τις απαιτήσεις σχεδιασμού. Κάθε υποψήφιος βέλτιστος σχεδιασμός αξιολογείται χρησιμοποιώντας αυτούς τους περιορισμούς. Όλοι [15] οι έλεγχοι του EC2 πρέπει να ικανοποιηθούν για τα φορτία βαρύτητας χρησιμοποιώντας τον ακόλουθο συνδυασμό φορτίων

$$S_d = 1.35\sum_j G_{kj} \text{"+"} 1.50\sum_i Q_{ki} \quad (6)$$

όπου "+" υπονοεί "για να συνδυαστεί με", το σύμβολο "Σ" αθροίσματος υπονοεί ότι "η συνδυασμένη επίδραση", το G_{KJ} δείχνει τη χαρακτηριστική τιμή "κ" της μόνιμης δράσης j και το q_{ki} αναφέρεται στη χαρακτηριστική τιμή "κ" της μεταβλητής δράσης i. Εάν οι ανωτέρω περιορισμοί ικανοποιούνται, η φασματική ανάλυση απόκρισης εκτελείται, σύμφωνα με τον EC8, και τη φόρτιση σεισμού που εξετάζεται χρησιμοποιώντας το ακόλουθο συνδυασμό φορτίσεως

$$S_d = \sum_j G_{kj} \text{"+"} E_d \text{"+"} \sum_i \psi_{2i} Q_{ki} \quad (7)$$

όπου το E_δ είναι η τιμή σχεδιασμού της σεισμικής δράσης για τις δύο συνιστώσες (διαμήκη και εγκάρσια) αντίστοιχα και ψ_μ είναι ο συντελεστής συνδυασμού για τη μεταβλητή δράση i, εδώ ληφθείς ίσος σε 0,30. Όλοι αυτοί οι έλεγχοι εκτελούνται για κάθε υποψήφιο σχεδιασμό που εξετάζεται από τον βελτιστοποιητή.

Η κύρια αρχή των νέων κανονισμών, του EC8 συμπεριλαμβανόμενου, είναι να σχεδιαστούν τα δομικά συστήματα βασισμένα στην απορρόφηση ενέργειας και στην πλαστιμότητα προκειμένου να ελεγχθεί η ανελαστική σεισμική απόκριση. Ο σχεδιασμός ενός πολυώροφου κτηρίου ΟΣ για την απορρόφηση ενέργειας περιλαμβάνει τα ακόλουθα χαρακτηριστικά γνωρίσματα: (i) εκπλήρωση του ικανοτικού σχεδιασμού, (ii) επαλήθευση μελών από την άποψη των δυνάμεων και των αντιστάσεων για οριακή κατάσταση αστοχίας υπό το σεισμό σχεδιασμού (με την περίοδο επαναφοράς 475 ετών, την πιθανότητα υπέρβασης 10% σε 50 έτη), με το ελαστικό φάσμα που μειώνεται από το συντελεστή συμπεριφοράς q, (iii) περιορισμός ζημιών για την οριακή κατάσταση λειτουργικότητας (iv) ικανοτικός σχεδιασμός έναντι τέμνουσας

1.4 Αποτίμηση υπαρχόντων κριτηρίων σχεδιασμού

Τα κριτήρια σχεδιασμού κτηριακών φορέων έναντι στρέψης που εξετάστηκαν στην Διδακτορική Διατριβή είναι: (i) ελάχιστη απόσταση μεταξύ του κέντρου μάζας και κέντρου ελαστικής στροφής, (ii) ελάχιστη τετραγωνική ρίζα του αθροίσματος των τετραγώνων των αποστάσεων του κέντρου μάζας του κάθε ορόφου από το κέντρο συστροφής του συγκεκριμένου ορόφου, (iii) ελάχιστη απόσταση μεταξύ του κέντρου μάζας και του κέντρου αντοχών του κάθε ορόφου και (iv) ελάχιστη στρεπτική ροπή βάσης του φορέα. Το κάθε κριτήριο σχεδιασμού ικανοποιήθηκε μέσω διαδικασίας βελτιστοποίησης σε ικανό αριθμό κτηριακών κατασκευών. Αντικείμενο της παρούσας Διδακτορικής Διατριβής αποτέλεσε η σύγκριση αυτών των σχεδιασμών, καθώς και των κριτηρίων σχεδιασμού έχοντας ως βάση αξιολόγησης την επίδοσή τους κατά τη σεισμική φόρτιση. Οι τελικοί σχεδιασμοί συγκρίνονται με κριτήριο το κόστος κύκλου ζωής το οποίο είναι το άθροισμα του αρχικού κόστους και του κόστους επισκευής. Ο στόχος είναι να προταθεί μια μεθοδολογία που θα βελτιώνει τη φιλοσοφία σχεδιασμού τριδιάστατων κτηρίων από οπλισμένο σκυρόδεμα με βάση την επίδοσή τους σε σεισμικές δράσεις.

1.5 Λόγος Στρέψης: Νέο κριτήριο σχεδιασμού κατασκευών έναντι στρέψης

Μέσω ενός σημαντικού αριθμού αναλύσεων, με βάση τα υπάρχοντα κριτήρια σχεδιασμού της βιβλιογραφίας, διαπιστώθηκε ότι κανένα από αυτά δεν έχει γενική ισχύ, δηλαδή ικανοποιητική επίδοση τόσο σε ελαστική όσο και σε ανελαστική συμπεριφορά. Σε αυτό το πλαίσιο προτείνεται ένα γενικότερο κριτήριο σχεδιασμού κατασκευών έναντι στρέψης με την ονομασία: *Λόγος Στρέψης*. Το κριτήριο αυτό προέκυψε ύστερα από την διαπίστωση ότι το πρόβλημα της στρέψης κατασκευών δεν οφείλεται σε στρεπτικές ροπές στα υποστυλώματα αλλά σε πλεονάζοντα ζεύγη τεμνουσών δυνάμεων σε αυτά. Συγκεκριμένα σε ασύμμετρες κατασκευές ισχύει η συνθήκη:

$$\sum_{k=1}^{n} |Vkij| \neq \sum_{k=1}^{n} Vkij$$

Όπου τα εντατικά μεγέθη *Vkij* (που φαίνονται στο Σχήμα 1) είναι οι τέμνουσες των υποστυλωμάτων. Έτσι διατυπώθηκε ο λόγος της στρέψης ως το πηλίκο των πλεοναζουσών τεμνουσών της με την τέμνουσα βάσης της κατασκευής:

$$\text{ROT} = \sum_1^n \sum_{i=x,j=y}^{y,x} ROTij$$

$$\text{όπου } ROTij = \frac{\sum_{k=1}^{n} |Vkij| - a * \sum_{k=1}^{n} Vkij}{\sum_{k=1}^{n} Vkij}$$

1.6 Παραδείγματα

Ένα διώροφο χωρικό πλαίσιο ΟΣ, που παρουσιάζεται στο σχήμα 1, έχει εξεταστεί για την αξιολόγηση της προτεινόμενης μεθοδολογίας. Σε όλες τις περιπτώσεις δοκιμής οι ακόλουθες ιδιότητες υλικών έχουν εξεταστεί: σκυρόδεμα με το συντελεστή της ελαστικότητας E_c = 30GPa και χαρακτηριστική θλιπτική αντοχή f_{ck} = 20MPa, διαμήκης χάλυβας με μέτρο ελαστικότητας E_s = 210GPa και χαρακτηριστική δύναμη διαρροής $f_{yk,s}$ = 500MPa και εγκάρσιος οπλισμός με το μέτρο ελαστικότητας E_s = 210GPa και χαρακτηριστική τιμή διαρροής $f_{yk,s}$ = 220MPa. Το φάσμα σχεδιασμού που έχει χρησιμοποιηθεί έχει τα ακόλουθα χαρακτηριστικά: A=0.16g (σεισμικό επίπεδο επικινδυνότητας ΙΙ), τύπος εδάφους Β (T_1 = 0.15sec και T_2 = 0.60sec) και συντελεστής συμπεριφοράς q=3.5 σύμφωνα με Eurocode 8 [14] (EC8 1996). Η εγκάρσια διατομή των δοκών είναι 25 $\times$ 60 εκατ.^{2}. Οι στύλοι έχουν θεωρηθεί ως πλήρως πακτωμένοι και στους όρους δεν έχουν ληφθεί υπόψη οι συνθήκες θεμελίωσης.

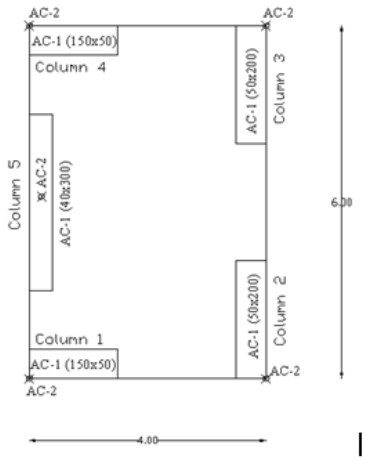

Column	AC_1	
	AC_{1x}	AC_{1y}
C1	150	50
C2	50	200
C3	50	200
C4	150	50
C5	40	300

Εικόνα 1. Αρχιτεκτονικοί περιορισμοί

Οι ακόλουθες τέσσερις διατυπώσεις του προβλήματος βελτιστοποίησης έχουν εξεταστεί: (i) αρχικό κόστος κατασκευής (ii) ελάχιστη εκκεντρότητα CM-CR (iii) ελάχιστη CM-CV εκκεντρότητα (iv) πέντε συνδυασμένες διατυπώσεις όπου δύο τιμές του συντελεστή βάρους (0,1 και 0.9) της εξίσωσης (5) έχουν εξεταστεί. Οι πέντε συνδυασμένες διατυπώσεις μπορούν να περιγραφούν ως εξής:

$$\begin{aligned}
&\text{Min}\{0.1\cdot C^{*}_{\text{IN}} + 0.9\cdot e^{*}_{\text{CM-CR}}\} && \text{Comb(1)}\\
&\text{Min}\{0.1\cdot C^{*}_{\text{IN}} + 0.9\cdot e^{*}_{\text{CM-CV}}\} && \text{Comb(2)}\\
&\text{Min}\{0.1\cdot C^{*}_{\text{IN}} + 0.9\cdot \max(e^{*}_{\text{CM-CR}}, e^{*}_{\text{CM-CV}})\} && \text{Comb(3)}\\
&\text{Min}\{0.9\cdot C^{*}_{\text{IN}} + 0.1\cdot e^{*}_{\text{CM-CR}}\} && \text{Comb(4)}\\
&\text{Min}\{0.9\cdot C^{*}_{\text{IN}} + 0.1\cdot e^{*}_{\text{CM-CV}}\} && \text{Comb(5)}
\end{aligned} \qquad (8)$$

Τρία διαφορετικά κριτήρια έχουν χρησιμοποιηθεί προκειμένου να αξιολογηθούν οι βέλτιστοι σχέδιασμοί που επιτυγχάνονται μέσω των προαναφερθεισών διατυπώσεων: το αρχικό κόστος κατασκευής το συνολικό κόστος κύκλου της ζωής και το στρεπτικό κριτήριο απόκρισης. Για τις δεύτερες και τρίτες σεισμικές κινήσεις που επιλέγονται από τη [16] βάση δεδομένων των Somerville και Collins, που ανήκει στο 50/50, 10/50 και 2/50 επίπεδα επικυνδυνότητας, χρησιμοποιούνται. Τα αρχεία κάθε επιπέδου επικυνδυνότητας κανονικοποιούνται στο ίδιο PGA προκειμένου να εξασφαλιστεί συμβατότητα μεταξύ των αρχείων, σύμφωνα με τις καμπύλες επικυνδυνότητας για την Ελλάδα που λαμβάνεται από την εργασία Papazachos et του Al [17] (πίνακας 1).

Πίνακας 1: Επίπεδα Επικινδυνότητας [17]

Γεγονός	Περίοδος Επαναφοράς	Πιθανότητα Υπέρβασης	PGA (g)
Συνήθης	21 χρόνια	90% στα 50 χρόνια	0.06
Περιστασιακός	72 χρόνια	50% στα 50 χρόνια	0.11
Σπάνιος	475 χρόνια	10% στα 50 χρόνια	0.31
Πολύ σπάνιος	2475 χρόνια	2% στα 50 χρόνια	0.78

Πίνακας 2: Μέσες τιμές της στρεπτικής απόκρισης στα τρία επίπεδα επικινδυνότητας

Design philosophy	Hazard Level					
	50/50		10/50		2/50	
	max (10^{-3} rad)	min (10^{-3} rad)	max (10^{-3} rad)	min (10^{-3} rad)	max (10^{-3} rad)	min (10^{-3} rad)
Min{$0.1C_{IN}$+ $0.9e_{CM-CR}$}	0.509	-0.543	1.87	-1.84	9.14	-9.02
Min{$0.1C_{IN}$+ $0.9e_{CM-CV}$}	0.569	-0.533	3.77	-3.64	3.20	-3.71
Min{$0.1C_{IN}$+ $0.9\max(e_{CM-CR}, e_{CM-CV})$}	0.505	-0.351	1.43	-1.20	4.46	-4.42
Min{$0.9C_{IN}$+ $0.1e_{CM-CR}$}	2.29	-1.83	9.72	-9.92	23.10	-15.00
Min{$0.9C_{IN}$+ $0.1e_{CM-CV}$}	3.47	-2.94	6.39	-6.53	9.31	-9.45
Min{e_{CM-CR}}	0.254	-0.293	0.953	-1.28	5.26	-5.05
Min{e_{CM-CV}}	1.51	-1.40	2.46	-2.33	3.50	-5.05
Min{C_{IN}}	1.69	-1.34	7.90	-7.91	13.90	-13.40

Στο παράδειγμα που εξετάστηκε υπάρχει μόνο μια ομάδα ορόφων δεδομένου η κάτοψη είναι η ίδια για όλους τους ορόφους. Για αυτό το παράδειγμα 6 μεταβλητές σχεδιασμού έχουν χρησιμοποιηθεί: 5 ενεργές μεταβλητές τοπολογίας και 1 μεγέθους για την ενιαία ομάδα ορόφων. Πρέπει να διαπιστωθεί ότι όλα τα σχέδια που λαμβάνονται από τις διαφορετικές διατυπώσεις ικανοποιούν τις απαιτήσεις των EC2 και EC8.

Προκειμένου να αξιολογηθεί η επίδοση των βέλτιστων λύσεων, οι μη γραμμικές timehistory αναλύσεις εκτελούνται για τις καταγραφές από τη βάση δεδομένων [16]. Στα σχήματα 2 (a) έως 2 (c) μια αριθμητική μελέτη διεξάγεται συγκρίνοντας τη στρεπτική απόκριση του διαφράγματος του δεύτερου ορόφου, ενώ στον πίνακα 2 οι μέγιστες και ελάχιστες τιμές της περιστροφής διαφραγμάτων δίνονται. Μπορεί να φανεί ότι η μέγιστη περιστροφή του διαφράγματος αντιμετωπίζεται στα βέλτιστοι σχεδιασμοί αποκτηθέντα όταν το C_{IN} ήταν το κυρίαρχο κριτήριο και για τα τρία επίπεδα επικινδυνότητας που εξετάστηκαν. Αφ' ετέρου, στο συχνό (50/50) και περιστασιακό (10/50) επίπεδο επικινδυνότητας, το κριτήριο Min{e_{CM-CR}} συμπεριφέρεται καλύτερα ενώ στα σπάνια (2/50) επίπεδα κινδύνου οι διατυπώσεις όπου το e_{CM-CV} είναι το κυρίαρχο κριτήριο δίνουν τους καλύτερους σχεδιασμούς. Αυτή η παρατήρηση δικαιολογείται από τα συμπεράσματα των Paulay [11,12] και Tso και Myslimaj [13].

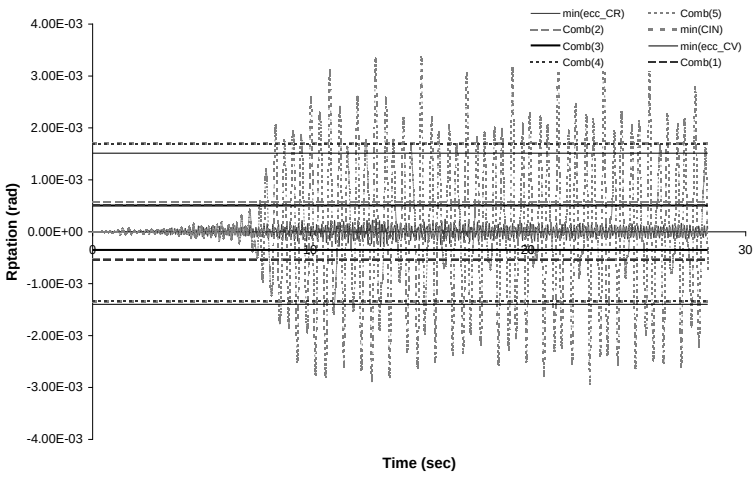

(a)

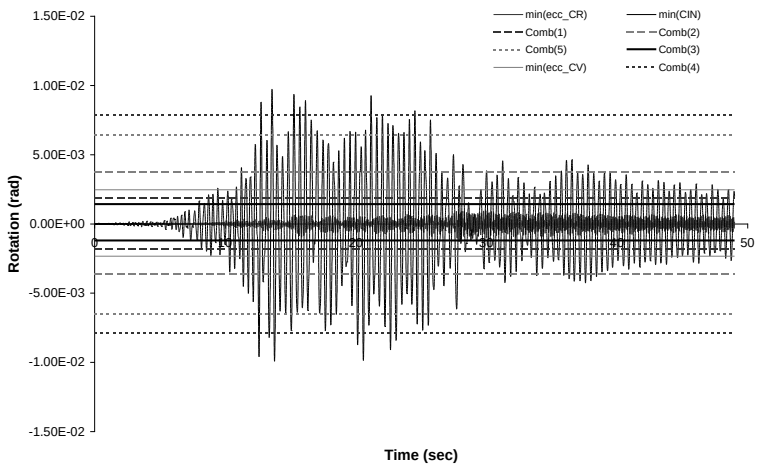

(b)

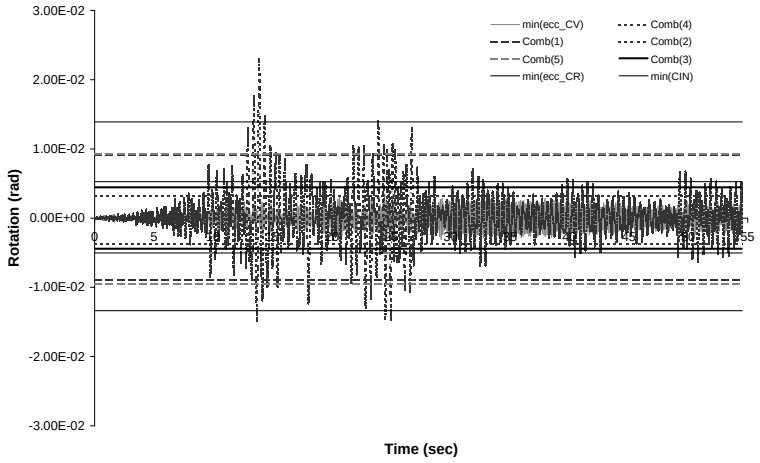

(c)

Σχήμα 2: Χρονοιστορία της στροφής για τα τρία επίπεδα επικινδυνότητας (a) 50/50, (b) 10/50 και (c) 2/50

Το τελευταίο μέρος της σύγκρισης δίνεται στον πίνακα 3 όπου οι βέλτιστοι σχεδιασμοί συγκρίνονται όσον αφορά το αρχικό, της οριακής κατάστασης και το συνολικό κόστος κύκλου της ζωής. Μέσω αυτής της σύγκρισης μπορεί να φανεί ότι το C_{IN} δεν είναι το κατάλληλο κριτήριο για ένα σχεδιασμό κύκλου της ζωής μιας κατασκευής ΟΣ δεδομένου ότι η δομική συμπεριφορά ενάντια στο σεισμό επιβάλλεται ως περιορισμοί του κανονισμού.

Αφ' ετέρου, οι διατυπώσεις που έχουν το κριτήριο e_{CM-CR} ως το κυρίαρχο οδηγούν στους βέλτιστους σχεδιασμούς με το ελάχιστο C_{TOT} έναντι αυτού των άλλων βέλτιστων.

Πίνακας 3: Σύγκριση των σχεδιασμών σε σχέση με το κόστος

	$Min\{0.1C_{IN}+0.9e_{CM-CR}\}$	$Min\{0.1C_{IN}+0.9e_{CM-CV}\}$	$Min\{0.1C_{IN}+0.9max(e_{CM-CR}, e_{CM-CV})\}$	$Min\{0.9C_{IN}+0.1e_{CM-CR}\}$	$Min\{0.9C_{IN}+0.1e_{CM-CV}\}$	$Min\{e_{CM-CR}\}$	$Min\{e_{CM-CV}\}$	$Min\{C_{IN}\}$
C_{IN} (in € 1,000)	51.92	50.33	49.23	43.13	46.15	52.80	51.24	43.81
C_{LS}/C_{IN}	3.53	18.57	7.19	22.53	23.56	3.65	13.07	29.18
C_{TOT}(in € 1,000)	235.46	984.92	403.31	1015.01	1133.73	245.61	721.32	1322.33

1.7 Συμπεράσματα

Σε αυτή την εργασία, ένα πλήθος προσεγγίσεων σχεδιασμού για τρισδιάστατα κτήρια από οπλισμένο σκυρόδεμα (ΟΣ) διατυπώνονται σαν προβλήματα βέλτιστου δομοστατικού σχεδιασμού και αποτιμώνται με βάση την επίδοση υπό σεισμικά φορτία. Επίσης, το κόστος κύκλου ζωής λαμβάνεται υπόψη ως μέτρο αποτίμησης της συμπεριφοράς των σχεδιασμών που προκύπτουν. Τρείς φιλοσοφίες σχεδιασμού κτηρίων από ΟΣ θεωρούνται στην παρούσα εργασία. Στην πρώτη το αρχικό κατασκευαστικό κόστος θεωρείται ως αντικειμενική συνάρτηση ελαχιστοποίησης, η δεύτερη διατυπώνεται ως πρόβλημα ελαχιστοποίησης της στρεπτικής απόκρισης ενώ σαν τρίτη προσέγγιση σχεδιασμού εξετάζεται μια συνδυασμένη διατύπωση. Η δεύτερη προσέγγιση θεωρείται με δύο διακριτές διατυπώσεις. Σύμφωνα με την πρώτη η στρεπτική συμπεριφορά ελαχιστοποιείται μέσω της ελαχιστοποίηση της απόστασης του κέντρου μάζας από το κέντρο ελαστικής στροφής ενώ στη δεύτερη αυτό επιτυγχάνεται ελαχιστοποιώντας την εκκεντρότητα μεταξύ του κέντρου αντοχών και του κέντρου μάζας. Γίνεται φανερό ότι οι σχεδιασμοί που λαμβάνονται σύμφωνα με την ελαχιστοποίηση της εκκεντρότητας του κέντρου ελαστικής στροφής συμπεριφέρονται καλά σε συχνούς (50/50 επίπεδο επικινδυνότητας) και συνήθεις (10/50 επίπεδο

επικινδυνότητας) σεισμούς, ενώ οι σχεδιασμοί που λαμβάνονται σύμφωνα με την ελαχιστοποίηση της εκκεντρότητας του κέντρου αντοχής επιδεικνύουν καλή συμπεριφορά στα σπάνια (2/50 επίπεδο επικινδυνότητας) σεισμικά γεγονότα. Σχεδιασμοί βασισμένοι σε μια συνδυασμένη διατύπωση δείχνουν καλή συμπεριφορά και στα τρία επίπεδα επικινδυνότητας που εξετάστηκαν.

Η επιρροή των μεγάλων εκκεντροτήτων των κέντρων ακαμψίας και αντοχής σε σχέση με το κέντρο μάζας αξιολογείται όσον αφορά τη σεισμική απόκριση των κτηρίων. Ειδικότερα, οι διάφορες διατυπώσεις βέλτιστου σχεδιασμού αξιολογούνται όσον αφορά την ελάχιστη στρεπτική απάντηση σε τρία επίπεδα επικινδυνότητας (συχνός, περιστασιακός και σπάνιος) και όσον αφορά το συνολικό κόστος κύκλου της ζωής. Σε αυτήν την μελέτη ένας εξελικτικός αλγόριθμος βελτιστοποίησης έχει εφαρμοστεί για τη λύση των προβλημάτων βελτιστοποίησης. Δύο είναι τα κύρια συμπεράσματα αυτής της παραμετρικής μελέτης:

- Τα αποτελέσματα Paulay, Tso και Myslimaj ότι η κεντρική εκκεντρικότητα ακαμψίας είναι σημαντική μόνο όταν συμπεριφέρεται γραμμικά το δομικό σύστημα, ενώ όταν αρχίζει να συμπεριφέρεται μη γραμμικά η εκκεντρότητα αντοχών γίνονται σημαντικότερη ελέγχονται, στα πλαίσια της δομικής βελτιστοποίησης.
- Η δεύτερη εύρεση έχει να κάνει με τη διατύπωση που οδηγεί στους σχεδιασμούς με το ελάχιστο συνολικό κόστος κύκλου της ζωής. Στις ιδιαίτερες διατυπώσεις ότι το κριτήριο εκκεντρότητας ακαμψίας είναι το κυρίαρχο οδηγούν στους βέλτιστους σχεδιασμούς που έχουν το ελάχιστο συνολικό κόστος κύκλου της ζωής έναντι των βέλτιστων που έχουν λήφθει μέσω των διατυπώσεων όπου το αρχικό κόστος κατασκευής ή το κριτήριο εκκεντρότητας αντοχών ήταν το κυρίαρχο.

Σε αυτή την εργασία παρουσιάζεται η μέθοδος του στρεπτικού λόγου ως μια νέα μέθοδος σχεδιασμού κατασκευών από οπλισμένο σκυρόδεμα (ΟΣ). Συγκεκριμένα, ένα πλήθος προσεγγίσεων σχεδιασμού για τρισδιάστατα κτήρια από ΟΣ διατυπώνονται σαν προβλήματα βέλτιστου δομοστατικού σχεδιασμού και αποτιμώνται με βάση την επίδοση υπό σεισμικά φορτία, έτσι ώστε να συγκριθεί και να αξιολογηθεί η παρούσα μέθοδος σε σχέση με τις κυρίαρχες μεθόδους της διεθνούς βιβλιογραφίας για σχεδιασμό σε στρέψη. Τέσσερεις φιλοσοφίες σχεδιασμού κτηρίων από ΟΣ θεωρούνται στην παρούσα εργασία. Στην πρώτη το αρχικό κατασκευαστικό κόστος θεωρείται ως αντικειμενική συνάρτηση ελαχιστοποίησης, η δεύτερη διατυπώνεται ως πρόβλημα ελαχιστοποίησης της εκκεντρότητας μεταξύ του κέντρου μάζας και του κέντρου ελαστική στροφής ενώ σαν τρίτη προσέγγιση σχεδιασμού εξετάζεται η ελαχιστοποίησης της εκκεντρότητας μεταξύ του

κέντρου μάζας και του κέντρου αντοχών. Στην τέταρτη εκδοχή, παρουσιάζονται σχεδιασμοί που προέκυψαν από βελτιστοποίηση με αντικειμενική συνάρτηση το Στρεπτικό Λόγο.

Η διαδικασία βελτιστοποίησης χωρίζεται σε δύο ομάδες. Στην πρώτη, σε κάθε κύκλο της διαδικασίας βελτιστοποίησης εκτελούνται αναλύσεις με βάση τους κανονισμούς Ε.Α.Κ. και Ε.Κ.Ω.Σ. ενώ στη δεύτερη, σε κάθε κύκλο της διαδικασίας βελτιστοποίησης εκτελούνται έξι μη γραμμικές δυναμικές αναλύσεις (δύο για κάθε επίπεδο σεισμικής επικινδυνότητας) και ελέγχονται οι σχεδιασμοί με βάση την επιτελεστικότητα. Ο τελικοί σχεδιασμοί που προκύπτουν από την επίλυση των προβλημάτων βελτιστοποίησης αναλύονται με μη-γραμμική δυναμική μέθοδο και αξιολογούνται με βάση τις καμπύλες στρέψης - τέμνουσας βάσης. Τέλος συγκρίνονται τα αποτελέσματα για κάθε αντικειμενική συνάρτηση – φιλοσοφία σχεδιασμού για τα τρία επίπεδα σεισμικής επικινδυνότητας (50/50, 10/50, 2/50).

1.8 Συμβολή της Διδακτορικής Διατριβής

Αξιολογήθηκε η επιρροή των μεγάλων εκκεντροτήτων των κέντρων ακαμψίας και αντοχής σε σχέση με το κέντρο μάζας όσον αφορά τη σεισμική απόκριση των κτηρίων. Ειδικότερα, οι διάφορες διατυπώσεις βέλτιστου σχεδιασμού αξιολογούνται ως προς την ελάχιστη στρεπτική απόκριση σε τρία επίπεδα επικινδυνότητας (συχνός, περιστασιακός και σπάνιος) και ως προς το συνολικό κόστος κύκλου της ζωής. Σε αυτήν τη Διδακτορική Διατριβή έχει εφαρμοστεί ένας εξελικτικός αλγόριθμος βελτιστοποίησης για τη λύση των προβλημάτων βελτιστοποίησης. Η συμβολή καθώς και τα κύρια συμπεράσματα αυτής της Διδακτορικής Διατριβής είναι:

- Ανάπτυξη μεθοδολογίας βέλτιστου σχεδιασμού γενικών τριδιάστατων κτηρίων με μεταβλητές τοπολογίας και μεγέθους.
- Ανάπτυξη λογισμικού εφαρμογής της μεθοδολογίας βέλτιστου σχεδιασμού συμπεριλαμβανομένων των κανονισμών και μη γραμμικής δυναμικής ανάλυσης με αντικειμενικές συναρτήσεις τα επιμέρους κριτήρια στρεπτικής συμπεριφοράς.
- Η μη επιβεβαίωση των ευρημάτων των Paulay, Tso και Myslimaj ότι η κεντρική εκκεντρικότητα ακαμψίας σε πολυώροφα κτήρια είναι σημαντική μόνο όταν συμπεριφέρεται γραμμικά το δομικό σύστημα, ενώ όταν αρχίζει να συμπεριφέρεται μη γραμμικά η εκκεντρότητα αντοχών γίνεται σημαντικότερη.

- Οι σχεδιασμοί με βάση το ROT δίνουν καλύτερα αποτελέσματα σε γενικούς κτηριακούς φορείς τόσο στην ελαστική όσο και στην ανελαστική περιοχή με αξιολόγηση παραμορφώσεων και στρεπτικών ροπών βάσης κατά Chopra.

1.9 Μελλοντική Έρευνα

Τομείς για μελλοντική έρευνα σχετικά με την αξιοπιστία του λόγου της στρέψης όσον αφορά αποτίμηση συμπεριφοράς κατασκευών έναντι στρέψης:

- Η εφαρμογή αυτού του νέου πλαισίου σχεδιασμού σε μεγαλύτερο πλήθος κατασκευών για τεκμηρίωση αποτελεσμάτων
- Η εφαρμογή της προτεινόμενης μεθόδου αξιολόγησης σε μεταλλικές κατασκευές.
- Ανάπτυξη διαδικασιών, λογισμικών εργαλείων και μεθοδολογιών σχεδιασμού για άμεση χρήση από μηχανικούς της πράξης του σχεδιασμού που βασίζεται στα ευρήματα της Διατριβής αυτής.
- Χρήση προηγμένων υπολογιστικών μεθόδων επίλυσης των αριθμητικών προβλημάτων προκειμένου να αξιολογηθεί η αξιοπιστία της προτεινόμενης μεθόδου σε μεγαλύτερο εύρος κτηριακών κατασκευών.

1.10Επιστημονικές εργασίες

Το συνολικό δημοσιευμένο έργο στο οποίο ο κος Νικόλαος Π. Μπάκας συνέβαλε στο πλαίσιο της Διδακτορικής της Διατριβής συνοψίζεται ως εξής:

<u>Πρωτότυπες εργασίες σε κεφάλαια βιβλίων διεθνών εκδοτικών οίκων</u>

Mitropoulou Ch.Ch., **Bakas N.P.**, Lagaros N.D., M. Papadrakakis, Advances in design optimization of reinforced concrete structural systems, in Computational Structural Dynamics and Earthquake Engineering, M. Papadrakakis, D.C. Charmpis, N.D. Lagaros and Y. Tsompanakis (Eds.), Taylor & Francis, (November 2008).

<u>Δημοσιεύσεις σε διεθνή επιστημονικά περιοδικά με κριτές</u>

N.D. Lagaros, M. Papadrakakis, **N.P. Bakas** Automatic minimization of the rigidity eccentricity of 3d reinforced concrete buildings, J. Earth. Engrg., Vol. 10, No. 4, pp. 533-564, 2006.

N.D. Lagaros, **N.P. Bakas**, M. Papadrakakis "Optimum Design Approaches for Improving the Seismic Performance of 3D RC Buildings", Journal Earthquake Engineering, Vol. 13, No. 3, pp. 345-363, 2009.

N. P. Bakas, N.D. Lagaros, Ch. Stathi, M. Papadrakakis "Ratio of Torsion: A new assessment and design criterion", Earthquake Engineering & Structural Dynamics, υπό κρίση.

<u>Δημοσιεύσεις σε πρακτικά επιστημονικών συνεδρίων</u>

N.P. Bakas, N.D. Lagaros, M. Papadrakakis, "Earthquake resistant optimum design of 3d reinforced concrete buildings", 7th WCCM, Northwestern and UCLA universities, Los Angeles, California, USA, July 16-22, 2006.

N.P. Bakas, N.D. Lagaros, Manolis Papadrakakis, "Minimizing the torsional response of RC buildings under earthquake loading", The First South-East European Conference on Computational Mechanics, Kragujevac, Serbia, June 28-30, 2006.

N.P. Bakas, N.D. Lagaros, M. Papadrakakis. Assessment of Code's Torsional Provisions using Evolutionary Optimization Algorithms, COMPDYN 2007, June 13-16, 2007, Rethymno, Crete, Greece.

N.P. Bakas, N.D. Lagaros, M. Papadrakakis, Substratum Assessment of Various Minimum Torsional Design Philosophies via Structural Optimization Techniques, 8th WCCM and 5th ECCOMAS, Venice, Italy, June 30 – July 4, 2008.

N.P. Bakas, N.D. Lagaros, M. Papadrakakis, Assessment of design recommendations for torsionally unbalanced structures using structural optimization, CST2008, The 9th International Conference on Computational Structures Technology, Athens, Greece, 2-5 September 2008.

N.P. Bakas, N.D. Lagaros, M. Papadrakakis, A new method for assessing tortional effects in irregular buildings, COMPDYN 2009, June 22-24, 2009, Island of Rhodes, Greece.

N.D. Lagaros, **N.P. Bakas**, M. Papadrakakis, Assessment of design approaches for multistorey rc buildings under earthquake loading, using evolutionary optimization algorithms, 8th HSTAM International Congress on Mechanics, Patras,12 – 14 July, 2007

Ν.Π. Μπάκας, Ν.Δ. Λαγαρός, Μ. Παπαδρακάκης, Βέλτιστος σχεδιασμός κτηρίων από Οπλισμένο Σκυρόδεμα υπό σεισμικές δράσεις,15ο_Συνέδριο_Σκυροδέματος,Αλεξανδρούπολη,Οκτώβριος 2006

M. Papadrakakis, N.D. Lagaros, **N.P. Bakas**, D.C. Charmpis, M. Fragiadakis, Ch. Mitropoulou, Computational chalenges in optimum structural design, 7th World Congress on Computational Mechanics, Hyatt Regency Century Plaza Hotel Los Angeles, California, July 16 - 22, 2006.

M. Papadrakakis, N.D. Lagaros, M. Fragiadakis, D. Charmpis, Y. Tsompanakis, **N.P. Bakas**, Seismic design procedures in the framework of evolutionary based structural optimization, III European Conference on Computational Mechanics,ECCM-Lisbon, Portugal,5-8 June 2006

M. Papadrakakis, N. D. Lagaros, M. Fragiadakis, **N.P. Bakas**, Optimum performance based design of structures, Extreme Man-Made and Natural Hazards in Dynamics of Structures - NATO Advanced Research Workshop,NATO-ARW Croatia,May28 - June 1 2006

N.P. Bakas, Earthquake resistant optimum design of 3d reinforce concrete buildings,Greek-Serbian Joint course: Selected Topics in Modelling, Simulation & Programming,National Technical University of Athens, Athens, Greece, 31/1-10/2/2006

1.11Αναφορές

[1] Sarma, K. C., and Adeli, H. (1998). Cost Optimization of Concrete Structures. J. Struct. Engrg., ASCE, 124(5), 570-578.

[2] Ganzerli, S., Pantelides, C. P., and Reaveley, L. D. (2000). Performance-based design using structural optimization. Earthquake Engrg. Struct. Dynamics, 29(11), 1677-1690.

[3] Fragiadakis, M., Lagaros, N.D., Papadrakakis, M., (2005) Optimization of irregular RC buildings under earthquake loading, 6th European Conference on Structural Dynamics (EURODYN 2005), Paris, France, September 4-7.

[4] Chan, C.-M., Zou, X.-K. 2004 Elastic and inelastic drift performance optimization for reinforced concrete buildings under earthquake loads, Earthquake Engrg. Struct. Dynamics 33 (8), pp. 929-950.

[5] Zou, X.-K., Chan, C.-M. 2005 Optimal seismic performance-based design of reinforced concrete buildings using nonlinear pushover analysis, Engineering Structures 27 (8), 1289-1302.

[6] Bachmann, H. (2002). Seismic Conceptual Design of Buildings - Basic principles for engineers, architects, building owners, and authorities, Order Number: 804.802e, Swiss Federal Office for Water and Geology, Swiss Agency for Development and Cooperation, BWG, Biel.

[7] Bertero, R.D. (1995). Inelastic torsion for preliminary seismic design. J. Struct. Engrg., ASCE, 121(8), 1183-1189.

[8] Wong, C.M., Tso, W.K. (1995). Evaluation of seismic torsional provisions in uniform building code. J. Struct. Engrg., 121(10), 1436-1442.

[9] Duan, X.N., Chandler, A.M. (1997). An optimized procedure for seismic design of torsionally unbalanced structures. Earthquake Engrg. Struct. Dynamics, 26, 737-757.

[10] Lagaros, N.D., Papadrakakis, M., Bakas, N., Earthquake resistant optimum design of 3D reinforced concrete structures, J. Earth. Engrg., (to appear), 2006.

[11] Paulay, T., A mechanism-based design strategy for torsional seismic response of ductile buildings. European Earthquake Engineering; 2: 33–48, 1998.

[12] Paulay T. Some design principles relevant to torsional phenomena in ductile buildings. Journal of Earthquake Engineering 2001; 5:273–308.

[13] W. K. Tso; and B. Myslimaj A yield displacement distribution-based approach for strength assignment to lateral force-resisting elements having strength dependent stiffness Earthquake Engng Struct. Dyn. 2003; 32:2319–2351.

[14] Eurocode 8. (1996), "Design provisions for earthquake resistance of structures." ENV1998, CEN European Committee for standardization, Brussels.

[15] Eurocode 2. (1992). "Design of concrete structures." ENV1992, CEN European Committee for standardization, Brussels.

[16] Somerville, P, Collins, N. Ground motion time histories for the Humboldt bay bridge, Pasadena, CA, URS Corporation, 2002, www.peertestbeds.net/humboldt.htm.

[17] Papazachos, BC, Papaioannou, ChA, Theodulidis, NP. Regionalization of seismic hazard in Greece based on seismic sources, Natural Hazards 1993; 8(1), 1-18.

2 Preface

I'm grateful to my family for their moral and overall support throughout the duration of my studies and particularly during the preparation of this thesis.

I would like to thank Professor M. Papadrakakis for his willingness to consult me and select the thematic area and for his general guidance during this work.

I would also like to thank Dr. N. Lagaros for his support especially on the part of the computational algorithms and his suggestions on the theoretical sections of this work. His contribution was great and decisive.

Finally, I must give thanks to Dr. Ch. Mitropoulou for the cooperation on programming structural codes checks and Ph.D. Candidate Chrysanthi Stathi for the cooperation in the nonlinear simulations and analysis of this work.

Nikolaos P. Bakas

16/12/2011

3 Introduction

Designing earthquake resistant structures has been a subject of great concern amongst engineers and scientists, aiming ατ a structural design that would acceptably resist seismic excitation. The vertical seismic resisting elements (columns and shear walls) in particular, in connection with the plates (slabs) of a reinforced concrete building, constitute the structural system that must resist the seismic excitation. The response and the behavior of such a structural system under seismic loading

conditions depend mainly on the cross sectional size and the topological arrangement of the columns and the shear walls. A high percentage of building damages, and even collapses, has been attributed to the wrong plan arrangement of the columns and the shear walls, permitting the activation of the combined torsional-translational vibration of the structural system [1-6]. This is a common problem in most reinforced concrete buildings, due to architectural and code constraints. These types of buildings are called irregular and are faced with additional loading due to torsion.

As we will see in the following chapters, torsion creates additional forces in structural members. In order to take into consideration the effect of torsion, many researchers have proposed several design and/or evaluation criteria. Some of these are connected to the: center of stiffness, center of resistance, center of strength, BST curves, torsional ductility, etc. At the early stages of this work, we examined structures designed according to these criteria. In order to evaluate the performance of these criteria, we used structural optimization techniques to design the structures. Many studies have been performed over the past three decades devoted to the subject of structural optimization of concrete structures and most of them were devoted to cost.

The minimum design optimization of a steel structure is a good approximation of the structure minimum cost. For a concrete structure, however, the weight of the structure is not linked directly to the cost of the structure since other factors can decisively influence the final cost. Furthermore the relation between the weight of the structure and its cost varies according to the type of concrete structure: steel reinforced, fiber reinforced or pre-stressed concrete structure. An article review on the cost optimization of concrete structures [7] concluded that most of the research work published on this scientific area deal with simple structural elements, such as beams or slabs. Only few papers deal with framed structures and even fewer with realistic three-dimensional structures. Fadaee and Grierson [8] have studied the minimum cost design of 3D reinforced concrete frames, with the beams and the columns having

rectangular cross sections. Balling and Xiao [9] presented a comparative study of optimization of 3D reinforced concrete frames with rectangular columns and rectangular T- or L-shaped beams.

When dealing with reinforced concrete buildings, apart from optimizing the cost a more realistic procedure is to attempt an optimum design based on the structural performance. Duan and Chandler [10] have proposed an optimization procedure for torsionally unbalanced structures subjected to earthquake loading, considering both serviceability and ultimate limit states. Ganzerli et al. [11] have proposed a new optimization methodology for seismic design considering performance based constraints.

The objective of the present study is to propose a methodology for improving the conceptual design of 3D steel reinforced concrete structural systems, in terms of their performance, under seismic excitation according to the seismic demands of the Eurocode8 design requirements [12], in an effort to minimize the cost of the structure. The definition of the cost of a 3D concrete building is a complicated task since construction methodology, functionality, life-cycle conditions, operation, maintenance and marketability, among other factors, have to be taken into account. In this study the term 'cost optimization' refers to the material and labor cost for the construction of the building's structural elements.

During the first stages of this work, we examined the effect of torsion on the total cost and then on the life cycle cost of the structure. We performed the minimum cost optimization algorithms using a torsional criterion as an objective function. The torsional effect is activated when the mass center and the rigidity center of a structural system do not coincide. Then the system is called eccentric. When such a system is subjected to dynamic excitations, the inertia forces can be modeled as acting through the mass center and the resisting forces through the rigidity center. This couple of opposing forces creates the torsional effect to the structural system coupled with the lateral motion. Although structural systems can be designed to meet code requirements related to torsional effect, buildings with severe torsion are less likely to perform

predictably well in earthquakes. A first approach in meeting the seismic demands of the design codes is to make the structure massive and rigid in order to prevent damage at the expense of making its cost prohibitive. A cost-effective approach proposed in this study aims at improving the seismic performance of 3D reinforced concrete buildings by minimizing the eccentricity between the mass centre and the rigidity centre at each storey thus minimizing the effect of torsion on the structure.

This aim is achieved with optimization algorithms and in particular with the family of evolutionary optimization algorithms. The most well-known algorithms in this class are the genetic algorithms (GA) [13] and the Evolution Strategies (ES) [14]. Evolution-based algorithms maintain a population of potential solutions instead of a single one. These algorithms have some selection processes based on fitness of individuals and some recombination operators imitating the biological evolution in nature and combine the concept of artificial survival of the fittest with evolutionary operators in order to form a robust search mechanism of the design space. The proposed methodology has no limitations regarding the material type of the structure (whether it is steel or reinforced concrete), the size of the structure and the complexity of the architectural morphology of the structure.

Further down in this thesis, we will present a short description of the guidelines for the seismic design codes, the formulation of the optimization problem as well as an outline of the Evolution Strategies algorithm. In chapter 7 the implemented simplified and the more accurate structural design procedures as recommended by the EC8 are described. A number of test examples are presented demonstrating the potential of the proposed approach in designing realistic structures combining safety and cost efficiency.

As we mentioned above, most of the buildings exhibit some degree of asymmetry in plan due to strength, mass or stiffness. This irregularity induces an uneven distribution to these buildings of coupled lateral and torsional response which increases the vulnerability of this type of buildings to earthquakes. Several researchers studied the elastic response

of asymmetric in plan buildings and evaluated the torsional provisions in seismic codes. Only recently some studies extended the investigation to inelastic behavior but they were restricted to asymmetric single-storey systems.

As far as the elastic behavior is concerned, Hejal and Chopra [15] defined the location of center of rigidity, center of resistance, center of twist, shear center for one-storey as well as multi-storey systems. They also proved that for one-storey systems with symmetric plans all theese centers are coincident. In their investigation, it was also shown that for a special class of multy-storey buildings, with lateral stiffness matrices of all resisting elements mutually proportional, the locations of the centers of rigidity and twist were shown to be coincident, independent of the lateral forces and they are lying on a vertical line. Cheung and Tso [16] suggested a generalized center of rigidity and a generalized center of twist. Based on these definitions, the storey torsional moments are evaluated for the design of torsionally unbalanced regular multi-storey systems. In the case of the generalized center of rigidity, the torsional moment is calculated using the floor eccentricity, while for the generalized center of twist it is calculated using the storey eccentricity. Xenidis, Makarios and Athanasopoulou [18] proposed the fictitious vertical elastic axis or optimum torsion axis. Poole [20] suggested that the shear center below each floor can be taken as the center of rigidity to compute the floor eccentricity. Humar [21] interpreted the center of rigidity at each floor as the point through which the resultant lateral forces passing from that point does not inflict any rotation at the floor. Smith and Vezina [22] defined the center of rigidity, at a particular level of a multi-storey structure subjected to a particular vertical distribution of horizontal loading, as the point where the external horizontal load acting at that point does not produce any torque to the structure. Riddell and Vaquez [23] interpreted the concept of eccentricity in the dynamic sense, and concluded that the centers of rigidity exist only for a very special class of multi-storey buildings, namely buildings with proportional framing.

In the domain of inelastic seismic behavior of asymmetric in plan buildings, Llera and Chopra [24] proposed the base shear and torque surface (BST) for the building, which represents all combinations of shear and torque that when applied statically lead to the collapse of the structure. They also proposed a simplified model, which is based on a super-element per building storey capable of representing the elastic and inelastic properties of the storey. They accomplished that by matching the stiffness matrices and ultimate yield surface of the storey to that of the super-element [25]. Paulay [26] defined the center of resistance and identified the plastic mechanism developed in a three-dimensional system in order to estimate torsional effects on the seismic response of ductile building structures. They are classified as either torsionally unrestrained or torsionally restrained. Tso [28] proved that the torsional effects can be minimized by having the strength distribution such that results in the location of the center of strength and the center of rigidity on the opposite sides of the center of mass for asymmetric wall-type systems. Castillo and Restrepo [29] suggested monitoring the strength distribution of the structure elements of the system as a means of reducing or eliminating strength eccentricity. This can produce a reduction of the system rotation and allows the structure to be modeled as an equivalent single degree of freedom system.

A number of studies have been presented in the past dealing with the problem of optimum design of reinforced concrete (RC) buildings. Optimum design of reinforced concrete buildings with performance criteria is a relatively new field of recearch. In most cases the performance criteria are imposed as constraints to the objective function to be minimized which is usually the initial construction cost. Based on this approach Ganzerli et al. [11] have proposed an optimization methodology for seismic design considering performance-based constraints. Sebastian [30] presented a computational procedure which beneficially offsets the undesirable effect of limited ductility, while Zou and Chan [31] have shown that steel reinforcement, compared to concrete, appears to be the more appropriate material that can be effectively used to control interstorey drift.

A high percentage of building damages, or even collapses, has been attributed to the wrong plan arrangement of the columns and the shear walls, due to the activation of the combined torsional-translational vibration of the structural system [1,6]. For this reason a number of studies have been published in the past where the seismic response of the structure is examined under the coupling of the lateral-torsional response [32-37].

In the first stage of this work we perform structural optimization of RC building having as object function the minimum distance between the center of mass and the center of rigidity (chapter 5). In the second stage of this work (chapter 7) the optimized structures obtained through three different design approaches are assessed with respect to the minimum seismic torsional effect and their performance against three earthquake hazard levels. In the first design approach, the initial construction cost is considered as the main objective. In the second one, performance criteria are implemented, where the eccentricity of the rigidity and the strength centers with respect to the mass centre is minimized. In the third one, both cost minimization and performance criteria are applied. All three design approaches are formulated as a combined topology-sizing optimization problem. The location and the size of the columns and the shear walls of the structure, of each storey layout, constitute the design variables. Apart from the constraints imposed by the seismic and reinforced concrete structure design codes, architectural restrictions are also taken into account in all formulations of the optimization problems. The aim of the present study is to propose a methodology for improving the conceptual design of 3D reinforced concrete buildings, in terms of their performance under seismic excitation according to the seismic demands of the design codes [38]. For this reason the final designs are compared with respect to the total life cycle cost, which is the sum of the initial and the limit state cost. The limit state cost, as considered in this study, represents monetary-equivalent losses due to seismic events that are expected to occur during the design life of the structure. Additionally, fragility analysis is also performed for four limit states to assess the optimum designs obtained through the optimization procedure.

In this study a new index associated with the torsional behavior of irregular RC buildings is proposed. According to this approach, a ratio of torsion (ROT) is calculated using the shear forces that are developed in the elements of the structure. The ratio of torsion is based on the principle that the sum of the absolute values of the internal forces in the structure is always bigger than the external seismic horizontal force. This difference is pronounced with the degree of asymmetry of the structure. The precise methodology is described more extensively in chapter seven.

REFERENCES:

[1] H. Bachmann, "Seismic Conceptual Design of Buildings - Basic principles for engineers, architects, building owners, and authorities," *Order Number: 804.802e, Swiss Federal Office for Water and Geology, Swiss Agency for Development and Cooperation, Bwg, Biel.*, 2002.

[2] W. K. Tso & R. Bergmann, "Dynamic Study of an unsymmetric high rise building," *Canadian J. Civil Eng.*, vol. 3, no. 1, pp. 107–118, 1976.

[3] W. K. Tso & P. F. Ast, "Special Considerations In design of an asymmetrical shear wall building," *Canadian J. Civil Eng.*, vol. 5, no. 3, pp. 403–413, 1978.

[4] "Three-Dimensional Inelastic Response of an RC Building during the Northridge Earthquake," 2001.

[5] D. Mitchell, R. H. Devall & K. Kobayashi & R. Tinawi & W. K. Tso, "Damage to concrete structures due to the January 17, 1995, Hyogo-ken Nanbu (Kobe) earthquake," *Canadian J. Civil Eng.*, vol. 23, no. 3, pp. 757–770, 1996.

[6] R. D. Bertero, "Inelastic torsion for preliminary seismic design," *J. Struct. Engrg., Asce*, vol. 121, no. 8, pp. 1183–1189, 1995.

[7] Sarma & Adeli, "Cost optimization of concrete structures," *J. Structural Eng.*, vol. 124, no. 5, pp. 570–578, 1998.

[8] M. J. Fadaee & G. E. Donald, "Design optimization of 3D reinforced concrete structures having shear walls," *Eng. With Computers*, vol. 14, no. 2, pp. 139–145, 1998.

[9] R. J. Balling & X. Xiao, "Optimization of reinforced concrete frames," *J. Struct. Engrg., Asce*, vol. 123, no. 2, pp. 193–202, 1997.

[10] X. N. Duan & A. M. Chandler, "An optimized procedure for seismic design of torsionally unbalanced structures," *Earthquake Engrg. Struct. Dynamics*, vol. 26, no. 1, pp. 737–757, 1997.

[11] S. Ganzerli, C. P. Pantelides & L. D. Reaveley, "Performance-based design using structural optimization," *Earthquake Engrg. Struct. Dynamics*, vol. 29, no. 11, pp. 1677–1690, 2000.

[12] "Eurocode 8, Design provisions for earthquake resistance of structures, ENV1998," *Vol Cen European Committee for Standardization, Is Brussels*, 1996.

[13] J. Holland, "Adaptation in natural and artificial systems," *University of Michigan Press, Ann Arbor*, 1975.

[14] Rechenberg, "Evolution strategy: optimization of technical systems according to the principles of biological evolution," *Frommann-Holzboog, Stuttgart*, 1973.

[15] Hejal Reem & Anil K. Chopra, "Earthquake Response of Torsionally-Coupled Buildings," *Earthquake Eng. Research Center, College Engineering, University California Berkeley*.

[16] V. Cheung, W. T. & W. K. Tso, "Eccentricity in irregular multistorey buildings," *Canadian J. of Civ. Engrg*, vol. 13, no. 1, pp. 46–52.

[17] Wai K. Tso, "Static Eccentricity Concept for Torsional Moments Estimations," *J. Structural Eng.*

[18] Har. Xenidis, Trian. Makarios & As. Athanasopoulou, "The Properties of the Optimum Torsion Axis In Asymmetric Multi-storey Buildings," *Tech. Chron. Sci. J.tcg,i*, no. 2-3, 2005.

[19] T. Makarios, "Torsion Axis and Torsional Radii of Gyration in Multi-Storey Buildings," *Tech. Chron. Sci. J. Tcg,I*, no. 1, 2000.

[20] R. A. Poole, "Analysis for torsion employing provisions of NZRS 4203: 1974," *New Zealand Society for Earthquake Eng*, vol. 10, no. 4, p. 219–225, 1977.

[21] J. K. Humar, "Design for seismic torsional forces," *Canadian J. of Civ. Engrg.*, vol. 12, no. 2, pp. 150–163, 1984.

[22] Smith, B. Stafford & S. Vezina, "Evaluation of centers of resistance in multistorey building structures," *Proc. Instn. Civ. Engrs., Part 2, Institution of Civil Engineers*, vol. 79, no. 4, pp. 623–635, 1985.

[23] R. Riddel, J. Vasquez "Existence of centres of resistance and torsional uncoupling of earthquake response of buildings," *Proc. 8th World Conf. Earthquake Eng., 4*, pp. 187–194, 1984.

[24] Juan C. De La Llera & Anil K. Chopra, "A simplified model for analysis and design of asymmetric plan buildings," *Earthquake Eng. Structural Dynamics*, vol. 24, pp. 573–594, 1995.

[25] T. Paulay, "Torsional mechanisms in ductile building systems," *Earthquake Eng. Structural Dynamics 27*, pp. 1101–1121, 1998.

[26] T. Paulay, "Displacement-based design approach to earthquake induced torsion in ductile buildings," *Eng. Structures*, vol. 9, no. 9, pp. 699–707, 1997.

[27] B. Mylimaj & W. K. Tso, "A strength distribution criterion for minimizing torsional response of asymmetric wall-type systems," *Earthquake Engng Struct. Dyn.*, vol. 31, pp. 99–120, 2002.

[28] R. Castillo, A. J. Carr & J. I. Restrepo, "The rotation of asymmetric plan structures," *Nzsee 2001 Conf.*, 2001.

[29] W. M. Sebastian, "Optimisation of flexural stiffness profiles to compensate for reduced ductility in hyperstatic reinforced concrete structures," *Eng. Struct.* , vol. 28, no. 6, pp. 893–902, 2006.

[30] X. K. Zou & C. M. Chan, "Optimal seismic performance-based design of reinforced concrete buildings using nonlinear pushover analysis," *Eng. Struct*, vol. 27, no. 8, pp. 1289–1302, 2005.

[31] P. Fajfar, D. M. Marušić & I. Peruš, "Torsional effects in the pushover-based seismic analysis of buildings," *J. Earthquake Eng.*, vol. 9, no. 6, pp. 831–854, 2005.

[32] J. D. Pettinga, M. J. N. Priestley & S. Pampanin & C. Christopoulos, "The role of inelastic torsion in the determination of residual deformations," *J. Earthquake Eng.*, vol. 11, no. 1, pp. 133–157, 2007.

[33] C. L. Kan, A. K. Chopra "Effect of torsional coupling on earthquake forces in buildings," *J. Struct. Division Asce*, vol. 103, no. 4, pp. 805–819, 1977.

[34] S. H. Jeong & A. S. Elnashai, "New three-dimensional damage index for RC buildings with planar irregularities," *J. Structural Eng.*, vol. 132, no. 9, pp. 1482–1490, 2006.

[35] W. K. Tso "Static eccentricity concept for torsional moment estimations," *J. Struct. Engrg.* , vol. 116, no. 5, pp. 1199–1212, 1990.

[36] S. H. Jeong & A. S. Elnashai, "Analytical assessment of an irregular RC frame for full-scale 3D pseudo-dynamic testing part I: Analytical model verification," *J. Earthquake Eng.*, vol. 9, no. 1, pp. 95–128, 2005.

[37] "Eurocode 8. Design provisions for earthquake resistance of structures. ENV1998," *Cen European Committee for Standardization, Brussels*, 1996.

4 Torsionally unbalanced elastic buildings – An overview

4.1 One-storey Buildings

4.1.1 Basic Concepts

The lateral-torsional coupling has great impact on the dynamic response of buildings. Coupled lateral-torsional motions occur in buildings subjected to ground shaking if their structural plan do not have two axes of mass and stiffness symmetry or ground shaking includes a torsional component. They can also appear due to unbalanced load distributions in the floor-plan or differences between actual and assumed mass and stiffness distributions. A special class of multi-storey buildings has been considered to consist of resisting elements idealized as shear beams, whose acceptance may be inappropriate. This makes it necessary to analyze the relation between those multi-storey buildings and the associated one-storey systems. Subsequently the analysis of one-storey systems is presented.

The systems considered are single-storey buildings consisting of a rigid diaphragm, where the mass of the structure is lumped, supported by massless, axially inextensible resisting elements (i.e. portal frames, shear walls, columns or shear-wall cores), which are symmetrically arranged about the X-axis (axis of symmetry for the building plan) (Figure 3.1). The dynamic response of such systems to the horizontal component of ground motion along the Y-axis is investigated. As long as the building is not symmetric about the Y-axis, it will be subjected to coupled lateral-torsional motions. For thesimulation of the earthquake ground motion two idealized design spectra are included: (i) a flat or period independent pseudo-acceleration spectrum, and (ii) a hyperbolic pseudo-acceleration spectrum (Figure 3.2).

In order to derive the equations of motion for this system, the building stiffness matrix should be formed. Because of the rigidity of the diaphragm and the symmetry about the X-axis, this single-storey system has two dynamic degrees of freedom: (i) the translational displacement uy of the center of mass (CM) of the diaphragm along the Y-axis and (ii) the rotation uθ of the diaphragm about a vertical axis. The degrees of freedom for each vertical structural resisting element (Figure 3.1b) are defined below:

Shear wall: one translational degree of freedom at the floor level, along the plane of the shear wall and a rotational degree of freedom about the horizontal axis perpendicular to its plane.

Frame: one translational degree of freedom at the floor level, along the plane of the frame and a rotational degree of freedom per joint about the horizontal axis perpendicular to the plane of the frame.

Column: two translational degrees of freedom at the floor level along the X- and Y- axes and two rotational degrees of freedom about the X- and Y-axes.

Shear Wall Core: two translational degrees of freedom along the principal axes of the core, two rotations about these axes, and one torsional rotation about a vertical axis passing through the shear center of the core.

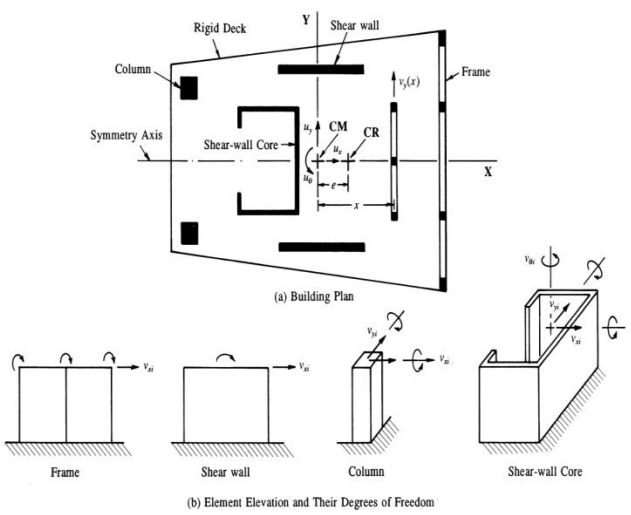

Figure 3.1 *Single-storey / General plan of a building [1]*

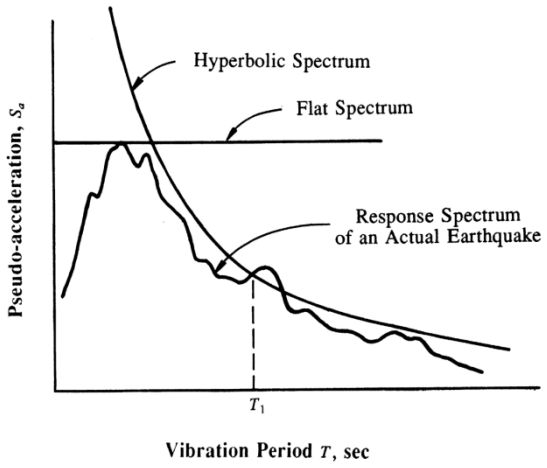

Figure 3.2 *Flat and hyperbolic response spectra [1]*

4.1.2 Equations of Motion

As far as one-storey systems are concerned, it has been proven [1] that the center of rigidity, the center of twist, the shear center and the center of stiffness coincide. It has also been shown that their location does not depend on the applied load but on the stiffnesses and the locations of their vertical structural elements. The definitions of these centers are given below [1].

The **centre of rigidity** is the point on the diaphragm through which the application of a static horizontal force causes no rotation of the deck, regardless the direction of the applied force. [1]

The **principal axes**, **I** and **II**, of the system are two orthogonal axes passing through the center of rigidity, such that if a static horizontal force is applied along one of the principal axes of the system, the diaphragm translates only in the direction of the force without any twist.

The **center of twist** is the point on the diaphragm which remains stationary when the diaphragm is subjected to a statically applied torsional moment, i.e. the diaphragm undergoes pure twist about this point.

The **shear center** is the point on the diaphragm through which the resultant of the shear forces of all resisting vertical structural elements passes when the diaphragm is subjected to a system of lateral static loads whose resultant passes through the center of rigidity of the building, thus causing no rotation or twist of the diaphragm.

The **center of mass** of the system is the point on the diaphragm through which the resultant of the inertia forces of the diaphragm is applied. If the masses of individual resisting elements are negligible, the center of mass of the diaphragm with uniform mass distribution coincides with its geometric center. [1]

Subsequently, the linear equations of motion for the one-storey system, under consideration, subjected to earthquake ground motion written with respect to the reference point O, at the center of mass and the center of rigidity, as follows:

Reference point O

$$\begin{bmatrix} m & 0 & -my_M \\ 0 & m & mx_M \\ -my_M & mx_M & J_0 \end{bmatrix} \begin{Bmatrix} \ddot{u} \\ \ddot{u} \\ \ddot{u} \end{Bmatrix} + \begin{bmatrix} K_x & K_{xy} & K_{x\theta} \\ K_{yx} & K_y & K_{y\theta} \\ K_{\theta x} & K_{\theta y} & K_\theta \end{bmatrix} \begin{Bmatrix} u_x \\ u_y \\ u_\theta \end{Bmatrix} = -m \begin{Bmatrix} a_{gx}(t) \\ a_{gy}(t) \\ -y_M a_{gx}(t) + x_M a_{gy}(t) \end{Bmatrix} \quad (3.1)$$

Center of Mass

$$\begin{bmatrix} m & 0 & 0 \\ 0 & m & 0 \\ 0 & 0 & mr^2 \end{bmatrix} \begin{Bmatrix} \ddot{u} \\ \ddot{u} \\ \ddot{u} \end{Bmatrix} + \begin{bmatrix} K_x & K_{xy} & K_{x\theta} \\ K_{yx} & K_y & K_{y\theta} \\ K_{\theta x} & K_{\theta y} & K_\theta \end{bmatrix} \begin{Bmatrix} u_x \\ u_y \\ u_\theta \end{Bmatrix} = -m \begin{Bmatrix} a_{gx}(t) \\ a_{gy}(t) \\ 0 \end{Bmatrix} \quad (3.2)$$

Center of Rigidity

$$\begin{bmatrix} m & 0 & -me_y \\ 0 & m & me_x \\ -me_y & me_x & J_R \end{bmatrix} \begin{Bmatrix} \ddot{u} \\ \ddot{u} \\ \ddot{u} \end{Bmatrix} + \begin{bmatrix} \widetilde{K_x} & \widetilde{K_{xy}} & 0 \\ \widetilde{K_{yx}} & \widetilde{K_y} & 0 \\ 0 & 0 & \widetilde{K_\theta} \end{bmatrix} \begin{Bmatrix} \tilde{u} \\ \tilde{u} \\ \tilde{u} \end{Bmatrix} = -m \begin{Bmatrix} a_{gx}(t) \\ a_{gy}(t) \\ -e_y a_{gx}(t) + e_x a_{gy}(t) \end{Bmatrix} \quad (3.3)$$

where J_0 is the polar moment of inertia of the diaphragm with respect to point O accelerations $a_{gx}(t)$ and $a_{gy}(t)$ along the X- and Y- axes are given given by

$$J_o = m(r^2 + x_M^2 + y_M^2) \quad (3.4)$$

r is the radius of gyration; x_M, y_M are the x and y coordinates of the center of mass J_R is the polar moment of inertia about a vertical axis passing through the center of rigidity

$$J_R = m(e^2 + r^2) \quad (3.5)$$

x_R, y_R are the x and y coordinates of the center of rigidity.

The **static eccentricity e** of the single-storey building is defined as the distance between the CR and the CM of the floor.

$$e=\frac{K_{y\theta}}{K_y}=\frac{\sum_i x_i K_{yi}}{\sum_i K_{yi}} \quad (3.6)$$

Other scientists define the static eccentricity as the distance between the center of mass and shear center of the building. For one-storey systems this definition is meaningless, since the center of rigidity and the shear center of the system coincide, contrary to multi-storey buildings.

The **dynamic eccentricity e_d** is defined as the distance from the CR of the system where the uncoupled base shear should be applied statically to cause a base torque equal to T_R (base torque of coupled system at its CR) at the CR of the system. [3,7]

Specifically the undamped equations of motion for the single-storey system described above, assuming linear behavior, subjected to earthquake ground motion acceleration $a_{gy}(t)$ along the Y- axes are written as follows:

With respect to the CM:

$$\begin{bmatrix} m & 0 \\ 0 & m \end{bmatrix} \begin{Bmatrix} \ddot{u}_y(t) \\ r\ddot{u}_\theta(t) \end{Bmatrix} + \begin{bmatrix} K_y & \frac{e}{r}K_y \\ \frac{e}{r}K_y & K_\theta \end{bmatrix} \begin{Bmatrix} u_y(t) \\ ru_\theta(t) \end{Bmatrix} = -m \begin{Bmatrix} 1 \\ 0 \end{Bmatrix} a_{gy}(t) \quad (3.7)$$

With Respect to the CR:

$$\begin{bmatrix} m & -m\frac{e}{r} \\ -m\frac{e}{r} & m[1+(e/r)^2] \end{bmatrix} \begin{Bmatrix} \ddot{v}_y(t) \\ r\ddot{u}_\theta(t) \end{Bmatrix} + \begin{bmatrix} K_y & 0 \\ 0 & \frac{1}{r^2}K_{\theta R} \end{bmatrix} \begin{Bmatrix} v_y(t) \\ ru_\theta(t) \end{Bmatrix} = -m \begin{Bmatrix} 1 \\ -\frac{e}{r} \end{Bmatrix} a_{gy}(t) \quad (3.8)$$

It is obvious from the above equations that the translational ground motion along the Y- axis causes lateral displacement of the CM as well as torsional rotation of the floor about a vertical axis.

4.1.3 Coupled Equations

As it is previously mentioned coupled lateral-torsional motion occurs in buildings subjected to ground shaking if the CM CR does not coincide. Coupled motion can also appear due to unbalanced load distributions or differences between the actual and assumed mass and stiffness distributions.

It is also apparent that if the static eccentricity, e, is zero, then equations (3.7) and (3.8) are transformed in two identical uncoupled equations.

On this occasion the earthquake ground motion only causes lateral displacement governed by the first uncoupled equation, where the lateral vibration frequency of the corresponding uncoupled system is:

$$\omega_y = \sqrt{\frac{K_y}{m}} \tag{3.9}$$

While the second uncoupled equation leads to the torsional vibrational frequency of the corresponding torsionally-uncoupled system:

$$\omega_\theta = \sqrt{\frac{K_{\theta R}}{mr^2}} = \sqrt{\frac{K_\theta}{mr^2} - \left(\frac{e}{r}\right)\omega_y^2} \tag{3.10}$$

The uncoupled system is derived from the actual by modifying the configuration of resisting elements or the mass properties, so that the center of mass (CM) and the center of rigidity (CR) coincide.

The undamped equations of motion are further simplified to:

$$\begin{Bmatrix} \ddot{u}(t) \\ r\ddot{u}(t) \end{Bmatrix} + \omega_y^2 \begin{bmatrix} 1 & \frac{e}{r} \\ \frac{e}{r} & \Omega^2 + (e/r) \end{bmatrix} \begin{Bmatrix} u_y(t) \\ r u_\theta(t) \end{Bmatrix} = -\begin{Bmatrix} 1 \\ 0 \end{Bmatrix} a_{gy}(t) \tag{3.11}$$

in which $\Omega = \frac{\omega_\theta}{\omega_y}$ (3.12)

the uncoupled torsional to lateral frequency ratio. The coupled and the uncoupled frequencies are close for systems with smallest ratio e/r.

Actually, the coupled lateral-torsional response of the system to ground motion $a_{gy}(t)$, depends on these four parameters: e/r, Ω,ω_y (in case of

arbitrary shaped spectra) and ξ, the damping ratio which is considered to be the same in each mode of vibration.

4.1.4 Lateral-Torsional Coupling characteristics

Some very important findings are presented by Hejal and Chopra [1], using the response spectrum analysis (RSA) method. For torsionally-stiff (Ω>1) systems, the fundamental mode is predominantly lateral and the second mode is the torsional. Unlike torsionally-stiff systems, for torsionally-flexible (Ω<1) systems the modes are not predominantly lateral or torsional, unless e/r is very small. Finally for systems with closely spaced uncoupled frequencies (Ω=1) the lateral and torsional motions are similar. These systems with small e/r ratios have a significant cross-correlation term. Systems with Ω equal to zero are unstable as long as the fundamental frequency ω_1 is zero.

As mentioned above, the response of the system is also dependent on the shape of the spectra (or T_y or ω_y) when the arbitrary shape of the system is arbitrary. For instance, the normalized base shear $\bar{v}$ for systems with small e/r ratio is insensitive to the shape of the spectrum. But as the e/r ratio increases, the acceleration-controlled region $\bar{v}$ remains the same for a flat spectrum, while the velocity-controlled region $\bar{v}$ remaining the same for both the arbitrary and hyperbolic spectra. The divergence of the idealized response spectrum shapes increases as e/r increases and is larger for torsionally-flexible systems.

The lateral-torsional coupling tends to decrease the base shear, the base overturning moment and the lateral displacement at the center of rigidity, but increases the torque and ratio e_d/r. These effects are not so pronounced for torsionally-stiff systems, since the reduction in the base shear is negligible and there is no dynamic amplification of static eccentricity. Contrary to torsionally-stiff systems, theese with closely spaced uncoupled frequencies present maximum dynamic amplification of static eccentricity, especially for smaller e/r ratios.

Although the overall earthquake response of the system depends on the parameters, e/r, Ω, Ty, ξ, the local response of the system depends on

the degree of frame action, except for the parameters above. The degree of frame action determines the in-plane stiffness of the diaphragm. The degree of frame action is defined through parameter ρ.

The joint rotation index ρ [2], of a frame, is defined as the ratio of the sum of the stiffnesses of all beams at the mid-height storey of the frame to the summation of the stiffnesses of all the columns at the same storey.

$$\rho=\frac{\sum_{beams} EI_b/L_b}{\sum_{columns} EI_b/L_b} \tag{3.13}$$

where various values of ρ represent different functions of the frame:

(i) ρ=0 represents a flexural column with beams imposing no constraint to joint rotations.

(ii) ρ=∞ represents a shear frame in which joint rotations are completely restrained and the deformations occur only through double curvature bending of the columns.

Intermediate values of ρ represent frames with both beams and columns undergoing bending deformations with joint rotations. [1]

The joint rotation index, ρ, does not affect the maximum lateral displacement of the frame $v_y(x)$ but influences the member forces (the frame base shear, the column base moment, the beam moment, the column axial force), whose equations are given below:

$$V(x)=\frac{EI}{h^3}\frac{6(1+12\rho)}{1+3\rho}v_y(x) \tag{3.14}$$

$$M_c(x)=\frac{EI}{h^2}\frac{3(1+6\rho)}{1+3\rho}v_y(x) \tag{3.15}$$

$$M_b(x)=P_c(x)\frac{L}{2}=\frac{EI}{h^2}\frac{18\rho}{1+3\rho}v_y(x) \tag{3.16}$$

In accordance with Figure 3.5 member forces increase with an increase in ρ, on a condition that the other parameters are kept constant.

All member forces are proportional to lateral floor displacements. Consequently maximum member forces of the coupled system may increase or decrease due to the lateral-torsional coupling. They are

influenced by the location of the element and the other parameters of the system. Therefore, regardless of the element's location, whether it's on the flexible or the stiff side of the building, its member forces are larger than the corresponding uncoupled ones.

4.1.5 Center of Rigidity, Center of Twist and Shear Center

The coordinates of the center of rigidity are defined through the following procedure:

$$\widetilde{K} = \begin{bmatrix} K_x & K_{xy} & 0 \\ K_{yx} & K_y & 0 \\ 0 & 0 & \widetilde{K_\theta} \end{bmatrix} \tag{3.17}$$

$$\widetilde{K}=\tilde{a}^{T}K\tilde{a} \tag{3.18}$$

$$u=\begin{Bmatrix} u_x \\ u_y \\ u_\theta \end{Bmatrix} = \begin{bmatrix} 1 & 0 & y_R \\ 0 & 1 & -x_R \\ 0 & 0 & 1 \end{bmatrix} \begin{Bmatrix} \tilde{u} \\ \tilde{u} \\ u_\theta \end{Bmatrix} = \tilde{a}\tilde{u} \tag{3.19}$$

in which:

K: the building stiffness matrix with respect to the degrees of freedom u at reference point O

$\widetilde{K}$: the building stiffness matrix with respect to the degrees of freedom u at the center of rigidity of the system

a: the transformation matrix relating u to $\tilde{u}$

Utilizing the equations above, results in:

$$\widetilde{K} = \begin{bmatrix} K_x & K_{xy} & K_x y_R - K_{xy} y_R + K_{x\theta} \\ K_{yx} & K_y & K_{yx} y_R - K_y x_R + K_{y\theta} \\ K_{\theta x} + y_R K_x - x_R K_{yx} & K_{\theta y} + y_R K_{xy} - x_R K_y & \widetilde{K_\theta} \end{bmatrix} \tag{3.20}$$

Both matrices (3.18) and (3.20) should be identical leading to the conditions:

$$K_x y_R - K_{xy} x_R + K_{x\theta} = 0 \tag{3.21a}$$

$$K_{yx} y_R - K_y x_R + K_{y\theta} = 0 \tag{3.21b}$$

According to conditions (3.19) the coordinates of the center of rigidity:

$$x_R = \frac{K_x K_{y\theta} - K_{xy} K_{x\theta}}{K_x K_y - K_{xy}^2} \quad (3.22a)$$

$$y_R = -\frac{K_y K_{x\theta} - K_{xy} K_{y\theta}}{K_x K_y - K_{xy}^2} \quad (3.22b)$$

The equations above are further simplified on two special occasions:

The building has one axis of symmetry, which coincides with one of the principal axes of the system and the other is perpendicular to it. In this case, the X-axis is assumed as the symmetry axis, the terms K_{xyi} and $K_{x\theta i}$ are of the same value but of opposite algebraic signs. As a result $K_{xy}=K_{yx}=0$ and $K_{x\theta=}K_{\theta x}=0$, which leads to the equations:

$$x_R = \frac{K_{y\theta}}{K_y} \quad (3.23a)$$

$$y_R = -\frac{K_{x\theta}}{K_x} = 0 \quad (3.23b)$$

for the coordinates of the center of rigidity.

The resisting elements of the building are arranged such that their principal axes form an orthogonal grid in plan (e.g. Figure 3b). The principal axes of the system are also in the directions of the elemental principal axes. The coordinates of the center of rigidity are simplified to:

$$x_R = \frac{K_{y\theta}}{K_y} = \frac{\sum_i k_{yi} x_i}{\sum_i k_{yi}} \quad (3.24a)$$

$$y_R = -\frac{K_{x\theta}}{K_x} = \frac{\sum_i k_{xi} y_i}{\sum_i k_{xi}} \quad (3.24b)$$

As mentioned above, the center of twist, the shear center and the center of rigidity of the one-storey system are coincident. This derives from:

Center of twist

Since the center of twist is the point in the plane of diaphragm that does not undergo any translational displacement when the diaphragm is subjected to a static horizontal torsional moment (definitions [1]), the

building stiffness matrix is identical to (3.17) (if degrees of freedom of the diaphragm are defined at its center of twist). The same procedure as the one followed for the center of rigidity leads to the same expressions for the coordinates of the center of twist. Utilizing energy principles results to the same conclusions.

Shear center

The shear center is the point in the plane of the diaphragm through which the resultant of the shear forces of the resisting elements passes when the diaphragm is subjected to a system of horizontal lateral forces causing no twist (u_θ=0) of the diaphragm (definitions [1]). Substituting u_θ=0 and utilizing the equilibrium of moments of all shearing forces acting in the plane of the diaphragm about a vertical axis passing through O, gives an equation which leads to the same expressions as the center of rigidity.

To sum up the center of rigidity, the center of twist and the shear center for one-storey systems are coincident and do not depend on the applied load.

4.2 Multi-Storey Buildings

4.2.1 Equations of Motion

Contrary to one-storey systems, the defined centers for multi-storey buildings are not coincident. Apart from the stiffness properties, their locations depend on the applied lateral or torsional loadings. But there is still a special class of multi-storey buildings, for which the centers for each floor coincide, that is the centers of all floors lie on a vertical line and are load-independent. Definitions about the various centers follow next.

The **center of rigidity** of the building's floors are points on the floor diaphragms through which any set of static horizontal forces of arbitrary magnitude and direction causes no rotation or twisting of any of the floors.[1]

Another definition for the center of rigidity of a floor is given in [3], as the point of the floor through which a static horizontal force where applied

produce pure translation without rotation or twist; other floors, however, may twist or rotate.

The principal axes of a floor are two orthogonal axes passing through its center of rigidity, such that any set of static horizontal forces applied simultaneously along one of the principal axes of each floor, causes each floor to displace literally in the direction of its applied force without any twist.

The centers of twist of the building's floors are points on the floor diaphragms which remain stationary when the building is subjected to any set of static horizontal torsional moments, applied at the floor levels, i.e. the floor diaphragms undergo pure twist about these points.

The shear center of a buiding's floor is the point on the floor through which the resultant of the interstorey shear forces of all resisting elements at that level passes (due to static forces applied at the floors above including the floor under consideration) when the building's floors are subjected to static horizontal forces passing through the centers of rigidity of the floors, thus causing no twist in any of the floors.

The center of mass of a building's floor is the point on the floor through which the resultant of the floor's inertia forces passes. If the masses of individual resisting elements are negligible compared to that of the floors' masses, then the building's center of mass with floors of uniform mass distribution coincide with the geometric centers of the floors.

The static eccentricity ej of the jth floor is defined as the distance between its center of mass and its center of rigidity.

According to some building codes [4] the static eccentricity is defined as the distance between the center of mass and the shear center. The centers of rigidity of multi-storey buildings do not coincide with the shear centers. Consequently, there is more than one definition for static eccentricity.

The undamped equations of motion for the multi-storey building, assuming linear behavior, subjected to earthquake ground motion accelerations

agx(t) and agy(t) along the X- and Y- axes are given, written with respect to the degrees of freedom defined at the reference point O, at the center of mass and at the center of rigidity, respectively:

Reference Point O

$$\begin{bmatrix} m & 0 & -my_M \\ 0 & m & mx_M \\ -my_M & mx_M & J_0 \end{bmatrix} \begin{Bmatrix} \ddot{u}_x \\ \ddot{u}_y \\ \ddot{u}_\theta \end{Bmatrix} + \begin{bmatrix} K_x & K_{xy} & K_{x\theta} \\ K_{yx} & K_y & K_{y\theta} \\ K_{\theta x} & K_{\theta y} & K_\theta \end{bmatrix} \begin{Bmatrix} u_x \\ u_y \\ u_\theta \end{Bmatrix} = - \begin{Bmatrix} m1a_{gx}(t) \\ m1a_{gy}(t) \\ -y_M m1a_{gx}(t) + x_M m1a_{gy}(t) \end{Bmatrix} \quad (3.25)$$

Reference Point CM

$$\begin{bmatrix} m & 0 & 0 \\ 0 & m & 0 \\ 0 & 0 & J_M \end{bmatrix} \begin{Bmatrix} \ddot{u}_x \\ \ddot{u}_y \\ \ddot{u}_\theta \end{Bmatrix} + \begin{bmatrix} K_x & K_{xy} & K_{x\theta} \\ K_{yx} & K_y & K_{y\theta} \\ K_{\theta x} & K_{\theta y} & K_\theta \end{bmatrix} \begin{Bmatrix} u_x \\ u_y \\ u_\theta \end{Bmatrix} = - \begin{Bmatrix} m1a_{gx}(t) \\ m1a_{gy}(t) \\ 0 \end{Bmatrix} \quad (3.26)$$

Reference Point CR

$$\begin{bmatrix} m & 0 & -me_y \\ 0 & m & me_x \\ -me_y & me_x & J_R \end{bmatrix} \begin{Bmatrix} \ddot{\tilde{u}}_x \\ \ddot{\tilde{u}}_y \\ \ddot{u}_\theta \end{Bmatrix} + \begin{bmatrix} \tilde{K}_x & \tilde{K}_{xy} & 0 \\ \tilde{K}_{yx} & \tilde{K}_y & 0 \\ 0 & 0 & \tilde{K}_\theta \end{bmatrix} \begin{Bmatrix} \tilde{u}_x \\ \tilde{u}_y \\ u_\theta \end{Bmatrix} = - \begin{Bmatrix} m1a_{gx}(t) \\ m1a_{gy}(t) \\ -e_y m1a_{gx}(t) + e_x m1a_{gy}(t) \end{Bmatrix} \quad (3.27)$$

where J0 : diagonal matrix of dimension N with diagonal entries J0i, the polar moment of inertia of the jth floor diaphragm about Z, the reference vertical axis passing through reference point Oj given by

$$J_{oj}=m_j(r_j^2 + x_{Mj}^2 + y_{Mj}^2) \quad (3.28)$$

r is the radius of gyration; x_M, y_M are the diagonal matrices of dimension N with diagonal entries equal to x_{Mj} and y_{Mj}, the coordinates of the center of mass of the jth floor relative to reference axes X_j and Y_j, J_M is a diagonal matrix of dimension N with diagonal entries $J_{Mj} = m_j r_j^2$, the polar mass moment of inertia of the jth floor about a vertical axis passing through its center of mass, J_R is diagonal matrix of dimension N with diagonal entries J_{Rj} equal the polar moment of inertia of the jth deck about a vertical axis passing through the center of rigidity given by

$$J_{Rj} = m_j\left(e_j^2 + r_j^2\right) \quad (3.29)$$

e_x, e_y : diagonal matrices of dimension N with diagonal entries e_{xj} and e_{yj}, the x and y components of the static eccentricity of the jth floor given by:

$$e_{xj} = x_{Mj} - x_{Rj} \tag{3.30a}$$

$$e_{yj} = y_{Mj} - y_{Rj} \tag{3.30b}$$

x_{Mj}, y_{Mj} are the x and y coordinates of the center of rigidity of the j^{th} floor relative to its reference axes X_j and Y_j

The centers of rigidity and the centers of twist should be uniquely defined in order to determine a building stiffness matrix in the form of k given in equation (3.27).

4.2.2 Center of Rigidity, Center of Twist and Shear Center

4.2.2.1 Center of rigidity

The coordinates of the center of rigidity are defined through the following procedure:

$$\widetilde{K} = \begin{bmatrix} K_x & K_{xy} & 0 \\ K_{yx} & K_y & 0 \\ 0 & 0 & \widetilde{K_\theta} \end{bmatrix} \tag{3.31}$$

$$\widetilde{K} = \tilde{a}^T K \tilde{a} \tag{3.32}$$

$$u = \begin{Bmatrix} u_x \\ u_y \\ u_\theta \end{Bmatrix} = \begin{bmatrix} 1 & 0 & y_R \\ 0 & 1 & -x_R \\ 0 & 0 & 1 \end{bmatrix} \begin{Bmatrix} \tilde{u} \\ \tilde{u} \\ u_\theta \end{Bmatrix} = \tilde{a}\tilde{u} \tag{3.33}$$

$$\widetilde{K} = \begin{bmatrix} K_x & K_{xy} & K_x y_R - K_{xy} x_R + K_{x\theta} \\ K_{yx} & K_y & K_{yx} y_R - K_y x_R + K_{y\theta} \\ K_{\theta x} + y_R K_x - x_R K_{yx} & K_{\theta y} + y_R K_{xy} - x_R K_y & \widetilde{K_\theta} \end{bmatrix} \tag{3.34}$$

in which:

K: the building stiffness matrix with respect to the degrees of freedom u at reference point O

$\widetilde{K}$: the building stiffness matrix with respect to the degrees of freedom u at the center of rigidity of the system

$\tilde{a}$: the transformation matrix relating u to $\tilde{u}$

Comparing (3.31) and (3.34):

$$x_R = \frac{K_{y\theta} - K_{yx}K_x^{-1}K_{x\theta}}{K_y - K_{yx}K_x^{-1}K_{xy}} \quad (3.35a)$$

$$y_R = -\frac{K_{x\theta} - K_{xy}K_y^{-1}K_{y\theta}}{K_x - K_{xy}K_y^{-1}K_{yx}} \quad (3.35b)$$

The matrices x_R and y_R should be diagonal matrices in order to specify unique centers of rigidity. Otherwise, unique centers of rigidity do not always exist and are load-dependent, where different load distributions lead to different locations of the center of rigidity.

If the equations (3.35) do not lead to diagonal matrices, the locations of the center of rigidity depend on the applied set of static lateral forces. The coordinates of the center of rigidity, x_R and y_R, can be determined through the procedure below:

$\tilde{P}$=$\tilde{K}\tilde{u}$

$$\begin{Bmatrix} \widetilde{P_x} \\ \widetilde{P_y} \\ \widetilde{T_\theta} \end{Bmatrix} = \begin{bmatrix} K_x & K_{xy} & K_x y_R - K_{xy}x_R + K_{x\theta} \\ K_{yx} & K_y & K_{yx}y_R - K_y x_R + K_{y\theta} \\ K_{\theta x} + y_R K_x - x_R K_{yx} & K_{\theta y} + y_R K_{xy} - x_R K_y & \widetilde{K_\theta} \end{bmatrix} \begin{Bmatrix} \tilde{u} \\ \tilde{u} \\ u_\theta \end{Bmatrix} \quad (3.36)$$

For the set of forces P, with $P_x \neq 0$ and $P_y \neq 0$ but $T_\theta = 0$, according to definitions $u_x \neq 0$

and $u_y \neq 0$ but $u_\theta = 0$:

$$\{x_R\} = \left[\widetilde{P_y}\right]\text{^}(-1)\frac{K_{\theta y} - K_{\theta x}K_x^{-1}K_{xy}}{K_y - K_{yx}K_x^{-1}K_{xy}}\widetilde{P_y} \quad (3.37a)$$

$$\{y_R\} = -\left[\widetilde{P_x}\right]\text{^}(-1)\frac{K_{\theta x} - K_{\theta y}K_y^{-1}K_{yx}}{K_x - K_{xy}K_y^{-1}K_{yx}}\widetilde{P_x} \quad (3.37b)$$

Since $[P_y]$ and $[P_x]$ are diagonal matrices, the equations (3.37) are simplified to equations (3.35). Consequently, the locations of the centers of rigidity are unique and independent of the applied loading.

The centers of rigidity can also be identified as **load centers**, as long as the x- and y- coordinates of the center of rigidity of a floor can be determined by finding the location of the resultant elemental loads at that level [8], as it is proved from the expressions below:

$$x_R = \frac{\sum_i [\pm d_{ai}Q_{aij} + (\pm)d_{bi}Q_{bij}]}{\widetilde{P_{yJ}}} \quad (3.38a)$$

$$y_R = \frac{\sum_i [\pm d_{ai} Q_{aij} + (\pm) d_{bi} Q_{bij}]}{\widetilde{P_{xj}}} \quad (3.38b)$$

The terms Q_{aij} and Q_{bij} are different in equations (3.38a) and (3.38b). Those involved in equation (3.38a) are computed for the applied forces P_x and those in (3.38b) for P_y.

4.2.2.2 Centers of twist

According to the definition, the building stiffness matrix written with respect to degrees of freedom defined at the center of twist would be of the form of equation (3.31). Following the same procedure as that of the center of rigidity leads to the same expressions for the coordinates of the center of twist as the center of rigidity (3.5). If these expressions yield diagonal matrices, then centers of twist and centers of rigidity are coincident.

If the equations (3.37) do not lead to diagonal matrices, then the locations of the center of twist depend on the applied set of static torsional moments. The coordinates of the center of twist, x_T and y_T, can be determined through the procedure below:

$\tilde{P}=\widetilde{K}\tilde{u}$

$$\begin{Bmatrix} \widetilde{P_x} \\ \widetilde{P_y} \\ \widetilde{T_\theta} \end{Bmatrix} = \begin{bmatrix} K_x & K_{xy} & K_x y_T - K_{xy} x_T + K_{x\theta} \\ K_{yx} & K_y & K_{yx} y_T - K_y x_T + K_{y\theta} \\ K_{\theta x} + y_T K_x - x_T K_{yx} & K_{\theta y} + y_T K_{xy} - x_T K_y & \widetilde{K_\theta} \end{bmatrix} \begin{Bmatrix} \tilde{u} \\ \tilde{u} \\ u_\theta \end{Bmatrix} \quad (3.39)$$

For the set of forces P with $P_x = P_y = 0$ and $T_\theta \neq 0$, according to definitions $u_x = u_y = 0$ but $u_\theta \neq 0$:

$$\{x_T\} = [u_\theta]\text{^}(-1) \frac{K_{y\theta} - K_{yx} K_x^{-1} K_{x\theta}}{K_y - K_{yx} K_x^{-1} K_{xy}} u_\theta \quad (3.40a)$$

$$\{y_T\} = [u_\theta]\text{^}(-1) \frac{K_{x\theta} - K_{xy} K_y^{-1} K_{y\theta}}{K_x - K_{xy} K_y^{-1} K_{yx}} u_\theta \quad (3.40b)$$

The equations above are further simplified on two special occasions:

The building has a vertical plane of stiffness symmetry. In this case, the terms K_{xyi} and $K_{x\theta i}$ are of the same value but of opposite algebraic signs. As a result $K_{xy}=K_{yx}=0$ and $K_{x\theta=}K_{\theta x}=0$, which leads to the equations:

X_j direction in the direction of the symmetry plane:

$$\{x_T\} = [u_\theta]\text{^}(-1)K_y^{-1}K_{y\theta}u_\theta \text{ and } \{y_T\} = -[u_\theta]\text{^}(-1)K_x^{-1}K_{x\theta}u_\theta=0 \qquad (3.41)$$

Y_j direction along the symmetry plane:

$$\{x_T\} = [u_\theta]\text{^}(-1)K_y^{-1}K_{y\theta}u_\theta = 0 \text{ and } \{y_T\} = -[u_\theta]\text{^}(-1)K_x^{-1}K_{x\theta}u_\theta \qquad (3.42)$$

The resisting elements of the building are arranged such that their principal planes are parallel or orthogonal, or for buildings consisting of frames they are arranged in an orthogonal grid in plan [14]:

$$\{x_T\} = [u_\theta]\text{^}(-1)K_y^{-1}K_{y\theta}u_\theta \text{ and } \{y_T\} = -[u_\theta]\text{^}(-1)K_x^{-1}K_{x\theta}u_\theta \qquad (3.43)$$

4.2.2.3 Shear centers

The location of the shear center of a floor is determined by finding the centroid of the interstorey shear forces experienced by individual resisting elements due to a static loading that causes no twist ($u_\theta=0$) of any of the storeys. [1]

Substituting the equations of vectors of lateral displacements of the ith resisting element along its principal planes, v_{ai} and v_{bi}, into the equations of vectors of applied lateral loads on the ith resisting element along its principal axes, V_{ai} and V_{bi} are given by:

$V_{ai}=SQ_{ai}=Sk_{ai}(\cos\beta_i\, u_x + \sin\beta_i\, u_y)$ (3.44a)

$V_{bi}=SQ_{bi}=Sk_{bi}(-\sin\beta_i\, u_x + \cos\beta_i\, u_y)$ (3.44b)

in which S is a summation matrix which is upper triangular, of dimension N and of the form:

$$S=\begin{bmatrix}1 & \dots & 1\\ 0 & \dots & \dots\\ 0 & \dots & 1\end{bmatrix}$$

Substituting and solving the equation of equilibrium of moments about the reference axis Z of all shear forces acting at each floor level, leads to the coordinates of shear centers:

$$\{x_S\} = \left[P_y'\right]\text{^}(-1)S\frac{K_{\theta y}-K_{\theta x}K_x^{-1}K_{xy}}{K_y-K_{yx}K_x^{-1}K_{xy}}\widetilde{P_y} \quad (3.45a)$$

$$\{y_S\} = -[P_x']\text{^}(-1)S\frac{K_{\theta x}-K_{\theta y}K_y^{-1}K_{yx}}{K_x-K_{xy}K_y^{-1}K_{yx}}\widetilde{P_y} \quad (3.45b)$$

where $[P_x']$ and $[P_y']$ denote the diagonal matrix forms of vectors SP_x and SP_y respectively.

When equations (3.45) lead to a diagonal matrix with equal diagonal entries, equations (3.45) simplify to (3.35) and are load-independent. In such a case shear centers, centers of rigidity and centers of twist are coincident.

In conclusion, the centers of rigidity, the centers of twist and the shear centers of the floors of a multi-storey building do not generally coincide, apart from a special class of buildings, and are load-dependent.

4.2.2.4 A Special Type of Multi-Storey Buildings

Although it is impossible to define unique centers of rigidity of the various storeys of a multi-storey building (that means non force-dependent centers), there is a special class of buildings that allows the unique definition of the center of rigidity and possesses the following properties: a) the centers of mass of all floors lie on a vertical line, b) the resisting elements are arranged such that their principal axes form an orthogonal grid in plan and are connected at each floor level by a rigid diaphragm and c) the lateral stiffness matrices of all resisting elements along one direction are proportional to each other. As a result of the two last properties, the centers of rigidity of all storeys lie on a vertical line. Consequently the static eccentricity of each floor is the same. [1]

For the analysis procedure the torsionally-coupled N-storey system was divided into two smaller systems: a) a corresponding torsionally-uncoupled, N-storey system and b) an associated torsionally-coupled one-storey system. The Response Spectrum Analysis was applied for each

system. However for the corresponding torsionally-uncoupled N-storey system in order to evaluate the maximum response quantity the Square-Root of the Sum of Squares (SRSS) the combination rule was applied, while for the associated torsionally-coupled one-storey system the Complete Quadratic Combination was applied. The results are combined through the following relation:

$$r_{nj} = \overline{r_{nj}} r_j \tag{3.46}$$

where

r_{nj}: the maximum value of any response quantity of the torsionally-coupled, N-storey building

due to its njth vibration mode

$\overline{r_{nj}}$: the normalized maximum value of any response quantity of the associated torsionally-coupled one-storey system with uncoupled lateral vibration frequency ω_y equal to ω_{yj}, in its nth vibration mode, where the normalization is with respect to the maximum value of the corresponding response quantity in the corresponding torsionally-uncoupled, one-storey system.

r_j: the maximum value of the same response quantity of the corresponding torsionally-uncoupled, N-storey system in its jth lateral vibration mode

Similarly for one-storey systems, the coupled lateral-torsional response of the building depends on the following parameters: e/r, Ω, ρ, T_{y1} and ξ. For fixed values of e/r, Ω and ρ the response contributions of higher vibration modal-pairs increase by increasing $T_{y1.}$ For fixed values of e/r, Ω and T_{y1} the response contributions of higher vibration modal-pairs increase by increasing ρ. The response contributions of higher modal-pairs are different for the various response quantities. They affect more profoundly the base shear and base torque, for the local response quantities the column moments, and are insensitive to e/r and Ω.

Similarly for the one-storey system, the effects of lateral-torsional coupling on the responses of a multi-storey building decrease in the base shear, the base overturning moment and the top floor lateral displacement at the center of rigidity, but increase at the base torque. The difference between the multi-storey building and its associated one-storey system is the cross-correlation term. In addition the lateral-torsional coupling has no great effect on the height-wise variations of forces.

Finally, the analysis is further simplified, since the first two pairs of vibration modes associated with the first two vibration modes of the torsionally-uncoupled system have been proved to be sufficient. [1]

4.3 Torsional Axis and Torsional Radii of Gyration of Multi-Storey Buildings

A very important parameter for the torsionally coupled motions of irregular buildings is the **optimum torsion axis.** This is the theoretical part of the Greek Aseismic Code and is a good base to understated and design multi-storey buildings. **This axis of a system** is an axis upon which when the level of lateral static seismic forces is placed then the twist of the whole system is minimized [4-6] while the twist is equal to zero in the limit case where the relevant axis is a real elastic axis of the system [7]. Its contribution to the definition of the principal directions of the system and torsional radii of gyration is quite remarkable.

4.3.1 Optimum Torsion Axis

In order to define the location of the optimum torsion axis a continuum model of the structure is used. According to this model, a multi-storey spatial frame-wall system is divided into two spatial subsystems, the bending one and the shear one. Each of them contain the elastic centers K and S, respectively, and its principal elasticity axes I and II, provided that they maintain their elastic and geometric characteristics unchanged in elevation. The frame-wall multi-storey systems have proved [8] to possess three vertical torsion axis, Ω_1, Ω_2, Ω_3, which are not upon the same line. The final response of the system, due to the lateral static loading F(z) continuous distribution in elevation, arises from the

superposition of the three enforced rotations of the system around the relevant axes (Figure 3.3). It has been proved [8] that when there is a vertical real elastic axis in the system and is identified with Ω3 while the Ω1, Ω2 axes move to infinity (Figure 3.4).

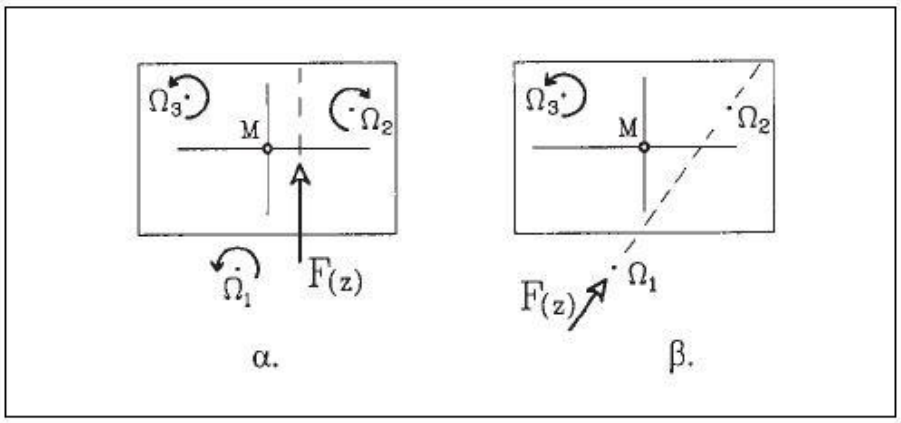

Figure 3.3 *Axes of enforced torsion in a frame-wall multi-storey system [8]*

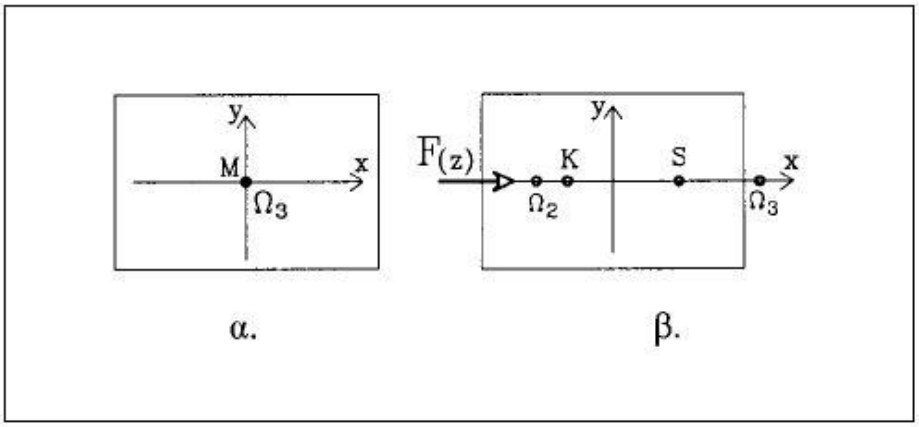

Figure 3.4 *Axes of enforced torsion in symmetrical system [8]*

On the special occasion where the multi-storey frame-wall system is monosymmetric, symmetrical axis x-x, the axis Ω_1 moves to the y-infinity while the other two axes Ω_2, Ω_3 are upon x-x. The elastic centers K and S of the bending and the shear subsystem correspondingly are also upon x-x. The axes Ω_2, Ω_3 are always outside of the (KS) space. [7] When the lateral static loading F(z) has a direction perpendicular to the symmetric axis of the system and is inside the (Ω_2, Ω_3) space the two rotations have

an opposite direction (Figure 3.5). When the following expression is satisfied (3.47) the effects of torsion on the system are minimized.

$$\min\theta^2=\frac{\theta_1^2+\theta_2^2+\cdots+\theta_N^2}{N} \quad (3.47)$$

in which θ_i: rotation angle of the i^{th} floor

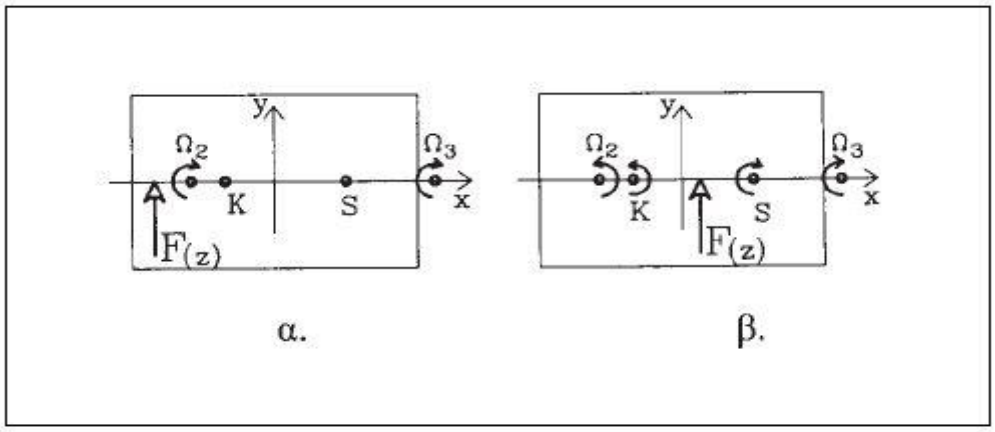

Figure 3.5 *Superposition of two rotations about Ω_1, Ω_2 [7]*

The relation (3.47) is satisfied when the rotation angle of the floor is equal to zero at level z=0.8H (Figure 3.6). [4], [5], [6] Solving the equation that stems from this condition, the location of the Optimum Torsion Axis is defined, point P_o.

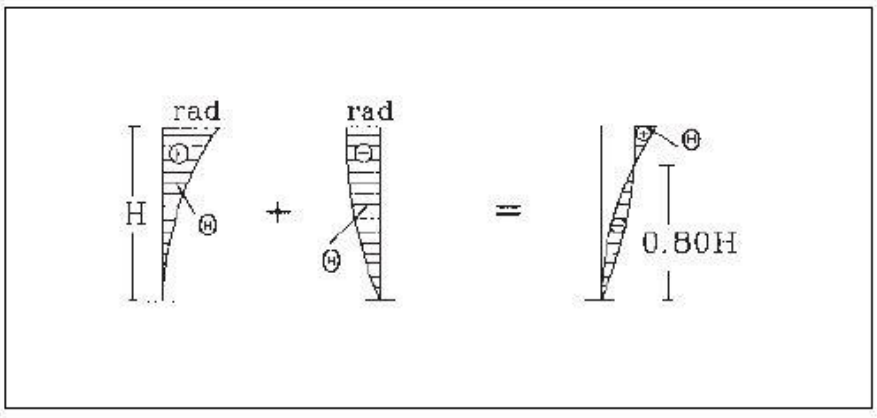

Figure 3.6 *State Optimum Torsion in a multi-storey frame-wall building [4]*

The Optimum Torsion Axis satisfies the following boundary conditions [6]:

Its position in the plan coincides with point K, called the elastic/stiffness centre, in the boundary case where the multi-storey system reduces to a single-storey system.

Its position in the plan coincides with point K when the system transforms into a purely bending one.

Finally its position in the plan coincides with point S when the building transforms into a purely shear one.

The properties of the Optimum Torsion Axis in asymmetric multi storey buildings

According to a study on a five-storey asymmetric building the optimum torsion axis is characterized by the following attributes:

The sum of the squares of the deck rotations and the sum of the squares of the deck displacements along the fictitious principal II-axis is minimum, when the vertical plane of the lateral static seismic forces passes through the fictitious elastic centre P_o and is parallel to the fictitious principal I-axis. The results are similar for lateral seismic forces along the II-axis.

The translational and rotational components are weakly coupled when the vertical mass axis coincides with the fictitious elastic axis.

The earthquake ground motion along the fictitious principal I-axis or II-axis causes almost a translational vibration along the same axis when the vertical mass axis coincides with the fictitious elastic axis. The maximum deck rotations are very small.

The translational and the rotational components of motion are strongly coupled when the mass axis does not coincide with the fictitious elastic axis. [9]

4.3.2 Torsional Radii of Gyration

The **torsional radius of gyration ρ_I** represents the lever arm, according to K, of the elastic forces of restoration during the torsional loading of the single-storey/monosymmetric system. [7]

It can be calculated in two different ways, resulting to the same value:

It can be calculated directly from the relation:

$$\rho_I=\sqrt{\frac{K_{Ш}}{K_{Ц}}} \quad (3.48)$$

where K_{III}: the torsional stiffness of the single-storey system about the axis III

K_{II}: the translational stiffness of the single-storey system according to principal axis II

It can also be calculated according to the ratio of special displacement:

$$\rho_I=\sqrt{\frac{K_{Ш}}{K_{Ц}}}=\sqrt{\frac{F_{Ц}/\theta_z}{F_{Ц}/u_{Ц}}}=\sqrt{\frac{u_{Ц}}{\theta_z}} \quad (3.49)$$

where $u_Ц=F_{Ц}/K_{Ц}$: the displacement for static load force $F_Ц$ at the point K

$\theta_z=F_{Ц}/K_{Ш}$: the twist angle about K for torsional loading $M=1\cdot F_Ц$ of the system

The torsional radius of gyration ρI of the frame-wall monosymmetric systems does not have the same value for every level ξ, but the one in diagrams of figures 3.7a and 3.7b. It is suggested that the torsional radius of gyration of level z=0.8H is approximately equal to the torsional radius of gyration of the whole system, since the optimum torsional axis is defined at this level. According to the relation between the torsional radius of gyration ρI at the center of mass and the radius of gyration of the diaphragm r the torsional flexibility of the system for dynamic translational excitation is defined. Actually if $\rho_{mx}\leq r$ the system is torsionally flexible.

$$\rho_{mx}=\sqrt{\rho_I^2+e_{ox}^2} \quad (3.50)$$

e_{ox}: the static eccentricity along x axis

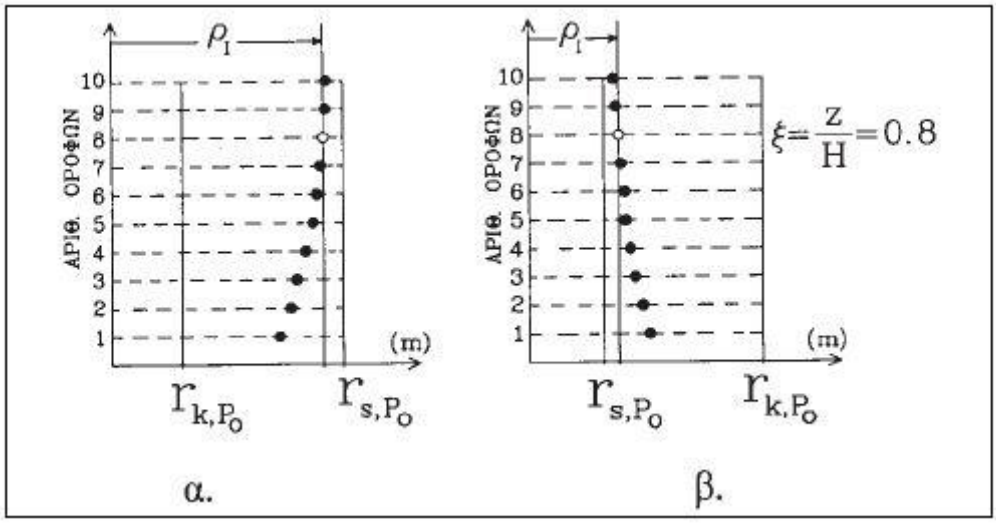

Figure 3.7 *Distribution of the torsional radius of the floors [7]*

Another criterion for the torsional flexibility of a building is the coordinates of the center of vibration O_i of the floors. A system is characterized as torsionally flexible when the vibration centers, calculated for the first and the second modal shape, occur inside the circle of the radius of inertia of the diaphragm, which means that the torsional vibrations of the diaphragm dominate the translational ones for pure translational excitation. The coordinates of the center of vibration O_i (e_{xi},e_{yi}) are given by the expressions below:

$$\varepsilon_{yi}=\frac{\varphi_{xi}}{\varphi_{zi}} \quad (3.51a)$$

$$\varepsilon_{xi}=-\frac{\varphi_{yi}}{\varphi_{zi}} \quad (3.51b)$$

4.3.3 Equivalent Static Eccentricities

The equivalent static eccentricities e_f, e_r are used in order to define the location of the point of application of the lateral static seismic forces and are given by the expressions (3.52) and (3.53), respectively. The accidental eccentricity $e_{\tau i}$ is also taken into consideration.

$$e_f=\frac{\rho_l^2}{r}\cdot R_f \quad (3.52)$$

$$e_r=\frac{\rho_l^2}{r}\cdot\frac{1-D_r}{l_r-\varepsilon_o}\leq\frac{1}{2}\cdot e_o \quad (3.53)$$

where

$R_f=\frac{sin2\theta}{2}\cdot\left(\frac{1}{A_1^{2n}}+\frac{1}{A_2^{2n}}-2\varepsilon_{12}\cdot\frac{1}{A_1^n\cdot A_2^n}\right)^{1/2}$

$D_r=\frac{sin2\theta}{2}\cdot\left(\frac{\delta_{r1}^2}{A_1^{2n}}+\frac{\delta_{r2}^2}{A_2^{2n}}+2\varepsilon_{12}\cdot\frac{\delta_{r1}^2\cdot\delta_{r2}^2}{A_1^n\cdot A_2^n}\right)^{1/2}$

$\text{tana}_o=\frac{2\varepsilon_o}{\varepsilon_o^2+\mu^2-1}$

If $\text{tana}_o\geq 0$, then $\theta=\alpha_o/2$.

If $\text{tana}_o<0$, then $\theta=90-|a_o|/2$

$\varepsilon_o=\frac{e_o}{r}$, $\rho_l=\sqrt{\frac{K_{Ш}}{K_{Ц}}}=\sqrt{\frac{u_{,F}}{\theta_{,M}}}$, $\mu=\frac{\rho_l}{r}$

$A_1=1-\varepsilon_o\cdot\tan\theta$, $A_2=1+\varepsilon_o\cdot\cot\theta$

$\delta_{r1}=\cot\theta-l_r$, $\delta_{r2}=\tan\theta-l_r$, $l_r=\frac{L_r}{r}$

$\varepsilon_{12}(\zeta=5\%)$, $r_{12}=\sqrt{A_2/A_1}$

$\varepsilon_{12}=\frac{8\zeta^2\cdot(1+r_{12})\cdot r_{12}^{3/2}}{(1-r_{12}^2)+4\zeta^2\cdot r_{12}\cdot(1+r_{12})}$

On the special occasion of the double asymmetric system, the procedure is applied for both of its principal axis.

A five-storey building, made of reinforced concrete, with asymmetric arrangement of the stiffness elements has been examined. [7] The equivalent static method, the dynamic spectral method, the dynamic spectral solution and the spatial superposition have been applied to the five-storey building leading to the conclusion that although the building is highly torsionally flexible, if the application of the equivalent static method is used (by using the optimum torsion axis and the equivalent static eccentricities) then the results contain the results of the corresponding response of the dynamic spectral method.

4.4 Torsional Moment Assessment through the Static Eccentricity Concept

It is urgent to assess the torsional effect due to structural asymmetry in the seismic design of buildings, since the most damages during an earthquake are caused by this effect. In most cases, torsional effect is computed as the product of static eccentricity and equivalent static load. Several approaches have been proposed in order to compute the static eccentricity in multi-storey buildings [10]. The main problem is that this eccentricity depends on the horizontal load pattern. Two of these approaches are described below through an example.

A two-bay building (Figure 3.8) with frames A, B and C showing fig 3.8 is considered. In the y-direction the frames are considered with rigid floor diaphragms. In the first two storeys frames A, B and C are spanned, while in the last two storeys just frames A and B. The building is symmetrical along the x-direction and undergoes a static torsional load P_i ($i = 1,2,3,4$) acting at the center of mass of each floor. Due to the irregularity in plan, torsional moments are developed at each storey level $(M_i)_k$ $(i = 1,2,3,4)$.

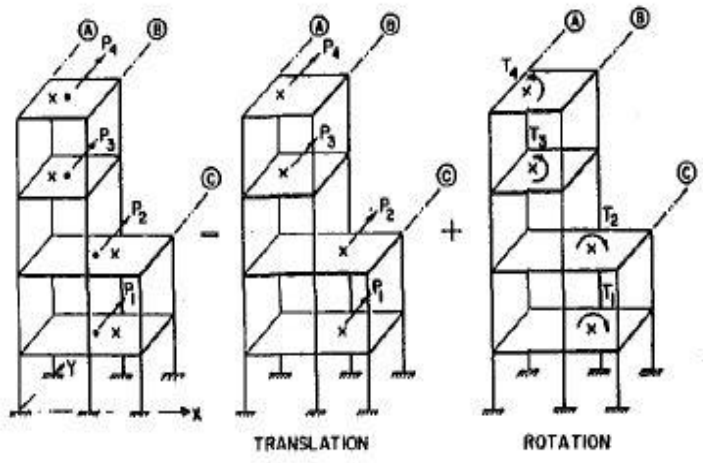

Figure 3.8 *Loads used in the eccentricity concept to multi-storey Buildings [10]*

4.4.1 First evaluation method by Tso

In this case, the torsional moment is assessed through the developed floor torques. The load is divided in two components, the translational and the rotational, as shown in Fig. 3.9The load at each floor is relocated acting at

the generalized center of the floor's rigidity (the definition of the generalized center of rigidity is given below). According to assumption, the floor torques $T_i\ (i = 1,2,3,4)$ are computed through the following expressions:

$$T_i = P_i\ e_i\ (i = 1,2,3,4) \tag{3.54}$$

$$e_i = (x_m)_i - (x_R)_i \tag{3.55}$$

where **e_i: the floor eccentricity**, the distance between the center of mass and the generalized center of rigidity at that floor [10].

The generalized centers of rigidity are defined as points at the floor levels in a multi-storey structure such that when lateral load is applied at them, the structure deflects laterally without any floor rotation [10].

In order to specify the location of the generalized centers of rigidity at each floor, free body diaphragms of each floor under the translational loading are considered (Figure 3.9).

The frame reaction at the floor i is given by the following equation:

$$\left(V_{i,j} - V_{i+1,j}\right) = f_{i,j}\ (i = 1,2,3,4)\ (j = A, B, C) \tag{3.56}$$

where $V_{i,j}$: the storey shears below level i of frames j

Translational equilibrium at each floor (Figure 2.12b) gives the following equation:

$$f_{iA} + f_{iB} + f_{iC} = P_i \quad (i = 1,2,3,4) \tag{3.57}$$

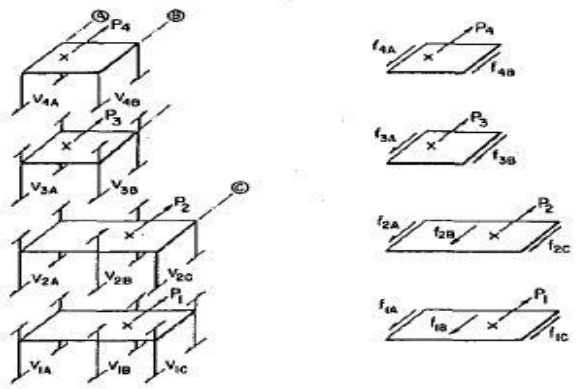

Figure 3.9 *Free Body Diagram of Each Floor [10]*

It is assumed that there is no rotation of the floors. The moment equilibrium about a vertical axis for each floor is computed when the loads act through the 'centroids' of the floors' frame actions. Provided that the frame reactions for a floor are known, the location of the floor's centers of rigidity can be defined as the sum of the first moments of the frame reactions divided by the total of the floor's frame reaction. Thus, the generalized centers of rigidity of a multi-storey building are characterized also as frame reaction centers.

4.4.2 Second evaluation method

In this case, the torsional moments are assessed through storey shear and storey eccentricity.

The torsional moment at storey k is expressed by the following equation:

$$(M_t)_k = V_k e_k^* \tag{3.58}$$

where V_k is the storey shear and e_k^*: the storey eccentricity at storey k, defined as the horizontal distance between the shear center at the storey and the resultant of all lateral forces above the storey being considered [10] (computed from the equilibrium of the free body diaphragm above a cut at storey k-(Figure 3.10)).

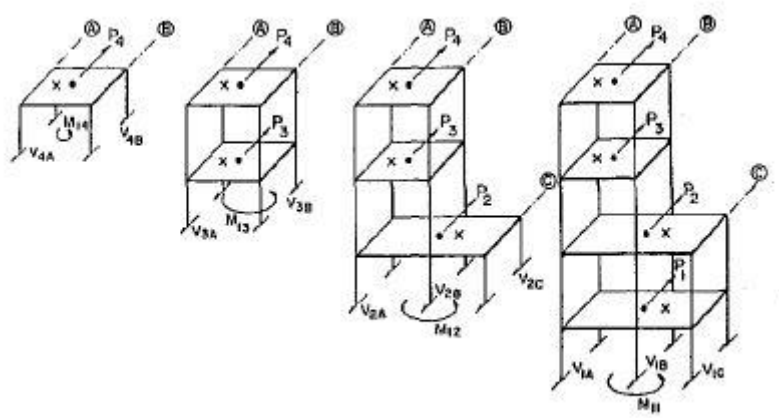

Figure 3.10 *Free Body Diagram of Substructures [10]*

The torsional moment at storey k is expressed through the equation:

$$(M_t)_k = \sum_{i=k}^{4} P_i[(x_m)_i - (x_s)_k] \tag{3.59}$$

From the equilibrium of the cut at storey k:

$$\widehat{V_k} = \sum_{i=k}^{4} P_i \tag{3.60}$$

Through (1.7), (1.6) is transformed into:

$$(M_t)_k = \sum_{i=k}^{4} P_i (x_m)_i - V_k (x_s)_k \tag{3.61}$$

The x-coordinate of the resultant of all applied loads above storey k can be obtained as the ratio of the sum of the first moment of the applied loads to the sum of these loads [10]:

$$(x^*)_k = \frac{\sum_{i=k}^{4} P_i (x_m)_i}{V_k} \tag{3.62}$$

$$(M_t)_k = V_k e_k^* [(x^*)_k - (x_s)_k] \tag{3.63}$$

At Reference [10] it has been proved that both approaches reach the same result provided that the appropriate definitions for the eccentricities are assumed.

At the same Reference [10] it has also been proved through the given example that the storey eccentricity is less sensitive to load distribution than the floor eccentricity (Table 3.1). Therefore, a second approach is supposed to be more appropriate for a structural asymmetry assessment.

Table 3.1 *Comparison of Results for Two Different Load Distributions [10]*

	Uniform Distribution Loading				Triangular Distribution Loading			
Story (1)	Floor eccentricity (m) (2)	Story eccentricity (m) (3)	Story shear (kN) (4)	Torsional moment (kN-m) (5)	Floor eccentricity (m) (6)	Story eccentricity (m) (7)	Story shear (kN) (8)	Torsional moment (kN-m) (9)
4	−0.96	−0.96	10	−9.6	−1.00	−1.00	16	−16.0
3	−1.20	−1.08	20	−21.6	−1.22	−1.09	28	−30.6
2	−8.62	−3.59	30	−107.8	−15.05	−4.19	36	−151.0
1	0.82	−2.49	40	−99.6	2.95	−3.48	40	−139.2

But there is a special class of buildings that the floor and the storey eccentricity are identical. The features of this special class of buildings are: (i) that they have proportional framing resulting to proportional stiffness properties of resisting elements, (ii) their generalized centers of rigidity lie on a vertical line and their position is independent of load

distribution and (iii) their floors' centers of mass lie along a vertical axis. As a result their floor and storey eccentricities are identical, as mentioned before, and remain constant along the height. It can easily be concluded that the centers of rigidity coincide with the shear centers.

REFERENCES:

[1] Reem Hejal and Anil K. Chopra, 1987, "*Earthquake Response of Torsionally-Coupled Buildings"*, Earthquake Engineering Research Center, College of Engineering, University of California at Berkeley.

[2] J. A. Blume "Dynamic Characteristics of Multi-storey Buildings," *J. Structural Division, Asce*, vol. 94, no. ST2, pp. 337–402, 1968.

[3] J. L. Humar & A. M. Awad, "Design for Seismic Torsional Forces," *Proc., 4th Canadian Conf. Earthquake Eng., Vancouver, Canada*, pp. 251–260, 1983.

[4] T. Makarios & K. Anastassiadis, "Real and Fictitious Elastic Axis of Multi-storey Buildings: Application," *Tech. Chron*, no. 17, 1997.

[5] T. Makarios & K. Anastassiadis, "Real and Fictitious Elastic Axis of Multi-storey Buildings: Application," *Tech. Chron*, no. 18, 1998.

[6] T. Makarios & K. Anastassiadis, "Real and Fictitious Elastic Axis of Multi-storey Buildings: Application," *PhD School Civil Eng., Thessaloniki*, 1994.

[7] T. Makarios "Optimum Torsion Axis and Torsional Radii of Gyration in Multi-Storey Buildings," *Tech. Chron. Sci. J. Tcg*, vol. I, no. 1,

[8]K. Anastassiadis, "Analyse Statique tridimensionelle du contreventement des batiments. La method des trios pivots," *Annales De I' I.t.b.t.p.*, no. 435, 1987.

[9] Har. Xenidis, Trian. Makarios & As. Athanasopoulou, "The Properties of the Optimum Torsion Axis In Asymmetric Multi-storey Buildings," *Tech. Chron. Sci. J.tcg*, vol. I, no. 2-3, 2005.

[10] Wai T. Tso, "Eccentricity Concept for Torsional Moments Estimations," *J. Structural Eng.*, 1990.

5 Torsionally unbalanced inelastic buildings – An overview

It is a matter of vital importance for engineers to define the torsional collapse mechanisms of building systems, since this knowledge is valuable in predicting the seismic response of torsional vulnerable structures. The existing codes deals with the problem of torsion assuming elastic behavior of structures. However it is the plastic mechanisms that give the engineer the opportunity to estimate the displacement ductility demand of the system and compare it with the displacement ductility capacity of the structural resisting elements. In order to define the critical elements, inelastic structures are classified as torsionally unrestrained or restrained, resulting in two different classes of mechanism.

5.1 Torsional mechanisms in ductile building systems

Torsionally unrestrained systems are the systems, which cannot resist torsion in the post-yield range. Thus, torsion can be undertaken by the structural elements with the elastic domain since they are unable to resist torsional effects at the inelastic stage. As a result one corner element may be subjected to excessive plastic deformations while the other, at the opposite side, may be in the elastic domain. This is associated with a reduction of the base shear capacity of the system. [1]

For instance, the system of Figure 4.1 is considered assuming that the response of the lateral force resisting elements is perfectly elastic-plastic. When element (2) is about to yield and its displacement ductility capacity

$\mu_{\Delta 2max}$ should not be exceeded, the system displacement ductility demand should be limited to:

$$\mu_{\Delta} \leq \beta \frac{\Delta_{y1}}{\Delta_y} + \alpha \mu_{\Delta 2max} \frac{\Delta_{y2}}{\Delta_y} \quad (4.1)$$

where

Δ_y: the system yield displacement (for torsionally unrestrained systems), relevant to CM

$$\Delta_y = \beta \Delta_{y1} + \alpha \Delta_{y2} \quad (4.2)$$

with the introduction of a geometric system parameter:

$$\psi = \frac{\alpha \Delta_{y2}}{\beta \Delta_{y1}} = \frac{a l_{w1}}{\beta l_{w2}} \quad (4.3)$$

Expression (4.1) simplifies to:

$$\mu_{\Delta} \leq \frac{\mu_{\Delta 2max}+1}{1+\psi} \quad (4.4a)$$

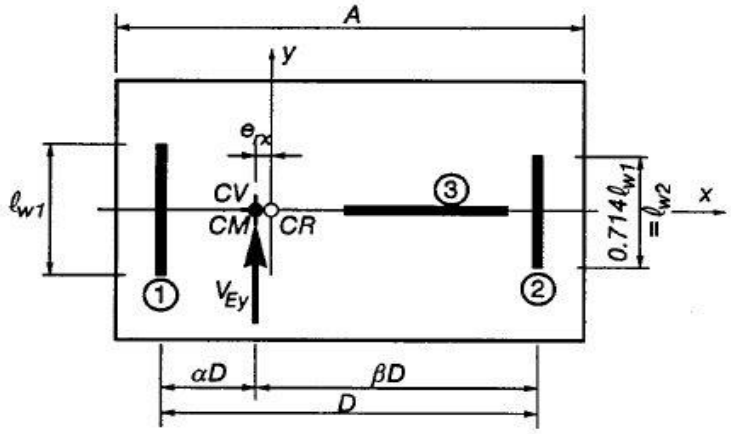

Figure 4.1 *Arrangement of lateral forces resisting elements in a torsionally unrestrained system [1]*

When it is found that element (1) is about to yield and its displacement ductility capacity should not be exceeded, the system displacement ductility should be limited to:

$$\mu_{\Delta} \leq \frac{\mu_{\Delta 1max}+\psi}{1+\psi} \quad (4.4b)$$

Finally, in the design of such a system, the system ductility demand should be limited to the lesser of the two values (4.4a and b).

Limited torsional restrained systems are the systems, whose elements exhibit post-yield stiffness, $k_{pi}=\sigma k_i$ (σ:post-yield stiffness coefficient), i.e. for typical reinforced concrete elements $\sigma<0.06$. In this case, the nominal strength of one element is in excess of that assigned to it, for example the element (1), $V_{n1}=\lambda_1 V_1$ where $\lambda_1> 1.00$. An upper limit is established, which reassures the development of post-yield deformation of element (1). Beyond this value and for a given post-yield stiffness of element (2), element (1) cannot yield. This limit is expressed by the equation:

$$\lambda_1 < 1 + \sigma(\mu_{\Delta 2max} - 1) \quad (4.5)$$

It has been proved [1] that in the case of limited torsional restraint the system ductility demand should be restricted to:

$$\mu_\Delta = \mu_{\Delta 2max} - \frac{\lambda_1 - 1}{\sigma(1+\psi)} \quad (4.6)$$

Torsionally restrained systems can resist earthquake-induced torque up to their ultimate limit state with transverse elements remaining within the elastic range, which also control the system twist, while translatory elements are subjected to inelastic displacements of different magnitudes. The center of resistance of these inelastic translator elements, CV, can be found by strength eccentricity. Torsionally restrained mechanisms subjected to inelastic skew displacements must be expected to degenerate into torsionally ones.

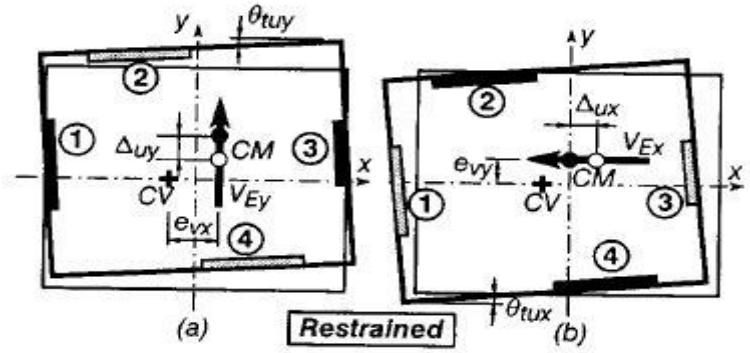

Figure 4.2 *Arrangement of lateral forces resisting elements in a torsionally unrestrained system [1]*

Strength eccentricity is the distance between CM and CV defined by the equation:

$$e_{vx=\frac{\sum x_i V_{ni}}{\sum V_{ni}}} \quad (4.7)$$

Where x_i is the distance of the element of CM

When one or more of the elements do not respond to their nominal strength, then the reduced one must be used in equation (4.7). This case is usually encountered in torsionally unrestrained systems or in restrained systems, when the transverse elements, providing torsional resistance, yield before all translator elements develop their nominal strength.

The wise assignment of the nominal strength of translatory elements would lead the system to the optimum response, provided that $\sum V_{ni} \geq V_E$. The location of CV is of crucial importance, since during a damaging earthquake some of the lateral force resisting elements yield and stiffness eccentricity is inappropriate to represent the asymmetry of the structure. In this case, the structure is subjected for portions of time in the elastic state and for others in the plastic state. It has been proved that the produced rotations in the different states cancel one another when stiffness and strength eccentricity have opposite signs, which means that the location of the centre of rigidity and the centre of strength are on the opposite sides of the centre of mass. [2]

5.2 Inelastic seismic behavior of asymmetric in plan buildings

In order to understand the seismic inelastic behavior of asymmetric-plan buildings, the base shear and torque historeys are superimposed to the base shear and torque surface (BST) of the building. The main advantage of the BST surface is that in cooperation with the base shear and torque historeys it offers a conceptual evaluation before the dynamic analysis. Subsequently, the construction of the base-shear and torque surface is

described, as well as, the parameters that affect its shape and its properties.

Single storey buildings consisting of a rigid diaphragm, where all the storey mass is lumped, are analyzed. The i_{th} resisting plane in the x-direction has stiffness kxi, lateral strength fxi and is located at distance yi from the center of mass (CM) of the building. Similarly, for the jth resisting plane in the y-direction kyj, fyj and xj, respectively (Figure 4.3).

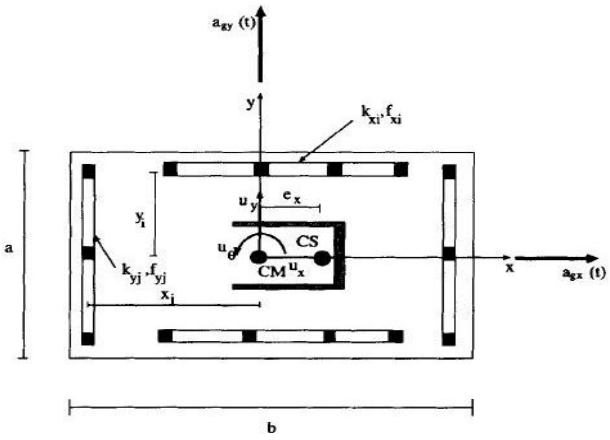

Figure 4.3 *Typical plan of buildings considered (asymmetric-plan buildings) [3]*

The equation of motion that describes the dynamic response of the system to base accelerations $a_{gx}(t)$ and $a_{gy}(t)$ in the x- and y-directions, is:

$$M\ddot{u} + C\dot{u} + R(\delta, \dot{\delta}) = -Mra_g \quad (4.8)$$

where: $u = \begin{Bmatrix} u_x \\ u_y \\ u_\theta \end{Bmatrix}$

$\ddot{u}$,$\dot{u}$: the accelerations and velocities of the diaphragm

$\ddot{\delta}$,$\dot{\delta}$: the vectors containing the deformation and deformation rates of the different resisting elements, which are computed from the displacements u and velocities $\dot{u}$ as $\delta = Lu$ and $\dot{\delta} = L\dot{u}$, where L is the displacement-deformation transformation matrix; M and C are the mass and damping matrices; R($\delta, \dot{\delta}$) is the vector of restoring forces in the system

r: a 3×2 matrix with its two columns $r_x = \begin{Bmatrix} 1 \\ 0 \\ 0 \end{Bmatrix}$ and $r_y = \begin{Bmatrix} 0 \\ 1 \\ 0 \end{Bmatrix}$, the influence vector for excitations $a_{gx}(t)$ and $a_{gy}(t)$, respectively

$$a_g(t) = \begin{Bmatrix} a_{gx}(t) \\ a_{gy}(t) \end{Bmatrix}$$

The base shear and torque surface (BST) and base shear and torque historeys are presented in a space spanned by the base shears V_x and V_y in the x- and y-directions, respectively, and base torque T.

The BST surface consists of all combinations of base shear and torque that applied statically leading to the collapse of the system. The force space is divided by the BST surface in two regions, the interior and the exterior. The interior consists of points which represent base shear and torque combinations causing elastic behavior of the structure. The exterior contains statically inadmissible base shear and torque combinations. The BST surface is the limit between the two regions where the inelastic behavior of the system is developed.

The BST surface below is computed for a symmetric single-storey system (Figure 4.4).

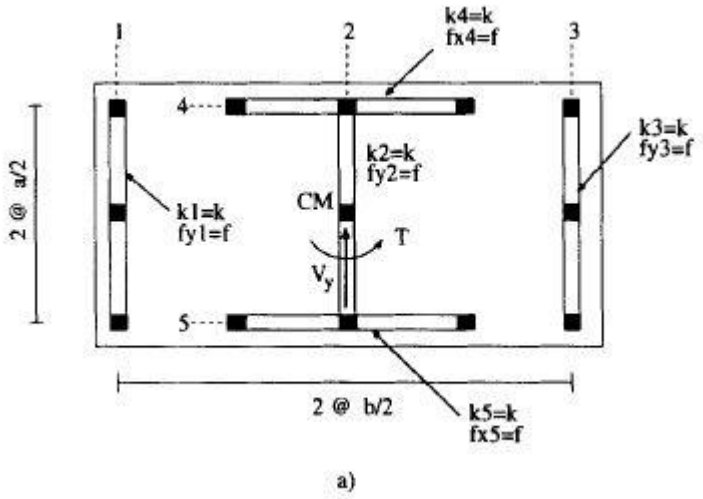

a)

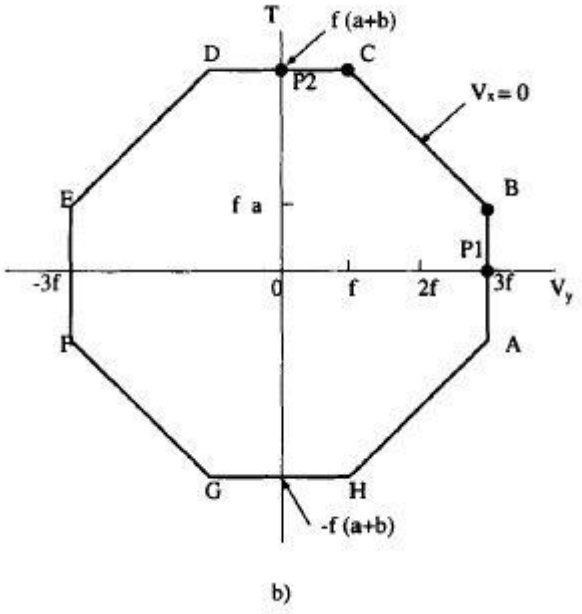

Figure 4.4 *Example for the construction of a BST ultimate surface [3]*

Next, the procedure of computing the first quadrant is carried out; the other three quadrants are symmetric.

Point P1 represents a purely translational mechanism of the plan (Figure 4.5a,b) – simultaneous yielding all resisting planes in the y-direction, V_y=3f and T=0. Branch P1-B represents mechanisms involving rotation of the plan (Figure 4.5c,d) – the plan rotation increases linearly always leaving the deformation of resisting plane 1 equal to u_y, V_y=3f and T=fa. Branch B-C represents mechanisms always leaving the resisting plane 1 in the elastic range (Figure 4.5e,f) – point C, V_y=f and T= f(a+b). Branch C-P2 represents mechanisms always leaving the resisting plane 2 in the elastic range (Figure 4.5g) - rotation is fixed at its maximum value and the base shear in the y-direction is decreasing. Point P2 represents a purely torsional mechanism (Figure 4.5h) - V_y=0 and T=f(a+b).

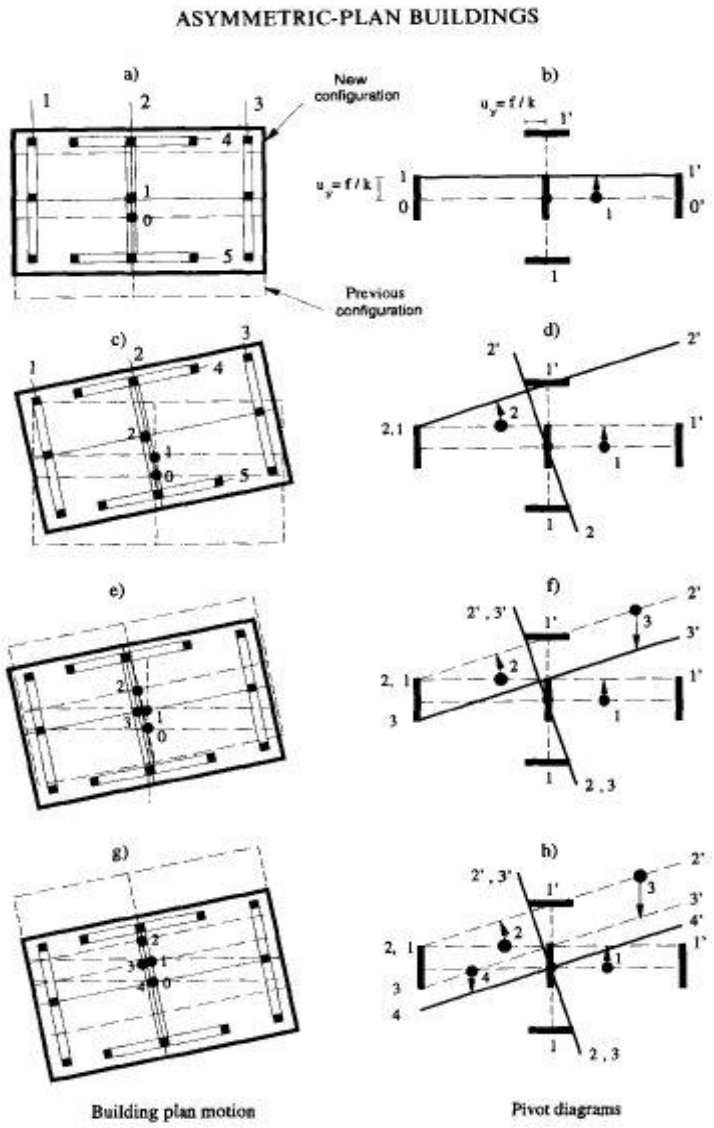

Figure 4.5 *Construction of the BST surface in the first quadrant [3]*

5.2.1 Properties of the BST surface

The BST surface is convex and it is composed of linear branches [3].

The slope of a tangent to the BST surface tells the position of the element in the building plan that remains elastic during the mechanism (or branch) considered. Besides, this slope also defines the center of plastic rotation of the building [3].

The BST ultimate surface has as many branches with a finite slope as twice the number of resisting planes in the structure in the direction of the ground motion. Starting in a counter-clockwise sense from the branch of

constant base shear in the first quadrant, the first branch is associated with mechanisms that leave the leftmost resisting plane in the elastic range, the second branch the second farthest plane to the plane, and so forth until we reach the rightmost resisting plane [3].

The BST surface is point-symmetric with respect to the origin if the element yield displacements are the same under load reversals [3].

The BST surface of the system contracts along the torque axis as the base shear in the x-direction V_x increases from zero to its maximum value V_{xo} [3]. All these properties are proved in Reference [4].

5.2.2 Parameters affecting the BST surface

The inelastic behavior of a building is described by the shape of the BST surface. As a result, the parameters that affect the shape of the BST surface affect the inelastic behavior of the building. These parameters are:

The strength of the resisting planes in the x- and y-directions. An isotropic change of the resisting planes' strength causes proportional change (dilation or contraction) of the surface (Figure 4.6b).

The strength of the resisting planes in the orthogonal direction. An increase of the strength of the resisting planes causes an increase of the torsional capacity of the system and of the length of the constant base shear branches of the BST surface (Figure 4.6c).

Asymmetry in stiffness. The BST surface is independent of the stiffness eccentricity.

Asymmetry in strength. The skewness and stretching of the BST surface are affected by strength asymmetry. The inelastic behavior of a building developed along the long branches implies that the strongest resisting plane remains elastic while the others yield significantly (Figure 4.6d).

Planwise distribution of strength.

Number of resisting planes. According to the properties of the BST surface, the number of branches with a finite slope are more since we

have more resisting elements. As a result the BST surface looks rounder in comparison with the reference system (Figure 4.6f).

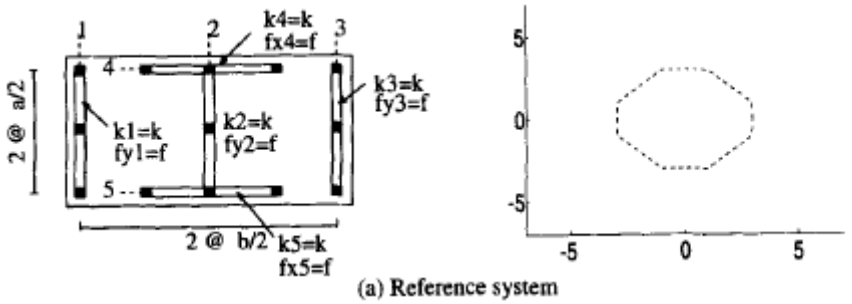

(a) Reference system

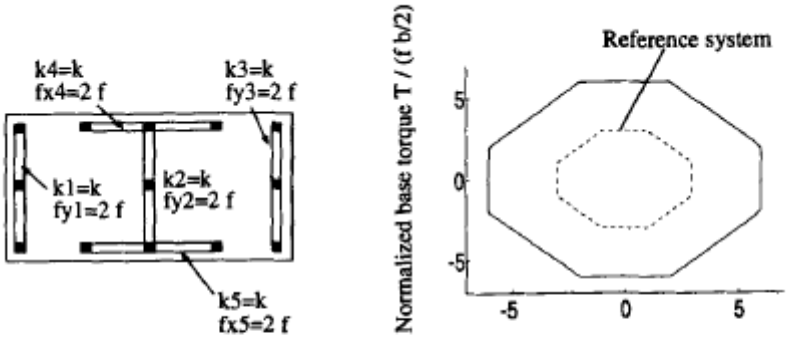

(b) Global increase in strength

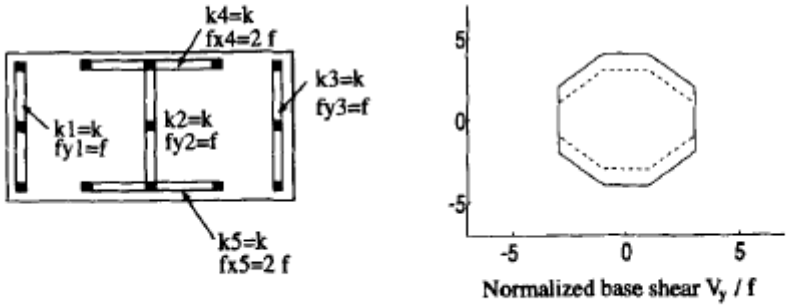

(c) Increase in strength of orthogonal resisting planes

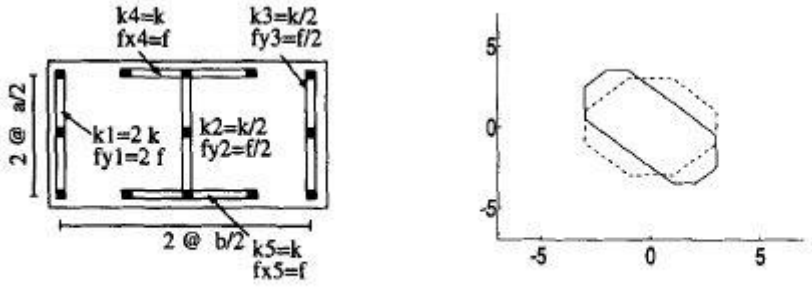

(d) Strength asymmetry

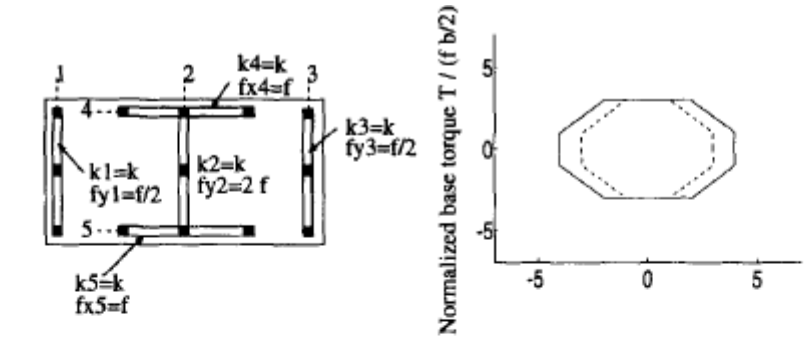

(e) Planwise distribution of strength

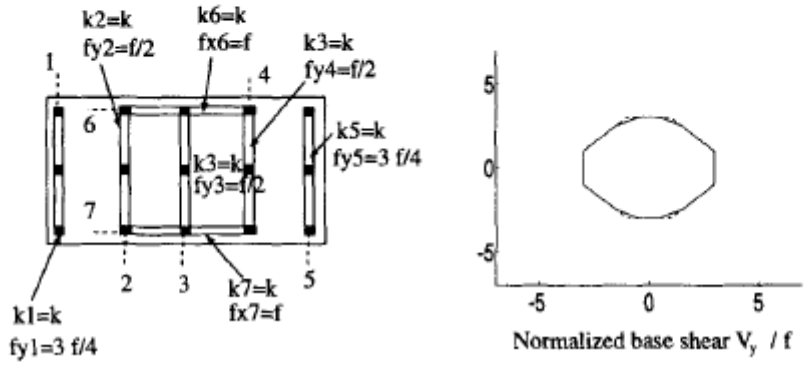

(f) Number of resisting planes

Figure 4.6 *Effect of different parameters on the shape of the BST surface [3]*

5.3 A simplified model for analysis and design

The difficulties of defining the earthquake response of asymmetric buildings, such as analysis cost, computational effort and the inefficiency of current analyses methods to design any ground motion characteristics, led engineers to search for other methods. The new methods should overcome all the obstacles mentioned above and should also offer

accurate results through a simpler analysis procedure. A new simplified analysis method proposed by Llera and Chopra [5] is based on one structural super-element (SE) per building storey, which sufficiently represents the elastic and inelastic properties of the storey.

In order to give results, the systems considered in the investigation above [5] are single and multi-storey buildings consisting of rigid diaphragms, flexurally and axially, where all the storey masses are lumped; lateral resistance is provided by resisting planes in the x- and y-directions [Figure 4.7(a)] composed of elasto-plastic resisting elements. The systems are symmetric in stiffness and strength about the x-axis.

Next the equation of motion of the system is given in order to assess the dynamic response of it to base acceleration a_{gy}(t) in the y-direction:

$$M\ddot{u} + Cu + \dot{R}(\delta, \dot{\delta}) = -Mr\, a_{gy}(t) \qquad (4.9)$$

where $u = \begin{Bmatrix} u_x \\ u_y \\ u_\theta \end{Bmatrix}$

u_x: the vector of displacements $u_x^{(j)}$ of the jth floor CM along the x-direction

u_y: the vector of displacements $u_y^{(j)}$ of the jth floor CM along the y-direction

u_θ: the vector of rotations $u_\theta^{(j)}$ of the jth rigid floor diaphragm about a vertical axis through the CM [Figure 4.6(a)]

M: the mass matrix given by

$$M = \begin{bmatrix} m & 0 & 0 \\ 0 & m & 0 \\ 0 & 0 & I_p \end{bmatrix}$$

where m and I_p are diagonal matrices containing the masses and polar moments of inertia for each building storey

C: the linear viscous damping matrix

$R(\delta, \dot{\delta})$: the vector of restoring forces in the system

$r = \begin{Bmatrix} 0 \\ 1 \\ 0 \end{Bmatrix}$: the influence vector for the ground acceleration a_{gy}(t)

The equation of motion (4.9) above will be integrated numerically using the partitioned predictor-corrector scheme developed in Reference [6].

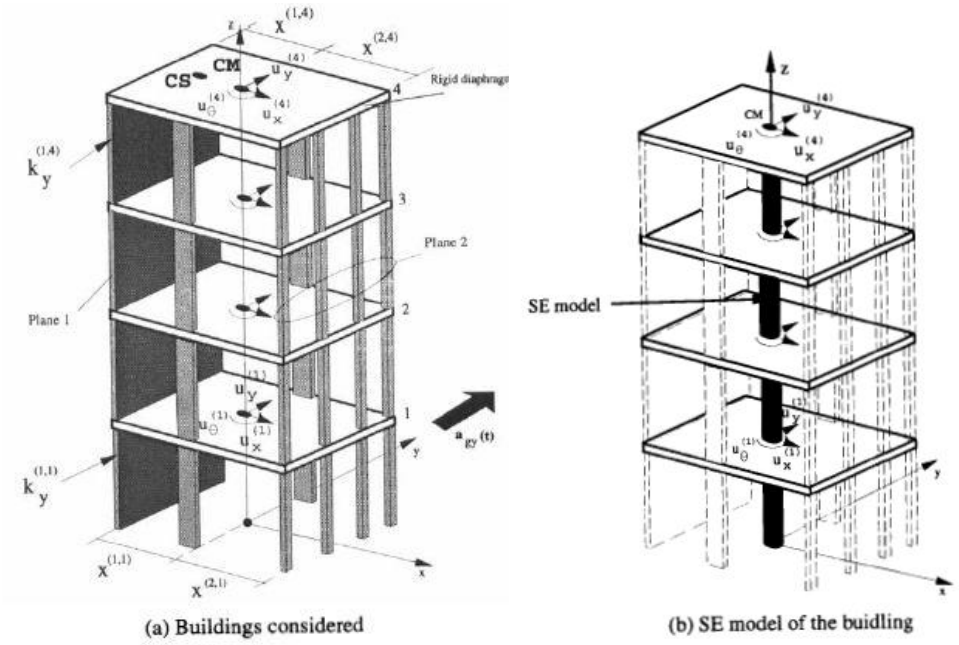

Figure 4.7 *Buildings considered and the SE model [5]*

The SE model of a building consists of a single fictitious structural element per storey. This element has three degrees of freedom per node (Figure 4.7b), the two translations and the rotation of floors are connected by the element, and is appropriate for representing the elastic and inelastic properties of the storey.

Subsequently, the elastic and inelastic properties of the SE model are presented.

5.3.1 Elastic properties of the SE model

On the elastic occasion, the SE model has the same stiffness matrix as the storey considered:

$$K_{SE} = \begin{bmatrix} K & -K \\ -K & K \end{bmatrix} \qquad (4.10)$$

where $K = \begin{bmatrix} K_x & 0 & 0 \\ 0 & K_y & K_{y\theta} \\ 0 & K_{y\theta} & K_\theta \end{bmatrix}$

$K_x, K_y, K_{y\theta}, K_\theta$: are scalar quantities for the storey considered

A possible obstacle, as far as K_{SE} is concerned, may appear when the center of mass of the different storeys do not lie on the same vertical line (Figure 4.7). In order to overcome this problem, a linear transformation a_u between the degrees of freedom $u^{(1)}$ at the CM of the first floor and the degrees of freedom $u^{(1)\prime}$ at the bottom of the second storey SE, is used:

$$\begin{Bmatrix} u_x^{(1)\prime} \\ u_y^{(1)\prime} \\ u_\theta^{(1)\prime} \end{Bmatrix} = \begin{bmatrix} 1 & 0 & 0 \\ 0 & 1 & \chi_1 \\ 0 & 0 & 1 \end{bmatrix} \begin{Bmatrix} u_x^{(1)} \\ u_y^{(1)} \\ u_\theta^{(1)} \end{Bmatrix} = [a_u] \begin{Bmatrix} u_x^{(1)} \\ u_y^{(1)} \\ u_\theta^{(1)} \end{Bmatrix} \tag{4.11}$$

The stiffness matrix of the second-storey SE with respect to the degrees of freedom at the CM of floors 1 and 2 can be expressed as:

$$K_{SE} = \begin{bmatrix} K & -Ka_u \\ -a_u^T K & a_u^T K a_u \end{bmatrix} \tag{4.12}$$

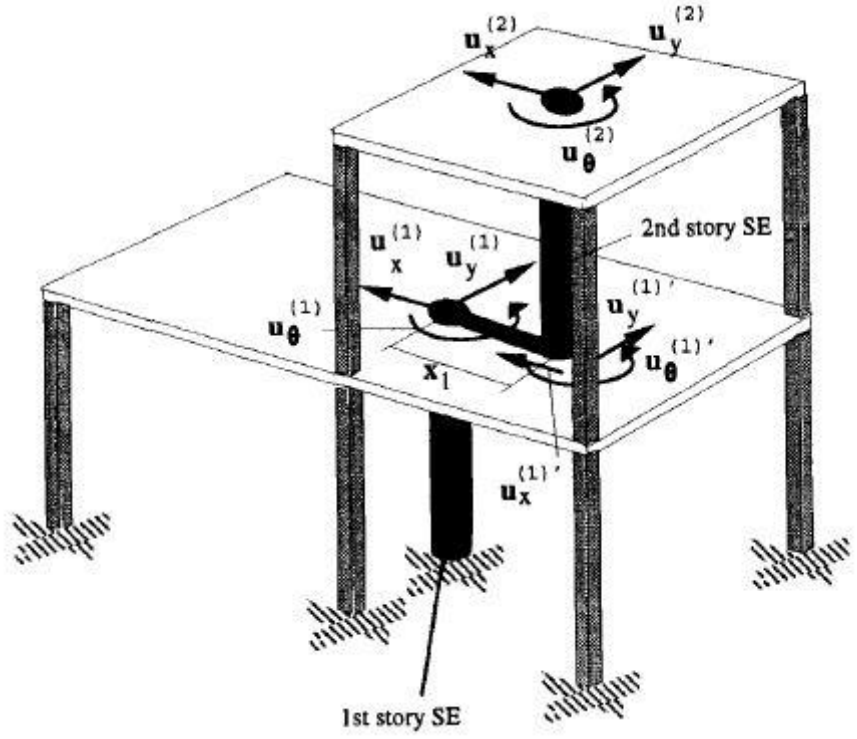

Figure 4.8 *SE model for a building with non-aligned centers of mass [5]*

5.3.2 Inelastic properties of the SE model

In order to match the inelastic properties of the storey and the SE model, the storey shear and torque (SST) ultimate surface is used. The SST surface consists of all combinations of storey shears and torque that applied statically and would lead to the collapse of the storey.

The exact model of a section of the SST (Figure 4.9-solid line) surface is presented below, for a storey with three resisting planes along the y-axis (the direction of asymmetry and of ground motion) and two resisting planes in the orthogonal direction, with constant storey shear Vx. Later on this model will prove to predict accurately the response of systems regardless of the number of resisting planes they consist of. The seven parameters that affect the shape of the SST surface will also be investigated.

The following expressions define the coordinates (xj, yj) of the vertices of this surface:

$$
\begin{aligned}
&x_1 = V_{yo}, && y_1 = V_{yo}x_p + T_\perp(1-\widehat{V_x})\\
&x_2 = V_{yu} + V_{yc}, && y_2 = T_o + T_\perp\widehat{V_x}\\
&x_3 = V_{yu} - V_{yc}, && y_3 = T_o - T_\perp\widehat{V_x}\\
&x_4 = -V_{yo}, && y_4 = -V_{yo}x_p + T_\perp(1-\widehat{V_x})\\
&x_5 = -x_1, && y_5 = -y_1\\
&x_6 = -x_2, && y_6 = -y_2\\
&x_7 = -x_3, && y_7 = -y_3\\
&x_8 = -x_4, && y_8 = -y_4
\end{aligned}
\tag{4.13}
$$

where:

$\widehat{V_x} = \frac{V_x}{V_{xo}}$: the normalized storey shear in the x-direction; $V_{xo} = \sum_{i=1}^{M} f_x^{(i)}$: the lateral capacity of the storey in the x-direction; $f_x^{(i)}$: the capacity of the

ith resisting plane in the x-direction; and M: the number of resisting planes in the x-direction

$V_{yo} = \sum_{i=1}^{N} f_y^{(i)}$: the lateral capacity of the storey in the y-direction; $f_y^{(i)}$: the capacity of the ith resisting plane in the y-direction; and N: the number of resisting planes in the y-direction

V_{yc}: the capacity of resisting planes in the y-direction passing through the CM of the system; in practical terms, it will represent the capacity of all resisting planes 'close' to the CM

$T_o = \sum_{i=1}^{N} \left| f_y^{(i)} x^{(i)} \right| + \sum_{i=1}^{M} \left| f_x^{(i)} y^{(i)} \right|$: the torsional capacity of the system

$T_{\perp} = \sum_{i=1}^{M} f_x^{(i)} y^{(i)}$: the torque provided by the resisting planes in the orthogonal direction

$x_p = \frac{\sum_{i=1}^{N} f_y^{(i)} x^{(i)}}{V_{yo}}$: the strength eccentricity, or the first moment of strength

$V_{yu} =_{i \neq 2} \frac{\sum_{i=1}^{N} f_y^{(i)} x^{(i)}}{|x^{(i)}|}$: 'strength unbalance' in the storey

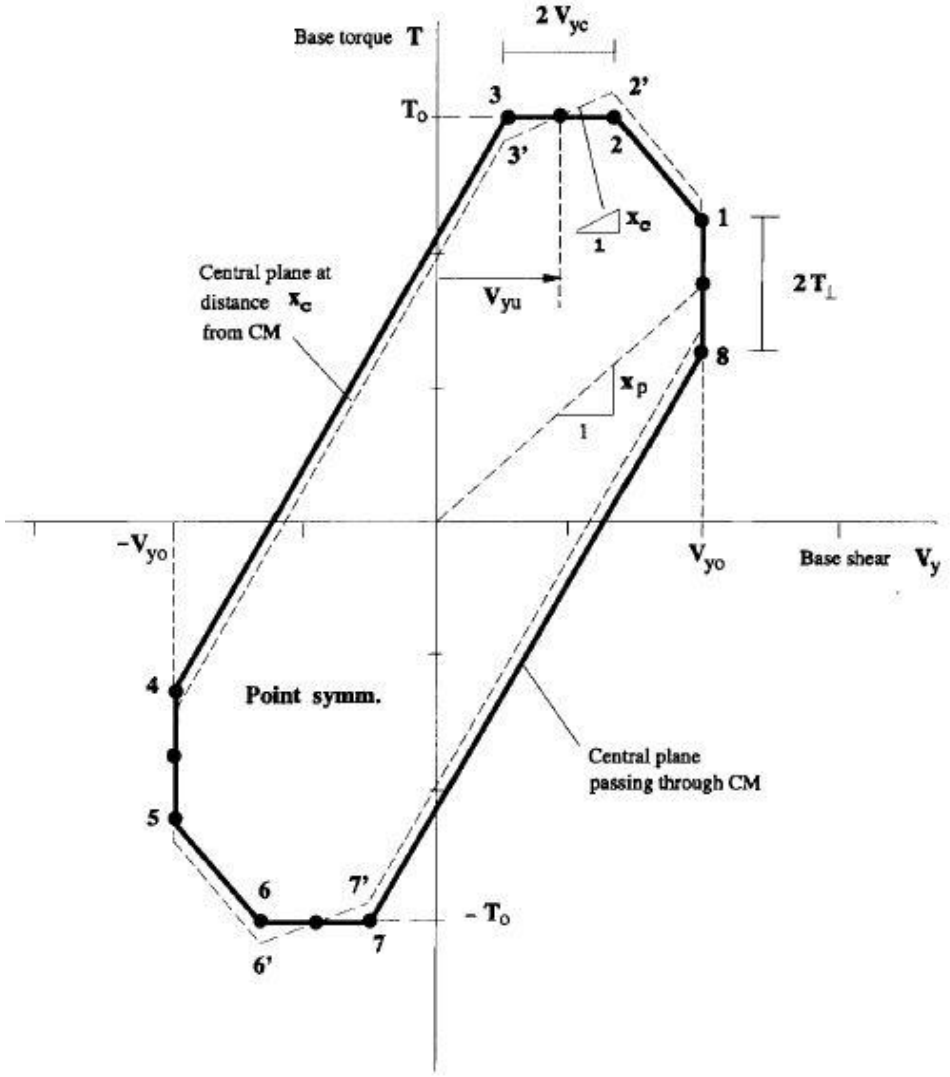

Figure 4.9 *Parametric representation of the SST surface [5]*

Subsequently, the seven parameters that control the shape of the SST surface are analyzed:

The normalized storey shear $\widehat{V_x}$ varies from 0 ($V_x = 0$) to 1 ($V_x = V_{xo}$) and is responsible for the variation of the SST surface along the Vx shear axis. This variation arises due to a lesser contribution to the torsional capacity of the system (because of the x-direction component of ground motion). In this case, the planes must be subjected to translation along this direction, which lead to a decrease in force-couple, consequently in torque resistance.

The lateral capacity V_{yo} represents the maximum shear of a purely translational mechanism of the storey and the limits of abscissas of the SST surface.

The capacity V_{yc} represents the capacity of the resisting planes passing through the CM. This capacity controls the length of the constant torque branches of the SST surface. These branches correspond to predominantly torsional mechanisms. This parameter should also contain the capacity of resisting planes 'close' to the CM.

The torsional capacity To represents the torque of a purely torsional mechanism of the storey and establishes the limits of the ordinates of the SST surface. Large values of To means that there are strong resisting planes along the edges while small values of To means that there are central cores on the plane.

The torsional capacity $T_{\perp}$ of the resisting planes in the orthogonal direction affects the length of the constant base shear branches of the SST surface, which represent predominantly translational mechanisms.

The strength eccentricity x_p is equal to the slope of the ray connecting the centre of the surface and the middle point of the constant base shear branch 1-8 (Figure 4.4). The value of x_p controls the skewness and width of the SST surface (i.e. large values of strength eccentricity lead to skewed and narrow surfaces).

The 'strength unbalance' V_{yu} affects the abscissa of the central point of the constant torque branch of the SST surface at positive torque (Figure 4.8). This parameter also controls the skewness of the surface and is equal to zero when the lateral capacities of the resisting planes on both sides of the CM are identical. Its physical meaning is that it represents the storey shear of the system for a purely torsional mechanism about a vertical axis passing through the central resisting plane.

The SST surface leads to two significant conclusions:

The SST surfaces for the exact and the SE models for two three-plane single-storey systems are identical (Figure 4.10).

The constant torque branches 2-3 and 6-7 of the SST surface means that the system has one (or several) central resisting planes passing through or 'close' to the CM. The SST surface of a storey with an eccentric central resisting plane located at distance x_c is the one with dashed lines (Figure 4.10). The abscissas of the vertices for the two SST surfaces are the same, while the ordinates varie. The ordinates of vertices 1, 2, 7 and 8 need to add the torque $V_{yc}x_c$, whereas the ordinates of the vertices 3, 4, 5 and 6 need to subtract the torque $V_{yc}x_c$.

The co-ordinates of the vertices 1, 4, 5 and 8 are defined still from equation (4.12), but the strength eccentricity is the one of the new system.

The ordinates from the vertices 2, 3, 6 and 7 are given from the following expressions:

$$\begin{aligned} y_2 &= T_o - \ T_{\perp}\widehat{V}_x + V_{yc}x_c \\ y_3 &= T_o - \ T_{\perp}\widehat{V}_x - V_{yc}x_c \\ y_6 &= -y_2 \\ y_7 &= -y_3 \end{aligned} \tag{4.14}$$

It is important to notice that the eccentric central plane causes an inclination of the segment 2-3 (6-7) in a slope equal to x_c.

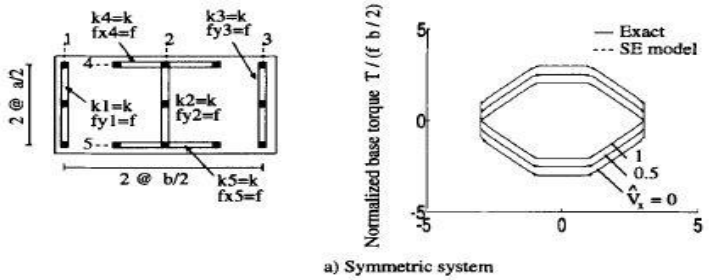

a) Symmetric system

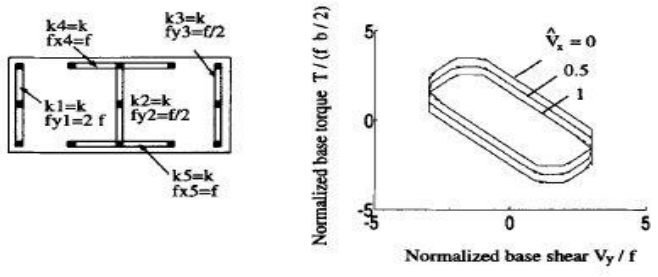

(b) Strength asymmetric system

Figure 4.10 *Comparison between the actual and theoretical SST surface in a symmetric and an asymmetric structure [5]*

Finally, the accuracy of the SE model is questioned. After experiments upon several asymmetric plan buildings [6], the following conclusions were derived:

The SE model can lead to safe conceptual evaluation.

The error of the SE is less than 20 percent - in terms of differences in peak deformations. Especially, for systems with stiffness and strength asymmetries in the same direction, the error in peak is even smaller (below 10 percent).

Because of the inaccuracy of the prediction of the plan rotation, errors arise, since this model can not describe the inelastic behavior of the system in the transition between its elastic and completely plastic states.

REFERENCES:

[1] T. Paulay, "Torsional mechanisms in ductile building systems," *Earthquake Eng. Structural Dynamics*, vol. 27, pp. 1101–1121, 1998.

[2] B. Mylimaj & W. K. Tso, "A strength distribution criterion for minimizing torsional response of asymmetric wall-type systems," *Earthquake Engng Struct. Dyn.*, vol. 31, pp. 99–120, 2002.

[3] Juan C. De La Llera & Anil K. Chopra, "Understanding the inelastic seismic behaviour of asymmetric-plan buildings," *Earthquake Eng. Structural Dynamics*, vol. 24, pp. 549–572, 1995.

[4] J. C. De La Llera & A. K. Chopra, "Accidental and natural torsion in earthquake response and design of buildings," *Report No. Eerc 94/07, University at California, Berkeley*, 1994.

[5] Juan C. De La Llera & Anil K. Chopra, "A simplified model for analysis and design of asymmetric plan buildings," *Earthquake Eng. Structural Dynamics*, vol. 24, pp. 573–594, 1995.

[6] J. A. Inaudi & J. C. De La Llera, "Dynamic analysis of nonlinear structures using state-space formulation and partitioned integration schemes," *Report No. Eerc 92/18, University of California, Berkeley*, 1992.

[7] T. A. Paulay "Displacement-based design approach to earthquake induced torsion in ductile buildings," *Eng. Structures*, vol. 9, no. 9, pp. 699–707, 1997.

6 Reaching the best possible design with optimization tools

Engineers' objective is to design resistant structures, which satisfy all the constraints (defined by codes) and also acquire specific attributes (low cost, low weight, small displacements just to name a few). This can be accomplished by the optimization process through a trial and error procedure, which is a computationally intensive task. Thanks to developments in Computational Mechanics the solution of this problem is feasible using evolutionary algorithms. Inspired by the Darwinian evolution, this procedure is an imitation of it.

The best known evolutionary algorithms include Genetic Algorithms (Gas) [1], Evolutionary Programming (EP) [2], Genetic Programming (GP) [3] and Evolution Strategies (ESs) [4,5].

6.1 Formulation of the optimization problem for torsionally balanced systems

Structural optimization problems are characterized by various objective and constraint functions that are generally non-linear functions of design variables. These functions are usually implicit, discontinuous and non-convex. The mathematical formulation of structural optimization problems with respect to the design variables, the objective and the constraint functions depends on the type of application. However, most optimization problems can be expressed in standard mathematical terms as a non-linear programming problem. A discrete structural optimization problem can be formulated in the following form:

$$\begin{aligned} &\min && F(\mathbf{s}) \\ &\text{subject to} && g_j(\mathbf{s}) \le 0 \quad j=1,...,m \\ & && s_i \in R^d, \quad i=1,...,n \end{aligned} \tag{5.1}$$

where $F(\mathbf{s})$ and $g_j(\mathbf{s})$ denote the objective and constraints functions respectively, R^d is a given set of discrete values, while the design variables s_i (i=1,...,n) can take values only from this set.

There are three main classes of structural optimization problems depending on the type of design variables employed: (i) sizing, (ii) shape and (iii) topology. In sizing optimization problems the aim is usually to minimize the weight of the structure under certain behavioral constraints on stresses and displacements. The design variables are most frequently chosen to be dimensions of the cross-sectional areas of the structure's members. In structural shape optimization problems the aim is to improve the performance of the structure by modifying its shape. The design variables are either some of the coordinates of the key points in the boundary of the structure or some other parameters that influence the shape of the structure. Structural topology optimization assists the designer to define the type of structure, which is best suited to satisfy the operating conditions for the problem at hand. In the current study the task of topology optimization is to define the position of the columns and the shear walls in each storey layout, while the task of sizing optimization is related to the size of the cross sections of the columns and the shear walls.

6.1.1 Definitions

There are some definitions that have to be given in order to facilitate the description of the problem and its handling of the optimization algorithm in the present study.

Torsionally balanced: A structural system is defined as torsionally balanced when, in any storey of the structure, the mass center coincides or almost coincides with the rigidity center.

For every column and shear wall, two architectural constraints are defined:

Architectural constraint 1: The first architectural constraint (AC-1) is related to the boundaries of the plan where a column or shear wall could be located. It is implemented as a rectangle with dimensions AC-1x × AC-1y. A design is considered as feasible, with respect to the AC-1 constraint, when the cross section of the columns and shear walls are contained in the corresponding rectangles. In Figures 5.1a and 5.1b two AC-1 rectangles are shown for a typical plan view of a concrete building.

Architectural constraint 2: The second architectural constraint (AC-2) is related to the topological position of the beams in conjunction with their supporting columns and/or shear walls. This constraint is implemented as a point located within the rectangle AC-1. The AC-2 is essential in assisting the optimization procedure to reach layouts where the beams and their cross points are supported by columns or shear walls. In any feasible design the AC-2 point should correspond to a joint of horizontal (beam) and vertical (column/shear wall) elements. In Figures 5.1a and 5.1b the AC-2 points are shown.

Column type: Two types of columns/shear walls are considered. *Type I* is defined as the column/shear wall where the AC-2 point corresponds to one of the corners of the rectangle AC-1 (see Figure 5.1a, the AC-2 point coincides with one of the corners of the AC-1 rectangle labeled as F); *Type II* is defined as the column/shear wall where the AC-2 point is located inside the rectangle AC-1 (see Figure 5.1b, the AC-2 point is located inside the AC-1 rectangle).

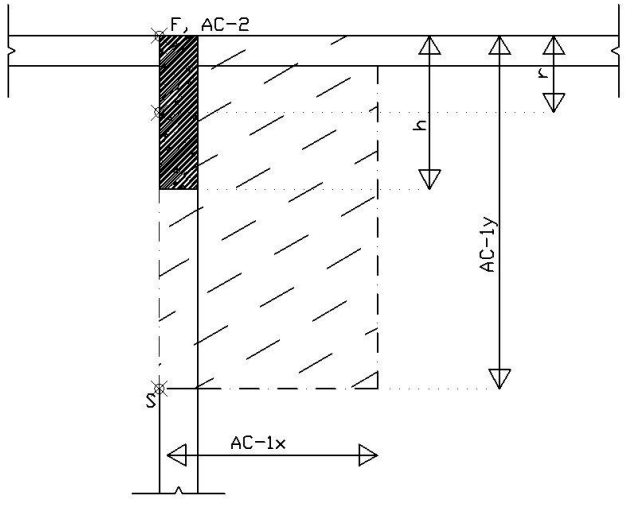

Figure 5.1a *Sample column Type I with its architectural constraints AC-1 and AC-2.*

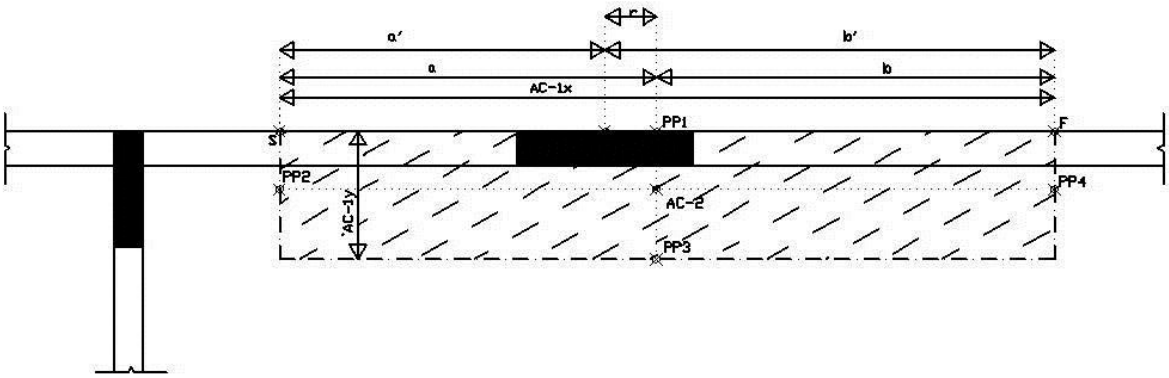

Figure 5.1b *Sample column Type II with its architectural constraints AC-1 and AC-2.*

6.1.2 Combined topology and sizing optimization

In the column/shear wall topology-sizing optimization problem for each storey pursued in this study, the basic goal is to formulate an optimization procedure that could lead to designs with improved earthquake resistance. The objective is to create torsionally balanced designs by minimizing the mass eccentricity eMC-RC between the mass center and the rigidity center of each storey subject to the behavioral constraints imposed by the design codes as well as to the architectural constraints. The design variables are divided in two categories: (i) topology design variables corresponding to the topology or layout of the columns and shear walls of the building and (ii) sizing design variables corresponding to the dimensions of the cross sections. The mathematical formulation of the problem can be stated as follows:

$$\begin{aligned} &\min && e_{\text{MC-RC}} = \sqrt{(x^i_{\text{MC}} - x^i_{\text{RC}})^2 + (y^i_{\text{MC}} - y^i_{\text{RC}})^2},\ i=1,2,...,n_{\text{storeys}} \\ &\text{subject to} && g_k(\mathbf{s}) \le 0,\ k=1,2,...,m \text{ (behavioral)} \\ &&& \left.\begin{aligned} t^i_{\text{lb,j}} \le r^i_j \le t^i_{\text{ub,j}},\ j=1,2,...,n_{\text{columns}} \\ s^i_{\text{lb,j}} \le h^i_j \le s^i_{\text{ub,j}},\ j=1,2,...,n_{\text{columns}} \end{aligned}\right\} \text{(architectural)} \end{aligned} \qquad (5.2)$$

where $(x^i_{MC}, y^i_{MC}), (x^i_{RC}, y^i_{RC})$ are the coordinates of the of the Mass Center (MC) and the Rigidity Center (RC), respectively, in the i-th group of storeys having the same layout in the plan. $n_{storeys}$ is the total number of groups of storeys in the structure, $g_k(\mathbf{s})$ are the behavioral constraints imposed by the design codes, r^i_j is the distance of the individual element center of the j-th column/shear wall in the i-th group of storeys from its corresponding AC-2 point (see Figure 1b where for simplicity reasons the superscript *i* and subscript *j* are omitted). $t^i_{lb,j}, t^i_{ub,j}$ are the lower and upper bounds of the topology design variables imposed by the architectural constraints. h^i_j is the largest edge of the j-th column/shear wall in the i-th group of storeys, corresponding to the sizing design variables (see Figure 1a where for simplicity reasons the superscript *i* and subscript *j* are omitted). $s^i_{lb,j}, s^i_{ub,j}$ are the lower and upper bounds of the sizing design variables imposed by the architectural constraints. As it will be seen in the following subsection of the problem's description there is a relation between the two kinds of design variables, topology and sizing, as well as their bounds.

6.1.3 Type of design variables

In this study the columns/shear walls are of rectangular shape with dimensions $h \times b$, where $h \geq b$. In our implementation the smallest column that is permitted to be allocated is 25×30 cm^2. In our formulation the sizing design variables of the columns and shear walls depend on the topology design variables which are defined first. This way, we solved the coupled topology – sizing problem that is a very difficult problem in structural optimization of buildings because of its complexity.

6.1.3.1 Topology design variables

As mentioned above the columns are divided in two categories. For Type I column/shear walls if AC-1x > AC-1y the final position of the individual element center of the column/shear wall will be allocated along the AC-1x rectangular edge, otherwise it will be allocated along the AC-1y edge. In the case of a square architectural constraint with AC-1x = AC-1y, the selection of the edge is random. For Type I column/shear walls the lower

bound of the topology design variable depends on the indicative minimum column size:

$$t^{i}_{lb,j} = \frac{h_{min}}{2} \tag{5.3}$$

where h_{min} is the minimum column size, which is equal to 30 cm, as mentioned above. The upper bound is equal to half the size of the corresponding architectural constraint edge (AC-1x or AC-1y):

$$t^{i}_{ub,j} = \frac{1}{2}\sqrt{(x_S - x_F)^2 + (y_S - y_F)^2} \tag{5.4}$$

In Figure 1a the largest edge of the AC-1 architectural constraint is AC-1y which will be selected as the edge to which the individual element center of the column/shear wall will be allocated. Furthermore, S (x_S, y_S) is the starting point and F (x_F, y_F) is the finishing point of the AC-1y edge, while the AC-2 point coincides with the finishing point F.

In Type II column/shear walls the edge of the AC-1 architectural rectangle, where the individual element center of the column will be allocated, has either been selected beforehand or it will be selected by the smallest distance of the projection of the AC-2 point to the four edges of the AC-1 rectangle. In Figure 5.1b the four projections points PPi, i=1,…,4 are shown. It can be seen that the distance between the points AC-2 and PP1 is the smallest one, so the edge AC-1x of the corresponding architectural constraint is selected for the allocation of the individual element center of the column/shear wall and the PP1 projection point is renamed to AC-2. S (xS,yS) is the starting point and F (xF,yF) is the finishing point of this edge. The allocation of the mass center of the column/shear wall is either on the left or on the right side of the renamed projection point PP1. Irrespectively of the side to which the individual element center will be allocated, the lower bound is defined to be equal to zero:

$$t^{i}_{lb,j} = 0 \tag{5.5}$$

The definition of the upper bound depends on which side of the projected AC-2 point the column mass center will be allocated.

$$t^{i}_{ub,j} = \frac{a}{2} \text{ (if on the left side)}$$
$$t^{i}_{ub,j} = \frac{b}{2} \text{ (if on the right side)} \quad (5.6)$$

where a is the distance of the new position of the AC-2 point from point S and b is the distance of the new position of the AC-2 point from point F (see Figure 5.1b).

6.1.3.2 Sizing design variables

As mentioned above topology design variables are defined first, followed by the sizing design variables, which are related to the topology design variables. In the case of Type I columns/shear walls there is a direct relation between the topology and sizing design variables for each column/shear wall. This sizing design variable is defined as *inactive*.

$$h^{i}_{j} = 2r^{i}_{j} \quad (5.7)$$

In the case of Type II column/shear walls there is an indirect relation between the two types of design variables defined by:

$$s^{i}_{lb,j} = 2r^{i}_{j}$$
$$s^{i}_{ub,j} = 2\min(a',b') \quad (5.8)$$

where a’ and b’ refer to the distance of the individual element center of the column/shear wall from points S and F, respectively, as it can be seen in Figure 5.1b. This sizing design variable is defined as *active*. In the case of Type II column/shear walls the sizing design variable is active, since their dimensions have to be defined by the optimizer and not by the topology design variables as in the case of Type I. The bounds of the size of the column/shear walls are dependent on the topological design variable r^{i}_{j}.

6.2 Optimization Procedures

Computer algorithms based on the process of natural evolution have been found capable to produce very powerful and robust search mechanisms although the similarity between these algorithms and the natural evolution is based on a crude imitation of biological reality. The resulting Evolutionary Algorithms (EA) are based on a population of individuals, each of which represent a search point in the space of potential solutions of a given problem. These algorithms adopt a selection process based on the fitness of the individuals and some recombination operators. The best known EA in this class include evolutionary programming (EP) [6], Genetic Algorithms (GA) [7,8] and Evolution Strategies (ES) [9,10]. The first attempt to use evolutionary algorithms took place in the sixties by a team of biologists [11] and was focused on building a computer program that would simulate the process of evolution in nature.

Both GA and ES imitate the biological evolution in nature and have three characteristics that differ from other conventional optimization algorithms: (i) In place of the usual deterministic operators, they use randomized operators: mutation, selection and recombination. (ii) Instead of a single design point, they work simultaneously with a population of design points in the space of design variables. (iii) They can handle - with minor modifications continuous, discrete or mixed optimization problems. The second characteristic allows for a natural implementation of GA and ES on a parallel computing environment [12,13,14].

In structural optimization problems, where the objective function and the constraints are highly non-linear functions of the design variables, the computational effort spent in gradient calculations required by the mathematical programming algorithms is usually large. In two recent studies by Papadrakakis et al. [15,16] it was found that probabilistic search algorithms are computationally efficient even if a greater number of analyses are needed to reach the optimum. These analyses are computationally less expensive than in the case of mathematical programming algorithms since they do not require gradient information. Furthermore, probabilistic methodologies were found to be more robust in

finding the global optimum due to their random search. Whereas mathematical programming algorithms may be trapped in local optima.

6.3 Solution of the structural optimization problem

6.3.1 Evolutionary optimization algorithms

ES were proposed for parameter optimization problems in the seventies by Rechenberg [90] and Schwefel [96]. Some differences between GA and ES stem from the numerical representation of the design variables used by these two algorithms. The basic GA operate on fixed-sized bit strings which are mapped to the values of the design variables, while ES work on real-valued vectors. Another difference can be found in the use of the genetic operators. Although, both GA and ES use the mutation and recombination (crossover) operators, the role of these genetic operators is different. In GA mutation only serves to recover lost alleles, while in ES mutation implements some kind of hill-climbing search procedure with self-adapting step sizes σ (or γ). In both algorithms recombination serves to enlarge the diversity of the population, and thus the covered search space. There is also a difference in treating constrained optimization problems where in the case of ES the death penalty method is always used, while in the case of GA only the augmented Lagrangian method can guarantee the convergence to a feasible solution. The ES, however, achieve a high rate of convergence than the GA due to their self-adaptation search mechanism and are considered more efficient for solving real world problems [61]. The ES were initially applied for continuous optimization problems, but recently they have also been implemented in discrete and mixed optimization problems [106,107]. The ES algorithms used in the present study are based on the work of Thierauf and Cai who applied the ES methodologies in sizing structural optimization problems having discrete and/or continuous design variables [85,86]. In the following paragraphs different versions of ES algorithms are discussed and compared in some test examples.

6.3.2 Genetic Algorithms (GA)

GA are probably the best-known evolutionary algorithms, receiving substantial attention in recent years. The GA model used in this study and in many other structural design applications refers to a model introduced and studied by Holland and co-workers [1]. In general the term genetic algorithm refers to any population-based model that uses various operators (selection-crossover-mutation) to evolve. In the basic genetic algorithm each member of this population will be a binary or a real valued string, which is sometimes referred to as a *genotype* or, alternatively, as a *chromosome*.

Different versions of GA have appeared in literature in the last decade dealing with methods for handling the constraints or techniques to reduce the size of the design vectors' population. In this section basic genetic algorithms are considered along with some of the most frequently used versions of GA.

6.3.2.1 The Basic Genetic Algorithms

The three main steps of the basic GA

Step 0 Initialization

The first step in implementing any genetic algorithm is to generate an initial population. In most cases the initial population is generated randomly. After creating an initial population, each member of the population is evaluated by computing its fitness function.

Step 1 Selection

A selection operator is applied to the current population in order to create an intermediate one. In the first generation the initial population is considered as the intermediate one, while in the next generations this population is created by the application of the selection operator.

Step 2 Generation

In order to create the next generation crossover and mutation operators are applied to the intermediate population in order to create the next

population. Crossover is a reproduction operator, which forms a new chromosome by combining parts of each of the two parental chromosomes. Mutation is a reproduction operator that forms a new chromosome by making (usually small) alterations to the values of genes in a copy of a single parent chromosome. The process of moving from the current population to the next population constitutes one generation in the evolution process of a genetic algorithm. If the termination criteria are satisfied then the procedure stops. Otherwise it returns to step 1.

Encoding

The first step before the activation of any operator is to encode the design variables of the optimization problem into a string of binary digits (l's and 0's) called a chromosome. If there are n design variables in an optimization problem and each design variable is encoded as a L-digit binary sequence, then a chromosome is a string of n×L binary digits. In the case of discrete design variables each discrete value is assigned to a binary string, while in the case of continuous design variables the design space is divided into a number of intervals (to the power of 2). The number of intervals L+1 depends on the tolerance given by the designer. If $s \in [s^{\ell}, s^{u}]$ is the decoded value of the binary string $< b_L b_{L-1} \ldots b_0 >$ then

$$s = DE(< b_L b_{L-1} \ldots b_0 >) = s^{\ell} + \frac{s^{u} - s^{\ell}}{2^{L} - 1} \left(\sum_{i=0}^{L} b_i \cdot 10^{i}\right) \tag{5.9}$$

where DE(**.**) is the function that performs the decoding procedure. In order to code a real valued number into the binary form the reverse procedure is followed.

Evaluation of fitness function

Apart from the objective function, the so-called fitness function is also used by a genetic algorithm. The evaluation of a string refers to the evaluation of that string's objective function value and it is independent of the evaluation of any other string. The fitness of that string, however, is always defined with respect to other members of the current population. The fitness is used to determine the selection probability of the

chromosome that will become the parent chromosome for the generation of the new chromosomes. In the basic genetic algorithm, fitness is defined by: $F_i'/\overline{F}'$ where F_i' is the penalized objective function associated with string i. $\overline{F}'$ is the average penalized objective function value of all the strings in the population. Fitness can also be assigned based on a string's rank in the population [30] or by sampling methods, such as tournament selection [51].

Selection

There are a number of ways to perform the selection. According to the *Tournament Selection* scheme each member of the intermediate population is selected to be the best member from a randomly selected group of members belonging to the current population. According to the *Roulette Wheel* selection scheme, the population is laid out in random order as in a pie graph, where each individual is assigned a place on the pie graph in proportion to its fitness. Next an outer roulette wheel is placed around the pie graph with *N* equally spaced pointers, where N is the size of the population. A single spin of the roulette wheel will now simultaneously pick all N members of the intermediate population.

Crossover

Crossover is a reproduction operator, which forms a new chromosome by combining parts of both 'parent' chromosomes. The simplest form is called the single-point crossover, in which an arbitrary point in the chromosome is selected. According to this operator, two 'offspring' chromosomes are generated, the first one is generated by copying all the information from the start of the parent A to the crossover point and all the information from the crossover point to the end of parent B. The second 'offspring' chromosome is generated by the reverse procedure. Variations exist which use more than one crossover point, or combine information from parents in other ways.

Mutation

Mutation is a reproduction operator, which forms a new chromosome by making (usually small) alterations to the values of the genes in a copy of a single parent chromosome.

6.3.2.2 Micro Genetic Algorithms (μGA)

The micro genetic algorithm was introduced by Krishnakumar [67] and applied to simple mathematical test functions and to the wind shear optimal guidance problem. The main objective of this scheme is to reduce the size of the population compared to the basic one. This corresponds, in the case of structural optimization problems discretized with finite elements, to less finite element analyses per generation. It is a known fact that GA generally exhibit poor performance with a small population size due to insufficient information processed and premature convergence to non-optimal results. A solution to this problem, suggested by Goldberg [53], could be to restart the evolution process in case of nominal convergence with a new initial population, which will include the best solution already achieved. Based on this suggestion Krishnakumar proposed the μGA which can be described by the following steps:

Step 0 Initialization

The first step generates a population of size 5 either randomly or by generating 4 strings randomly and by selecting 1 good string from any previous search, or according to the experience of the designer.

Step 1 Fitness evaluation

In this step the fitness of each individual is evaluated and the best string is determined. The best string is labeled as string 5 and it is carried to the next generation (elitist strategy). This way there is a guarantee that the information about good strings is not lost.

Step 2 Generation

According to the previous step the best individual of the current generation is carried out to the next one. The remaining four members of the next generation are chosen according to the tournament selection

operator. After the selection operator is terminated the crossover operator is applied.

Step 3 Convergence check

If the termination criteria is satisfied the process ends. Otherwise check for nominal convergence which is measured by bit wise convergence in case of binary coding or by comparing the design variables in case of real valued strings. If it converges go to step 0, else return to step 1.

A modified version of μGA is tested in this study, where only feasible designs are accepted for the evolution process. This version, which resembles the death penalty treatment of the constraints adopted by ES, is abbreviated to mμGA.

6.3.2.3 Methods for handling the constraints

Although genetic algorithms are initially developed to solve unconstrained optimization problems during the last decade several methods have been proposed for handling constrained optimization problems as well. The methods based on the use of penalty functions are employed in the majority of cases for treating constraint optimization problems with GA. In this study methods belonging to this category have been implemented and will be briefly described in the following paragraphs.

Method of static penalties

In this simple method the objective function is modified as follows

$$F'(s) = \begin{cases} F^{(n)}(s), & \text{if } s \in F \\ F^{(n)}(s) + p \cdot viol^{(n)}(s), & \text{otherwise} \end{cases} \quad (5.10)$$

where p is the static penalty parameter, $viol^{(n)}(s)$ is the sum of the violated constraints

$$viol(s) = \sum_{j=1}^{m} f_j(s) \quad (5.11)$$

and $F^{(n)}(s)$ is the objective function to be minimized, both normalized in [0,1], while F is the feasible region of the design space.

The sum of the violated constraints is normalized before it is used to calculate the modified objective function. The main advantage of this method is its simplicity. However, there is no guidance on how to choose the single penalty parameter p. If it is chosen too small the search will converge to an infeasible solution and if it is chosen too large a feasible solution may be located but it would be far from the global optimum. A large penalty parameter will force the search procedure to work away from the boundary, where the global optimum is usually located, that divides the feasible region from the infeasible one.

Method of dynamic penalties

The method of dynamic penalties was proposed by Joines and Houck [43] and applied to mathematical test functions. As opposed to the previous method, the penalty parameter does not remain constant during the optimization process. Individuals are evaluated (at generation g) by the following formula

$$F'(s) = F^{(n)}(s) + (c \cdot g)^{\alpha} viol^{(n)}(s) \tag{5.12}$$

with

$$viol(s) = \sum_{j=1}^{m} f_j^{\beta}(s) \tag{5.13}$$

where c, α and β are constants. A reasonable choice for these parameters was proposed as follows: c = 0.5÷2.0, α = β =1 or 2. However, for a high generation number the $(c \cdot g)^{\alpha}$ component of the penalty term takes on extremely large values which makes even the slightly violated designs not to be selected in subsequent generations. Thus, the system has little chances to escape from local optima. In most experiments reported by Michalewicz [71] the best individual was found in early generations.

6.3.2.4 Augmented Lagrangian method

The Augmented Lagrangian method (AL-GA) was proposed by Adeli and Cheng [1,3]. According to this method the constrained problem is transformed to an unconstrained one, by introducing two sets of penalty

coefficients γ [$(\gamma_1,\gamma_2,\ldots,\gamma_{M+N})$] and μ [$(\mu_1,\mu_2,\ldots,\mu_{M+N})$]. The modified objective function, for generation g, is defined as follows

$$F'(s,\gamma,\mu)=\frac{1}{L_f}F(s)+\frac{1}{2}\left\{\sum_{j=1}^{N}\gamma_j^{(g)}[(q_j-1+\mu_j^{(g)})^+]^2+\sum_{j=1}^{M}\gamma_{j+N}^{(g)}\left[\left(\frac{|d_j|}{|d_j^a|}-1+\mu_{j+N}^{(g)}\right)^+\right]^2\right\} \quad (5.14)$$

where L_f is a factor for normalizing the objective function; q_j is a non-dimensional ratio related to the stress constraints of the j^{th} element group (see eqs. (62), (63)); d_j is the displacement in the direction of the j^{th} examined degree of freedom, while d_j^a is the corresponding allowable displacement; N, M correspond to the number of stress and displacement constraint functions, respectively:

$$\left(q_j-1+\mu_j^{(I)}\right)^+=\max\left(q_j-1+\mu_j^{(I)},0\right) \quad (5.15)$$

$$\left(\frac{|d_j|}{|d_j^a|}-1+\mu_{j+N}^{(I)}\right)^+=\max\left(\frac{|d_j|}{|d_j^a|}-1+\mu_{j+N}^{(I)},0\right) \quad (5.16)$$

There is an outer step I and the penalty coefficients are updated at each step according to the expressions $\gamma_j^{(I+1)}=\beta\cdot\gamma_j^{(I)}$ and $\mu_j^{(I)}=\mu_j^{(I)}/\beta$, where $\mu_j^{(I+1)}=\mu_j^{(I)}+\max[\,con_{j,ave}^{(I)},-\mu_j^{(I)}]$ and $con_{j,ave}^{(I)}$ is the average value of the j^{th} constraint function for the I^{th} outer step, while the initial values of γ's and μ's are set equal to 3 and zero, respectively. Coefficient β is taken equal to 10 as recommended by Belegundu and Arora [32].

6.3.2.5 Segregated GA

The basic idea of the segregated GA (S-GA) [69] is to use two static penalty parameters instead of one, as in the method of static penalties. The two values of the penalty parameters are associated with two populations that have a different level of satisfaction of the constraints. Each of the groups correspond to the best performing individuals with respect to the associated penalty parameter.

The segregated GA can be described as follows:

Step 0 Initialization

Random generation of *2N* designs. The objective functions of the designs 1,2,...,N are evaluated using the p_h penalty parameter, while the remaining designs N+1,...,2N are evaluated using the p_ℓ penalty parameter.

Step 1 Selection

An intermediate population of size N is created by selecting the best individuals from both populations.

Step 2 Generation

Generate N offsprings using the basic operators mutation and crossover. The parents are evaluated using the p_h penalty parameter while the offsprings are evaluated using the p_ℓ. The process is then repeated by returning to *step 1*.

This version was used in [48] for the minimal weight design problem of a composite laminated plate.

6.3.3 Evolution Strategies (ES)

6.3.3.1 The Evolution Strategy algorithm

At the beginning of the procedure (in generation t=0) the initial parent population, composed by μ design vectors, is generated randomly (line 3). Lines 5 to 12 describe the main part of the ES algorithm, where every generation λ offspring vectors are generated by means of recombination and mutation. Recombination and mutation operators, described in lines 7 to 10, act on both design variable vectors s_l and distribution parameter vectors σ_l and a_l (both distribution parameter vectors denoted as y_l in the pseudo-code). In line 11 the objective and constraint functions are calculated in order to assess the design vectors in terms of the objective function value and feasibility. Figure 5.2 includes a pseudo-code of the ES algorithm which describes the procedure above.

Procedure $(\mu/\rho \dagger \lambda)$-ES; line

Begin 1

$g := 0;$ 2

$\texttt{initialize}\left(\mathfrak{P}_{\mathrm{p}}^{(0)} := \left\{\left(\mathbf{y}_m^{(0)}, \mathbf{s}_m^{(0)}, F(\mathbf{y}_m^{(0)})\right),\ m = 1, \ldots, \mu\right\}\right);$ 3

Repeat 4

For $l := 1$ **To** λ **Do Begin** 5

$\mathfrak{E}_l := \texttt{marriage}\left(\mathfrak{P}_{\mathrm{p}}^{(g)}, \rho\right);$ 6

$\mathbf{s}_l := \texttt{s\_recombination}(\mathfrak{E}_l);$ 7

$\mathbf{y}_l := \texttt{y\_recombination}(\mathfrak{E}_l);$ 8

$\tilde{\mathbf{s}}_l := \texttt{s\_mutation}(\mathbf{s}_l);$ 9

$\tilde{\mathbf{y}}_l := \texttt{y\_mutation}\left(\mathbf{y}_l, \tilde{\mathbf{s}}_l\right);$ 10

$\tilde{F}_l := F(\tilde{\mathbf{y}}_l)$ 11

End; 12

$\mathfrak{P}_{\mathrm{o}}^{(g)} := \left\{\left(\tilde{\mathbf{y}}_l, \tilde{\mathbf{s}}_l, \tilde{F}_l\right),\ l = 1, \ldots, \lambda\right\};$ 13

Case selection_type **Of** 14

(μ, λ) : $\mathfrak{P}_{\mathrm{p}}^{(g+1)} := \texttt{selection}\left(\mathfrak{P}_{\mathrm{o}}^{(g)}, \mu\right);$ 15

$(\mu + \lambda)$: $\mathfrak{P}_{\mathrm{p}}^{(g+1)} := \texttt{selection}\left(\mathfrak{P}_{\mathrm{o}}^{(g)}, \mathfrak{P}_{\mathrm{p}}^{(g)}, \mu\right)$ 16

End; 17

$g := g + 1;$ 18

Until termination_condition 19

End 20

Figure 5.2 *Pseudo-code of the ES algorithm*

6.3.3.2 Multi-Membered ES

In this case a population of μ parents will produce λ offsprings.

Formulation of the optimization problem

The optimization problem is considered:

$$F(s) \rightarrow min$$

$$s = \{s_1, s_2, \ldots\ldots, s_n\}^T$$

$$l_i \leq s_i \leq u_i, i = 1,2, \ldots\ldots, n$$

$$g_j(s) \geq 0, j = 1,2, \ldots\ldots, m$$

$$h_j(s) = 0, j = m+1, m+2, \ldots\ldots, t \qquad (5.17)$$

where

$F(s)$: the objective function

s: the vector corresponds to the design variables

$g_j(s), h_j(s)$: the constraint functions

Recombination

For every offspring vector a temporary parent vector $\tilde{s} = \{\tilde{s}_1, \tilde{s}_2, \dots\dots, \tilde{s}_n\}^T$ is initially built by means of recombination. For a continuous problem, five recombination cases which can be used selectively are given:

$$\begin{aligned} &\tilde{s}_i = s_{a,i} \; or \; s_{b,i} \quad randomly && (A) \\ &\quad 1/2\left(s_{a,i} + s_{b,i}\right) && (B) \\ &\quad s_{bj,i} && (C) \\ &\quad s_{a,i} \; or \; s_{bj,i} \quad randomly && (D) \\ &\quad 1/2\left(s_{a,i} + s_{bj,i}\right) && (E) \end{aligned} \tag{5.18}$$

where

$\tilde{s}_i$: the ith component of the temporary parent vector $\tilde{S}$

$s_{a,i}, s_{b,i}$: the ith components of the vectors S_a and S_b which are two parent vectors randomly chosen from the population

$s_{bj,i}$: the ith component of $\tilde{S}$ is chosen randomly from the ith components of all μ parent vectors

One of the advantages which recombination offers is that different good building blocks from different parents are mixed together, thus combining the good properties of the parents in the offspring. [1]

Mutation

The parent $S_p^{(g)}$ of the generation g produces an offspring $S_o^{(g)}$, whose genotype is slightly different from that of the parent:

$$S_o^{(g)} = S_p^{(g)} + Z^{(g)} \quad (5.19)$$

where

$Z^{(g)} = \left[Z_1^{(g)}, Z_2^{(g)}, \ldots\ldots, Z_n^{(g)}\right]^T$: a random vector

In order to choose the random vector, since the mutation is of random and purposeless events, a probability distribution is used according to which small changes occur frequently but large ones rarely. Two requirements arise together by analogy with the natural evolution: (i) the expectation value ξ_i for a component Z_i has the value zero; and (ii) the variance σ_i^2, the average squared deviation from the mean, is small. [2]

Selection

There are two different types of multi-membered ES:

$\underline{(\mu + \lambda) - ES}$: The best μ individuals are selected from a temporary population of $(\mu + \lambda)$ individuals to form the parents of the next generation.

$\underline{(\mu, \lambda) - ES}$: The μ individuals produce λ offsprings and the selection process defines a new population of μ individuals from the set of λ offsprings. Obviously, this strategy relies on a birth surplus, on $\lambda > \mu$ in a strict Darwinian sense of natural selection.

For the second type, the life of each individual is limited to one generation. This allows the $(\mu, \lambda) - ES$ selection to perform better on problems with an optimum moving over time, or on problems where the objective function is noisy.

6.3.3.3 The modified evolution strategies

For the solution of discrete optimization problems modified evolution strategies are proposed (Chai, 1995; Cai and Thierauf, 1993)

Formulation of the optimization problem

The discrete optimization problem is considered:

$F(s) \rightarrow min$

$s = \{s_1, s_2, \ldots\ldots, s_n\}^T$

$$l_i \le s_i \le u_i,\ i = 1,2,\ldots..,n$$

$$s_i \epsilon R^d,\ i = 1,2,\ldots..,n$$

$$g_j(s) \ge 0, j = 1,2,\ldots..,m$$

$$h_j(s) = 0, j = m+1, m+2,\ldots..,t \qquad (5.20)$$

where

$F(s)$: the objective function

s: the vector corresponds to the design variables

$g_j(s), h_j(s)$: the constraint functions

R^d: a given set of discrete design values, the design variables s_i can only take discrete values of this set

Recombination

For every offspring vector a temporary parent vector $\tilde{s} = \{\tilde{s}_1, \tilde{s}_2, \ldots\ldots, \tilde{s}_n\}^T$ is initially built by means of recombination. For a continuous problem, five recombination cases which can be used selectively are given:

$$\begin{aligned}
&\tilde{s}_i = s_{a,i}\ or\ s_{b,i}\ \ randomly && (A)\\
&\quad s_{m,i}\ or\ s_{b,i}\ randomly && (B)\\
&\quad s_{bj,i} && (C)\\
&\quad s_{a,i}\ or\ s_{bj,i}\ \ randomly && (D)\\
&\quad s_{m,i}\ or\ s_{bj,i}\ \ randomly && (E)
\end{aligned} \qquad (5.21)$$

where

$\tilde{s}_i$: the ith component of the temporary parent vector $\tilde{S}$

$s_{a,i}, s_{b,i}$: the ith components of vectors S_a and S_b which are two parent vectors randomly chosen from the population.

$s_{bj,i}$: the ith component of $\tilde{S}$ is chosen randomly from the ith components of all μ parent vectors.

$s_{m,i}$: the vector S_m is not chosen randomly but is the best of the μ vectors in the gth generation, in the cases of (B) and (E) if the information from the best parent is used it can lead to a better convergence.

One of the advantages which recombination offers is that different good building blocks from different parents are mixed together, thus combining the good properties of the parents in the offspring.[23]

Mutation

The parent $S_p^{(g)}$ of the generation g produces an offspring $S_o^{(g)}$, whose genotype is slightly different from that of the parent:

$$S_o^{(g)} = S_p^{(g)} + Z^{(g)} \tag{5.22}$$

where

$Z^{(g)} = \left[Z_1^{(g)}, Z_2^{(g)}, \ldots\ldots, Z_n^{(g)}\right]^T$: a random vector

The mutation operator, in the continuous version of the ES based optimization, produces a normally distributed random change vector $Z^{(g)}$, whose each component has a small standard deviation value σ_i and zero expectation. This means that there is a possibility that all components of a parent vector will need to be changed but the changes are usually small. [2]

In the discrete version of the ESs we have to change the generator of the random vector $Z^{(g)}$ in order to produce a modified vector that leads from one discrete value to another adjacent one. The difference between any two adjacent values is usually not small, which goes against the second requirement that arises by analogy to the natural evolution. For this reason, it is suggested that not all of the n components of a parent vector, but only few (say l) will be randomly changed every time. This means that (n-l) components of the randomly changed vector $Z^{(g)}$ have zero value. [23]

The components of the randomly changed vector $Z^{(g)}$ have the form:

$z_i^{(g)}$= (κ+1)δx$_i$ for l randomly chosen components and 0 for n-l other components (5.23)

Where:

δx$_i$: the current difference between two adjacent values in the discrete set

κ: a Poisson distributed integer random number with the following distribution

$$p(\kappa) = \frac{(\gamma)^{\kappa}}{\kappa!} e^{-\gamma} \quad (5.24)$$

where γ: the deviation and the expectation of the random number κ

From the equation above it is proved that the random change vector $Z^{(g)}$ depends on γ. A uniformly distributed random choice decides which l components should be changed according to equation (5.24). For structural optimization problems a suitable l value ranges from 8 to 12.

Selection

There are two different types of multi-membered ES:

$\underline{(\mu+\lambda)-ES}$: The best μ individuals are selected from a temporary population of $(\mu+\lambda)$ individuals to form the parents of the next generation.

$\underline{(\mu,\lambda)-ES}$: The μ individuals produce λ offsprings and the selection process defines a new population of μ individuals from the set of λ offsprings. Obviously, this strategy relies on a birth surplus, on $\lambda > \mu$ in a strict Darwinian sense of natural selection.

For the second type, the life of each individual is limited to one generation. This allows the $(\mu,\lambda)-ES$ selection to perform better on problems with an optimum moving over time, or on problems where the objective function is noisy.

The suggested **convergence criteria** for discrete optimization can be used selectively:

If the best value of the objective function in the last k$_I$(>4nμ/λ) generations has not been improved

If the mean value of the objective values from all parent vectors in the last k_{II}(>2nμ/λ) has not been improved by less than a given value ε_b

If the relative difference between the best objective function value and the mean value of the objective values from all parent vectors in the current generation is less than a given value ε_c(=0.0001)

If the ratio μ_b/μ has reached a given value ε_d(=0.5 to 0.8) where μ_b is the number of parent vectors in the current generation with the best objective function value.

The ES algorithm for structural optimization applications can be stated as follows [3]:

1. *Initialization step:* random generation of s_j (j = 1,2,...,μ) parent vectors
2. *Analysis step:* solve $\mathbf{K}(\mathbf{s}_i)\mathbf{u}_i = \mathbf{f}$, (i=1,2,...,μ)
3. *Constraints check :* all parent vectors become feasible
4. *Offspring generation:* generate $\mathbf{s}_j$, (j=1,2,...,λ) offspring vectors
5. *Analysis step:* solve $\mathbf{K}(\mathbf{s}_j)\mathbf{u}_j = \mathbf{f}$, (j=1,2,...,λ)
6. *Constraints check:* if satisfied continue, else change $\mathbf{s}_j$ and go to *step 4*
7. *Selection step:* selection of the next generation parents according to (μ+λ) or (μ,λ) schemes
8. *Convergence check:* If satisfied stop, else go to *step 3*

6.3.3.4 Evolution Strategies for discrete optimization problems

Evolution Strategies were proposed for parameter optimization problems in the seventies by Rechenberg (1973). ES was initially applied for continuous optimization problems, but recently they have also been implemented in discrete and mixed optimization problems (Lagaros et al. 2004; Papadrakakis and Lagaros 2002). In engineering practice the design variables are not continuous because the structural parts are usually constructed with certain variations of their dimensions. Thus design variables can only take values from a predefined discrete set. The basic differences between discrete and continuous ES are restricted to the mutation and the recombination operators.

6.3.3.5 Recombination and mutation

In any generation μ parents produce λ offsprings. The genotype of any descendant differs only slightly from that of its parents. For every offspring vector a temporary parent vector $\tilde{\mathbf{s}} = [\tilde{s}_1, \tilde{s}_2, ..., \tilde{s}_n]^T$ is first built by means of recombination. In our implementation the following discrete recombination scheme has been used

$$\tilde{s}_i = s_{a,i} \text{ or } s_{b,i} \text{ randomly} \tag{5.25}$$

$\tilde{s}_i$ is the i-th component of the temporary parent vector $\tilde{\mathbf{s}}$, $s_{a,i}$ and $s_{b,i}$ are the i-th components of vectors $\mathbf{s}_a$ and $\mathbf{s}_b$ which are two parent vectors randomly chosen from the population. From the temporary parent $\tilde{\mathbf{s}}$ an offspring can be created through the mutation operator.

An offspring $\mathbf{s}_o^{(g)}$ is generated through the temporary parent $\tilde{\mathbf{s}}^{(g)}$ of the g-th generation using the mutation operator as follows:

$$\mathbf{s}_o^{(g)} = \tilde{\mathbf{s}}^{(g)} + \mathbf{z}^{(g)} \tag{5.26}$$

where $\mathbf{z}^{(g)} = [z_1^{(g)}, z_2^{(g)}, ..., z_n^{(g)}]^T$ is a random vector. The terms of vector $\mathbf{z}^{(g)}$ is derived from:

$$z_i^{(g)} = \begin{cases} (\kappa + 1)\delta s_i & \text{for } \ell \text{ randomly chosen components} \\ 0 & \text{for n-}\ell \text{ other components} \end{cases} \tag{5.27}$$

where δs_i is the difference between two adjacent values in the discrete set and κ is a random integer number, which follows the Poisson distribution:

$$p(\kappa) = \frac{(\gamma)^\kappa}{\gamma!} e^{-\gamma} \tag{5.28}$$

γ is the standard deviation as well as the mean value of the random number κ. The choice of ℓ depends on the size of the problem and it is usually taken as being 1/5 of the total number of design variables, while the ℓ components are selected using a uniform random distribution.

Selection

There are two different types of selection schemes:

(μ+λ)-ESs: Where the best μ individuals are selected from a temporary population of (μ+λ) individuals to form the parents of the next generation.

(μ,λ)-ESs: Where the μ individuals produce λ offsprings ($\mu \leq \lambda$) and the selection process defines a new population of μ individuals from the set of λ offsprings only.

The optimization procedure terminates when the following termination criterion is satisfied: the ratio μ_b/μ has reached a given value ε_d (=0.8 in the current study) where μ_b is the number of the parent vectors in the current generation with the best objective function value.

6.3.3.6 Types of Algorithms

The ES can be divided into a two-membered evolution strategy (2-ES) or a multi-membered evolution strategy (M-ES).

The two−member ES

The earliest evolution strategies were based on a population consisting of one individual only. The two-membered scheme is the minimal concept for an organic evolution imitation. The two principles of mutation and selection, which Darwin recognized to be most important in 1859, are taken as rules for variation of the parameters and for recursion of the iteration sequence respectively.

The two-membered ES for the solution of the optimization problem works in two steps:

Step 1 (mutation). The parent $s_p^{(g)}$ of generation g produces an offspring $s_o^{(g)}$, whose genotype is slightly different from that of the parent

$$s_o^{(g)} = s_p^{(g)} + z^{(g)} \tag{5.29}$$

where $z^{(g)} = \left[z_1^{(g)}, \quad z_2^{(g)}, \quad \ldots, \quad z_n^{(g)}\right]^T$ is a random vector.

Step 2 (selection). The selection chooses the best individual between the parent and the offspring to survive

$$s_p^{(g+1)} = \begin{cases} s_o^{(g)} & \text{if } g_i(s_o^{(g)}) \le 0 \;\; i = 1,2,...,1 \;\; \text{and} \;\; f(s_o^{(g)}) \le f(s_p^{(g)}) \\ s_p^{(g)} & \text{otherwise} \end{cases} \tag{5.30}$$

The question of how to choose the random vector $z^{(g)}$ in *Step 1* is very important. This choice has the role of mutation. Mutation is understood to be random, purposeless events, which occur very rarely. If one interprets them, as is done here, as a sum of many individual events, it is then a natural choice to use a probability distribution according to which small changes occur frequently, but large ones only rarely. Two requirements arise together by analogy with the natural evolution: (i) the expected mean value ξ_i for a component $z_i^{(g)}$ to be zero; and (ii) the variance σ_i^2, the average squared deviation from mean value, is small.

The probability density function for normally distributed random events is given by

$$p(z_i^{(g)}) = \frac{1}{\sqrt{(2\pi)\sigma_i}} \exp\left(-\frac{(z_i^{(g)} - \xi_i)^2}{2 - \sigma_i^2}\right) \tag{5.31}$$

When $\xi_i=0$ the so-called $(0, \sigma_i)$ normal distribution is obtained. By analogy with other deterministic search strategies, σ_i can be called a step length, in the sense that it represents average values of the random steps' length. If the step length is too small the search takes an unnecessarily large number of iterations. On the other hand, if the step length is too large the optimum can only be crudely approached and the search might even get stuck far away from the global optimum. Thus, as in all optimization strategies, the step length control is the most important part of the algorithm after the recursion formula, and it is further more linked closely to the convergence behavior.

Multi-membered ES

The multi-membered evolution strategies differ from the previous two-membered strategies in the size of the population. In this case a population of μ parents will produce λ offsprings. Thus the two steps are defined as follows:

Step 1 (recombination and mutation). The population of μ parents at g-th generation produces λ offsprings. The genotype of any descendant differs only slightly from that of its parents.

Step 2 (selection). There are two different types of the multi-membered ES:

(μ+λ)-ES: The best μ individuals are selected from a temporary population of $(\mu+\lambda)$ individuals to form the parents of the next generation.

(μ,λ)-ES: The μ individuals produce λ offsprings ($\mu<\lambda$) and the selection process defines a new population of μ individuals from the set of λ offsprings only.

For the second type, the existence of each individual is limited to one generation. This allows the (μ,λ)-ES selection to perform better on problems with an optimum moving over time, or on problems where the objective function is noisy.

In *Step 1*, for every offspring vector a temporary parent vector $\tilde{s} = [\tilde{s}_1, \tilde{s}_2, ..., \tilde{s}_n]^T$ is initially built by means of recombination. For continuous problems the following recombination cases can be used

$$\tilde{s}_i = \begin{cases} s_{\alpha,i} \text{ or } s_{b,i} \text{ randomly} & \text{(a)} \\ 1/2(s_{\alpha,i} + s_{b,i}) & \text{(b)} \\ s_{bj,i} & \text{(c)} \\ s_{\alpha,i} \text{ or } s_{bj,i} \text{ randomly} & \text{(d)} \\ 1/2(s_{\alpha,i} + s_{bj,i}) & \text{(e)} \end{cases} \quad (5.32)$$

where $\tilde{s}_i$ is the i-th component of the temporary parent vector $\tilde{s}$, $s_{\alpha,i}$ and $s_{b,i}$ are the i-th components of vectors s_a and s_b which are two parent vectors randomly chosen from the population. In case (5.32c), $\tilde{s}_i = s_{bj,i}$ means that the i-th component of $\tilde{s}$ is chosen randomly from the i-th components of all μ parent vectors. From the temporary parent $\tilde{s}$ an offspring can be created in the same way as in two-membered ES (eq. (5.29)).

Multi-membered ES termination criteria are the following: (i) when the absolute or relative difference between the best and the worst objective function values is less than a given value ε_1, or (ii) when the mean value of the objective values from all parent vectors in the last $2*n$ generations has not been improved by less than a given value ε_2.

6.3.3.7 ES in structural optimization problems

In this work ESs methods are proposed for parameter optimization problems and have three characteristics that differentiate them from other conventional optimization algorithms: (i) in place of usual deterministic operators, they use randomized operators: recombination, mutation and selection; (ii) instead of a single design point, they work simultaneously with population of design points in the space of variables; (iii) they can handle continuous, discrete and mixed optimization problems. The ESs also achieve a higher rate of convergence than GAs owing to their self-adaptation search mechanism and are considered more efficient for solving real world problems. In the ES algorithm, each individual is equipped with a set of parameters:

$$a = [s, \sigma, a] \epsilon I_c$$

$$I_c = R^{n_s} \times R_+^{n_\sigma} \times [-\pi, \pi]^{n_a} \quad (5.33)$$

where

$s \epsilon R^{n_s}$: the vector of the design variables

$\sigma \epsilon R_+^{n_\sigma}$: vector σ corresponds to the standard deviations ($1 \leq n_\sigma \leq n_s$) of the normal distribution

$a \epsilon [-\pi, \pi]^{n_a}$: vector a corresponds to the inclination angles

($n_a = \left(n_c - \frac{n_\sigma}{2}\right)(n_\sigma - 1)$) defining linearly correlated mutations of the continuous design variables s.

The ES optimization procedure starts with a set of parent vectors and if any of these parent vectors give an infeasible design then this parent vector is modified until it becomes feasible. Subsequently, the offsprings are generated and checked if they are in the feasible region. The

computational efficiency of the multi-membered ES is affected by the number of parents and offsprings involved. It has been observed that values of μ and λ should be close to the number of the design variables in order to produce best results [64].

The ES algorithm for structural optimization applications can be stated as follows:

1. *Selection step:* selection of s_i (i = 1,2,...,μ) parent vectors of the design variables

2. *Analysis step:* solve $K(s_i)u_i = f$ (i=1,2,...,μ), where K is the stiffness matrix of the structure and f is the loading vector

3. *Constraints check:* all parent vectors become feasible

4. *Offspring generation:* generate s_j, (j=1,2,...,λ) offspring vectors of the design variables

5. *Analysis step:* solve $K(s_j)u_j = f$ (j=1,2,...,λ)

6. *Constraints check:* if satisfied continue, else change s_j and go to *step 4*

7. *Selection step:* selection of the next generation parents according to (μ+λ) or (μ,λ) selection schemes

Convergence check: If satisfied stop, else go to *step 3*

6.3.3.8 Contemporary ES (C-ES) - The (μ, λ, θ) Evolution Strategies

This is a more general ES version, which was proposed by Schwefel and Rudolph [74] for application in continuous problems but has not been applied either to continuous or to discrete optimization problems [71]. Considering the two schemes of the multi-membered evolution strategy, namely the (μ+λ) and the (μ,λ) ES, only empirical results have shown that the 'plus' version performs better in structural optimization problems [18,75]. The (μ,λ)-ES version is in danger to diverge because the so far best position is not preserved within the generation cycle (the so-called

elitist strategy). The 'comma' version implies that each parent can have children only once (duration of life: one generation or one reproduction cycle), whereas in the 'plus' version individuals may live eternally if no child achieves a better or at least the same improvement in the objective function.

The C-ES introduce a maximal life span of $\theta \geq 1$ reproduction cycles which gives the 'comma' scheme for $\theta = 1$ and the 'plus' one for $\theta = \infty$. If $\mu \geq 1$ is the number of parents, $\lambda > \mu$ is the number of offsprings, then ρ with $1 \leq \rho \leq \mu$ is the number of ancestors for each descendant. This ES version differs in two points from the basic one: (i) Free number of parents are involved in reproduction ranging from 1 to μ. (ii) A finite number of reproduction cycles per individual is performed, not one (1) or infinite (∞) as for the 'comma' and the 'plus' schemes, respectively. The selection operator used in the C-ES can be similar to the one used by the genetic algorithms.

6.3.3.9 Adaptive ES (A-ES)

The handling of the constraints by the basic ES is based on the death penalty approach [8], where every infeasible design point is discarded. Thus the process is directed to search only in the feasible region of the design space. Due to this approach many designs that are examined by the optimizer during the search process and are close to the acceptable design space are rejected leading to the loss of valuable information. The idea introduced in this work is to use soft constraints during the first stages of the search and as the search approaches the region of the global optimum the constraints to become more severe until they reach their real values.

The implementation of A-ES in structural optimization problems is straightforward and follows the same steps described in the section of the basic ES. The ES optimization procedure starts with a population of parent vectors, while a level of violation of the constraints is determined. If any of these parents corresponds to an infeasible design lying outside the extended design space then this parent is modified until it becomes 'feasible'. Then the offsprings are generated and checked if they are in the

'feasible' region according the current level of violation. In every generation the values of the objective function are compared between the parent and the offspring vectors and the worst vectors are rejected, while the remaining ones are considered to be the parent vectors of the new generation. This procedure is repeated until the termination criterion is satisfied.

In this adaptive scheme a nominal convergence check is adopted for the determination of the level of violation of constraints. Nominal convergence occurs when the mean value of the objective function of the designs of the current population is relatively close to the best design achieved until the current generation, according to the expression

$$\frac{\overline{F}^{(g)} - F_{best}^{(g)}}{\overline{F}^{(g)}} \leq \varepsilon_{ad} \tag{5.34}$$

where $\overline{F}^{(g)}$ is the mean objective function value, $F_{best}^{(g)}$ is the best objective function value of all parents in the g-th generation, and ε_{ad}=0.05.

The A-ES steps can be stated as follows:

1. Initialization step: Selection of s_i, (i = 1,2,...,μ) parent vectors of the design variables and the percentage of violation of the constraints v_0 (usually taken between 20-50%)

2. Analysis step: Solve $K(s_i)u_i = f$ (i=1,2,...,μ)

3. Constraints check: All parent vectors become "feasible", within the prescribed level of constraints violation v_0

4. Offspring generation: Generate s_j, (j=1,2,...,λ) offspring vectors of the design variables.

5. Analysis step: Solve $K(s_j)u_j=f$ (j=1,2,...,λ)

6. Nominal convergence check: If nominal convergence has occurred the level of violation v_g becomes more severe by reducing its value by a small quantity (usually 0.1 or 0.2)

7. Constraints check: If satisfied according to the current level of violation v_g continue, else change s_j and return to *step 4*

8. Selection step: Selection of the next generation parents according to (μ+λ) or (μ,λ) selection schemes

Convergence check: If satisfied stop, else return to *step 3*

6.3.3.10 ES for discrete optimization problems

In engineering practice the design variables are not continuous because the structural parts are usually constructed with certain variations of their dimensions. Thus design variables can only take values from a predefined discrete set. For the solution of discrete optimization problems Thierauf and Cai [85] have proposed a modified ES algorithm. The basic differences between discrete and continuous ES are focused on the mutation and the recombination operators. In the discrete version of ES the random vector $z^{(g)}$ is properly generated in order to force the offspring vector to move to another set of discrete values.

The fact that the difference between any two adjacent values can be relatively large is against the requirement that the variance σ_i^2 should be small. For this reason it is suggested that not all the components of a parent vector, but only a few of them (e.g. ℓ) should be randomly changed in every generation. This means that n-ℓ components of the randomly changed vector $z^{(g)}$ will have zero value. In other words, the terms of vector $z^{(g)}$ are derived from

$$z_i^{(g)} = \begin{cases} (\kappa + 1)\delta s_i & \text{for } \ell \text{ randomly chosen components} \\ 0 & \text{for n - } \ell \text{ other components} \end{cases} \tag{5.35}$$

where δs_i is the difference between two adjacent values in the discrete set and κ is a random integer number which follows the Poisson distribution

$$p(\kappa) = \frac{(\gamma)^{\kappa}}{\kappa!} e^{-\gamma} \tag{5.36}$$

γ is the standard deviation as well as the mean value of the random number κ. The choice of ℓ depends on the size of the problem and it is

usually taken as being 1/5 of the total number of design variables. The ℓ components are selected using uniform random distribution in every generation.

For discrete optimization the procedure terminates when one of the following termination criteria is satisfied: (i) when the best value of the objective function in the last $4*n*\mu/\lambda$ generations remains unchanged, (ii) when the mean value of the objective values from all parent vectors in the last $2*n*\mu/\lambda$ generations has not been improved by less than a given value ε_b (=0.0001), (iii) when the relative difference between the best objective function value and the mean value of the objective function values from all parent vectors in the current generation is less than a given value ε_c(=0.0001), (iv) when the ratio μ_b/μ has reached a given value ε_d (=0.5 to 0.8) where μ_b is the number of parent vectors in the current generation with the best objective function value.

6.3.4 Hybrid Optimization Algorithms

Several hybrid optimization algorithms which combine evolutionary computation techniques with deterministic procedures for numerical optimization problems have been recently investigated. Papadrakakis et al. [64] used evolution strategies with the SQP method, while Waagen et al. [91] combined evolutionary programming with the direction set method of Hooke and Jeeves [42]. The hybrid implementation proposed in [64] was found very successful on shape optimization problems, while the method proposed in [91] was applied to unconstrained mathematical test functions. Myung et al. [52] considered an approach similar to Waagen et al., but they experimented with constrained mathematical test functions. Myung et al. combined a floating-point evolutionary programming technique, with a method developed by Maa and Shanblatt [49] applied to the best solution found by the evolutionary programming technique. The second method iterates until the system defined by the combination of the objective function, the constraint functions and the design variables reach equilibrium.

A characteristic property of the SQP based optimizers is that they usually capture the right path to the nearest optimum very fast, irrespective of its

local or global optimum nature. However, after locating the area of this optimum it might oscillate until all constraints are satisfied since it is observed that even small constraint violations often slow down the convergence rate of the method. On the other hand, EA proceed with a slower rate, due to their random search, but the absence of strict mathematical rules, which govern the convergence rate of the mathematical programming methods, make EA less vulnerable to local optima. Therefore it is most likely to converge towards the global optimum in non-convex optimization problems. These two facts gave the motivation to combine EA with MP methodologies. Between the two EA examined in this study the basic genetic algorithms seem to be faster than evolution strategies since they do not always operate on the feasible region of the design space as the evolution algorithms. However, they are most often found unable to converge to feasible designs.

In order to benefit from the advantages of both methodologies a hybrid approach is proposed, which combines the two optimization methodologies in an effort to increase the robustness and the computational efficiency of the optimization procedure. Two combinations of SQP and EA methodologies are implemented : (i) In the first approach the SQP method is used first, giving a design very close to the optimum, followed by EA in order to accelerate convergence and avoid the oscillations of SQP due to small constraint violations around the optimum. The transition from one algorithm to the other is performed when

$$\left|\frac{f_{j+1}-f_j}{f_j}\right| \le \varepsilon \qquad (5.37)$$

where ε is taken to be 0.01. This approach appears to be more suitable when the design space is convex, i.e. there is a unique optimum irrespective of the starting design. (ii) In the second approach the sequence of the methods is reversed. An EA procedure, either GA or ES, is used first in order to locate the region where the global optimum lies, and then the SQP is activated in order to exploit its higher order of accuracy in the neighbourhood of the optimum. In this case the switch is performed when there is a small difference (ε=0.1) between the best designs of two

consecutive generations. This approach appears to be more rational in the general case when more complex and non-convex design problems are to be solved with many local optima and is perfectly suited to GA since it improves the fast-converged solution to an infeasible design by GA. Furthermore a combination of GA and ES are performed in which ES are used to improve the quality of the solution achieved by GA.

REFERENCES:

[1] J. A. Holland, "Adaptation in natural and artificial systems," *University of Michigan Press, Ann Arbor.*, 1975.

[2] A. J. Owens & M. J. Walsh, "Artificial Intelligence Through Simulated Evolution," *Wiley. New York*, 1966.

[3] "Genetic Programming: On the Programming of Computers by Means of Natural Selection," Koza 1992.

[4] Rechenberg, "Evolution strategy: optimization of technical systems according to the principles of biological evolution," *Frommann-Holzboog, Stuttgart.* 1973.

[5] H. G. Beyer & H. P. Schwefel, "Evolution Strategies: A Comprehensive Introduction," *J. Natural Comput.*, vol. 1, no. 1, p. 3–52, 2002.

[6] L. J. Fogel, A.J. Owens & M.J. Walsh, "Artificial intelligence through simulated evolution," *Wiley, New York*, 1966.

[7] D. E. Goldberg, "Genetic algorithms in search, optimization and machine learning," *Addison-Wesley Publishing Co., Inc., Reading, Massachusetts.*, 1989.

[8] J. Holland, "Adaptation in natural and artificial systems," *University of Michigan Press, Ann Arbor.*, 1975.

[9] Rechenberg, "Evolution strategy: optimization of technical systems according to the principles of biological evolution," *Frommann-Holzboog, Stuttgart*, 1973.

[10] H. P. Schwefel, "Numerical optimization for computer models," *Wiley & Sons, Chichester, UK*, 1981.

[11] N. A. Barricelli, "Numerical testing of evolution theories," *Act a Biotheoretica*, vol. 16, pp. 69–126, 1962.

[12] H. Adeli & N. T. Cheng, "Concurrent Genetic Algorithms for optimization of large structures," *J. Aerospace Eng., Asce*, vol. 7, no. 3, pp. 276–296, 1994.

[13] M. Papadrakakis, N. D. Lagaros & G. Thierauf & J. Cai, "Advanced Solution Methods in Structural Optimization Based on Evolution Strategies," *J. Engng. Comput.*, vol. 15, no. 1, pp. 12–34, 1998.

[14] G. Thierauf, J. Cai "A two level parallel evolution strategy for solving mixed-discrete structural optimization problems," *The 21th Asme Design Automation Conf., Boston MA, September,* pp. 17–221, 1995.

[15] M. Papadrakakis, N.D. Lagaros & Y. Tsompanakis, "Structural optimization using evolution strategies and neural networks," *Comp. Meth. Appl. Mechanics & Engrg*, vol. 156, pp. 309–333, 1998.

[16] M. Papadrakakis, Y. Tsompanakis & N.D. Lagaros, "Structural shape optimization using Evolution Strategies," *Eng. Optimization J.*, vol. 31, pp. 515–540, 1999.

[17] Manolis Papadrakakis, Nikolaos D. Lagaros & Georg Thierauf & Jianbo Cai, "Advanced solution methods in structural optimization based on evolution strategies"," *Eng. Computations*, vol. 15, no. 1, pp. 12–34, 1996.

[18] M. Fragiadakis, "Optimum Earthquake Resistant Design of Structures Performing Non-Linear Analysis," *PhD, Institute Structural Analysis Seismic Research, School Civil Eng., Ntua*, 2006.

[19] Nikolaos D. Lagaros, Manolis Papadrakakis & Nikolaos Bakas, "Automatic Minimization of the Rigidity Eccentricity of 3D Reinforced Concrete Buildings," *J. Earthquake Eng.*, vol. 10, no. 4, pp. 533–564, 2006.

[20] Nikolaos D. Lagaros, Nikolaos Bakas & Manolis Papadrakakis "Optimum Design Approaches for 3D Reinforced Concrete Buildings under Earthquake Loading," *J. Earthquake Eng. (to Appear)*, 2008.

[21] Hans-Georg Beyer and Hans-Paul Schwefel, 2002, *"Evolution Strategies"*, Natural Computing 1; 3-52

[22] H. D. Adeli & N. T. Cheng, "Augmented Lagrangian Genetic Algorithm for structural optimization," *J. Aerospace Eng., Asce*, vol. 7, no. 1, pp. 104–118, 1994. Adeli H. and Cheng N. T., 'Concurrent Genetic Algorithms for optimization of large structures', Journal of Aerospace Engineering, ASCE, 7(3), 276-296, (1994).

[23] H. D. Adeli & N. T. Cheng, "Integrated Genetic Algorithm for optimization of space structures," *J. Aerospace Eng., Asce*, vol. 6, no. 4, pp. 315–328, 1993.

[24] H. D. Adeli & Hyo Seon. Park, "Neural dynamics model for structural optimisation. - Theory," *Computers & Structures*, vol. 57, no. 3, pp. 383–399, 1995.

[25] Hyo Deon Adeli & H. S. Park, "Optimization of space structures by Neural dynamics," *Neural Networks*, vol. 8, no. 5, pp. 769–781, 1995.

[26] J. S. Arora "Computational Design Optimization: A review and future directions," *Structutal Safety*, vol. 7, pp. 131–148, 1990.

[27] M. A. Arslan & P. Hajela, "Counterpropagation Neural Networks in decomposition based optimal design," *Computers & Structures*, vol. 65, no. 5, pp. 641–650, 1997.

[28] T. Back, F. Hoffmeister & H. P. Schwefel, "A survey of evolution strategies', in R. K. Belew and L. B. Booker (eds.)," *Proc. 4th Int. Conf. Genetic Algorithms, Morgan Kaufmann*, pp. 2–9, 1991.

[29] J. Baker, "Adaptive selection methods for genetic algorithms," *in J. J. Grefenstette (ed.), Proc. Int. Conf. Genetic Algorithms Their Applications, Lawrence Erlbaum*, 1985.

[30] N. A. Barricelli, "Numerical testing of evolution theories," *Act a Biotheoretica*, vol. 16, pp. 69–126, 1962.

[31] A. D. Belegundu & J. S. Arora, "A computational study of transformation methods for optimal design," *Aiaa J.*, vol. 22, no. 4, pp. 535–542, 1984.

[32] M. P. Bendsoe & R. Kikuchi, "Generating optimal topologies in structural design using a homogenization method," *Comput. Methods Applied Mechanics Eng.*, vol. 71, pp. 197–224, 1988.

[33] L. Berke & Hajela P., "Applications of Artificial Neural Nets in Structural Mechanics," *Nasa*, vol. 71, pp. 331–348 TM-102420, 1990.

[34] L. Berke, S. N. Patnaik & P. L. N. Murthy, "Optimum Design of Aerospace Structural Components using Neural Networks," *Computers & Structures*, vol. 48, pp. 1001–1010, 1993.

[35] N. Bitoulas & M. Papadrakakis, "An optimised computer implementation of the incomplete Cholesky factorization," *Comp. Syst. Eng.*, vol. 5, no. 3, pp. 265–274, 1994.

[36] K. U. Bletzinger, S. Kimmich & E. Ramm, "Efficient modelling in shape optimal design," *Comput. Syst. Eng.*, vol. 2, no. 5/6, pp. 483–495, 1991.

[37] J. Cai, G. Thierauf, "Discrete structural optimization using evolution strategies," *B.h.v. Topping A.i. Khan (eds.), Neural Networks Combinatorial Civil Structural Eng., Edinburgh, Civil-comp Limited*, pp. 95–10, 1993.

[38] M. J. Embrechts "Metaneural-Version 4.1," *Rensselear Polytechnique Institute*, 1994.

[39] H. A. Eschenauer, A. Schumacher & T. Vietor, "Decision makings for initial designs made of advanced materials, in Bendsoe M. P. and Soares C.A.M. (eds.)," *Nato Arw 'topology Design of Structures', Sesimbra, Portugal, Kluwer Academic Publishers, Dordrecht, Netherlands*, pp. 469–480, 1993.

[40] Eurocode 3, Design of steel structures, Part1.1: General rules for buildings," *Cen, Env*, 1993-1-1/1992.

[41] C. Farhat, F. X. Roux, "Implicit Parallel Processing in Structural Mechanics," *Comp. Mec. Adv.*, vol. 2, pp. 1–124, 1994.

[42] C. Farhat & L. Crivelli & F. X. Roux, "Extending Substructure Based Iterative Solvers to Multiple Load and Repeated Analyses Comp. Meth.," *Appl. Mech. Eng*, pp. 195–209, 1994.

[43] C. Fleury, "Dual methods for convex separable problems, in Rozvany G.i.n. (ed), Nato/dfg Asi `optimization Large Structural Syst*.", Berchtesgaden, Germany, Kluwer Academic Publishers, Dordrecht, Netherlands*, pp. 509–530, 1993.

[44] L. J. Fogel, A. J. Owens & M. J. Walsh, "Artificial intelligence through simulated evolution," *Wiley, New York*, 1966.

[45] R. H. Gallagher, O. C. Zienkiewicz "Optimum Structural Design: Theory and Applications," *John Wiley & Sons, New York*, 1973.

[46] D. A. Gasparini & E. H. Vanmarke, "Simulated earthquake motions compatible with prescribed response spectra," *Massachusetts Institute Technology (MIT), Department Civil Eng., Publication*, no. R76-4, Jan. 1976.

[47] D. A. Gasparini, "SIMQKE - A program for artificial motion generation, User's manual and documentation," *Massachusetts Institute Technology (MIT), Department Civil Eng.*, Nov. 1976.

[48] P. E. Gill, W. Murray & M. H. Wright, "Practical Optimization," *Academic Press*, 1981.

[49] P. E. Gill, W. Murray & M. A. Saunders & M. H. Wright, "User's guide for NPSOL (Version 4.0): A Fortran Package for Nonlinear Programming," *Technical Report Sol 86-2, Dept. of Operations Research, Stanford University.*, 1986.

[50] D. Goldberg, "A note on Boltzmann tournament selection for Genetic Algorithms and population-oriented Simulated Annealing," *Tcga 90003, Eng. Mechanics, Alabama University*, 1990.

[51] D. E. Goldberg, "Genetic algorithms in search, optimization and machine learning," *Addison-Wesley Publishing Co., Inc., Reading, Massachusetts.*, 1989.

[52] D. E. Goldberg, "Sizing populations for serial and parallel genetic algorithms," *Tcga Report No 88004, University of Alabama*, 1988.

[53] D. J. Gunaratnam & J. S. Gero, "Effect of representation on the performance of Neural Networks in structural engineering applications," *Microcomputers Civil Eng.*, vol. 9, pp. 97–108, 1994.

[54] P. Hajela & L. Berke, "Neurobiological computational models in structural analysis and design," *Computers & Structures*, vol. 41, pp. 657–667, 1991.

[55] E. J. Haug & J. S. Arora, "Optimal mechanical design techniques based on optimal control methods," *Asme Paper No 64-dtt-10, Proc. 1st Asme Design Technology Transfer Conf., New York*, pp. 65–74, 1974.

[56] E. Hinton, "Some experiences in structural topology optimization, in B. H. V. Topping (ed.) Developments in Computational Techniques for Structural Engineering," *Civil-comp Press, Edinburgh*, pp. 323–331, 1995.

[57] E. Hinton & J. Sienz, "Aspects of adaptive finite element analysis and structural optimization, in Topping B.H.V & M. Papadrakakis (eds), "Advances in Structural Optimization," *Civil-comp Press, Edinburgh*, pp. 1–26, 1994.

[58] E. Hinton & J. Sienz, "Fully stressed topological design of structures using an evolutionary procedure," *J. Eng. Computations*, vol. 12, pp. 229–244, 1993.

[59] E. Hinton & J. Sienz, "Studies with a robust and reliable structural shape optimization tool, in B. H. V. Topping (ed) Developments in Computational Techniques for Structural Engineering," *Civil-comp Press, Edinburgh*, 1995.

[60] Hoffmeister & T. Back, "Genetic Algorithms and Evolution Strategies-Similarities and Differences, in Schwefel, H. P. & R. Manner (eds.), "Parallel Problems Solving from Nature," *Springel-Verlag, Berlin, Germany*, pp. 455–469, 1991.

[61] J. Holland, "Adaptation in natural and artificial systems," *University of Michigan Press, ann Arbor*, 1975.

[62] R. Hooke & T. A. Jeeves, "Direct Search Solution of Numerical and Statistical Problems," *J. Acm*, vol. 8, 1961.

[63] Joines & C. A. Houck, "On the use of non-stationary penalty functions to solve non- linear constrained optimization problems with GA', in Z. Michalewicz, J. D. Schaffer, H.-P. Schwefel, D. B. Fogel, and H. Kitano (eds.), Proceedings of the First IEEE International Conference on Evolutionary Computation," *IEEE Press*, pp. 579–584, 1994.

[64] Khan, A. I., Topping, B. H. V. and Bahreininejad, A. 'Parallel training of neural networks for finite element mesh generation', Neural Networks and Combinatorial Optimisation in Civil and Structural Engineering, B. H. V. Topping and A. I. Khan, eds, Civil-Comp Press, pp. 81-94, 1993.

[65] S. Kirkpatric, C. D. Gelatt & M.P. Vecchi, "Optimization by simulated annealing, Science," vol. 220, no. 1983, pp. 671–680.

[66] K. Krishnakumar, "Micro genetic algorithms for stationary and non stationary function optimization," *Spie Proc. Intelligent Control Adaptive Syst.*, vol. 1196, 1989.

[67] L. S. Lasdon, A. D. Warren & A. Jain, "Design and testing of a generalized reduced gradient code for nonlinear programming," *Acm Trans. Math. Softw.*, vol. 4, no. 1, pp. 34–50, 1978.

[68] R. G. Le Riche, C. Knopf-Lenoir & R.T. Haftka, "A segregated genetic algorithm for constrained structural optimization," *L. J. Eshelman (ed.), Proc. 6th Int. Conf. Genetic Algorithms*, pp. 558–565, 1995.

[69] C. Maa & M. Shanblatt, "A two-phase optimization neural network," *Ieee Trans. Neural Networks*, vol. 3, no. 6, pp. 1003–1009, 1992.

[70] Z. Michalewicz, "Genetic algorithms, numerical optimization and constraints," *L. J. Eshelman (ed.), Proc. 6th Int. Conf. Genetic Algorithms, Morgan Kaufmann*, pp. 151–158, 1995.

[71] F. Moses, "Mathematical programming methods for structural optimization," *Asme Structural Optimisation Symp. Amd*, vol. 7, pp. 35–48, 1974.

[72] H. Myung, J. M. Kim & D. Fogel, "Preliminary investigation into a two-stage method of evolutionary optimization on constrained problems'," *J. R. Mcdonnell, R. G. Reynolds D. B. Fogel (eds.), Proc. 4th Annual Conf. Evolutionary Programming, mit Press*, pp. 449–463, 1995.

[73] "NAG, Software manual, NAG Ltd, Oxford, UK." 1998.

[74] N. Olhoff, J. Rasmussen & E. Lund, "Method of exact numerical differentiation for error estimation in finite element based semi-analytical shape sensitivity analyses, Special Report," *Institute Mechanical Eng., Aalborg University, Aalborg, Dk.*, vol. 10,1992.

[75] Papadrakakis M., Domain decomposition techniques for computational structural mechanics, in M. Papadrakakis (Ed.), Solving Large-Scale Problems in Mechanics, Volume II, John Wiley, 1996.

[76] M. Papadrakakis, N. Bitoulas "Accuracy and effectiveness of preconditioned conjugate gradient method for large and ill-conditioned problems," *Comp. Meth. Appl. Mech. Eng.*, vol. 109, pp. 219–232, 1993.

[77] M. Papadrakakis, N. D. Lagaros & G. Thierauf & J. Cai, "Advanced Solution Methods in Structural Optimization Based on Evolution Strategies," *J. Engng. Comput*, vol. 15, no. 1, pp. 12–34, 1998.

[78] M. Papadrakakis, N. D. Lagaros & Y. Tsompanakis, "Optimization of large-scale 3D trusses using evolution strategies and neural networks," *Special Issue Int. J. Space Structures*, vol. 14, no. 3, pp. 211–223, 1999.

[79] M. Papadrakakis, N.D. Lagaros & Y. Tsompanakis, "Structural optimization using evolution strategies and neural networks," *Comp. Meth. Appl. Mechanics & Engrg*, vol. 156, pp. 309–333, 1998.

[80] M. Papadrakakis, V. Papadopoulos, "A computationally efficient method for the limit elasto plastic analysis of space frames," *Computational Mechanics*, vol. 16, no. 2, pp. 132–141, 1995.

[81] M. Papadrakakis, V. Papadopoulos "Efficient solution procedures for the stochastic finite element analysis of space frames using the Monte Carlo simulation, to appear in Comp," *Meth. Appl. Mech. Eng*, 1996.

[82] Papadrakakis M., Papadopoulos V. and Lagaros N. D., 'Structural reliability analysis of elastic-plastic structures using neural networks and Monte Carlo simulation', Comp. Meth. Appl. Mechanics & Engrg, Vol. 136, pp. 145-163, 1996.

[83] M. Papadrakakis & S. A. Smerou, "A new implementation of the Lanczos method in linear problems," *Int. J. Num. Meth. Eng.*, vol. 29, pp. 141–159, 1990.

[84] M. Papadrakakis, Y. Tsompanakis & L. D. Lagaros, "Structural shape optimization using Evolution Strategies," *Eng. Optimization J.*, vol. 31, pp. 515–540, 1999.

[85] M. Papadrakakis, Y. Tsompanakis & E. Hinton & J. Sienz, "Advanced solution methods in topology optimization and shape sensitivity analysis," *J. Eng. Computations*, vol. 3, no. 5, pp. 57–90, 1996.

[86] P. Pedersen, "Topology optimization of three dimensional trusses, in Bendsoe M.P. and Soares C.A.M. (eds.)," *Nato Arw 'topology Design of Structures', Sesimbra, Portugal, Kluwer Academic Publishers, Dordrecht, Netherlands*, pp. 19–31, 1993.

[87] G.G. Pope & L.A. Schmit (eds.), "Structural Design Applications of Mathematical Programming Techniques," *Agardograph 149, Technical Editing and Reproduction Ltd., London*, Feb., 1971.

[88] E. Ramm, K. U. Bletzinger & R. Reitinger & K. Maute , "The challenge of structural optimization, in Topping B.H.V. and Papadrakakis M. (eds) Advances in Structural Optimization," *Civil-comp Press, Edinburgh*, pp. 27–52, 1994.

[89] Rechenberg, "Evolution strategy: optimization of technical systems according to the principles of biological evolution," *Frommann-Holzboog, Stuttg*I.

[90] G. I. N. Rozvany & M. Zhou, "Layout and generalised shape optimization by iterative COC methods, in Rozvany G.I.N. (ed.)," *Nato/dfg Asi 'optimization Large Structural Syst.', Berchtesgaden, Germany, Kluwer Academic Publishers, Dordrecht, Netherlands*, pp. 103–120, 1993.

[91] G. Rudolph "Personal communication," 1999.

[92] D. E. Rummelhart & J. L. Mcclelland, "Parallel Distributed Processing," *Volume 1: Foundations, the Mit Press, Cambridge*, 1986.

[93] K. Schittkowski, C. Zillober & R. Zotemantel, "Numerical comparison of non-linear algorithms for structural optimization," Structural *Optimization*, vol. 7, pp. 1–19, 1994.

[94] H. P. Schwefel & G. Rudolph, "Contemporary Evolution Strategies in F. Morgan, A. Moreno, J. J. Merelo and P. Chacion (eds.). Advances in Artificial Life," *Proc. Third European Conf. On Artificial Life Granada, Spain, Springer, Berlin*, pp. 893–907, June 4-6, 1995.

[95] H. P. Schwefel, "Numerical optimization for computer models," *Wiley & Sons, Chichester, UK,* 1981.

[96] C. Y. Sheu & W. Prager, "Recent development in optimal structural design," *Applied Mechanical Reviews*, vol. 21, no. 10, pp. 985–992, 1968.

[97] Shieh R. C., "Massively parallel structural design using stochastic optimization and mixed neural net/finite element analysis methods", Computing Systems in Engineering, Vol. 5, No. 4-6, pp. 455-467, 1994.

[98] L. Spunt, "Optimum Structural Design," *Prentice-hall, Englewood Cliffs, New Jersey*, pp. 41–42, 1971.

[99] J. E. Stephens & D. Vanluchene, "Integrated assessment of seismic damage in structures," *Microcomputers Civil Eng.*, vol. 9, no. 2, pp. 119–128, 1994.

[100] K. Suzuki & N. Kikuchi, "Layout optimization using the homogenization method, in Rozvany G.I.N. (ed.), NATO/DFG ASI `Optimization of large structural systems," *Berchtesgaden, Germany, Kluwer Academic Publishers, Dordrecht, Netherlands*, pp. 157–175, 1993.

[101] K. Svanberg "The method of moving asymptotes, a new method for structural optimization," *Int. J. Num. Meth. Eng.*, vol. 23, pp. 359–373, 1987.

[102] C. A. Taylor, "A program for generating spectrum compatible earthquake ground acceleration time histories, Reference Manual," *Bristol Earthquake Eng. Data Acquisition Processing Syst.*, Dec. 1989.

[103] P. B. Thanedar, J. S. Arora & C. H. Tseng & O. K. Lim & G.J. Park, "Performance of some SQP methods on structural optimization problems," *Inter. J. Num. Meth. Engng*, vol. 23, pp. 2187–2203, 1986.

[104] P. S. Theocharis, P. D. Panagiotopoulos "Neural networks for computing in fracture mechanics. Methods and prospects of applications," *Comp. Meth. Appl. Mechanics & Engrg*, pp. 106 & 213–228, 1993.

[105] G. Thierauf & J. Cai, "A two level parallel evolution strategy for solving mixed-discrete structural optimization problems," *The 21th Asme Design Automation Conf., Boston Ma*, pp. 17–221, Sept. 1995.

[106] G. Thierauf & J. Cai, "Structural optimization based on Evolution Strategy, in Papadrakakis M. and Bugeda G. (eds)," *Advanced Computational Methods in Structural Mechanics, Cimne, Barcelona*, pp. 266–280, 1996.

[107] B. H. V. Topping & A. Bahreininejad, "Neural computing for structural mechanics," *Saxe Coburg, UK*, 1997.

[108] F. Van Keulen & E. Hinton, "Topology design of plate and shell structures using the hard kill method, in B.H.V. Topping (ed.) Advances in optimization for Structural Engineering," *Civil-comp Press, Edinburgh*, pp. 177–188, 1996.

[109] G.N. Vanderplaats "Numerical optimisation techniques for engineering design: with applications," *Mcgraw-Hill, New York*, 1984.

[110] V. B. Venkayya, N. S. Khot & L. Berke, "Application of optimality criteria approaches to automated design of large practical structures," *2nd Symp. Structural Optimisation Agard-cp-123, Milan, Italy, April*, 1973.

[111] D. Waagen, P. Diercks & J.Mcdonnell, "The stochastic direction set algorithm: A hybrid technique for finding function extrema', in D. B. Fogel and W. Atmar (eds.)," *Proc. 1st Annual Conf. Evolutionary Programming, Evolutionary Programming Society*, pp. 35–42, 1992.

[112] Y. M. Xie & G.P. Steven, "A simple evolutionary procedure for structural optimization," *Computers & Structures*, vol. 49, pp. 885–896, 1993.

[113] Y. M. Xie, G.P. Steven "Optimal design of multiple load case structures using an evolutionary procedure," *J. Eng. Computations*, vol. 11, pp. 295–302, 1994.

7 Elastic design of 3D reinforced concrete irregular buildings

In this chapter we present the results and conclusions derived from the first stage of our investigation. In these examples, we performed elastic static or response spectrum analyses as described below. The object function in most of the cases was the minimization of the distance between the center of mass and the center of rigidity of each floor plan. The results were very important and led us to the next steps of our investigation.

7.1 Structural response

Apart from the architectural constraints, behavioral constraints, imposed by the design codes, have to be satisfied in order to accept a design as feasible. These behavioral checks are performed following a structural analysis where internal forces and global displacements are calculated and checked according to the EC2 and EC8 design codes. In order to minimize the computational effort the optimization procedure is decomposed in two stages, depending on the type of the structural analysis and the corresponding behavioral constraints employed.

7.1.1 Structural analysis

Two different structural analysis procedures have been implemented in the proposed methodology: (i) a simplified analysis is applied during the first stage of the optimization procedure and (ii) a more accurate analysis, based on the EC8 design code, is applied during the second stage of the optimization procedure. A number of refinement steps are performed during the second stage in order to improve the optimum design achieved during the first stage and fulfil the requirements which are imposed by EC2 and and EC8 design codes.

7.1.1.1 Simplified structural analysis

Frames with almost rigid beams subjected to lateral forces exhibit zero moments at the mid-height of the columns and relative displacement proportional to the shear forces. These systems are called *shear frames*. In general, due to their T-section, beams exhibit a much larger stiffness compared to the supporting columns [15]. Therefore their behavior is very similar to the behavior of shear frames and thus a simplified structural analysis is justified during the first stage of the optimization procedure. In the simplified structural analysis the concrete structure is considered as a shear-type building where the rigidity of the horizontal structural elements is much higher than that of the vertical elements. For this type of modeling the simplified modal response spectrum analysis method can be effective where the structure is loaded with horizontal static forces at each storey level according to:

$$F_i = V_b \cdot \frac{z_i \cdot m_i}{\sum z_j \cdot m_j} \tag{6.1}$$

where V_b is the base shear force determined for each main direction, z_i and z_j are the heights of the storeys defined from the level of application of the seismic action (foundation) and masses m_i and m_j are the masses of the corresponding storey.

7.1.1.2 Detailed structural analysis

The detailed structural analysis implemented at the final stage after the convergence of the optimization procedure is based on the multi-Modal Response Spectrum (mMRS) analysis, by using the full modeling of the building. The mMRS analysis is a simplification of the mode superposition approach recommended by the Eurocode 8 (EC8 1996) and aims at avoiding time history analyses which are required by both direct integration and mode superposition approaches.

7.1.2 Behavioral constraints

In the intermediate optimization steps where the simplified structural analysis is performed for each vertical structural element the following behavioral constraints are checked:

$$\sigma_c \le \frac{f_{ck}}{\gamma_c}, \quad \sigma_t \le \frac{f_{yk,s}}{\gamma_s} \tag{6.2}$$

where σ_c, σ_t are the maximum axial compression and tension stresses, respectively, encountered in the cross-section of the vertical structural element, f_{ck} is the concrete's characteristic compressive cylinder strength at 28 days, and $f_{yk,s}$ is the characteristic yield strength of the steel reinforcement. The corresponding parameters γ_c and γ_s are the partial safety factors for the strength of materials which is equal to 1.50 for concrete and 1.15 for steel, respectively. The interstorey drift constraint employed in a frame structure can be written as:

$$\frac{d_r}{\nu} \le 0.004 \times h \tag{6.3}$$

where *v* is a reduction factor for the serviceability limit state (taken equal to 2.0 for the test examples considered in this study) and d_r is the relative drift between two consecutive storeys.

The optimum design achieved has to satisfy all performance requirements for resistance, serviceability and durability. These requirements are expressed through the limit states; beyond these states the structure no longer satisfies the design performance requirements. The limit states considered by Eurocode 2 (EC2 1992) and Eurocode 8 (EC8 1996) are classified into: (i) ultimate limit states, associated with collapse or with other forms of structural failure which may endanger the safety of people and (ii) serviceability limit states, corresponding to states beyond which specific service requirements are no longer satisfied.

7.1.3 Ultimate limit states

In the ultimate limit states the following verification check should be performed. When considering a limit state of static equilibrium or of gross displacements or deformations of the structure, it should be verified that:

$$E_{d,dst} < E_{d,stb}$$

where $E_{d,dst}$ and $E_{d,stb}$ are the design effects of destabilizing and stabilizing actions, respectively. When considering a limit state of rupture or

excessive deformation of a section, member or connection (fatigue excluded) it should be verified that:

$$S_d \leq R_d \tag{6.4}$$

where S_d is the design value of an internal force or moment (or of a respective vector of several internal forces or moments) and R_d is the corresponding design resistance, associating all structural properties with the respective design values.

When considering a limit state of transformation of the structure into a mechanism, it should be verified that a mechanism does not occur unless actions exceed their design values, associating all structural properties with the respective design values. When considering a limit state of stability induced by second-order effects it should be verified that instability does not occur unless actions exceed their design values, associating all structural properties with the respective design values. When considering a limit state of rupture induced by fatigue it should be verified that

$$D_d \leq 1 \tag{6.5}$$

where D_d is the design value of the damage indicator.

7.1.4 Serviceability limit states

In the serviceability limit states it should be verified that:

$$E_d \leq C_d \text{ or } E_d \leq R_d \tag{6.6}$$

where C_d is a nominal value or a function of certain design properties of materials related to the design effects of actions considered, and E_d is the design effect of actions.

7.2 Numerical results

Two 3D multi-storey concrete buildings, corresponding to real structures, have been considered for the evaluation of the proposed methodology. In all test cases the following material properties have been considered: concrete with modulus of elasticity E_c=27.5GPa and characteristic

compressive cylinder strength of concrete fck= 16MPa, longitudinal steel reinforcement with modulus of elasticity Es=210GPa and characteristic yield strength fyk,s=400MPa and transverse reinforcement with modulus of elasticity Es=210GPa and characteristic yield strength fyk,s=220MPa. The design spectrum that has been used has the following characteristics: A=0.16g (seismic hazard level II), ground type B (T1=0.15sec and T2=0.60sec) and behavior factor q=3.5 according to Eurocode 8 (EC8 1996). The cross section of the beams for both test examples is 25×60 cm^2.

7.2.1 Test example 6.1

The first test example is a three-storey concrete space frame. In this test example there is only one group of storeys since the plan layout of the columns/shear walls is the same for all storeys. For this test example 6.1 the design variables being used are: 10 topology and 2 active sizing design variables for the single group of storeys.

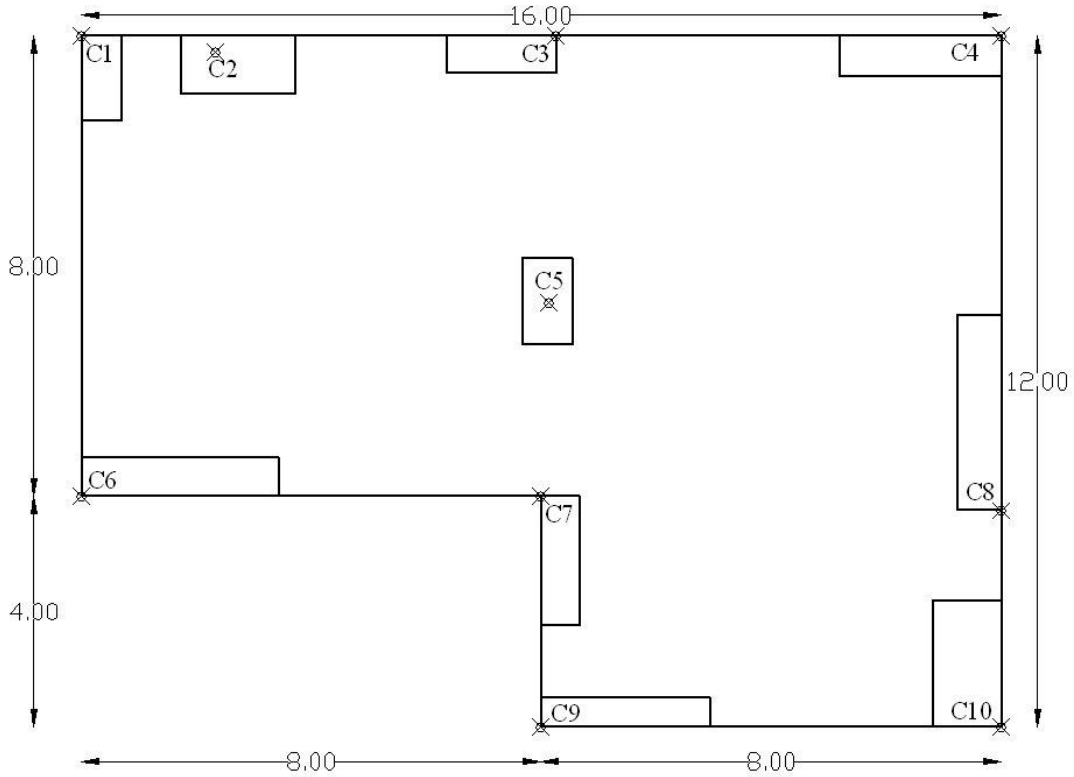

	AC - 1	
Column	**AC - 1x**	**AC - 1y**
C1	70	145
C2	200	100
C3	190	65
C4	280	70
C5	85	150
C6	345	65
C7	65	225
C8	75	340
C9	295	50
C10	120	220

Figure 6.1 *Test example 6.1 - Architectural constraints of a typical storey*

In Figure 6.1 both architectural constraints (AC-1 rectangles and AC-2 points) are presented for all columns/shear walls. In Figure 6.2a the applied solution provided by an experienced structural engineer is presented, while in Figure 6.2b the optimum design achieved by the proposed methodology is depicted.

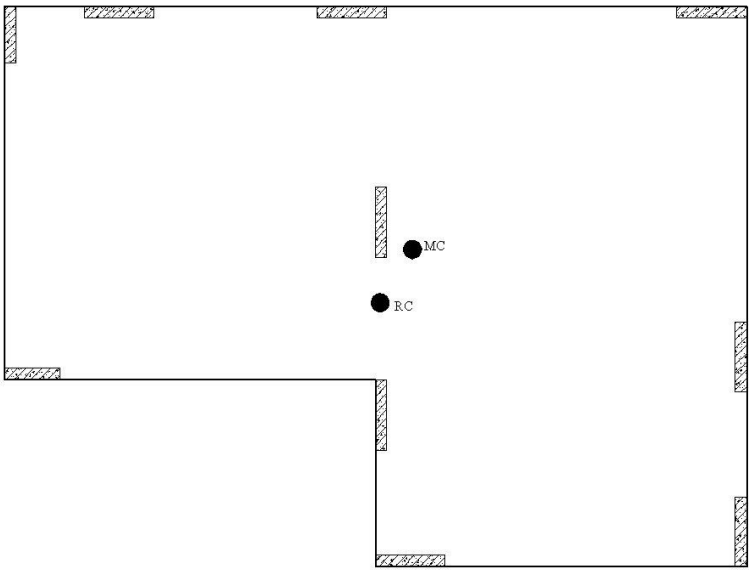

(a)

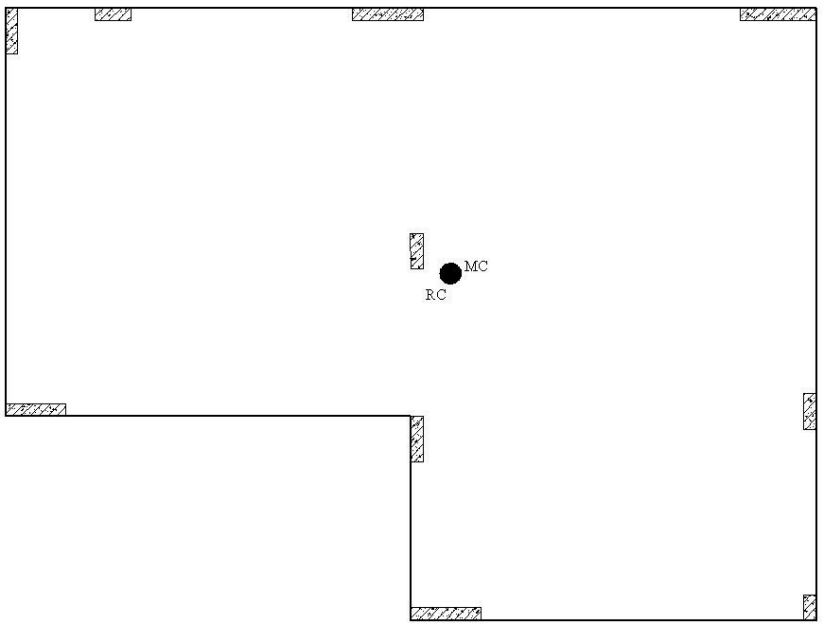

(b)

Solution	e_x (cm)	e_Y (cm)
Applied	69.50	114.40
Optimum	2.25	0.23

Figure 6.2 *Test example 6.1 – (a) Applied and (b) Optimum solutions (e_{MC-RC} eccentricity in x and y directions)*

It has to be noted that both solutions fulfil the requirements of EC2 and EC8 design codes. It can be seen from Table 1 that the distance between the rigidity center and the storey mass center is reduced from 133cm in Figure 6.2a to 2.26cm in Figure 6.2b.

Table 6.1. *Test example 6.1 – Final cross-sectional dimensions*

Column	Applied solution		Optimum solution	
	e_{MC-RC}=133cm		e_{MC-RC}=2.26cm	
	dim_x	dim_y	dim_x	dim_y
C1	25	120	25	90
C2	150	25	70	25
C3	150	25	140	25
C4	150	25	150	25
C5	25	150	25	70
C6	120	25	120	25
C7	25	150	25	90
C8	25	150	25	70
C9	150	25	140	25
C10	25	150	25	50

Table 6.2 *Test example 6.1 – Material required and relative costs of the vertical structural elements*

Solution	Concrete		Longitudinal reinforcement		Transverse reinforcement		Total
	(m^3)	cost	(tn)	cost	(tn)	cost	
Applied	38.85	C_1	2.93	C_2	5.46	C_3	C_{tot}
Optimum	22.89	$0.70C_1$	3.25	$1.11C_2$	3.31	$0.60C_3$	$0.73C_{tot}$

In Table 6.1 the cross-sections of the columns/shear walls for both solutions are given and it is clear that the sizes for the optimized solution are smaller than those of the applied ones. Respectively, the dimensions of the columns are denoted as dim_x and dim_y corresponding to the x and y axis. The importance of designing torsionally balanced structures is

presented in Table 6.2, where the relative cost of the columns and the shear walls of the structure is given. There are two reasons why the "Optimum" solution requires more longitudinal reinforcement than the "Applied" solution: (i) Comparing the "Optimum Solution" with the "Applied Solution", we can see that smaller column cross-sections are assigned in the first one, so more longitudinal reinforcement is required in order to fulfil EC2 and EC8 provisions. (ii) Bending behavior is dominant in a torsionally balanced structure, requiring more longitudinal than transverse reinforcement.

7.2.2 Test example 6.2

The second test example is a four-storey concrete space frame. In this test example there are two groups of storeys, the first group corresponds to storeys 1 and 2, while the second group corresponds to storeys 3 and 4. For this test example 6.2 design variables are used. These correspond to topology design variables only because all columns/shear walls are of Type I. 11 topology design variables correspond to the first group of storeys while 8 topology design variables correspond to the second group.

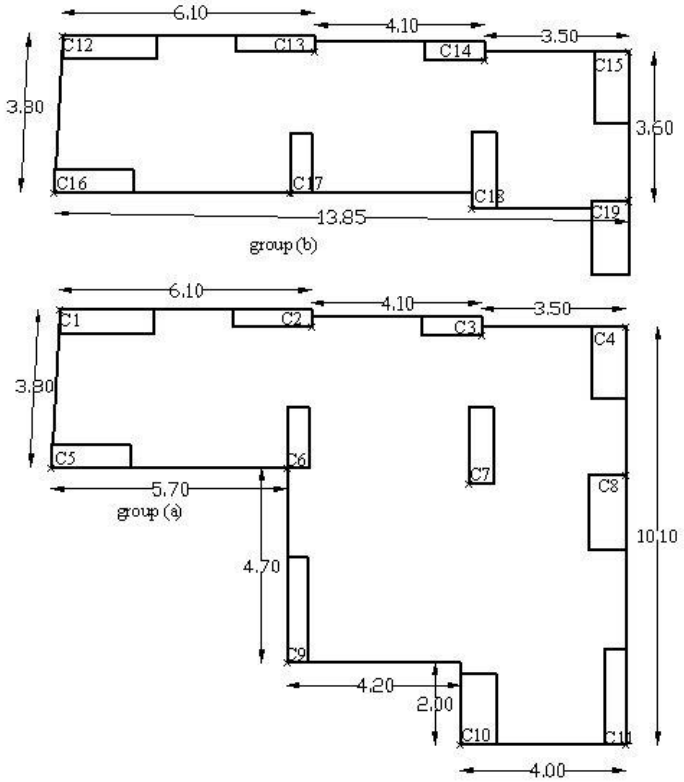

Column	AC - 1	
	AC - 1x	AC - 1y
Group (a)		
C1	230	55
C2	190	40
C3	145	45
C4	85	175
C5	195	55
C6	50	145
C7	60	185
C8	90	180
C9	50	250
C10	85	170
C11	50	230
Group (b)		
C12	230	55
C13	190	40
C14	145	45
C15	85	175
C16	195	55
C17	50	145
C18	60	185
C19	90	180

Figure 6.3 *Test example 6.2 – Architectural constraints of a typical storey*

In Figure 6.3 both architectural constraints (AC-1 rectangles and AC-2 points) for both groups of storeys are presented, where group (a)

corresponds to the layout of 1 and 2 storeys, while group (b) corresponds to the layout of 3 and 4 storeys. In Figure 6.4a the applied solution provided by an experienced structural engineer is presented. Figure 6.4b depicts the optimum design achieved by the proposed methodology considering only the optimization of the first group of storeys, while Figure 6.4c shows the optimum design achieved by the proposed methodology if both groups of storeys are optimized.

It can be seen in Table 6.3 that, in the first group of storeys, the distance between the rigidity center and the storey mass center is reduced from 176cm in Figure 6.4a to 0.23cm in Figure 6.4b (and Figure 6.4c) when either the first or both groups of storeys are optimized. Concerning the second group of storeys, only when the first group of storeys is optimized then the distance between the rigidity center and the storey mass center is increased from 100cm in Figure 6.4a to 130cm in Figure 6.4b. This distance in the second group of storeys is reduced from 100cm in Figure 6.4a to 4.56cm in Figure 6.4c if both groups of storeys are optimized.

Table 6.3 *Test example 6.2 – Final cross-sectional dimensions*

Column	Applied solution		Optimum solution I		Optimum solution II	
	layout group (a)					
	e_{MC-RC}=176cm		e_{MC-RC}=0.23cm		e_{MC-RC}=0.23cm	
	dim_x	dim_y	dim_x	dim_y	dim_x	dim_y
1	120	25	90	25	90	25
2	50	40	50	25	50	25
3	25	45	25	40	25	40
4	25	120	25	120	25	120
5	120	25	70	25	70	25
6	30	50	25	30	25	30
7	25	70	25	40	25	40
8	25	70	25	70	25	70

9	25	120	25	40	25	40
10	25	120	25	40	25	40
11	25	120	25	100	25	100
Column	layout group (b)					
	e_{MC-RC}=100cm		e_{MC-RC}=130cm		e_{MC-RC}=4.56cm	
12	120	25	90	25	70	25
13	50	40	50	25	30	25
14	25	45	25	40	25	30
15	25	120	25	120	25	80
16	120	25	70	25	50	25
17	30	50	25	30	25	30
18	25	70	25	40	25	40
19	25	70	25	70	25	60

Table 6.4 *Test example 6.2 – Material required and relative costs of the vertical structural elements*

Solution	Concrete		Longitudinal reinforcement		Transverse reinforcement		Total
	(m^3)	cost	(tn)	cost	(tn)	cost	
Applied	110.00	C_1	3.73	C_2	2.81	C_3	C_{tot}
Optimum I	19.38	$0.18C_1$	3.96	$1.06C_2$	1.93	$0.69C_3$	$0.32C_{tot}$
Optimum II	17.86	$0.16C_1$	3.93	$1.05C_2$	1.82	$0.65C_3$	$0.30C_{tot}$

In Table 6.3 the cross-sections of the columns/shear walls for all three designs are given. It is clear that the cross-sections of the optimized design are smaller than those obtained by the experienced engineer. The relative cost of the columns and the shear walls of the structure is given in Table 6.4. For the reasons described in test example 6.1 the "Optimum"

solution requires more longitudinal reinforcement than the "Applied" solution.

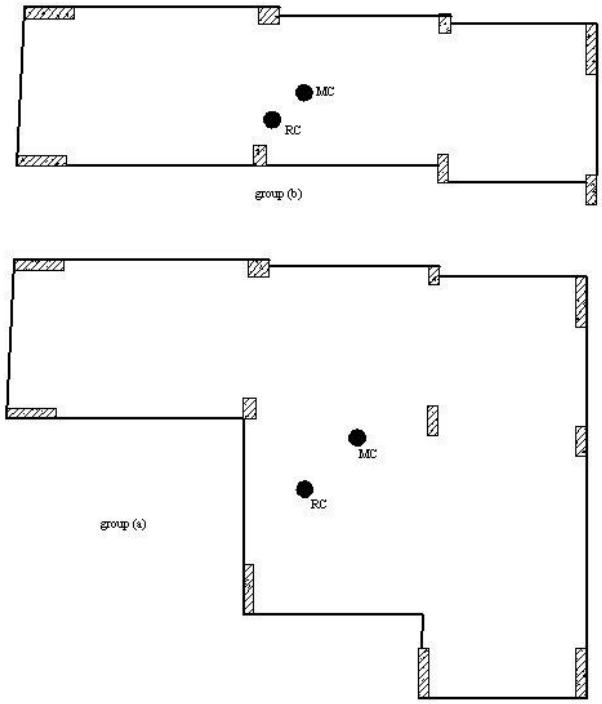

(a)

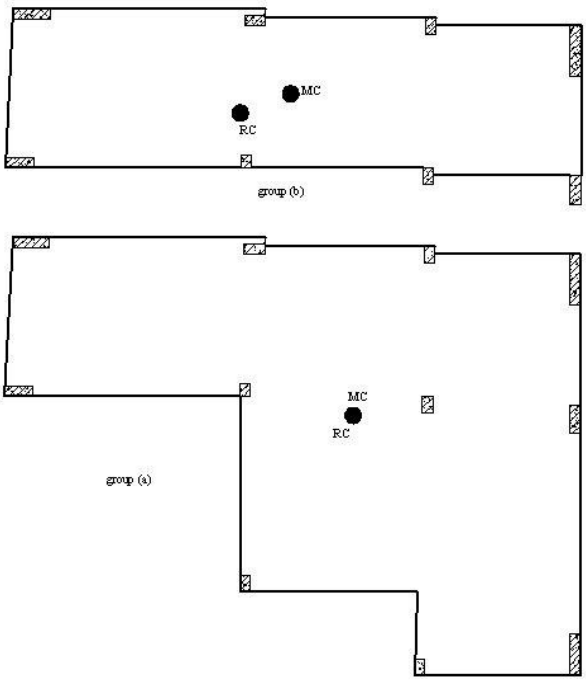

(b)

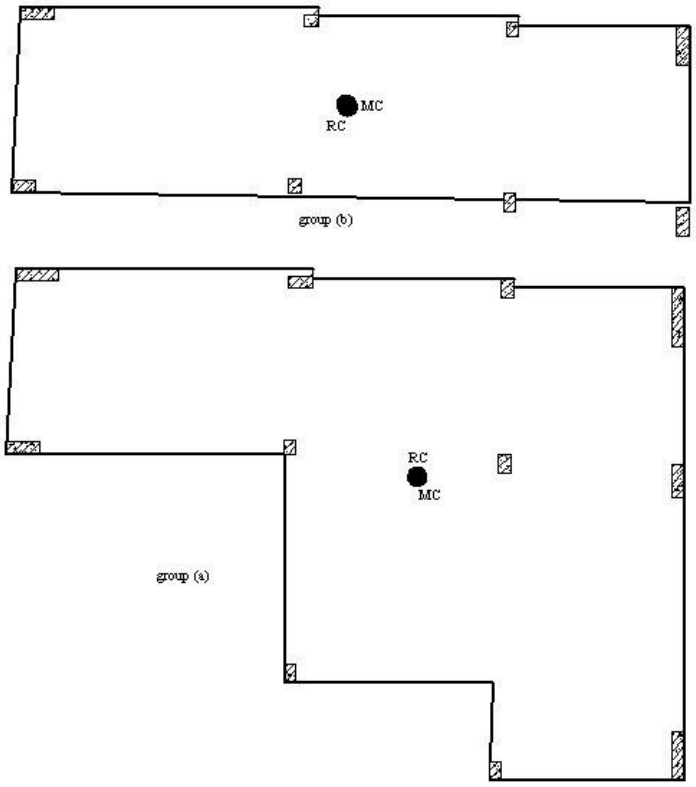

(c)

Solution	Group (a)		Group (b)	
	e_x (cm)	e_y (cm)	e_x (cm)	e_y (cm)
Applied	126.30	123.52	76.67	64.64
Optimum I	0.16	0.17	121.91	45.72
Optimum II	0.16	0.17	2.41	3.87

Figure 6.4 *Test example 6.2 – (a) Applied, (b) Optimum I and (c) Optimum II solutions (e_{MC-RC} eccentricity in x and y directions)*

7.3 Conclusions

The influence of a large eccentricity of the rigidity center in relation to the mass center is very important for the seismic response of buildings. In

this study Evolution Strategies have been implemented for the minimization of the distance between the mass center and the rigidity center of each floor layout of the building's vertical structural elements. The proposed design methodology is a two stage procedure leading to the coincidence of the mass and rigidity centers for each storey layout and fulfiling the EC2 and EC8 requirements. The minimization of the distance between the mass center and the rigidity center leads to a significant reduction of the torsional strain on the vertical elements of the structure and thus, leading implicitly to a cost-effective design of these elements. The beneficial effect of this kind of optimized layout arrangements of the columns and shear walls is directly observed on the cross-sectional and transverse reinforcement requirements for the structural systems' vertical elements. Evolution Strategies have proved to be a robust and efficient tool for the economically design optimization of seismic resistant reinforced concrete 3D frames.

REFERENCES

[1] H. Bachmann, "Seismic Conceptual Design of Buildings - Basic principles for engineers, architects, building owners, and authorities," *Order Number: 804.802e, Swiss Federal Office for Water and Geology, Swiss Agency for Development and Cooperation, Bwg, Biel*, 2002.

[2] R. J. Balling & X. Xiao, "Optimization of reinforced concrete frames," *J. Struct. Engrg., Asce*, vol. 123, no. 2, pp. 193–202, 1997.

[3] R. D. Bertero , "Inelastic torsion for preliminary seismic design," *J. Struct. Engrg., Asce*, vol. 121, no. 8, pp. 1183–1189, 1995.

[4] V. W. T. Cheung & W. K. Tso, "Eccentricity in irregular multistorey buildings," *Can. J. Civ. Engng.*, vol. 13, pp. 46–52, 1986.

[5] X. N. Duan & A. M. Chandler, "An optimized procedure for seismic design of torsionally unbalanced structures.," *Earthquake Engrg. Struct. Dynamics*, vol. 26, pp. 737–757, 1997.

[6] "Eurocode 2. Design of concrete structures," *Env1992, Cen European Committee for Standardization, Brussels*, 1992.

[7] "Eurocode 8. Design provisions for earthquake resistance of structures," *Env1998, Cen European Committee for Standardization, Brussels*, 1996.

[8] M.J. Fadaee & D.E. Grierson, "Design optimization of 3D reinforced concrete structures," *J. Struct. Opt.*, vol. 12, no. 2/3, pp. 127–134, 1996.

[9] "Federal Emergency Management Agency FEMA-310," *Handbook for the Seismic Evaluation of Buildings-a Prestandard, Prepared By the American Society of Civil Engineers for the Federal Emergency Management Agency, Washington, Dc.*, 1998.

[10] S. Ganzerli, C. P. Pantelides & L.D. Reaveley, "Performance-based design using structural optimization," *Earthquake Engrg. Struct. Dynamics*, vol. 29, no. 11, 1677-1690, 2000.

[11] J. Holland, "Adaptation in natural and artificial systems," *University of Michigan Press, Ann Arbor.*, 1975.

[12] N. D. Lagaros, M. Fragiadakis & M.Papadrakakis, "On the optimum design of shell structures with stiffening beams," *Aiaa J.*, vol. 42, no. 1, pp. 175–184, 2004.

[13] "National Building Code of Canada," Part 4 Structural Design.*" Issued By the Canadian Commission On Building and Fire Codes, Federal Publications Inc., Toronto*, 1995.

[14] M. Papadrakakis & N. D. Lagaros, "Reliability-based structural optimization using neural networks and Monte Carlo simulation," *Comput. Methods Appl. Mech. Engrg*, vol. 191, no. 32, pp. 3491–3507, 2002.

[15] G. G. Penelis & A. J. Kappos, "Earthquake-resistant concrete structures," *E&fn Spon*, 1997.

[16] Rechenberg "Evolution strategy: optimization of technical systems according to the principles of biological evolution," *Frommann-Holzboog, Stuttgart*, 1973.

[17] K. C. Sarma & H. Adeli, "Cost Optimization of Concrete Structures," *J. Struct. Engrg., Asce*, vol. 124, no. 5, pp. 570–578, 1998.

[18] K. W. Tso, "Static Eccentricity concept for torsional moment estimations," *J. Struct. Engrg., Asce*, vol. 116, no. 5, pp. 1199–1212, 1990.

[19] C. M. Wong & W. K. Tso, "Evaluation of seismic torsional provisions in uniform building code," *J. Struct. Engrg., Asce*, vol. 121, no. 10, pp. 1436–1442, 1995.

8 Performance Based Design of irregular buildings

8.1 Performance-based design procedure

Performance-based seismic design has the following distinctive features with respect to the prescriptive design codes: (i) it allows the owner, architect and structural engineer to choose both the appropriate level of seismic hazard and the corresponding performance level of the structure, and (ii) the structure is designed to meet a series of combinations of hazard levels in conjunction with corresponding performance levels.

The proposed PBD process is a displacement-based design procedure where the design criteria and the capacity demand comparisons are expressed in terms of displacements rather than forces [3], [4]. The main part in a performance-based seismic design procedure is the definition of the performance objectives that will be used. The proposed PBD process can be described by the following two steps:

(1) Proportioning of the longitudinal and transverse reinforcement of all members on the basis of the serviceability limit state.

(2) Use of non-linear dynamic analysis in order to estimate the structural capacities of the design for the different intensity levels employed. Revision of the reinforcement and the dimension of the members so that the capacities exceed the seismic demands [4].

The completion of *Step 1* is necessary for *Step 2* as the structural capacity depends both on the reinforcement and the dimensions of the members. The constraints considered for *Step 2* of the PBD procedure are related to the maximum interstorey drift limits Δ, which are the largest values of the height-wise peak interstorey drift ratios for each hazard level. This is a commonly used measure of both structural and non-structural damage because of its close relationship to plastic rotation demands on individual beam–column connection assemblies. In this study, three performance

objectives are considered that correspond to 50, 10 and 2% probabilities of exceedance in 50 years of hazard levels. The drift limits Δ, for the three performance objectives considered, are 0,5%, 1,0% and 3,0% for the three hazard levels 50in50, 10in50 and 2in50 respectively.

One performance objective is defined as the combination of a performance level for a specific hazard level. In this work three performance objectives have been considered corresponding to the 'Enhanced Objectives' of FEMA 356 [5]. The first step in defining the performance objectives is the selection of the performance levels. The performance levels that have been considered are the following:

(i) Operational: The overall damage level is characterized as very light. No permanent drift is encountered, while the structure essentially retains its original strength and stiffness.

To attain the Operational Building Performance Level, the structural components of the building need to meet the requirements for the Immediate Occupancy Structural Performance Level and the nonstructural components need to meet the requirements for the Operational Nonstructural Performance Level.

The immediate occupancy structural performance level shall be defined as the post-earthquake damage state that remains safe to occupy and essentially retains the pre-earthquake design strength and stiffness of the structure.

Also the immediate occupancy structural performance level means the post-earthquake damage state in which only very limited structural damage has occurred. The basic vertical- and lateral-force-resisting systems of the building retain nearly all of their pre-earthquake strength and stiffness. The risk of life threatening injury as a result of structural damage is very low, and although some minor structural repairs may be appropriate, these would generally not be required prior to reoccupancy.

And the operational nonstructural performance level shall be defined as the post-earthquake damage state in which the nonstructural components are able to support the pre-earthquake functions present in the building.

At this level, most nonstructural systems required for normal use of the building—including lighting, plumbing, HVAC and computer systems—are functional, although minor cleanup and repair of some items may be required. This Nonstructural Performance Level requires considerations beyond those that are normally within the sole province of the structural engineer. In addition to assuring that nonstructural components are properly mounted and braced within the structure, it is often necessary to provide emergency standby utilities. It may also be necessary to perform rigorous ability qualification testing of key electrical and mechanical equipment items to function during or after strong shaking. Users wishing to design this Nonstructural Performance Level will need to refer to appropriate criteria from other sources (such as equipment manufacturers' data) to ensure the performance of the mechanical and electrical systems.

So, buildings meeting this target Building Performance Level are expected to sustain minimal or no damage to their structural and nonstructural components. The building is suitable for normal occupancy and use, although possibly in a slightly impaired mode, with power, water and other required utilities provided from emergency sources, and possibly with some nonessential systems not functioning. Buildings meeting this target Building Performance Level pose an extremely low risk to life safety.

Under very low levels of earthquake ground motion, most buildings should be able to meet or exceed this target Building Performance Level. Typically, however, it will not be economically practical to design this target Building Performance Level for severe ground shaking, except for buildings that house essential services.

(ii) Life safety: The overall damage level is characterized as moderate. Permanent drift is encountered while strength and

stiffness has left in all storeys. Gravity-load bearing elements continue to function while there is no out-of plane failure of the walls. The overall risk of life-threatening injury as a result of structural damage is expected to be low. It should be possible to repair the structure; however, for economic reasons this may not be practical.

To attain the Life Safety Building Performance Level, the structural components of the building need to meet the requirements for the Life Safety Structural Performance Level and the nonstructural components need to meet the requirement for the Life Safety Nonstructural Performance Level.

The structural performance level shall be defined as the post-earthquake damage state that includes damage to structural components but retains a margin against onset of partial or total collapse.

Also the structural performance level means the post-earthquake damage state in which significant damage has occurred to the structure, but some margin against either partial or total structural collapse remains. Some structural elements and components are severely damaged, but this has not resulted in large falling debris hazards, either within or outside the building. Injuries may occur during the earthquake; however, the overall risk of life-threatening injury as a result of structural damage is expected to be low. It should be possible to repair the structure; however, for economic reasons this may not be practical. While the damaged structure does not pose an imminent collapse risk, it would be wise to implement structural repairs or install temporary bracing prior to its reoccupancy.

And the life safety nonstructural performance level shall be defined as the post-earthquake damage state that includes damage to nonstructural components but the damage is not life-threatening.

Also the life safety nonstructural performance level is the post-earthquake damage state in which potentially significant and costly damage has occurred to nonstructural components but they have not dislodged and fallen, threatening life safety either inside or outside the building. Egress

routes within the building are not extensively blocked, but may be impaired by lightweight debris. HVAC, plumbing and fire suppression systems may have been damaged, resulting in local flooding as well as loss of function. While injuries may occur during the earthquake from the failure of nonstructural components, overall, the risk of life-threatening injury is very low. Restoration of the nonstructural components may require extensive effort.

So, buildings meeting this level may experience extensive damage to structural and nonstructural components. Repairs may be required before reoccupancy of the building occurs, and repairing may be deemed as economically impractical. The risk to life safety in buildings meeting this target Building Performance Level is low.

This target Building Performance Level entails somewhat more damage than anticipated for new buildings that have been properly designed and constructed for seismic resistance when subjected to their design earthquakes. Many building owners will desire to meet this target Building Performance Level for severe ground shaking.

(iii) Collapse prevention: The overall damage level is characterized as severe. Substantial damage has occurred to the structure, including significant degradation in the stiffness and strength of the lateral-force resisting system. Large permanent lateral deformation of the structure and degradation of the vertical-load bearing capacity is encountered. However, all significant components of the gravity load-resisting system continue to carry their gravity load demands. The structure may not be technically practical to repair and is not safe for reoccupancy, since aftershock activity could induce collapse.

To attain the Collapse Prevention Building Performance Level, the structural components of the building need to meet the requirements for the Collapse Prevention Structural Performance Level. Nonstructural components are not considered.

The structural performance level shall be defined as the post-earthquake damage state that includes damage to structural components such that the structure continues to support gravity loads but retains no margin against collapse.

However, the structural performance level means the post-earthquake damage state in which the building is on the verge of partial or total collapse. Substantial damage to the structure has occurred, potentially including significant degradation in the stiffness and strength of the lateral-force-resisting system, large permanent lateral deformation of the structure, and—to a more limited extent— degradation of the vertical-load-carrying capacity. However, all significant components of the gravity load- resisting system must continue to carry their gravity load demands. Significant risk of injury due to falling hazards from structural debris may exist. Technically, the structure may not be practical to repair and is not safe for reoccupancy, as aftershock activity could induce collapse. And as nonstructural performance is not considered shall be classified a building rehabilitation that does not address nonstructural components.

Additionally, in some cases, the decision to rehabilitate the structure may be made without addressing the vulnerabilities of nonstructural components. It may be desirable to do this when rehabilitation must be performed without interruption of the building operation. In some cases, it is possible to perform all or most of the structural rehabilitation from outside occupied building areas. Extensive disruption of normal operation may be required to perform nonstructural rehabilitation. Also, since many of the most severe hazards to life safety occur as a result of structural vulnerabilities, some municipalities may wish to adopt rehabilitation ordinances that require structural rehabilitation only.

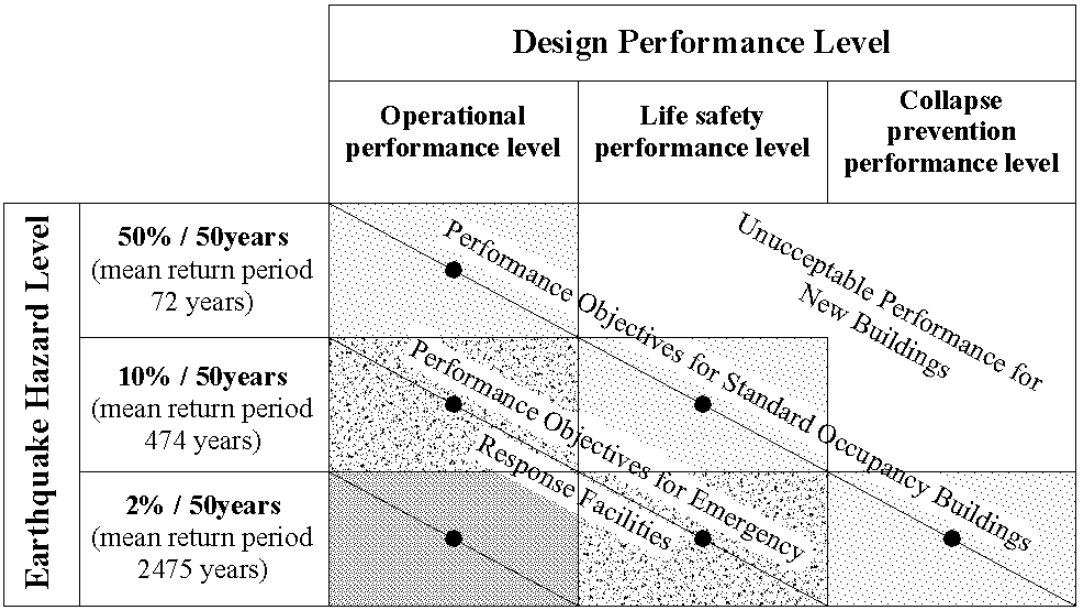

Figure 7.1 *The Design Performances [3]*

The second step in defining the performance objectives is to determine the earthquake hazard levels. Earthquake hazards include direct ground fault rupture, ground shaking, liquefaction, lateral spreading and land sliding FEMA-350 [6]. Ground shaking is the only earthquake hazard that the structural design provisions of the building codes directly address. Ground shaking hazards are typically characterized by a hazard curve, which indicates the probability that a given value of a ground motion parameter, for example peak ground acceleration, will be exceeded over a certain period of time. The ground shaking hazard levels that have been considered are the following:

(i) Occasional earthquake hazard level: with a probability of exceedance of 50% in 50 years with a 72 years interval of recurrence.

(ii) Rare earthquake hazard level: with a probability of exceedance of 10% in 50 years with a 475 years interval of recurrence.

(iii) Maximum considered event earthquake hazard level: with a probability of exceedance of 2% in 50 years with a 2475 years interval of recurrence.

8.2 Elastic response of reinforced concrete buildings

8.2.1 Design Principles

The main objective in the seismic resistant design of structural systems, like reinforced concrete buildings, is the proper conceptual design of the seismically resistant structural components and the appropriate planning arrangement of the vertical structural elements. It is obvious that the architectural layout of the structure imposes the principal restrictions related to the position of the structural elements of the building. The cooperation between the designer and the architect at the structural conceptual level might be crucial in the subsequent design stages. There are two general guidelines for the design engineer to take into account during the early designing stages of a concrete building: (i) guidelines related to the mass and stiffness distribution among the storeys of the structure and (ii) guidelines related to the plan arrangement of the vertical structural elements of the building where a rule of a minimum distance between the mass and the elastic centers for each storey (mass eccentricity) should be followed.

The elastic axis, which is the geometrical locus of the elastic centers of the storeys in a multi-storey building, cannot be accurately defined. The inability to accurately define the elastic axis has led to the following approximate approaches: (i) decomposition of the multi-storey structural system into single independent storey systems, (ii) use of the shear walls' center of gravity only and (iii) replacement of the elastic axis with an axis defined by the geometric locus of the rigidity centers of the stroreys (Cheung and Tso 1986; Tso 1990). In the present study, approach (iii), which has been adopted by the Eurocode 8 (EC8 1996) and the National Building Code of Canada (NBCC 1995), when an 'equivalent' elastic axis defined by the geometric locus of the rigid centers of each storey is considered.

According to the Federal Emergency Management Agency (FEMA-310 1998) it is suggested that, in order to minimize the influence of the

torsion, the distance between the storey's centre of mass and the storey's centre of rigidity is less than 20% of the building width in either plan dimension for Life Safety (LS) and Immediate Occupancy (IO) design states of the building. In most cases of building layouts it is not easy, even through a trial and error procedure, to define the plan arrangement of the columns and shear walls so that the rigidity center coincides closely with the mass center. What is needed is an automatic optimization procedure which is specially tailored for the solution of such a problem.

The optimum design of steel reinforced concrete 3D frames is formulated in this study on the basis of the FEMA-310 (1998) recommendation where the torsional response demands are to be reduced during a seismic event and thus implicitly enhance the seismic resistance of the structure. In this study, torsional response demands are reduced by minimizing the mass eccentricity, which is defined as the distance between the mass and the rigidity centers in each storey.

8.2.2 Seismic Design Procedures

The majority of the seismic design codes belong to the category of the prescriptive building design codes, which include: site selection and development of conceptual, preliminary and final design stages. According to a prescriptive design code, the strength of the structure is evaluated at one limit state between life-safety and near collapse using a response spectrum corresponding to one design earthquake [1]. In addition, serviceability limit state is usually checked in order to ensure that the structure will not deflect or vibrate excessively during its functioning. On the other hand, PBD is a different approach for the seismic design which includes, apart from the site selection and the development of the design stages, the construction and maintenance of a building in order to ensure reliable and predictable seismic performance over its life span. [2]

8.2.3 EAK-EKOS design procedures

According to the Greek national design codes, a number of checks must be considered in order to ensure that the structure will meet the design requirements. Each candidate design is assessed using these constraints.

All EKOS 2000 checks must be satisfied for the gravity loads using the following load combination:

$$S_d = 1.35 \sum_j G_{kj} + 1.5 \sum_i Q_{ki} \quad (7.1)$$

where '+' implies "to be combined with", the summation symbol 'Σ' implies "the combined effect of", G_{jk} denotes the characteristic value 'k' of the permanent action j and Q_{kj} refers to the characteristic value 'k' of the variable action i. If the above constraints are satisfied, the multi-modal response spectrum analysis is performed, according to EAK 2000, and the earthquake loading is considered using the following load combination:

$$S_d = \sum_j G_{kj} + E_d + \sum_i \psi_{2i} Q_{ki} \quad (7.2)$$

where E_d is the design value of the seismic action for the two components (longitudinal and transverse), respectively, and ψ_{2i} is the combination coefficient for the quasi-permanent action I, here taken to be equal to 0.30.

The main principle of new provisions, EAK 2000 included, is to design structural systems based on energy dissipation and ductility in order to control inelastic seismic response. Designing a multi-storey RC building for energy dissipation comprises the following features: (i) fulfilment of the strong column/weak beam rule, (ii) member verification in terms of forces and resistances for the ultimate limit strength limit state under the design earthquake (with a return period of 475 years and a 10% probability of exceedance in 50 years), with the elastic spectrum reduced by the q-factor equal to 3.5 times, (iii) damage limitation for the serviceability limit state and (iv) capacity design of beams and columns against shear failure.

8.3 Inelastic response of reinforced concrete buildings

8.3.1 Direct Integration of Equations of Motion

The one-storey sytems used in the models below are inelastic. The analytical solution of the equation of motion for nonlinear systems is not

possible, so numerical time-stepping methods for integration of differential equations are used.

The equation of motion of an inelastic system is:

$$mu + c\dot{u} + f_s(u, \dot{u}) = p(t) \quad (7.3)$$

In order to solve this equation, numerical integration is used, specifically Newmark's method (an implicit method). This method is based on the equations below:

$$\dot{u}_{i+1} = \dot{u}_i + [(1+\gamma)\Delta t]\ddot{u}_i + (\gamma \Delta t)\ddot{u}_{i+1} \quad (7.4)$$

$$u_{i+1} = u_i + (\Delta t)\dot{u}_i + [(0.5-\beta)(\Delta t)^2]\ddot{u}_i + [\beta(\Delta t)^2]\ddot{u}_{i+1} \quad (7.5)$$

The parameters β and γ usually take values $\gamma=\frac{1}{2}$ and $\frac{1}{6} \leq \beta \leq \frac{1}{4}$ and express the variation during a time step and affect the stability and accuracy of the method. Special occasions are for values $\gamma=\frac{1}{2}$ and $\beta=\frac{1}{4}$ (Average acceleration method) and $\gamma=\frac{1}{2}$ and $\beta=\frac{1}{6}$ (Linear acceleration method).

These two equations (7.3), (7.4) in combination with

$$mu_{i+1} + c\dot{u}_{i+1} + (f_s)_{i+1} = p_{i+1} \quad (7.6)$$

underlie in order to compute u_{i+1}, $\dot{u}_{i+1}$, $\ddot{u}_{i+1}$ at time i+1 from the known u_I, $\dot{u}_I$, $\ddot{u}_I$ at time i. Iteration is required to implement these computations because the unknown $\ddot{u}_{i+1}$ appears on the right-hand side of (7.3) and (7.5).

The key equation solved at each time step in Newmark's method, modified for nonlinear systems is:

$$\hat{k}_i \Delta u_i = \Delta \hat{p}_i \quad (7.7)$$

where

$$\Delta \hat{p}_i = \Delta p_i + \left(\frac{1}{\beta \Delta t} m + \frac{\gamma}{\beta} c\right)\dot{u}_i + \left[\frac{1}{2\beta} m + \Delta t \left(\frac{\gamma}{2\beta} - 1\right) c\right]\ddot{u}_i \quad (7.8)$$

$$\hat{k}_i = k_i + \frac{\gamma}{\beta \Delta t} c + \frac{1}{\beta (\Delta t)^2} m \quad (7.9)$$

For convenience in notation we replace i with T in k_i in order to emphasize that it is the tangent stiffness

$$\hat{k}_T \Delta u = \Delta \hat{p} \qquad (7.7')$$

$$\hat{k}_T = k_T + \frac{\gamma}{\beta \Delta t} c + \frac{1}{\beta (\Delta t)^2} m \qquad (7.9')$$

The first step of the iterative procedure is the application of equation (7.7'):

$$\hat{k}_T \Delta u^{(1)} = \Delta \hat{p} \qquad (7.7')$$

In this way $\Delta u^{(1)}$ is determined. The true force $\Delta f^{(1)}$ is associated with $\Delta u^{(1)}$ and is less than $\Delta \hat{p}$, so the residual force is defined:

$$\Delta R^{(2)} = \Delta \hat{p} - \Delta f^{(1)} \qquad (7.10)$$

The additional force displacement $\Delta u^{(2)}$ due to this residual force is determined from:

$$\hat{k}_T \Delta u^{(2)} = \Delta u^{(2)} = \Delta \hat{p} - \Delta f^{(1)} \qquad (7.11)$$

From this equation, additional displacement $\Delta u^{(2)}$ is computed and used to define a new value of residual force. The same procedure is continued until convergence. Table 7.1 describes the process for the time step i to i+1, which is the modified Newton-Raphson method (Figure 7.2).

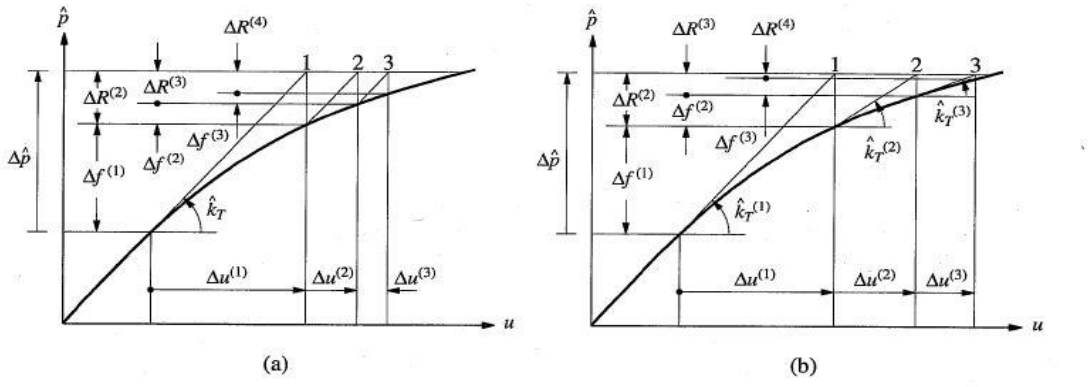

Figure 7.1 *Iteration within a time step for non-linear systems: a) modified Newton-Raphson iteration; b) Newton-Raphson iteration [7]*

1.0 *Initialize data.*

$$u_{i+1}^{(0)} = u_i \qquad f_S^{(0)} = (f_S)_i \qquad \Delta R^{(1)} = \Delta \hat{p}_i \qquad \hat{k}_T = \hat{k}_i$$

2.0 *Calculations for each iteration,* $j = 1, 2, 3, \ldots$

2.1 Solve: $\hat{k}_T \, \Delta u^{(j)} = \Delta R^{(j)} \Rightarrow \Delta u^{(j)}$.

2.2 $u_{i+1}^{(j)} = u_{i+1}^{(j-1)} + \Delta u^{(j)}$.

2.3 $\Delta f^{(j)} = f_S^{(j)} - f_S^{(j-1)} + (\hat{k}_T - k_T)\, \Delta u^{(j)}$.

2.4 $\Delta R^{(j+1)} = \Delta R^{(j)} - \Delta f^{(j)}$.

3.0 *Repetition for next iteration.* Replace j by $j + 1$ and repeat calculation steps 2.1 to 2.4.

Table 7.2 *Modified Newton-Raphson Iteration [7]*

When the incremental displacement $\Delta u^{(l)}$ satisfies the equation below the procedure is terminated:

$$\frac{\Delta u^{(l)}}{\Delta u} \leq \varepsilon \tag{7.12}$$

where

$\Delta u = \sum_{j=1}^{l} \Delta u^{(j)}$

The displacement over the time step i to i+1:

$$\Delta u_i = \sum_{j=1}^{l} \Delta u^{(j)} \tag{7.13}$$

Using the equations below (7.14) and (7.15) and deriving the value of Δu_i, $\Delta \dot{u}_i$, $\Delta \ddot{u}_I$ are defined:

$$\Delta \dot{u}_i = \frac{\gamma}{\beta \Delta t} \Delta u_i - \frac{\gamma}{\beta} \dot{u}_i + \Delta t \left(1 - \frac{\gamma}{2\beta}\right) \ddot{u}_I \tag{7.14}$$

$$\Delta \ddot{u}_i = \frac{1}{\beta (\Delta t)^2} \Delta u_i - \frac{\gamma}{\beta \Delta t} \dot{u}_i - \frac{1}{2\beta} \ddot{u}_I \tag{7.15}$$

Table 7.3 describes the analysis procedure using Newmark's method. [7]

Table 7.3 *Newmark's Method: Nonlinear Systems [7]*

Special cases

(1) Average acceleration method ($\gamma = \frac{1}{2}$, $\beta = \frac{1}{4}$)

(2) Linear acceleration method ($\gamma = \frac{1}{2}$, $\beta = \frac{1}{6}$)

1.0 *Initial calculations*

1.1 $\ddot{u}_0 = \dfrac{p_0 - c\dot{u}_0 - (fs)_0}{m}$.

1.2 Select Δt.

1.3 $a = \dfrac{1}{\beta \Delta t} m + \dfrac{\gamma}{\beta} c$; and $b = \dfrac{1}{2\beta} m + \Delta t \left(\dfrac{\gamma}{2\beta} - 1 \right) c$.

2.0 *Calculations for each time step, i*

2.1 $\Delta \hat{p}_i = \Delta p_i + a\dot{u}_i + b\ddot{u}_i$.

2.2 Determine the tangent stiffness k_i.

2.3 $\hat{k}_i = k_i + \dfrac{\gamma}{\beta \Delta t} c + \dfrac{1}{\beta (\Delta t)^2} m$.

2.4 Solve for Δu_i from $\hat{k}_i$ and $\Delta \hat{p}_i$ using the iterative procedure of Table 5.7.1.

2.5 $\Delta \dot{u}_i = \dfrac{\gamma}{\beta \Delta t} \Delta u_i - \dfrac{\gamma}{\beta} \dot{u}_i + \Delta t \left(1 - \dfrac{\gamma}{2\beta} \right) \ddot{u}_i$.

2.6 $\Delta \ddot{u}_i = \dfrac{1}{\beta (\Delta t)^2} \Delta u_i - \dfrac{1}{\beta \Delta t} \dot{u}_i - \dfrac{1}{2\beta} \ddot{u}_i$.

2.7 $u_{i+1} = u_i + \Delta u_i$, $\dot{u}_{i+1} = \dot{u}_i + \Delta \dot{u}_i$, $\ddot{u}_{i+1} = \ddot{u}_i + \Delta \ddot{u}_i$.

3.0 *Repetition for the next time step.* Replace i by $i + 1$ and implement steps 2.1 to 2.7 for the next time step.

8.3.2 DESIGNING AGAINST THE SEISMIC HAZARD

According to FEMA-310 [15] it is suggested that, in order to minimize the influence of the torsion for Life Safety (LS) and Immediate Occupancy (IO) design states of the building, the distance between the storey's center of mass and the storey's center of rigidity must be less than 20% of the building width in either plan dimension. In many cases of building layouts it is not easy, even though a trial and error procedure, to define the plan arrangement of the columns and shear walls so that the rigidity center to closely coincide with the mass center. What is needed is an automatic optimization procedure specially tailored for the solution of such a problem. According to the first approach, examined in this study, the minimum torsional response problem for 3D RC frames is formulated on the basis of the FEMA-310 [15] recommendations, where the torsional response demands are to be reduced during a seismic event and thus implicitly enhancing the seismic resistance of the structure. The response

demands are reduced, according to Bertero [6] by minimizing the mass eccentricity, which is defined as the distance between the mass and rigidity centers at each storey of the building. According to Pauley [16], strength can be assigned to the elements in any way that suits the designer's intentions. A desirable strength distribution is achieved when the center of strength is located close to or coincides with the center of mass of the system [16,17]. Based on this concept the second design approach of the minimum torsional response problem is formulated such that the eccentricity between strength and mass centers is minimized.

8.4 Optimum Design of RC buildings

Structural optimization problems are characterized by various objective and constraint functions that are generally non-linear functions of the design variables. These functions are usually implicit, discontinuous and non-convex. The mathematical formulation of the structural optimization problems with respect to the design variables, the objective and constraint functions depend on the type of the application. Most optimization problems can be expressed in standard mathematical terms as a non-linear programming problem. A structural optimization problem can be formulated in the following form:

$$\begin{aligned} &\min && F(\mathbf{s}) \\ &\text{subject to} && g_j(\mathbf{s}) \le 0 \quad j=1,...,m \\ & && s_i \in R^d, \quad i=1,...,n \end{aligned} \tag{7.16}$$

where $F(\mathbf{s})$ and $g_j(\mathbf{s})$ denote the objective and constraints functions, respectively, R^d is a given design set, while the design variables s_i (i=1,...,n) can take values only from this set.

8.4.1 Definitions

There are some definitions that have to be provided in order to facilitate the description of the problem and its handling by the adopted optimization algorithm.

Torsionally balanced: A structural system is defined as torsionally balanced when the mass center coincides or almost coincides with the rigidity center at any storey of the structure.

Center of rigidity (CR): Only in a special class of multi-storey structures can the centers of rigidity be defined in the strict sense [18]. The inability to define the centers of rigidity has led to the following approximate approaches: (i) Decomposing the multi-storey structural system into single independent storey systems. (ii) Using only the center of gravity of the shear walls. (iii) Replacing the elastic axis with an axis defined by the geometrical locus of the rigidity centers of the storeys [18]. In the present study, approach (iii) is considered, which has been adopted by Eurocode 8 [14] and the National Building Code of Canada [19].

Center of resistance or strength (CV): This center can be defined as follows:

$$x_{CV} = \frac{\sum_i x_i V_{n,i}}{\sum_i V_{n,i}} \tag{7.17}$$

where x_{CV} is the x-coordinate of the CV, $V_{n,i}$ is the nominal strength of the i-th vertical structural element and x_i is the distance of the i-th element from the center of mass.

For every column and shear wall, two architectural constraints are defined:

Architectural constraint 1: The first architectural constraint (AC_1) is related to the plan's boundaries where a column or shear wall should be located. It is implemented as a rectangle with dimensions $AC_{1x} \times AC_{1y}$. A design is considered feasible, with respect to the AC_1 constraint, when the cross sections of the columns and shear walls are contained in the corresponding rectangles. In Figures 7.2a and 7.2b two AC_1 rectangles are shown for a typical plan view of a concrete building.

Architectural constraint 2: The second architectural constraint (AC_2) is related to the topological position of the beams in conjunction with their

supporting columns and/or shear walls. This constraint is implemented through a point located within the rectangle AC_1. The AC_2 constraint, shown in Figures 7.2a and 7.2b, is essential in assisting the optimization procedure to reach layouts where the beams and their cross points are supported by columns or shear walls. In any feasible design the AC_2 point should correspond to a joint of horizontal (beam) and vertical (column/shear wall) elements.

Column type: Two types of columns/shear walls are considered. *Type I* is defined as the column/shear wall where the AC_2 point corresponds to one of the corners of the rectangle AC_1 labeled as F (see Figure 7.2a); *Type II* is defined as the column/shear wall where the AC_2 point is located inside the rectangle AC_1 (see Figure 7.2b).

8.4.2 Optimization based on the initial construction cost

In all design procedures that will be implemented in this study the design variables are divided in two categories: (i) Topology design variables, corresponding to the topology or layout of the columns and shear walls of the building. (ii) Sizing design variables, corresponding to the dimensions of the cross sections. The mathematical formulation of the optimization problem for the initial construction cost of RC buildings can be stated as follows:

$$\begin{aligned} \min \quad & C_{IN}(s) = C_b(s) + C_{sl}(s) + C_{cl}(s) \\ \text{subject to} \quad & g_k(s) \le 0,\ k=1,2,...,m \ \text{(behavioral)} \\ & \left.\begin{aligned} & t^i_{lb,j} \le r^i_j \le t^i_{ub,j},\ j=1,2,...,n_{columns} \\ & s^i_{lb,j} \le h^i_j \le s^i_{ub,j},\ j=1,2,...,n_{columns} \end{aligned}\right\} \text{(architectural)} \\ & i=1,2,...,n\_g_{storeys} \end{aligned} \tag{7.18}$$

where $C_{IN}(s)$ refers of the total initial construction cost of the structure, and $C_b(s)$, $C_{sl}(s)$, $C_{cl}(s)$ refer to the total initial construction cost of the beams, the slabs and the columns, respectively. The cost of the foundation has not been included in the initial cost. The term initial cost of a structure refers to the cost during its construction stage. The initial cost is related to the material and the labor cost for the construction of the building which includes concrete, steel reinforcement, labor cost for

placement and the non-structural components cost. The behavioral constraints $g_k(s)$ are imposed by the design codes, r_j^i is the distance of the j-th column/shear wall mass center in the i-th group of storeys from its corresponding AC_2 point (see Figure 7.3b, where for simplicity reasons the superscript i and subscript j are omitted in Figure 7.2). $n\_g_{storeys}$ is the total number of groups of storeys having the same layout in the plan, while $n_{storeys}$ is the total number of storeys. $t_{lb,j}^i, t_{ub,j}^i$ are the lower and upper bounds of the topology design variables imposed by the architectural constraints, while h_j^i is the largest edge of the j-th column/shear wall in the i-th group of storeys, corresponding to the sizing design variables (see Figure 7.2a). $s_{lb,j}^i, s_{ub,j}^i$ are the lower and upper bounds of the sizing design variables imposed by the architectural constraints. As it will be seen in the following subsection, there is a relation between the two kinds of design variables in topology and sizing optimization, as well as in the corresponding bounds.

8.4.3 Optimization design based on the minimum torsional response

In the minimum torsional response optimization problem the basic goal is to formulate an optimization procedure that could lead to designs with improved earthquake resistance and in particular to create designs having minimum torsional response. In this study two separate formulations of this problem have been considered. The first one is formulated as a minimization problem of the eccentricity $e_{CM\text{-}CR}$ between the mass center (CM) and the rigidity center (CR) of each storey, while the second formulation is stated as a minimization problem of the eccentricity $e_{CM\text{-}CV}$ between the mass center and the center of strength (CV). Both formulations are subjected to the behavioral constraints imposed by the design codes as well as to the architectural constraints.

The two formulations of the optimization problem can be stated as follows:

$$\text{(i)} \quad \min \quad e_{\text{CM-CR}} = \sqrt{(x^i_{\text{CM}} - x^i_{\text{CR}})^2 + (y^i_{\text{CM}} - y^i_{\text{CR}})^2},\ i=1,2,...,n\_g_{\text{storeys}}$$

$$\text{subject to} \quad g_k(\mathbf{s}) \le 0,\ k=1,2,...,m \quad \text{(behavioral)}$$

$$\left.\begin{array}{l} t^i_{\text{lb,j}} \le r^i_j \le t^i_{\text{ub,j}},\ j=1,2,...,n_{\text{columns}} \\ s^i_{\text{lb,j}} \le h^i_j \le s^i_{\text{ub,j}},\ j=1,2,...,n_{\text{columns}} \end{array}\right\} \text{(architectural)} \qquad (7.19a)$$

$$\text{(ii)} \quad \min \quad e_{\text{CM-CV}} = \sqrt{(x^i_{\text{CM}} - x^i_{\text{CV}})^2 + (y^i_{\text{CM}} - y^i_{\text{CV}})^2},\ i=1,2,...,n_{\text{storeys}}$$

$$\text{subject to} \quad g_k(\mathbf{s}) \le 0,\ k=1,2,...,m \quad \text{(behavioral)}$$

$$\left.\begin{array}{l} t^i_{\text{lb,j}} \le r^i_j \le t^i_{\text{ub,j}},\ j=1,2,...,n_{\text{columns}} \\ s^i_{\text{lb,j}} \le h^i_j \le s^i_{\text{ub,j}},\ j=1,2,...,n_{\text{columns}} \end{array}\right\} \text{(architectural)} \qquad (7.19b)$$

where $(x^i_{\text{CM}},y^i_{\text{CM}})$, $(x^i_{\text{CR}},y^i_{\text{CR}})$ and $(x^i_{\text{CV}},y^i_{\text{CV}})$ are the coordinates of the mass center, the rigidity center and the center of strength, respectively. It must be noted that both centers CR and CV are defined for each storey.

8.4.4 The combined optimization problem

In the third formulation, all three objectives defined in Eqs. (7.18), (7.19a) and (7.19b) are considered to lead to a three-objective optimization problem. A number of methods have been proposed for solving multi-objective optimization problems. The methods are divided into three major categories: (i) methods with a priori articulation of preferences, (ii) methods with a posteriori articulation of preferences, and (iii) methods with no articulation of preferences. In this study the weighted sum method that belongs to the methods with a priori articulation of preferences is considered. These methods allow the engineer to specify preferences, which are articulated in terms of the relative importance of different objectives. The mathematical formulation for the combined optimization problem can be stated as follows:

$$\begin{aligned} \min \quad & F(\mathbf{s}) = w \cdot C^{*}_{IN} + (1\text{-}w) \cdot \max(e^{*}_{CM\text{-}CR}, e^{*}_{CM\text{-}CV}) \\ \text{subject to} \quad & g_k(\mathbf{s}) \le 0,\ k=1,2,...,m \qquad \text{(behavioral)} \\ & \left.\begin{array}{l} t^{i}_{lb,j} \le r^{i}_{j} \le t^{i}_{ub,j},\ j=1,2,...,n_{columns} \\ s^{i}_{lb,j} \le h^{i}_{j} \le s^{i}_{ub,j},\ j=1,2,...,n_{columns} \end{array}\right\} \text{(architectural)} \end{aligned} \tag{7.20}$$

where C^{*}_{IN}, $e^{*}_{CM\text{-}CR}$ and $e^{*}_{CM\text{-}CV}$ are the normalized values of the three objectives, i.e. the initial construction cost and the two eccentricities, respectively, while w is the weight coefficient which articulates the preferences of the engineer regarding the relative importance of different objectives.

8.4.5 Type of design variables

In this study the columns/shear walls are of rectangular shape with dimensions $h \times b$, where $h \ge b$, while the smallest column that is permitted to be allocated is 30×30 cm^2. The sizing design variables of the columns and shear walls depend on the topology design variables which are defined first.

8.4.5.1 Topology design variables

As mentioned above the columns are divided in two categories. For Type I column/shear walls: if $AC_{1x} > AC_{1y}$ the final position of the individual element center of the column/shear wall will be allocated along the edge of AC_{1x}, otherwise it will be allocated along the edge of AC_{1y}. In the case of a square architectural constraint with $AC_{1x} = AC_{1y}$, the selection of the edge is random. For Type I column/shear walls the lower bound of the topology design variable depends on the indicative minimum column size

$$t^{i}_{lb,j} = \frac{h_{min}}{2} \tag{7.21}$$

where the minimum column size h_{min}, imposed by the design codes, is equal to 30cm. The above mentioned lower bound constraint is imposed in order to avoid obtaining columns with dimensions less than h_{min}. The

upper bound is equal to half the size of the corresponding architectural constraint edge (AC_{1x} or AC_{1y})

$$t_{ub,j}^{i} = \frac{1}{2}\sqrt{(x_S - x_F)^2 + (y_S - y_F)^2} \tag{7.22}$$

In Figure 7.2a the largest edge of the AC_1 architectural constraint is AC_{1y} which will be selected as the edge where the individual element center of the column/shear wall will be allocated. Furthermore, S (x_S, y_S) is the starting point and F (x_F, y_F) is the finishing point of the AC_{1y} edge, where the AC_2 point coincides with the finishing point F.

In Type II column/shear walls the edge of the AC_1 architectural rectangle, where the individual element center of the column will be allocated, has either been preselected or it will be selected by the smallest distance of the projection of the AC_2 point to the four edges of the AC_1 rectangle. The four projections points PPi, i=1,…,4 are shown in Figure 7.2b. It can be seen that the distance between the points AC_2 and PP1 is the smallest one, so the edge of AC_{1x} of the corresponding architectural constraint is selected for the allocation of the individual element center of the column/shear wall and the PP1 projection point is renamed to AC_2. Point S (x_S,y_S) is the starting point and F (x_F,y_F) is the finishing point of this edge. The allocation of the mass center of the column/shear wall is either on the left or on the right-hand side of the renamed projection point PP1.

Irrespectively of the side to which the individual element center will be allocated, the lower bound is defined to be equal to zero

$$t_{lb,j}^{i} = 0 \tag{7.23}$$

The definition of the upper bound depends on which side of the projected AC_2 point the column mass center will be allocated:

$$t^{i}_{ub,j} = \frac{a}{2} \quad \text{(if on the left side)}$$
$$t^{i}_{ub,j} = \frac{b}{2} \quad \text{(if on the right side)} \tag{7.24}$$

where "a" is the distance of the new position of the AC_2 point from point S and "b" is the distance of the new position of the AC_2 point from point F (see Figure 7.2b).

8.4.5.2 Sizing design variables

As mentioned previously, topology design variables are defined first followed by the sizing design variables which are related to the topology design variables. In the case of Type I columns/shear walls there is a direct relation between topology and sizing design variables for each column/shear wall. This sizing design variable is defined as inactive

$$h^{i}_{j} = 2r^{i}_{j} \tag{7.25}$$

In the case of Type II column/shear walls there is an indirect relation between the two types of design variables defined by:

$$s^{i}_{lb,j} = 2r^{i}_{j}$$
$$s^{i}_{ub,j} = 2\min(a',b') \tag{7.26}$$

where a' and b' refer to the distance of the individual element center of the column/shear wall from points S and F, respectively (see Figure 7.2b). In this case the sizing design variables are *active*, since their dimensions have to be defined by the optimizer and not by the topology design variables as in the case of Type I column/shear walls. The bounds of the size of the column/shear wall are dependent on the topological design variable r^{i}_{j}.

8.4.6 Behavioural Constraints

Apart from the architectural constraints, behavioral constraints, imposed by the design codes, have to be satisfied for an acceptable design. These behavioral checks are performed following a structural analysis where

stresses and displacements are calculated and checked according to the EC2 [20] and EC8 [14] design codes. The majority of the seismic design codes belong to the category of the prescriptive building design codes, which include site selection followed by the conceptual, preliminary and final design stages. According to a prescriptive design code the strength of the structure is evaluated at one limit state defined between life-safety and near collapse using a response spectrum corresponding to one design earthquake [14]. In addition, a serviceability limit state is usually checked in order to ensure that the structure will not deflect or vibrate excessively during its functioning.

According to the Eurocodes a number of checks must be considered in order to ensure that the structure will meet the design requirements. In particular, each candidate design should satisfy all EC2 [20] checks for the gravity loads using the following load combination:

$$S_d = 1.35\sum_j G_{kj} "+" 1.50\sum_i Q_{ki} \tag{7.27}$$

where '+' implies "to be combined with", the summation symbol 'Σ' implies "the combined effect of", G_{kj} denotes the characteristic value 'k' of the permanent action j and Q_{ki} refers to the characteristic value 'k' of the variable action i. If the above constraints are satisfied, the multi-modal response spectrum analysis is performed and the earthquake loading is considered using the following load combination:

$$S_d = \sum_j G_{kj} "+" E_d "+" \sum_i \psi_{2i} Q_{ki} \tag{7.28}$$

where E_d is the design value for the two components (longitudinal and transverse) of the seismic action and ψ_{2i} is the combination coefficient for the quasi-permanent action i, here taken to be equal to *0.30*. All these checks are performed for each candidate optimum design examined by the optimizer.

The main principle of new code provisions, EC8 inclusive, is to design structural systems based on energy dissipation and on ductility in order to control the inelastic seismic response. The following features have to be

taken into consideration in designing a multi-storey RC building for energy dissipation: (i) fulfilment of the strong column/weak beam rule, (ii) member verification in terms of forces and resistances for the ultimate strength limit state under the design earthquake (return period of 475 years, with a 10% probability of exceedance in 50 years) with the elastic spectrum reduced by the behavioral factor q, (iii) damage limitation for the serviceability limit state and (iv) capacity design of beams and columns against shear failure.

8.4.7 Initial and limit state cost

The total cost C_{TOT} of a structure, over a time period which may be the design life of a new structure or the remaining life of a retrofitted structure, can be expressed as a function of the time period and the design variable vector as follows [21]:

$$C_{TOT}(t,s) = C_{IN}(s) + C_{LS}(t,s) \tag{7.29}$$

where C_{IN} is the initial cost of a new or retrofitted structure, C_{LS} is the limit state cost, s is the design vector corresponding to the design loads, resistance and material properties while t is the time period. The term "limit state cost" refers to the potential damage cost from earthquakes that may occur during the life span of the structure. It accounts for the cost of repairs after an earthquake, the cost of loss of contents, the cost of injury recovery or human fatality and other direct or indirect economic losses. The quantification of the losses in economic terms depends on several socio-economic parameters. The limit state cost, for the i-th limit state, can be formulated as follows:

$$C_{LS}^{i} = C_{dam}^{i} + C_{con}^{i} + C_{ren}^{i} + C_{inc}^{i} \tag{7.30}$$

where C_{dam}^{i} is the damage repair cost, C_{con}^{i} is the loss of contents cost, C_{ren}^{i} is the loss of rental cost and C_{inc}^{i} is the income loss cost. Details about the calculation formula for each limit state cost can be found in [21,22], while Table 7.2 depicts how C_{LS}^{i} is calculated for the text example.

For the purpose of this study the exceedance cost of a damage state is obtained as a percentage of the initial cost as shown in Table 7.3 [23,24]. It is generally accepted that interstorey drift can be used to determine the expected damage. The relation between the drift limit ratios and the damage state, employed in this study (Tables 7.3 and 7.4), is based on the HAZUS project [25] for low-rise RC moment resisting frames for a moderate-code design, and on the work of Ghobarah [26] for ductile moment resisting frames. Based on analytical and experimental data, Ghoborah examined the correlation between drift and damage of various structural elements and systems and determined the relation between the interstorey drift and various damage levels of different reinforced concrete elements and structural systems, as given in Table 7.3.

Based on a Poisson process model of earthquake occurrences and an assumption that damaged buildings are immediately retrofitted to their original intact conditions after each major damage-inducing seismic attack, Wen and Kang [27] proposed the following formula for the limit state cost function considering *N* damage states:

$$C_{LS}(t,s) = \frac{\nu}{\lambda}\left(1-e^{-\lambda t}\right)\sum_{i=1}^{N} C_{LS}^{i} P_i \tag{7.31}$$

where

$$P_i = P(\Delta > \Delta_i) - P(\Delta > \Delta_{i+1}) \tag{7.32}$$

and

$$P(\Delta > \Delta_i) = (-1/t)\cdot \ln[1-\overline{P}_i(\Delta-\Delta_i)] \tag{7.33}$$

P_i is the probability of the ith damage state being exceeded given the earthquake occurrence and C_{LS}^{i} is the corresponding limit state dependent cost; $P(\Delta-\Delta_i)$ is the exceedance probability given occurrence; Δ_i, Δ_{i+1} are the drift ratios defining the lower and upper bounds of the ith damage state; $\overline{P}_i(\Delta-\Delta_i)$ is the annual exceedance probability of the maximum

interstorey drift value Δ_i; v is the annual occurrence rate of significant earthquakes, modeled by a Poisson process, and t is the service life of a new structure or the remaining life of a retrofitted structure. The first component of Eq. (7.31) that contains the exponential term is used in order to express the C_{LS} in a present value, where λ is the annual momentary discount rate considered to be constant and equal to 5%. It is assumed that after the occurrence of an earthquake the structure is fully restored to its initial state.

REFERENCES:

[1] Nikos D. Lagaros, Andreas F. Fotis & Stilianos A. Krikos, "Assessment of seismic design procedure bad on total cost," *Earthquake Engng. Struct.*, vol. 35, no. 10, pp. 1381–1401, 2006.

[2] Iordanis D. Naziris, "MSc Thesis "Influence of Masonry Infill Walls in the Framework of the Optimum Performance-Based Design of RC Buildings," *Institute Structural Analysis Seismic Research, School Civil Eng., Ntua*.

[3] T. J. Sullivan, G. M. Calvi & M. J. N. Priestley & M. J. Kowalsky, "The limitations and performances of different displacement based design methods," *J. Earthquake Eng.*, vol. 7, no. 1, pp. 201–241, 2003.

[4] T. B. Panagiotakos, M. N. Fardis "A displacement-based seismic design procedure for RC buildings and comparison with EC8," *Earthquake Eng. Structural Dynamics*, vol. 30, pp. 1439–1462, 2001.

[5] "American Society of Civil Engineers, Prestandard and Commentary for the Seismic Rehabilitation of Buildings," *Fema-356, Federal Emergency Management Agency, Washington, DC*, 2000.

[6] "Recommended Seismic Design Criteria for New Steel Moment-Frame Buildings," *Fema 350, Federal Emergency Management Agency, Washington, DC*, 2000.

[7] Anil K. Chopra, "Dynamics of Structures, Theory and Applications to Earthquake Engineering," *University California Berkeley, Prentice Hall Int., Inc*.

[8] "EKOS 2000, National code for concrete building structures of Hellas," 2000.

[9] "EAK 2000, National seismic code of Hellas," 2000.

[10] Raul D. Bertero & Vitelmo V. Bertero, "Performance-based seismic engineering: the need for a reliable conceptual comprehensive approach," *Earthquake Engng. Struct. Dyn*, vol. 31, pp. 627–652, 2002.

[11] M. Fragiadakis, "Optimum Earthquake Resistant Design of Structures Performing Non-Linear Analysis," *PhD, Institute Structural Analysis Seismic Research, School Civil Eng., Ntua*, 2006.

9 Numerical Tests of optimum design of RC irregular structures

9.1 Performance-based design examples

In this section two test examples are considered. In both test examples the following material properties have been considered: concrete with modulus of elasticity E_c=30GPa and characteristic compressive cylinder strength f_{ck}= 20MPa, longitudinal steel reinforcement with modulus of elasticity E_s=210GPa and characteristic yield strength $f_{yk,s}$=500MPa and transverse reinforcement with characteristic yield strength $f_{yk,s}$=220MPa. The design spectrum that has been used has the following characteristics: A=0.16g, ground type B and behavior factor q=3.0 according to EC8 [14]. The cross section of the beams is 25×60 cm^2.

The following four formulations of the optimization problem have been considered in the numerical study: (i) minimum initial construction cost (leading to design D_{Cin}); (ii) minimum CM-CR eccentricity (leading to design D_{Ecr}); (iii) minimum CM-CV eccentricity (leading to design D_{Ecv}); and (iv) one combined formulation (leading to design D_{Comb}) where two values of the weight coefficient of Eq. (5) have been examined (0.1 and 0.9). The combined formulation can be described as follows:

$$\mathrm{Min}\{0.1\cdot C_{IN}^{*}+0.9\cdot \max(e_{CM\text{-}CR}^{*}, e_{CM\text{-}CV}^{*})\} \quad (8.1)$$

The solution of all four formulations of the optimization problem is performed with the EA(μ+λ) optimization scheme [28] with ten parents and offsprings (μ=λ=10).

***Table 8.1**: Limit state dependent cost calculations (in € 1,000)*

Performance level	C_{dam}	C_{con}	C_{ren}	C_{inc}	C_{LS}^{i} Eq. (15)
1	0.00	0.00	0.00	0.00	0.00
2	0.26	0.07	0.02	0.16	0.52
3	2.64	0.72	0.20	1.60	5.16
4	10.56	2.88	0.81	6.40	20.65
5	23.76	6.48	1.81	14.40	46.45
6	42.24	11.52	3.23	25.60	82.59
7	52.80	14.40	4.03	32.00	103.23

***Table 8.2**: Damage state drift ratio limits and cost based on HAZUS [25]*

Performance level	Damage State	Interstorey Drift (%)	Cost (% of initial cost)
1	None	$\Delta<0.5$	0
2	Slight	$0.5<\Delta<0.9$	0.5
3	Moderate	$0.9<\Delta<2.3$	20
4	Major	$2.3<\Delta<6.0$	80
5	Destroyed	$6.0<\Delta$	100

Four different criteria have been used in order to assess the optimum designs achieved through the aforementioned formulations: (i) the initial construction cost; (ii) the total life-cycle cost; (iii) the torsional response criterion; and (iv) the limit state probabilities of exceedance of the optimum designs. For the second and third assessment criteria, ground motions from Table 8.4 are used which have been chosen from the Somerville and Collins [29] database. The records of each hazard level are scaled to the same PGA in order to ensure compatibility between the records, in accordance to the hazard curve taken from the work of Papazachos et al. [30] (see Table 8.5).

***Table 8.3**: Damage state drift ratio limits and cost based on the work of Ghobarah [26]*

Performance level	Damage State	Interstorey Drift (%)	Cost (% of initial cost)
1	None	$\Delta<0.1$	0
2	Slight	$0.1<\Delta<0.2$	0.5
3	Light	$0.2<\Delta<0.4$	5
4	Moderate	$0.4<\Delta<1.0$	20
5	Heavy	$1.0<\Delta<1.8$	45
6	Major	$1.8<\Delta<3.0$	80
7	Destroyed	$3.0<\Delta$	100

***Table 8.4**: Natural records [29]*

Earthquake	Station	Distance	Site
Records in 50/50 hazard level			
Honeydew (PT)	Cape Mendocino	20	rock
17 August 1991	Petrolia	17	soil
Cape Mendocino (CM)	Rio Dell	13	soil
25 April 1992	Butler Valley	37	rock
Cape Mendocino (C2)	Fortuna	43	soil
aftershock, 4/26/92	Centerville	28	soil
Records in 10/50 hazard level			
Tabas (TB)	Dayhook	14	rock
16 September 1978	Tabas	1.1	rock
Cape Mendocino (CM)	Cape Mendocino	6.9	rock
25 April 1992	Petrolia	8.1	soil
Chi-Chi (CC), Taiwan	TCU101	4.9	soil
20 September 1999	TCU102	3.8	soil
Records in 2/50 hazard level			
Valparaiso (VL), Chile	Vina del Mar	30	soil
3 May 1985	Zapaller	30	rock
Michoacan (MI), Mexico	Caleta de Campos	12	rock
19 September 1985	La Union	22	rock
	La Villita	18	rock
	Zihuatenejo	21	rock

The fragility analysis is performed following the methodology described in HAZUS [25], where uncertainties on the material properties affecting the capacity curve and on the ground shaking demand are considered. In order to perform the non-linear dynamic analyses required for the life-cycle cost and fragility analyses a centerline model was formed for both test examples. The members are modeled using the force-based fiber beam-column element while the same material properties are used for all the structural elements of both examples. Soil-structure interaction was not considered and the base of the columns at the ground floor is assumed to be fixed while no uncertainties in the foundation conditions have been taken into account.

***Table 8.5**: Seismic hazard levels [30]*

Event	Recurrence Interval	Probability of Exceedance	PGA (g)
Frequent	21 years	90% in 50 years	0.06
Occasional	72 years	50% in 50 years	0.11
Rare	475 years	10% in 50 years	0.31
Very Rare	2475 years	2% in 50 years	0.78

9.1.1 Test example 8.1 – Two storey building

The first test example, shown in Figure 8.1, is a two-storey 3D frame where the height of each storey is 3 meters, while the plan layout of the columns/shear walls is the same for both storeys. The following 6 design variables have been used corresponding to 5 topology and 1 active sizing design variables. In Figure 8.2 both architectural constraints (AC_1 rectangles and AC_2 points) are presented for all columns/shear walls. It must be noted that all designs obtained from the various formulations of the optimization problem fulfil the requirements of EC2 and EC8 design codes.

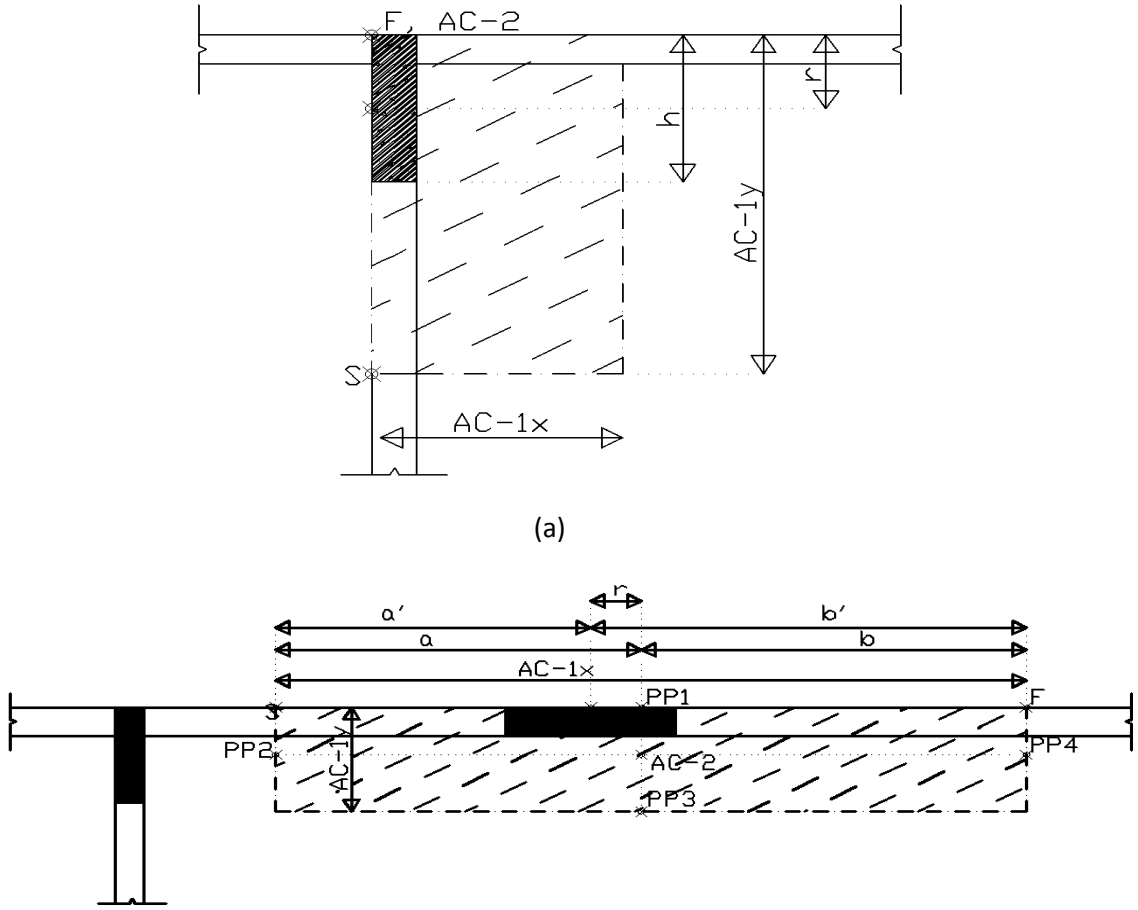

Figure 8.1: *(a) Sample column Type I with its architectural constraints AC_1 and AC_2, (b): Sample column Type II with its architectural constraints AC_1 and AC_2.*

Table 8.6 depicts the cross-sectional dimensions of the four optimum designs along with the corresponding eccentricities. It should be noted that the eCM-CV shown in Table 8.6 refers to its maximum values over the two storeys of the structure. The dimensions of the columns/shear walls are denoted as dimx and dimy corresponding to the x and y axis, respectively. As it can be seen the eccentricities ($e_{CM\text{-}CR}$, $e_{CM\text{-}CV}$) of D_{Cin} are larger than one meter, and while the Min $\{e_{CM\text{-}CR}\}$ and Min $\{e_{CM\text{-}CV}\}$ formulations improved only the eccentricity that was to be minimized, only the combined formulation managed to improve both eccentricities.

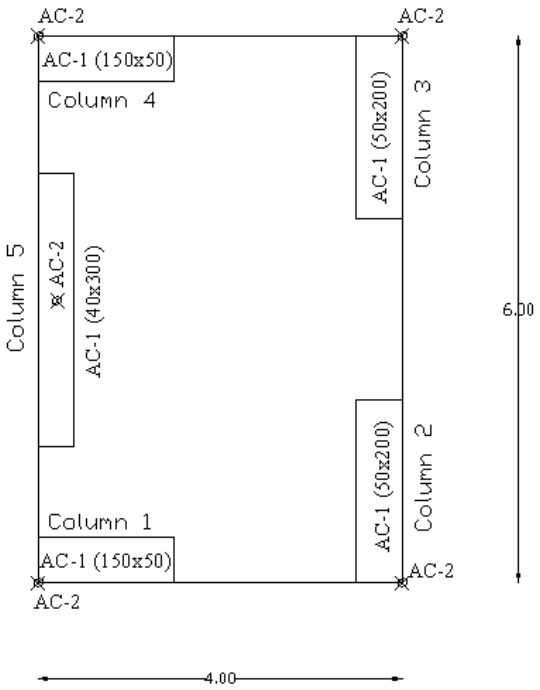

Column	AC_1	
	AC_{1x}	AC_{1y}
C1	150	50
C2	50	200
C3	50	200
C4	150	50
C5	40	300

***Figure 8.2**: Test example 8.1 - Architectural constraints of a typical storey*

In order to assess the structural performance of the optimum designs, nonlinear time-historey analyses are performed for the records from Table 8.4. Table 8.7 contains the maximum and minimum values of the top diaphragm rotation for each hazard level. It can be seen that the maximum rotation of the diaphragm, for all three hazard levels, is encountered for design D_{Cin}. On the other hand, in frequent (50/50) and occasional (10/50) hazard levels, design D_{Ecr} behaves better, while in rare (2/50) hazard levels it is design D_{Comb} that has the minimum torsional response. As far as the rare hazard level is concerned, between D_{Cin}, D_{Ecr} and D_{Ecv}, it is the latter that has the minimum rotation. The performance of designs D_{Ecr} and D_{Ecv} in the three hazard levels is in accordance with the findings of Paulay [16,17], Tso and Myslimaj [31] reported for one-storey structures.

In Table 8.8, the optimum designs are compared with respect to the initial limit state and total life-cycle costs. Through this comparison it can be seen that D_{Cin} is the worst design in terms of life-cycle cost irrespective of

the drift limits considered. The best design in terms of total life-cycle cost, though, depends on the drift limits used for calculating the limit state cost. When HAZUS [25] drift limits are employed designs D_{Ecr} and D_{Ecv} perform equally well too, while design D_{Comb} is the best optimum design. On the other hand, when the drift limits given by Ghobarah [26] are used for the calculation of the limit state cost then D_{Ecr} is the best design. This is due to the type of the architectural constraints imposed and the irregular plan view, the three formulations related with the minimization of eccentricities (Min $\{e_{CM-CR}\}$, Min $\{e_{CM-CV}\}$and combined) converging to optimum designs having shear-walls in both directions. On the other hand D_{Cin} has the minimum cross-sections, thus the maximum drifts obtained for each hazard level for D_{Cin} are much greater than those of the other three optimum designs.

The results of the last part of the comparative study, are shown in Table 8.9, where fragility analysis is performed for the slight, moderate, extensive and complete limit states. The four damage states are defined according to HAZUS for low rise buildings for the moderate code design level. More specifically, the probabilities of exceeding slight, moderate, extensive and complete limit states (defined according to HAZUS) are given in Table 8.9. In particular, for the case of the slight and moderate limit states the probabilities of violation, calculated for D_{Cin}, are one order of magnitude larger than those of D_{Ecv}. While for the extensive limit state, the probabilities of violation calculated for D_{Comb} is one order of magnitude less than those of D_{Ecr} and D_{Ecv} and two orders less than those for D_{Cin}. In the case of the complete limit state the probabilities calculated are less than 10^{-4}% for all designs.

9.1.2 Test example 8.2 – Three storey building

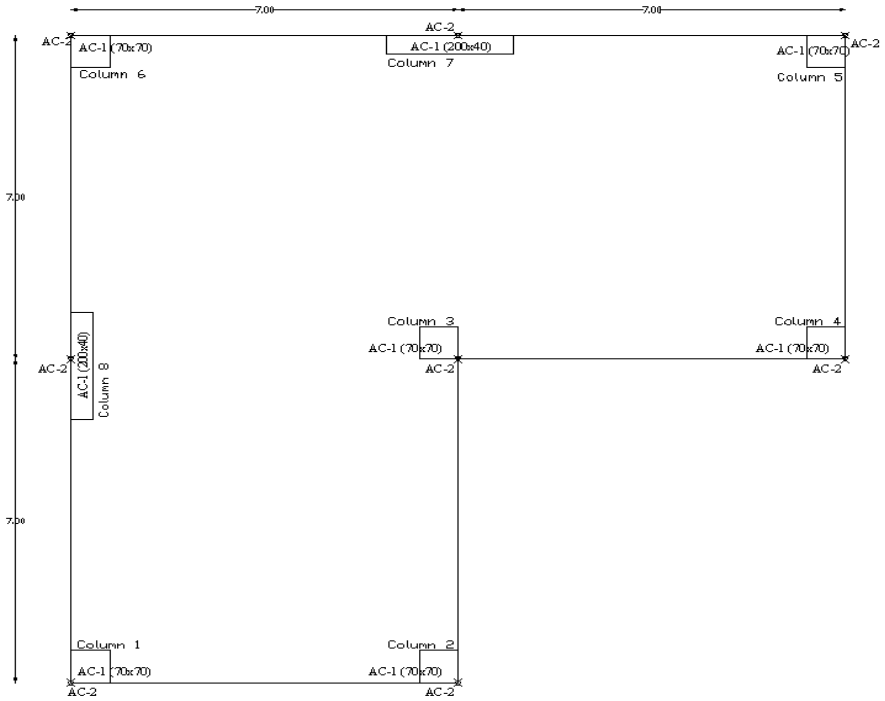

Column	AC_1	
	AC_{1x}	AC_{1y}
C1	70	70
C2	70	70
C3	70	70
C4	70	70
C5	70	70
C6	70	70
C7	200	40
C8	40	200

***Figure 8.3**: Test example 8.2 - Architectural constraints of a typical storey*

The second test example, shown in Figure 8.3, is a three-storey 3D frame where the height of each storey is 3 meters, while the plan layout of the columns/shear walls is the same for both storeys. The following 10 design variables have been used corresponding to 8 topology and 2 active sizing design variables. In Figure 8.3 both architectural constraints (AC_1 rectangles and AC_2 points) are presented for all columns/shear walls. Similarly to the first example designs fulfil the requirements of EC2 and EC8 design codes. Table 8.11 depicts the cross-sectional dimensions of the four optimum designs along with the corresponding eccentricities. The observations regarding the eccentricities are similar to those of the first example, where the combined formulation managed to improve both eccentricities. Table 8.12 contains the maximum and minimum values of the top diaphragm rotation for each hazard level obtained for the records from Table 8.4. It can be seen that the results are in exact accordance with the findings of Paulay [16,17], Tso and Myslimaj [31] reported for

one-storey structures, i.e. among all designs for the frequent and occasional hazard levels D_{Ecr} has the minimum rotation while in the rare hazard level it is design D_{Ecv} that has the best performance.

Table 8.13 depicts the initial limit state and total life-cycle costs of the four optimum designs. Similarly to the first test example D_{Cin} is the worst design in terms of the life-cycle cost irrespective of the drift limits considered, on the other hand D_{Comb} is the best design for both groups of drift limits. Moreover the performance of D_{Ecr} is almost the same with that of D_{Cin} for both groups of drift limits. This is due to the fact that no formulation concluded to optimum designs having shear-walls. Moreover, the probabilities of exceeding slight, moderate, extensive and complete limit states (defined according to HAZUS) are given in Tables 8.14 while the observations are similar to those obtained for the total life-cycle cost from Table 8.13.

Conclusions

In this work, various structural optimum design formulations are assessed with respect to the minimum torsional response of RC buildings in three hazard levels (frequent, occasional and rare) as well as through life-cycle cost and fragility analyses. An optimizer based on evolutionary algorithms has been implemented for the solution of the optimization problems. From the present study the following conclusions can be drawn:

The results reported by Paulay [16,17], Tso and Myslimaj [31], that the rigidity center eccentricity is important mainly when the structural system behaves linearly, while when the structure starts to behave nonlinearly the strength center eccentricity becomes more important to deal with, are verified, in a more rigorous and generalized framework provided by structural optimization procedures where a number of recommendations for designing RC buildings are incorporated. Moreover, these findings reported for single storey RC structures in the past by the two researchers are extended in multi-storey RC buildings.

The second finding is related to the most appropriate design criterion for reducing the torsional response. The proposed combined formulation,

where both e_{CM-CR} and e_{CM-CV} eccentricities are minimized, is the optimum design formulation that converges to designs having equally well response, in terms of rotation of the top diaphragm, in frequent, occasional and rare hazard levels. Moreover this design formulation shows the better performance with respect to the total life-cycle cost and limit state probabilities of exceedance.

TABLES

***Table 8.6**: Test example 8.1 - Optimum designs obtained through the formulations examined*

Column	D_{Comb}		D_{Ecr}		D_{Ecv}		D_{Cin}	
	e_{CM-CR}=9.01cm		e_{CM-CR}=0.04cm		e_{CM-CR}=150.2cm		e_{CM-CR}=179.6cm	
	e_{CM-CV}=12.7cm		e_{CM-CV}=99.7cm		e_{CM-CV}=4.26cm		e_{CM-CV}=118.3cm	
	dim_x	dim_y	dim_x	dim_y	dim_x	dim_y	dim_x	dim_y
C1	40	30	150	30	30	30	30	30
C2	30	130	30	90	30	150	30	30
C3	30	110	30	130	30	170	30	30
C4	40	30	150	30	70	30	30	30
C5	30	150	30	140	30	150	30	40

***Table 8.7**: Test example 8.1 - Maximum and minimum values of the torsional response in three hazard levels*

Design philosophy	Hazard Level					
	50/50		10/50		2/50	
	max (10^{-3} rad)	min (10^{-3} rad)	max (10^{-3} rad)	min (10^{-3} rad)	max (10^{-3} rad)	min (10^{-3} rad)
D_{Comb}	0.505	-0.351	1.43	-1.20	4.46	-4.42
D_{Ecr}	0.254	-0.293	0.953	-1.28	5.26	-5.05
D_{Ecv}	1.51	-1.40	2.46	-2.33	3.50	-5.05
D_{Cin}	1.69	-1.34	7.90	-7.91	13.90	-13.40

***Table 8.8**: Test example 8.1 - Comparison of the designs with respect to the cost*

		D_{Comb}	D_{Ecr}	D_{Ecv}	D_{Cin}
HAZUS [25]	C_{IN} (in € 1,000)	49.23	52.80	51.24	43.81
	C_{LS}/C_{IN}	0.41	0.81	0.82	3.88

Ghobarah [26]	C_{TOT}(in € 1,000)	69.56	95.92	93.21	213.93
	C_{LS}/C_{IN}	7.19	3.65	13.07	29.18
	C_{TOT}(in € 1,000)	403.31	245.61	721.32	1322.33

***Table 8.9**: Test example 8.1 - The probability of exceeding the four limit states (%)*

Limit state	D_{Comb}	D_{Ecr}	D_{Ecv}	D_{Cin}
Slight	1.67E+01	7.11E+00	4.22E+01	7.83E+01
Moderate	2.80E-01	1.22E+00	2.08E+00	3.02E+01
Extensive	7.20E-04	8.79E-03	5.90E-03	7.67E-02
Complete	1.44E-07	4.33E-06	2.50E-06	9.24E-05

***Table 8.10**: Test example 8.1 - The probability of exceeding the four limit states (%)Table 1*

Limit state	D_{Comb}	D_{Ecr}	D_{Ecv}	D_{Cin}
Slight	1.67E+01	7.11E+00	4.22E+01	7.83E+01
Moderate	2.80E-01	1.22E+00	2.08E+00	3.02E+01
Extensive	7.20E-04	8.79E-03	5.90E-03	7.67E-02
Complete	1.44E-07	4.33E-06	2.50E-06	9.24E-05

***Table 8.11**: Test example 8.2 - Optimum designs obtained through the formulations examined*

Column	D_{Comb}		D_{Ecr}		D_{Ecv}		D_{Cin}	
	e_{CM-CR}=8.51cm		e_{CM-CR}=7.54cm		e_{CM-CR}=150.3cm		e_{CM-CR}=236.8cm	
	e_{CM-CV}=14.9cm		e_{CM-CV}=310.1cm		e_{CM-CV}=10.6cm		e_{CM-CV}=527.4cm	
	dim_x	dim_y	dim_x	dim_y	dim_x	dim_y	dim_x	dim_y
C1	65	65	55	45	30	70	30	50
C2	55	50	55	40	45	50	35	70
C3	65	70	70	50	50	70	30	70
C4	70	60	50	45	50	40	70	70
C5	70	55	50	30	30	65	40	70
C6	50	70	70	40	60	70	35	50
C7	65	40	50	40	75	40	35	30
C8	40	50	30	35	30	35	30	35

***Table 8.12**: Test example 8.2 - Maximum and minimum values of the torsional response in three hazard levels*

Design philosophy	Hazard Level					
	50/50		10/50		2/50	
	max (10^{-3} rad)	min (10^{-3} rad)	max (10^{-3} rad)	min (10^{-3} rad)	max (10^{-3} rad)	min (10^{-3} rad)
D_{Comb}	0.815	-1.07	2.97	-3.28	4.39	-3.27
D_{Ecr}	0.731	-0.609	1.34	-0.987	5.19	-3.35
D_{Ecv}	1.26	-1.18	3.53	-3.55	3.56	-4.10
D_{Cin}	3.01	-3.56	8.28	-8.11	9.31	-11.20

***Table 8.13**: Test example 8.2 - Comparison of the designs with respect to the cost*

		D_{Comb}	D_{Ecr}	D_{Ecv}	D_{Cin}
HAZUS [25]	C_{IN} (in € 1,000)	464.97	471.65	485.10	413.85
	C_{LS}/C_{IN}	5.30	10.85	7.53	12.89
	C_{TOT}(in € 1,000)	2928.42	5590.37	4138.88	5749.96
Ghobarah [26]	C_{LS}/C_{IN}	17.25	21.14	16.46	24.85
	C_{TOT}(in € 1,000)	8485.03	10442.47	8470.46	10700.06

***Table 8.14**: Test example 8.2 - The probability of exceeding the four limit states (%)*

Limit state	D_{Comb}	D_{Ecr}	D_{Ecv}	D_{Cin}
Slight	9.14E+01	9.57E+01	9.33E+01	9.71E+01
Moderate	6.64E+01	7.69E+01	7.02E+01	8.21E+01
Extensive	1.63E+01	3.67E+01	1.77E+01	4.63E+01
Complete	2.25E-03	7.61E-01	1.02E-01	1.66E+00

9.2 Base shear torque examples

In this section of the study two models are performed in order to evaluate the behavior of optimized one-storey systems for the proposed methodology. Each model has been optimized for the following different objective functions: cost, static eccentricity e_{cr}, strength eccentricity e_{cv}, ratio and nonlinear ratio. The design variable considered is the column cross section. For every one of the objective functions above the model has been resolved according to constraints based on EAK and EKOS for the first case and Performance-Based Seismic Design for the second case (additionally to EAK and EKOS). Every example is examined through the design models below: Model_cost_ec, Model_cr_ec, Model_cv_ec, Model_rot_ec, Model_cost_nl, Model_cr_nl, Model_cv_nl, Model_rot_nl and Model_nl_nl, where the first component refers to the objective function and the second to the applied regulations.

The models designed based on EAK and EKOS are analyzed through the Modal Dynamic Analysis _ec, while those according to Performance-Based Seismic Design are analyzed through the Nonlinear Dynamic Procedure _nl, which are described in a previous section of the study (Design Procedures). The analysis above is carried out through the StereoSTATIKA commercial package (for the linear analysis) and the Opensees software framework (for the nonlinear analysis).

The optimization process is based on Evolution Strategies as described in a previous section. The optimization algorithm was written by Papadrakakis, Lagaros and Bakas.

9.2.1 Description of Model 1

A one-storey RC building is used for the study. The layout of the first model is shown in Figure 7.1, while the east and the south views are shown in Figure 8.4., 8.5, 8.6, and the 1-1 Section in Figure 8.7.

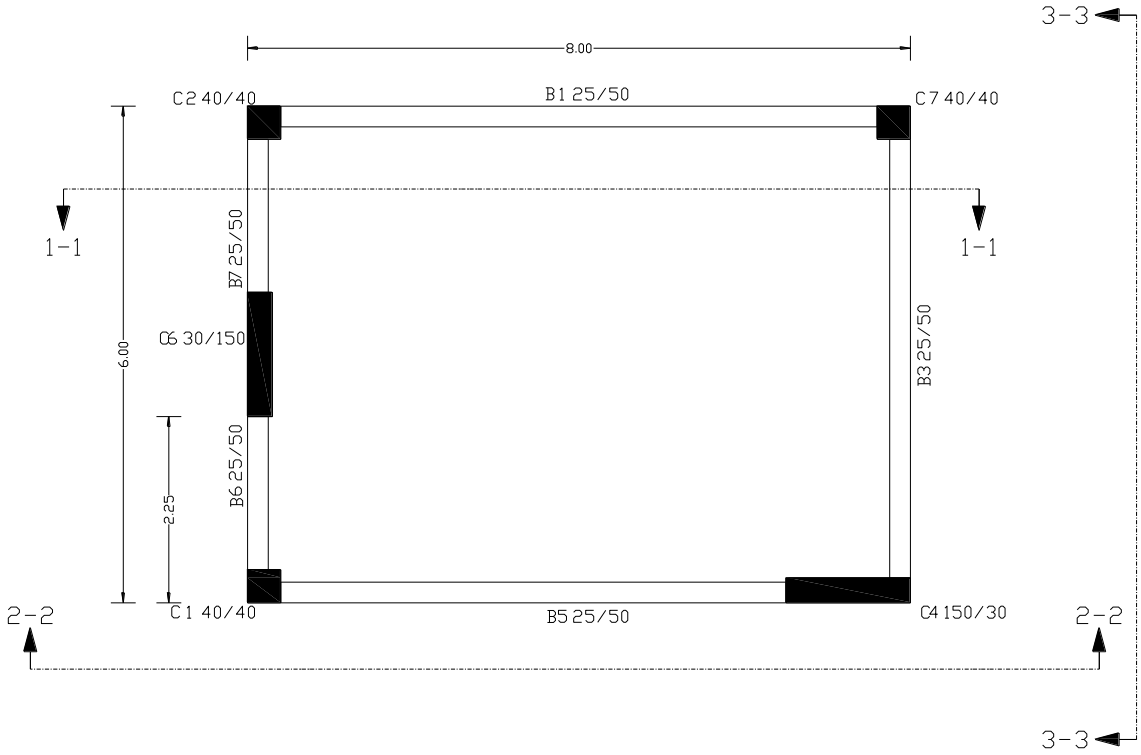

Figure 8.4 *Model1 layout of Model1*

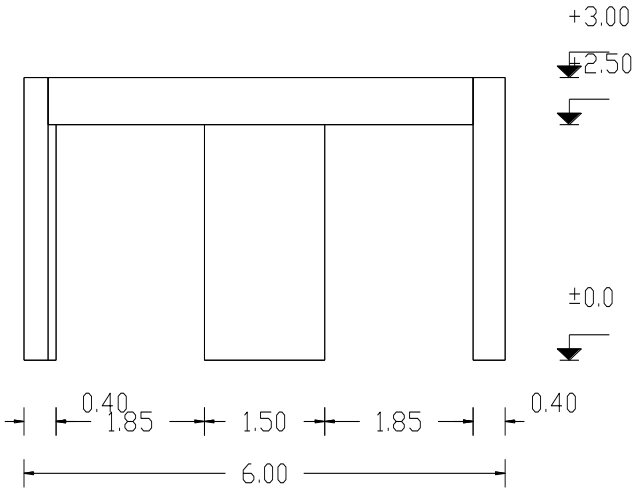

Figure 8.5 *The East view of Model1*

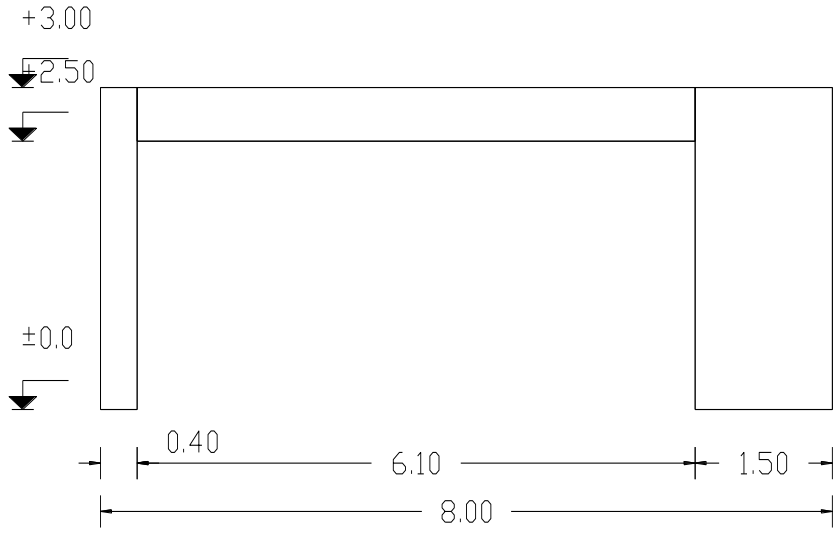

Figure 8.6 *The South view of Model1*

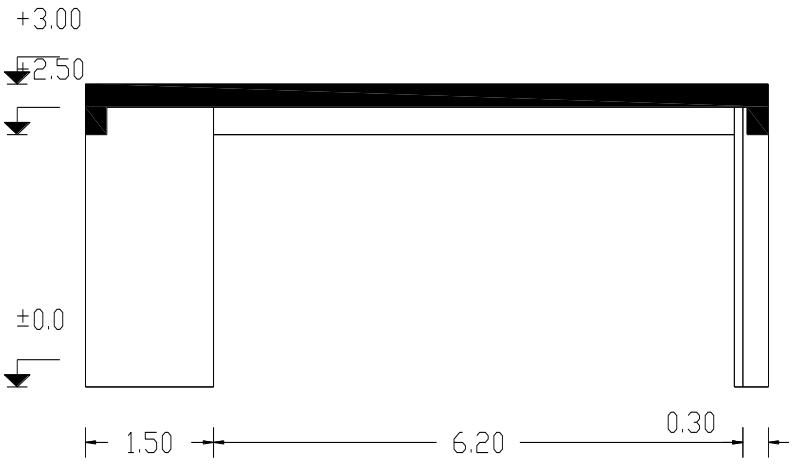

Figure 8.7 *The 1-1 Section of Model1*

In all test cases the following material properties have been considered:

Concrete:

Concrete modulus of elasticity: E_c=27.5 GPa

Concrete compressive strength at 28 days: f_c=25000 kPa

Reinforcing steel:

Steel modulus of elasticity: E_s=210 GPa

Steel yield strength: f_y=600000 kPa

The materials above correspond to the concrete class C20/25 (nominal cylindrical strength of 20 MPa) and steel class S500 (nominal yield stress of 500 MPa), while the slab thickness is equal to 13 cm.

The optimized layouts for the different designs procedures are presented below (Figures 8.8-8.16):

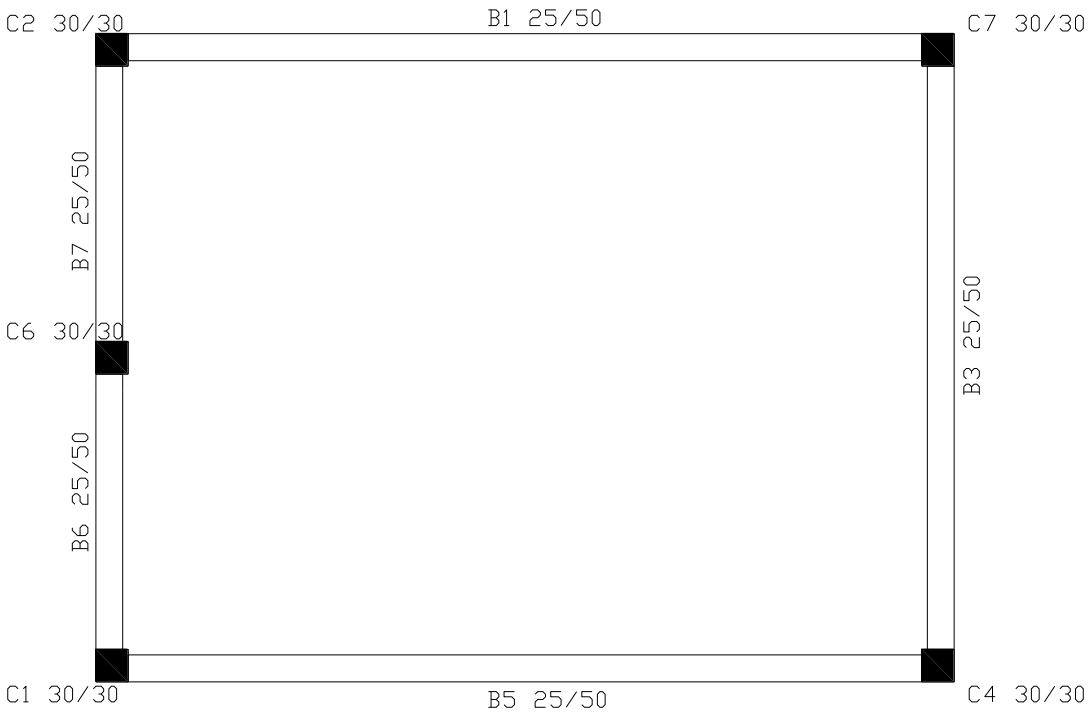

Figure 8.8 *Optimized layout through Model1_cost_ec design procedure*

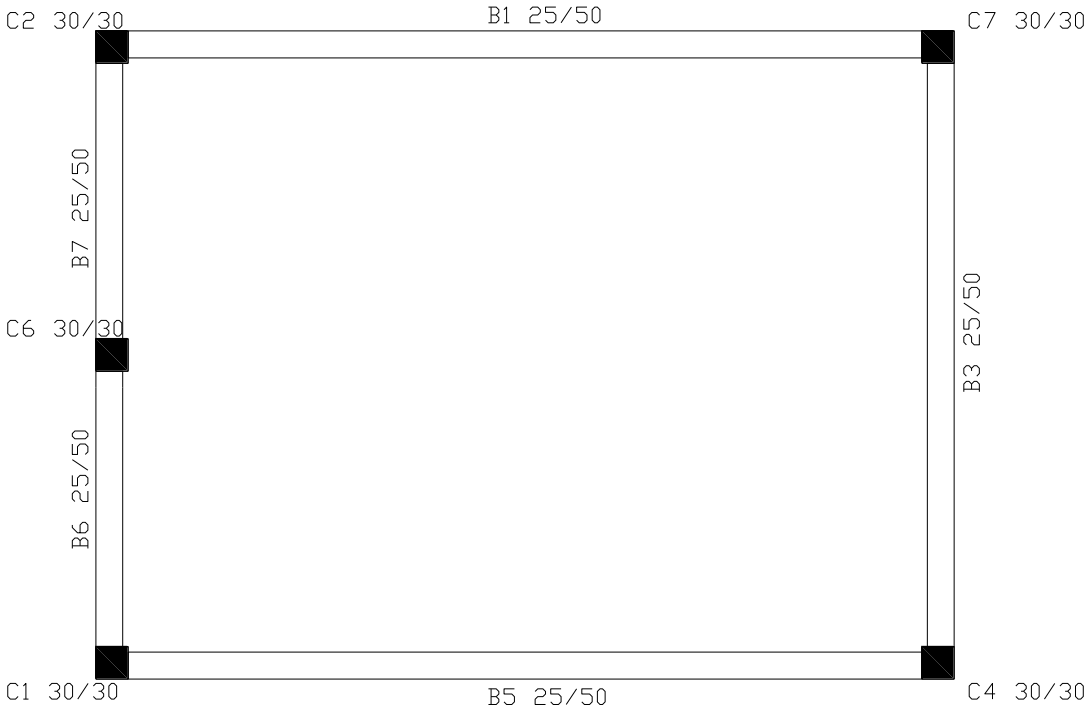

Figure 8.9 *Optimized layout through Model1_cost_nl design procedure*

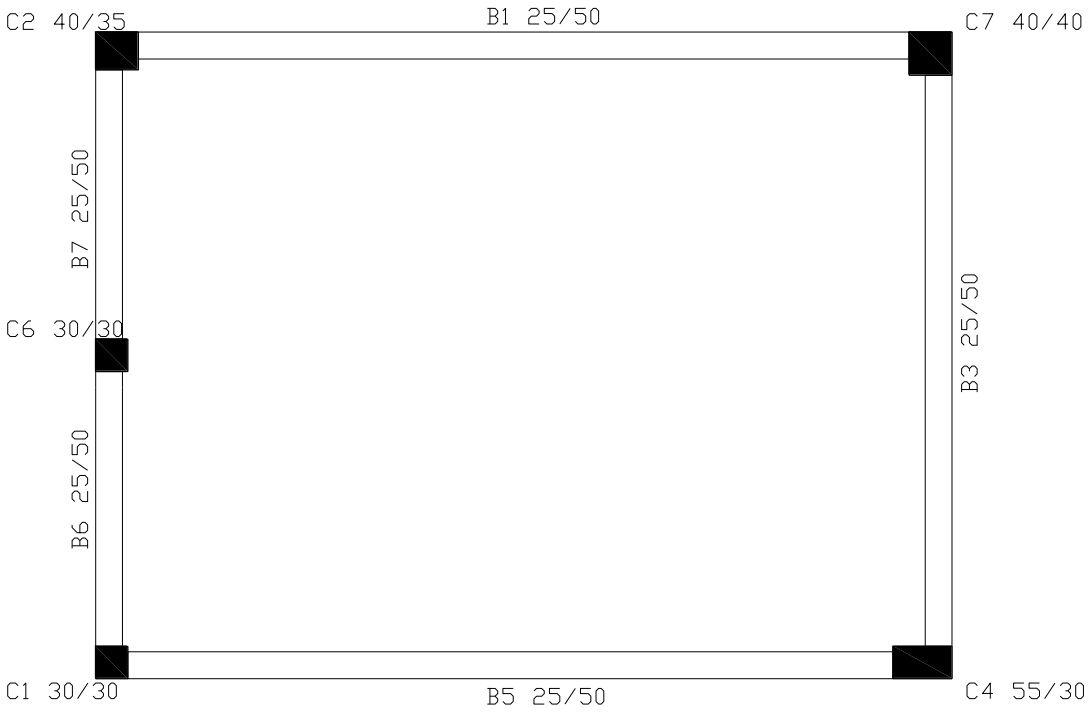

Figure 8.10 *Optimized layout through Model1_cr_ec design procedure*

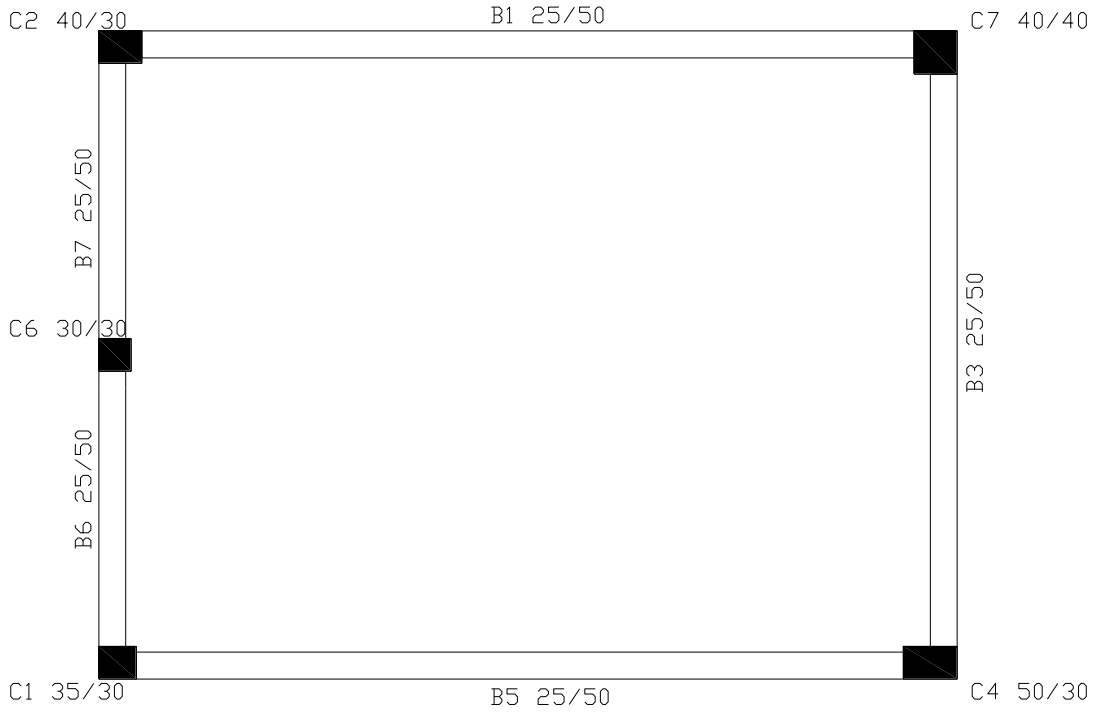

Figure 8.11 *Optimized layout through Model1_cr_nl design procedure*

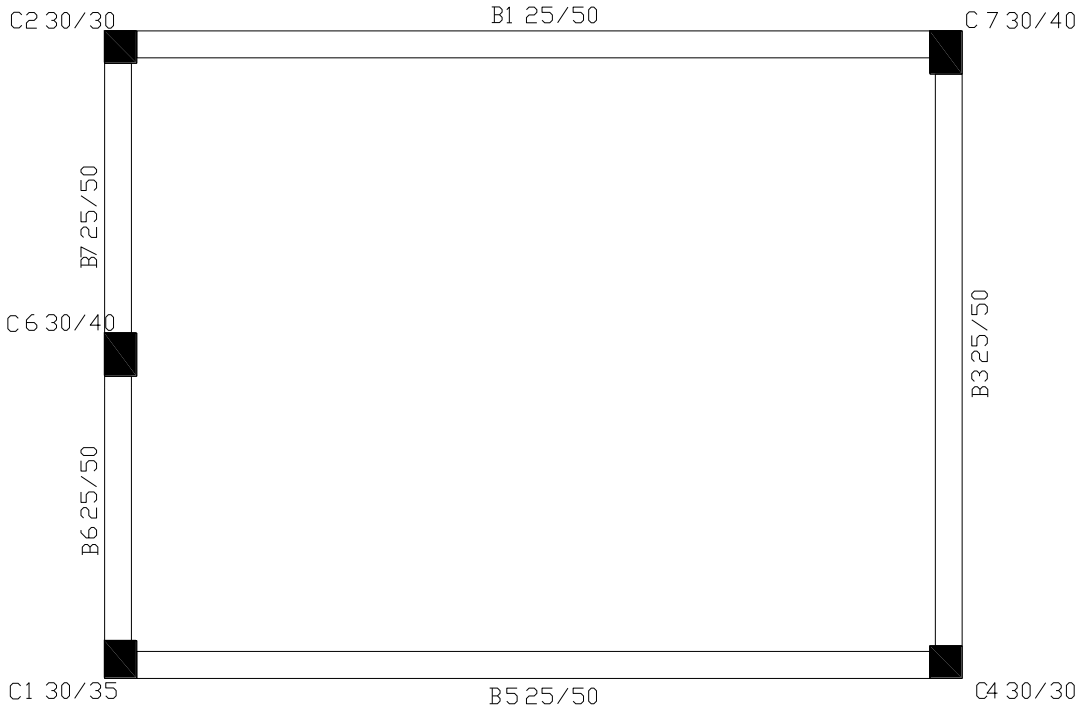

Figure 8.12 *Optimized layout through Model1_cv_ec design procedure*

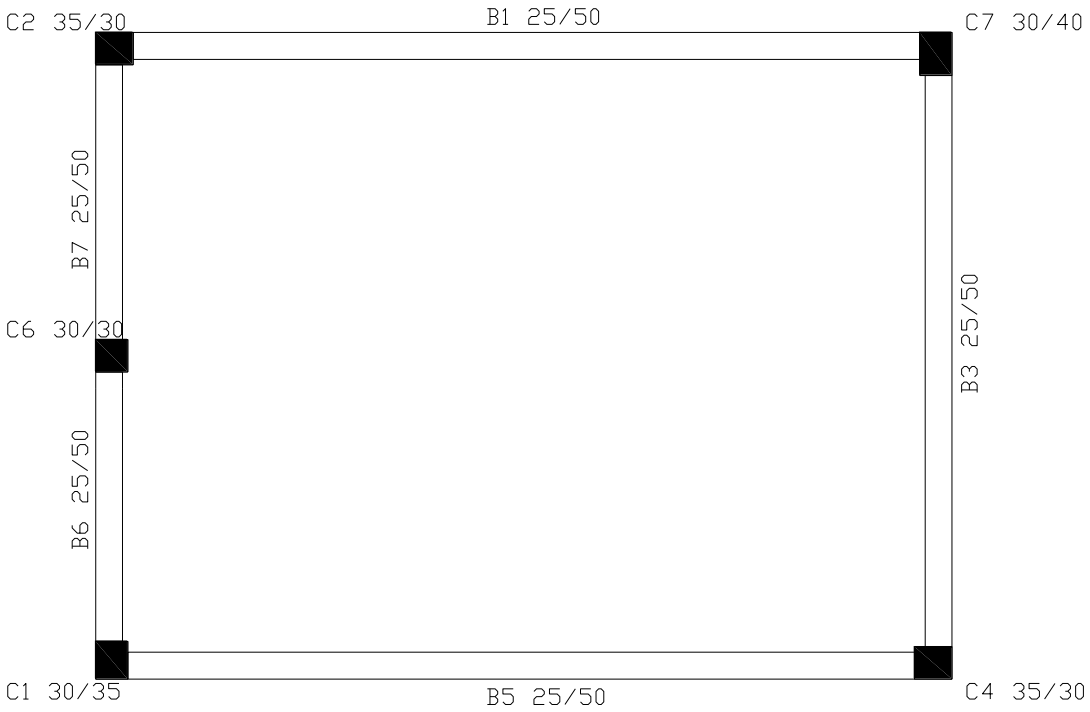

Figure 8.13 *Optimized layout through Model1_cv_nl design procedure*

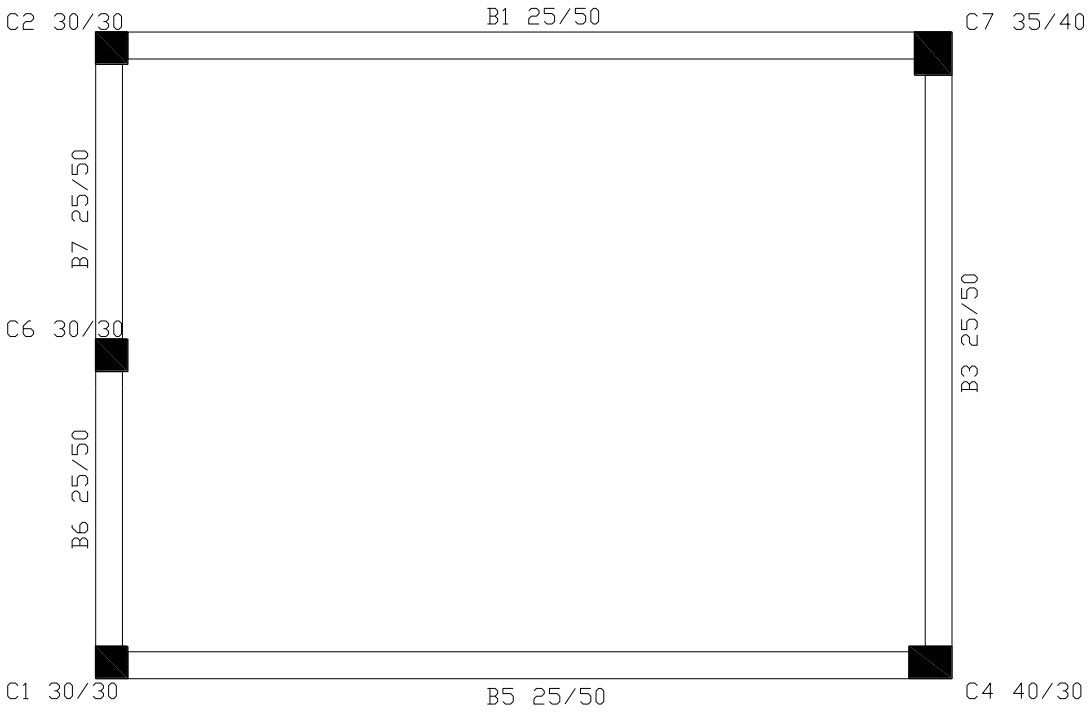

Figure 8.14 *Optimized layout through Model1_rot_ec design procedure*

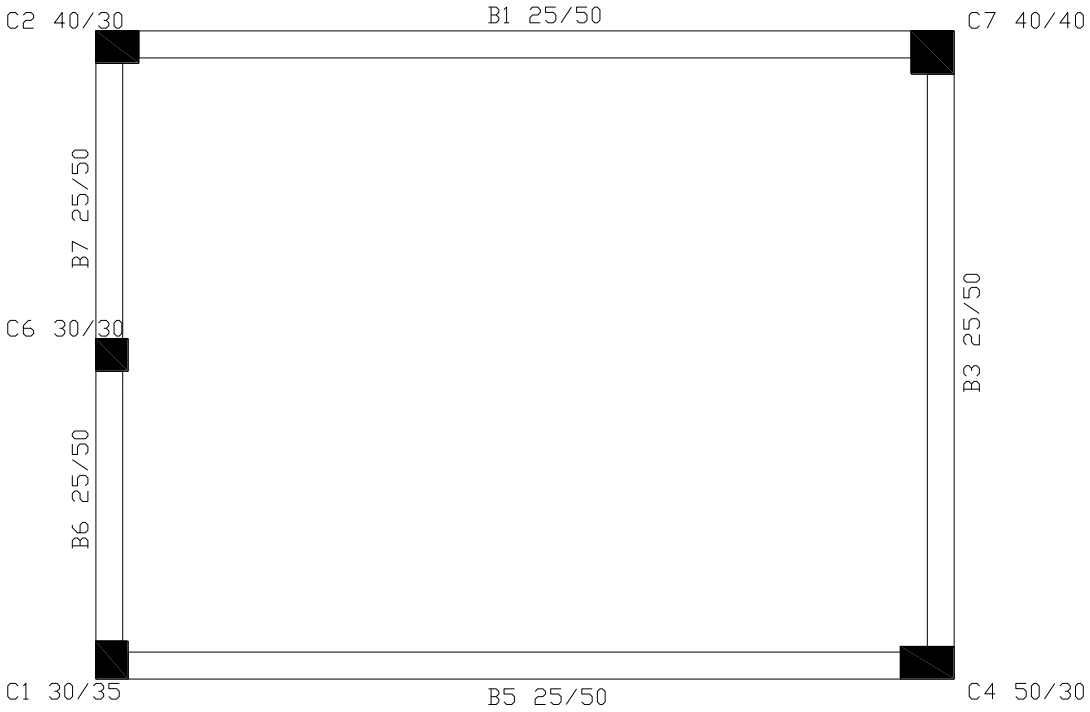

Figure 8.15 *Optimized layout through Model1_rot_nl design procedure*

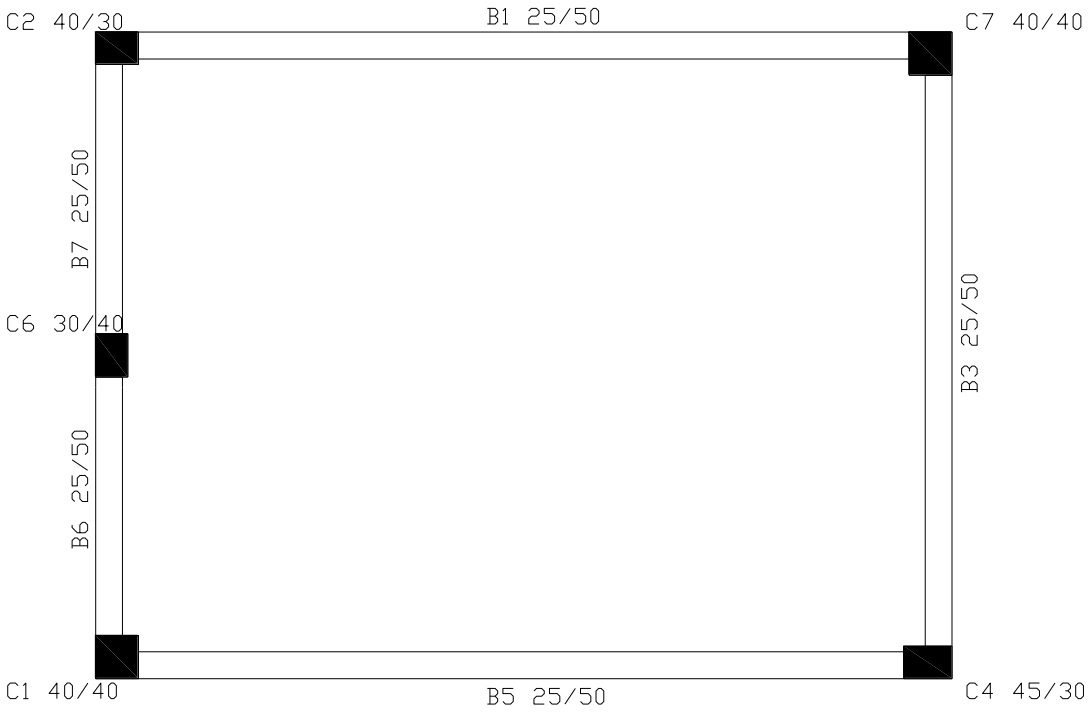

Figure 8.16 *Optimized layout through Model1_nl_nl design procedure*

Aiming at comparing various procedures in order to reduce the torsional effect, nine design procedures are compared. The model was subjected to two earthquake time historeys for every hazard level - C2_frtn and CM_riod in 50in50 level, CC_tcu101 and CC_tcu102 in 10in50 level, VL_pich and VL valu in 2in50 level.

For the first and the second design models (model_cost_ec, model_cost_nl) the objective function is the initial cost:

$$C = C_{IN} = C_{con} + C_{st} + C_{lab} \tag{8.2}$$

where $C = C_{IN}$: the initial cost of a new structure

C_{con}: the concrete cost

C_{st}: the cost of the steel of reinforcement

C_{lab}:the laboratory cost

For the third and the fourth design models (model_cr_ec, model_cr_nl) the objective function is the eccentricity of the center of rigidity:

$$e_{cr} = \sqrt{(x_{CM} - x_{CR})^2 + (y_{CM} - y_{CR})^2} \tag{8.3}$$

where x_{CM}, y_{CM}: the coordinates of the center of mass

x_{CR}, y_{CR}: the coordinates of the center of rigidity

For the fifth and the sixth design models (model_cv_ec, model_cv_nl) the objective function is the eccentricity of the center of rigidity:

$$e_{cv} = \sqrt{(x_{CM} - x_{CV})^2 + (y_{CM} - y_{CV})^2} \tag{8.4}$$

where x_{CM}, y_{CM}: the coordinates of the center of mass

x_{CV}, y_{CV}: the coordinates of the strength center

The difference between the models above with the same objective function is the behavioral constraints and the analysis procedure. The _ec design models are constrained by EAK and EKOS and analyzed with a modal analysis method. The _nl design models are designed in compliance with PBD and analyzed with a non-linear dynamic analysis.

For the seventh, eighth and the ninth design models (model_rot_ec, model_rot_nl, model_nl_nl) the objective function is the ratio of torsion:

$$ROTij = \frac{\sum_{k=1}^{n} |Vkij| - \sum_{k=1}^{n} Vkij}{\sum_{k=1}^{n} Vkij} \quad (8.5)$$

where n: the number of elements in a floor direction (x or y)

i: the corresponding shear force of the element

j: the direction of the earthquake motion

For the first two design models the ROT is calculated for shear forces result from modal dynamic analysis but the constraints are different at _ec model EAK and EKOS are applied and at _ nl model PBD is performed. For the third design model the ROT is calculated for shear forces result from non-linear dynamic analysis and PBD process is applied.

In Table 8.15 below the results of optimization for Model1 (using 9 different design models) are depicted.

Table 8.15 *Comparison between the initial values of the objective functions and the results of the optimization procedure for all the design models*

	Initial values					Final values					Variation Percentage				
Design Models	cost	e_cr	e_cv	rot	nl	cost	e_cr	e_cv	rot	nl	cost	e_cr	e_cv	rot	nl
Model1_cost_ec	3312,07	3,77	2,11	1,79	2,12E+267	2847,30	0,97	0,10	0,10	3124,25	-14,03	-74,27	-95,04	-94,29	-1,00E+00
Model1_cr_ec	3312,07	3,77	2,11	1,79	6,44E+263	2876,40	0,12	1,16	0,07	0,12	-13,15	-96,85	-44,96	-95,94	-1,00E+00
Model1_cv_ec	3585,14	3,77	2,50	1,78	0,00E+00	3130,07	1,16	0,01	0,22	0,00	-12,69	-69,22	-99,61	-87,87	0,00E+00
Model1_rot_ec	3312,07	3,77	2,11	1,79	7,75E+269	2865,72	0,09	0,26	0,02	0,04	-13,48	-97,67	-87,65	-98,79	-1,00E+00
Model1_nl_nl	3076,96	3,86	0,62	1,78	6,39E+01	2863,53	3,86	2,55	0,36	6,03	-6,94	-0,16	309,95	-79,73	-9,06E-01
Model1_cost_nl	3312,07	3,77	2,11	1,79	7,27E+262	2847,30	0,97	0,10	0,10	3107,16	-14,03	-74,27	-95,04	-94,29	-1,00E+00
Model1_cr_nl	3312,07	3,77	2,11	1,79	7,27E+262	2911,44	0,08	1,41	0,03	0,08	-12,10	-98,00	-33,24	-98,42	-1,00E+00
Model1_cv_nl	3585,14	3,77	2,50	1,78	0,00E+00	3122,09	0,51	0,03	0,12	0,00	-12,92	-86,45	-98,96	-93,18	0,00E+00
Model1_rot_nl	3312,07	3,77	2,11	1,79	5,53E+265	2917,01	0,14	1,18	0,04	0,04	-11,93	-96,24	-44,33	-97,76	-1,00E+00

In Figures 8.17- 8.25 below the time historeys of torsional moment and base shear in the x and y direction are presented for the three hazard levels for each design procedure.

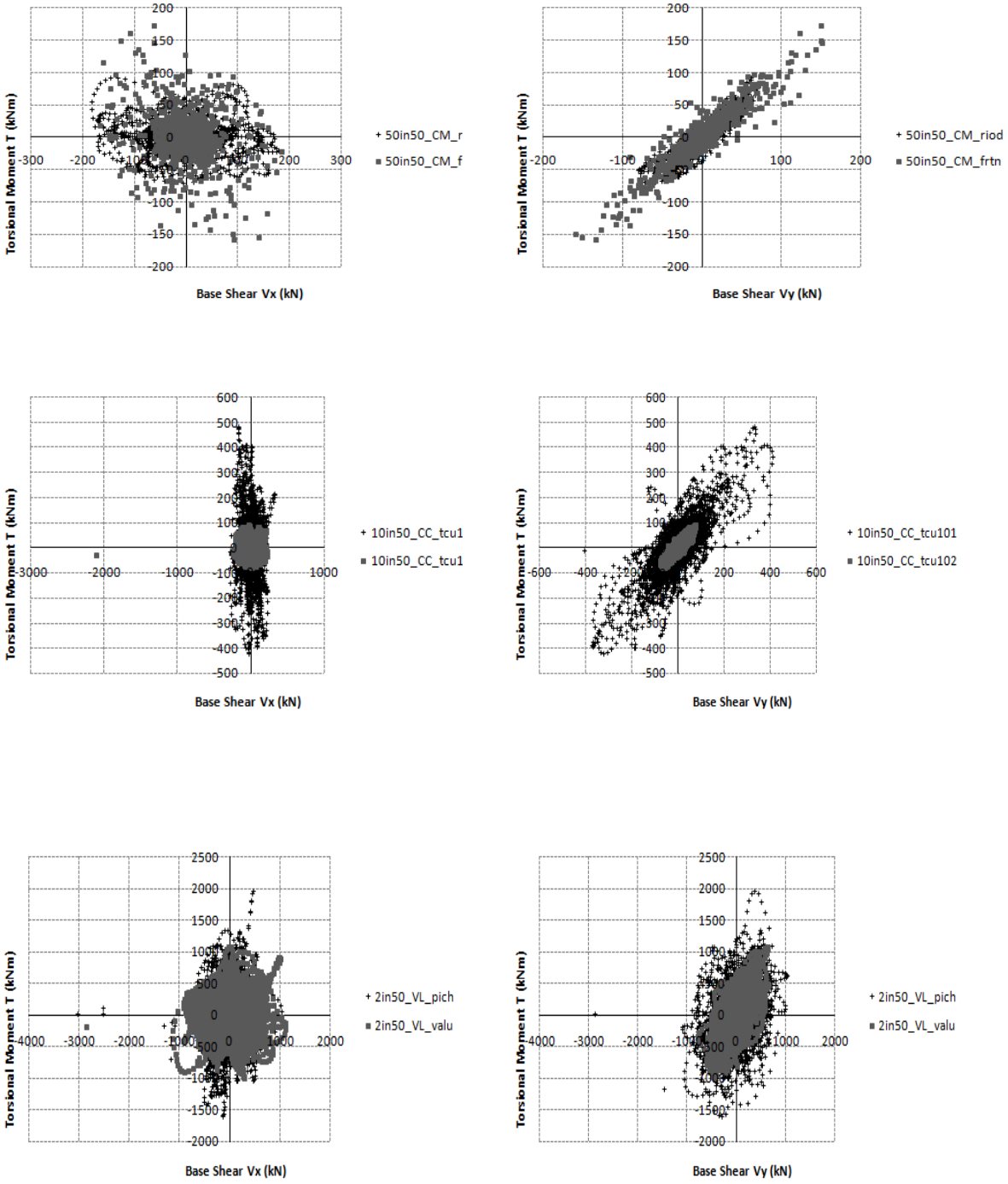

Figure 8.17 *Model1 cost ec base shear and torque time histories for the three hazard levels in x and y directions*

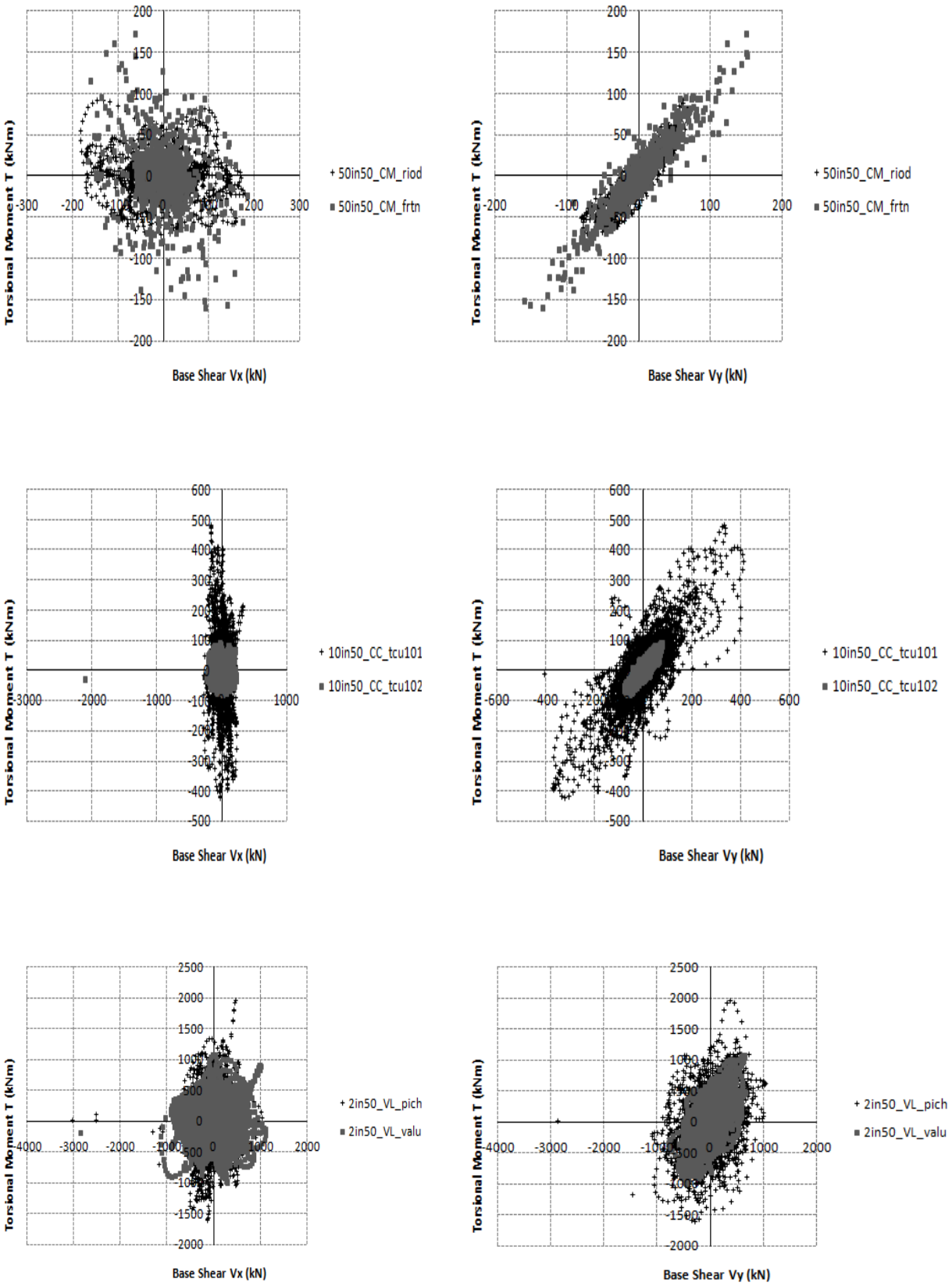

Figure 8.18 *Model1 cost nl base shear and torque time histories for the three hazard levels in x and y directions*

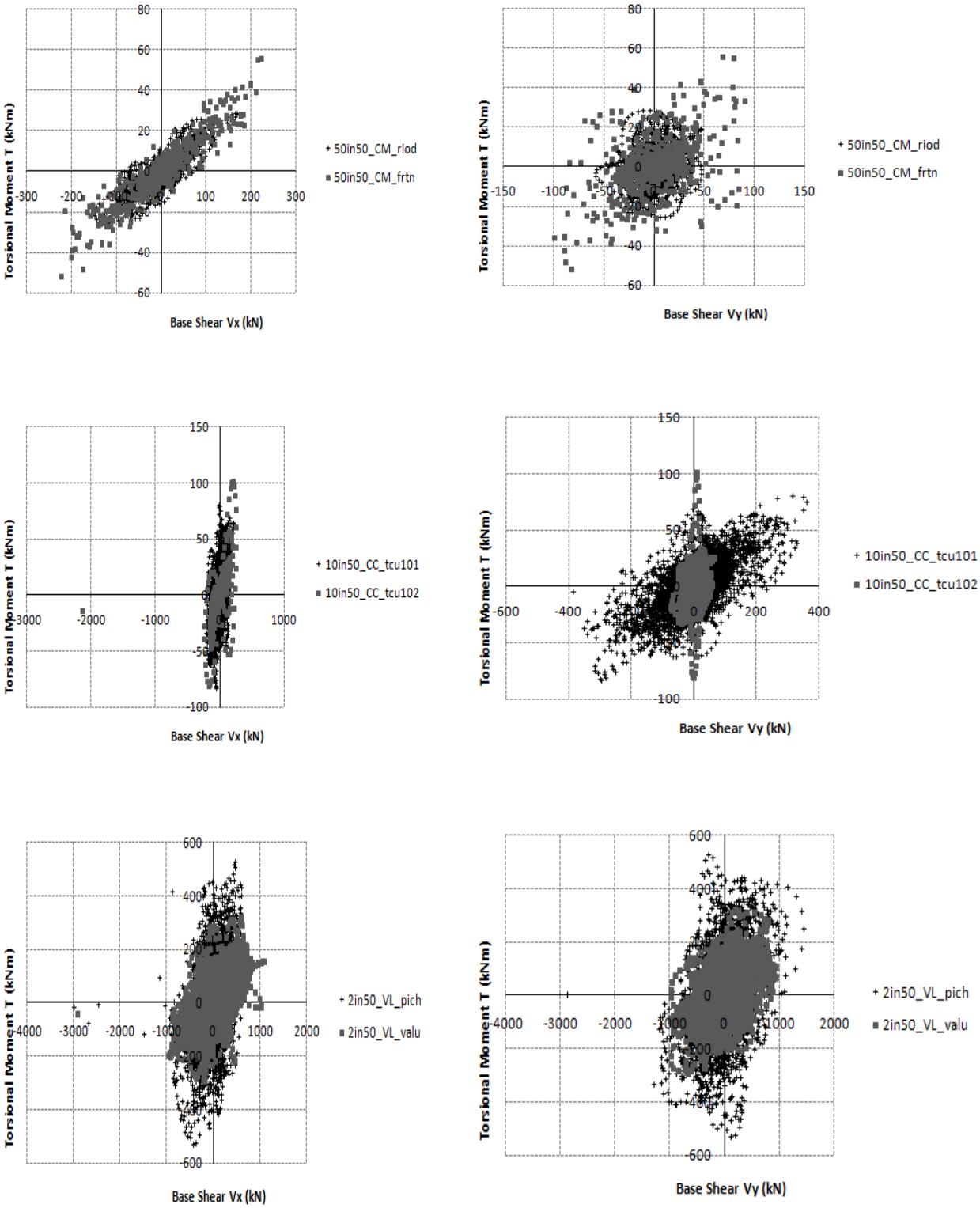

Figure 8.19 *Model1_cr_ec base shear and torque_time histories for the three hazard levels in x and y directions*

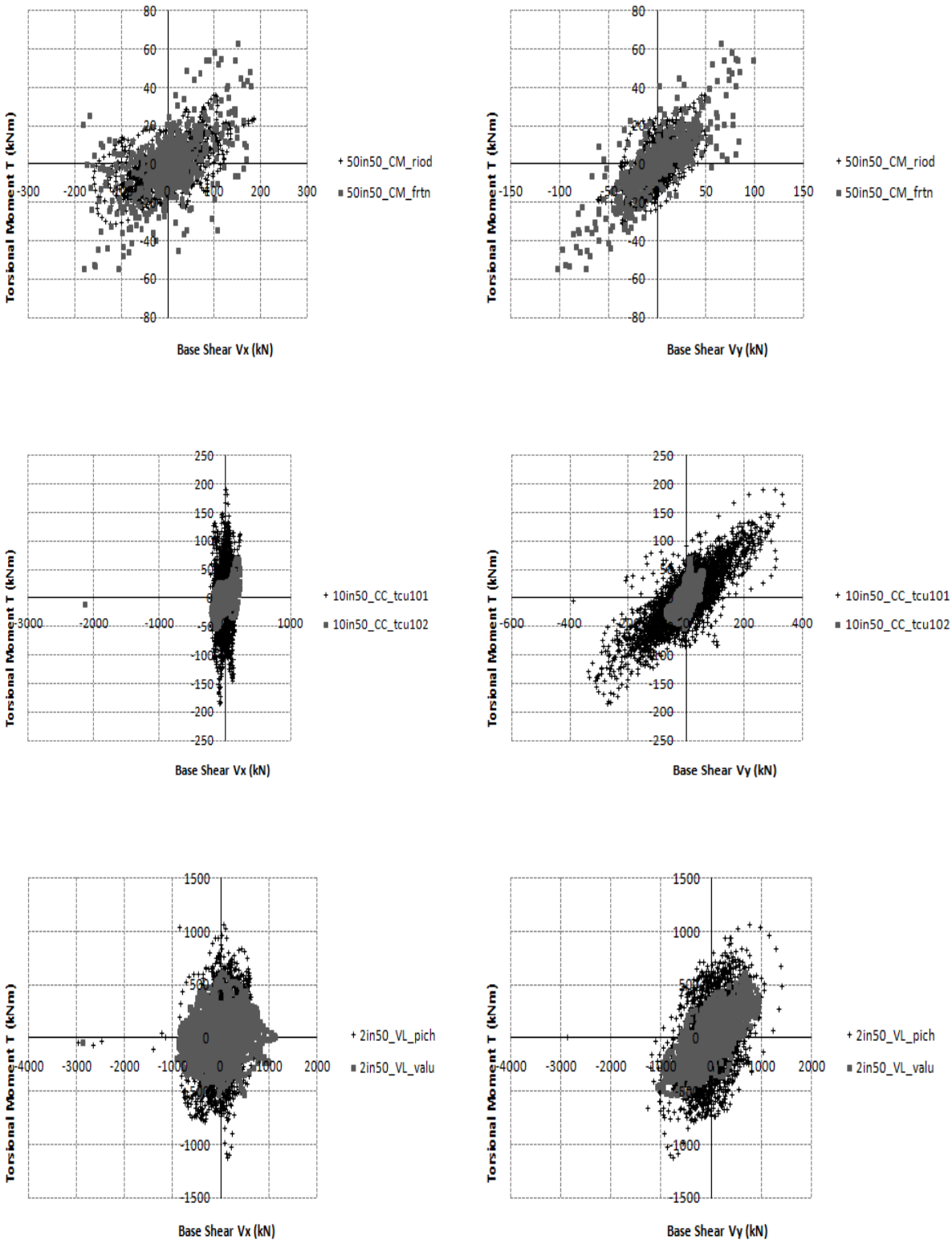

Figure 8.20 *Model1_cr_nl base_shear and torque_time histories for the three hazard levels in x and y directions*

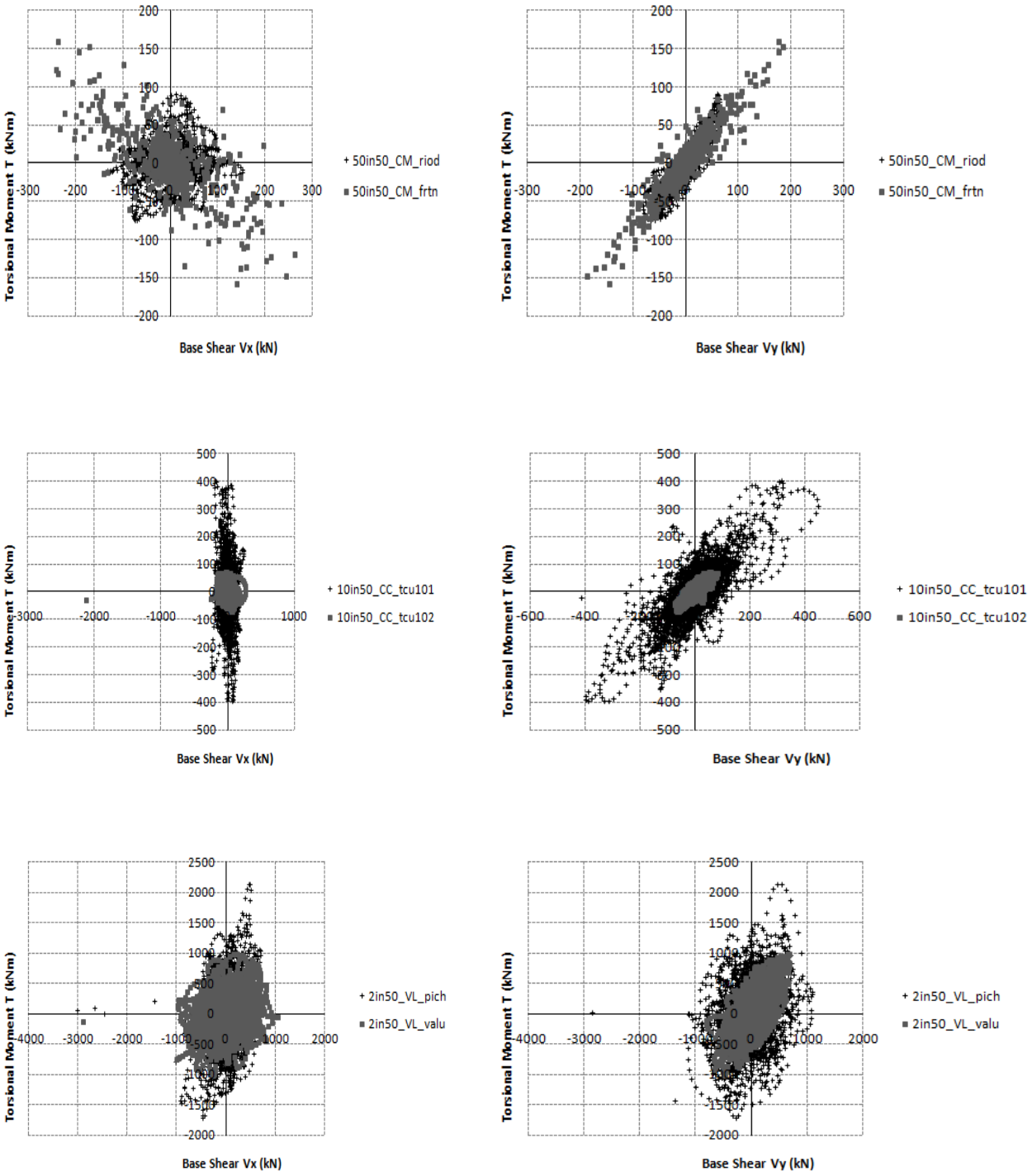

Figure 8.21 *Model1_cv_ec base_shear and torque_time histories for the three hazard levels in x and y directions*

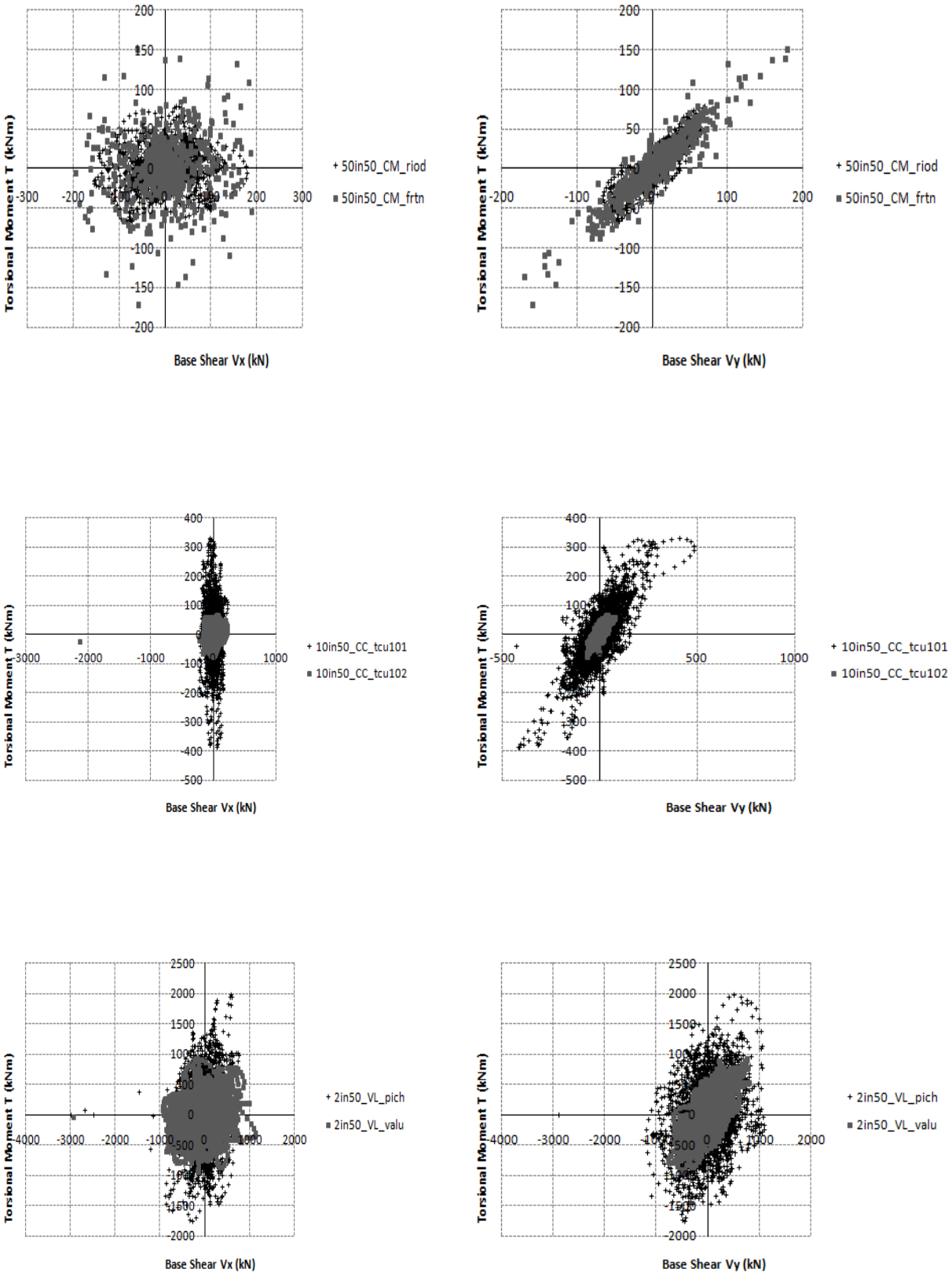

Figure 8.22 *Model1_cv_nl base_shear and torque_time histories for the three hazard levels in x and y directions*

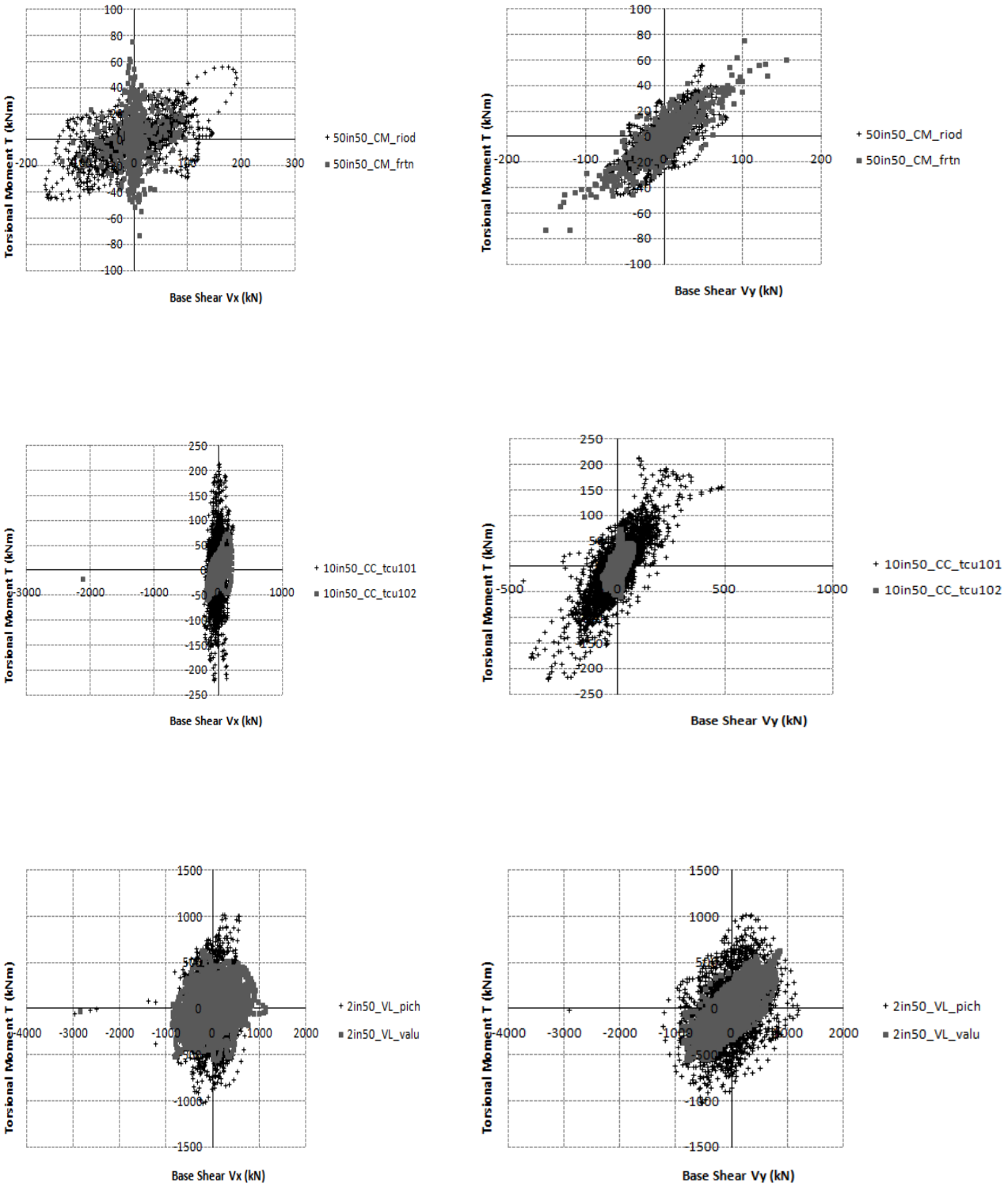

Figure 8.23 *Model1_rot_ec base_shear and torque_time histories for the three hazard levels in x and y directions*

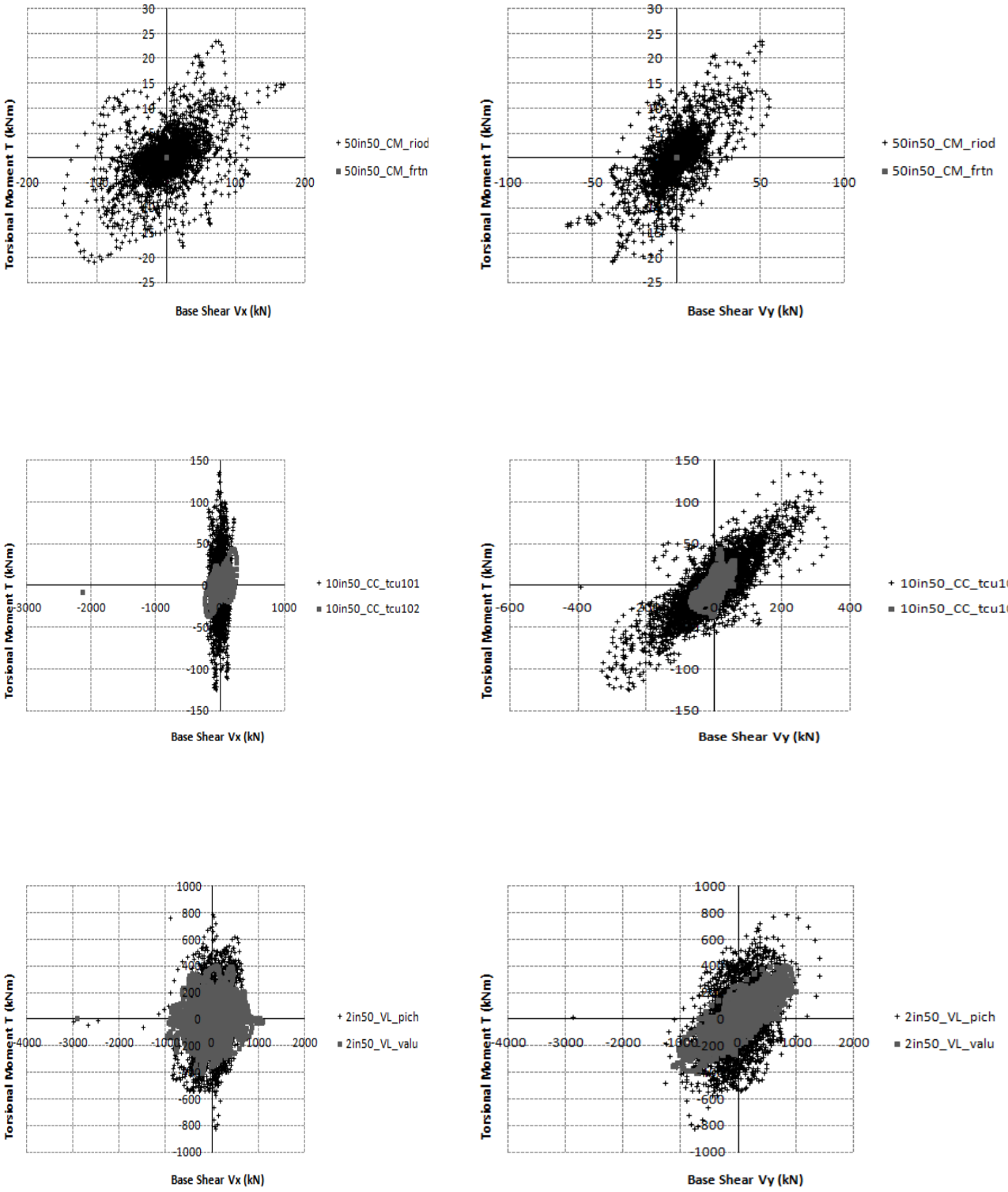

Figure 8.24 *Model1_rot_nl base_shear and torque_time histories for the three hazard levels in x and y directions*

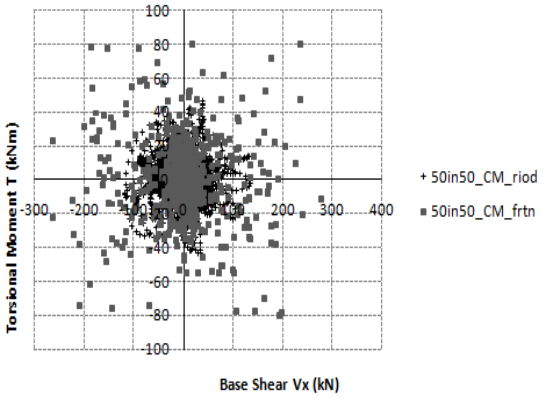

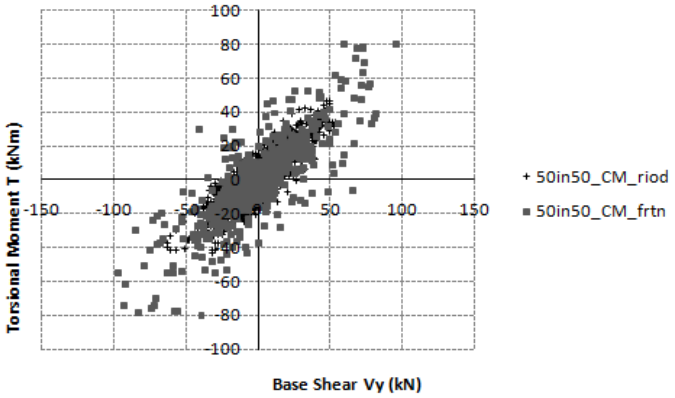

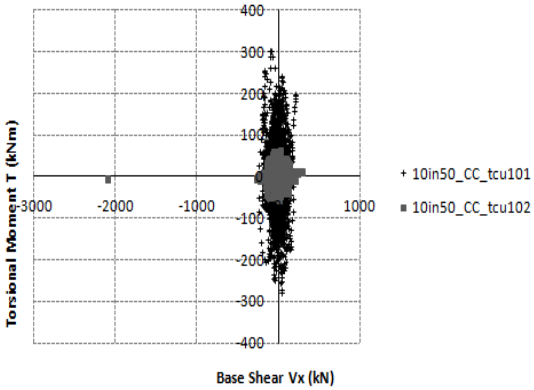

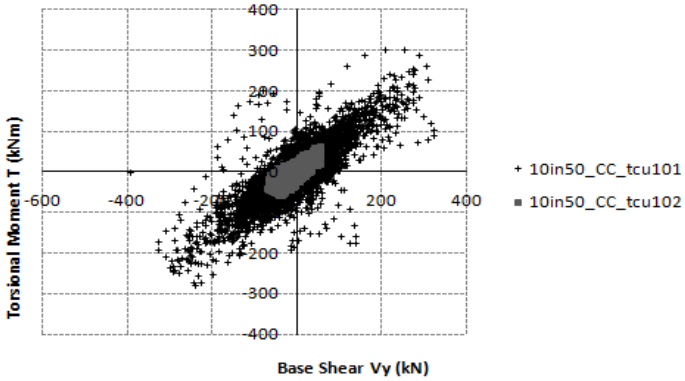

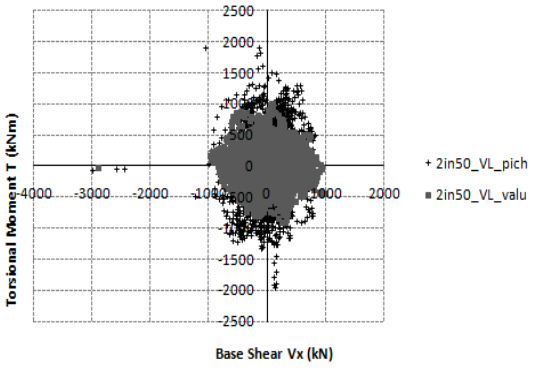

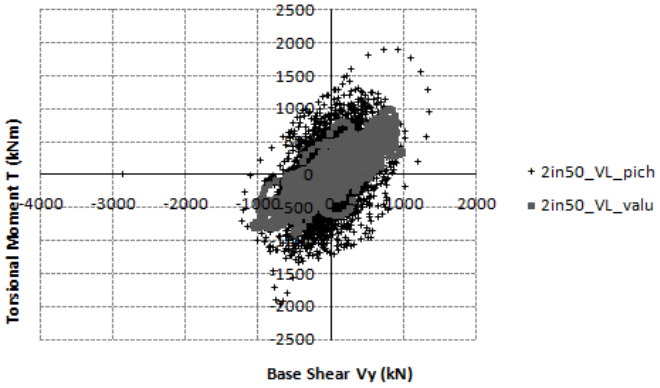

Figure 8.25 *Model1_nl_nl base_shear and torque_time histories for the three hazard levels in x and y directions*

In order to compare the various formulations of the optimization problem with reference to their performance against torsional effect, the envelopes of the base shear and torque time histories are developed. These envelopes are presented below so as to be able to reach any conclusions. (Figures 8.26-8.28)

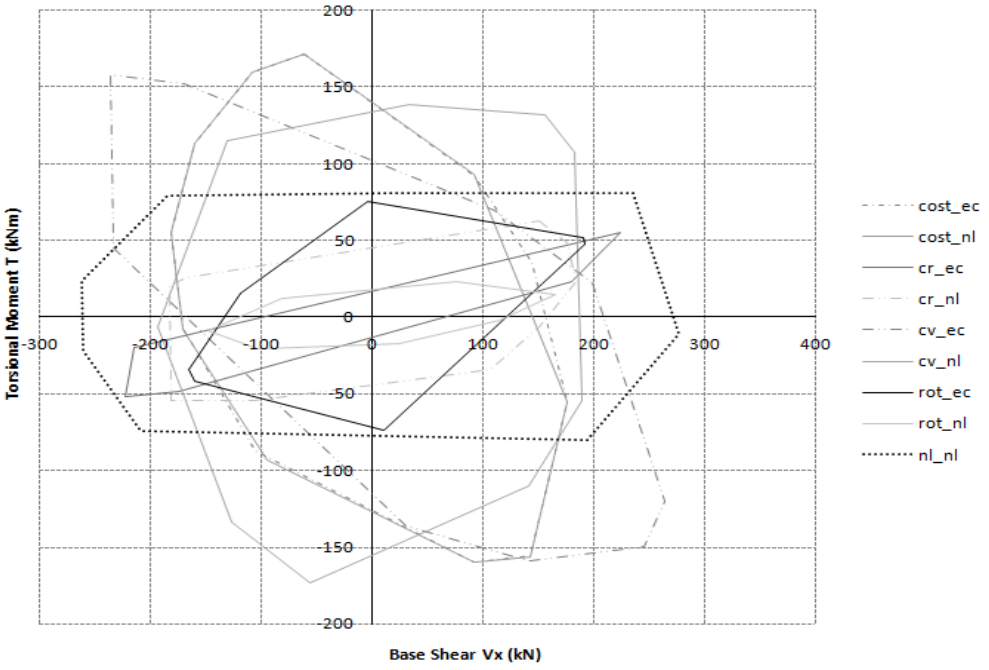

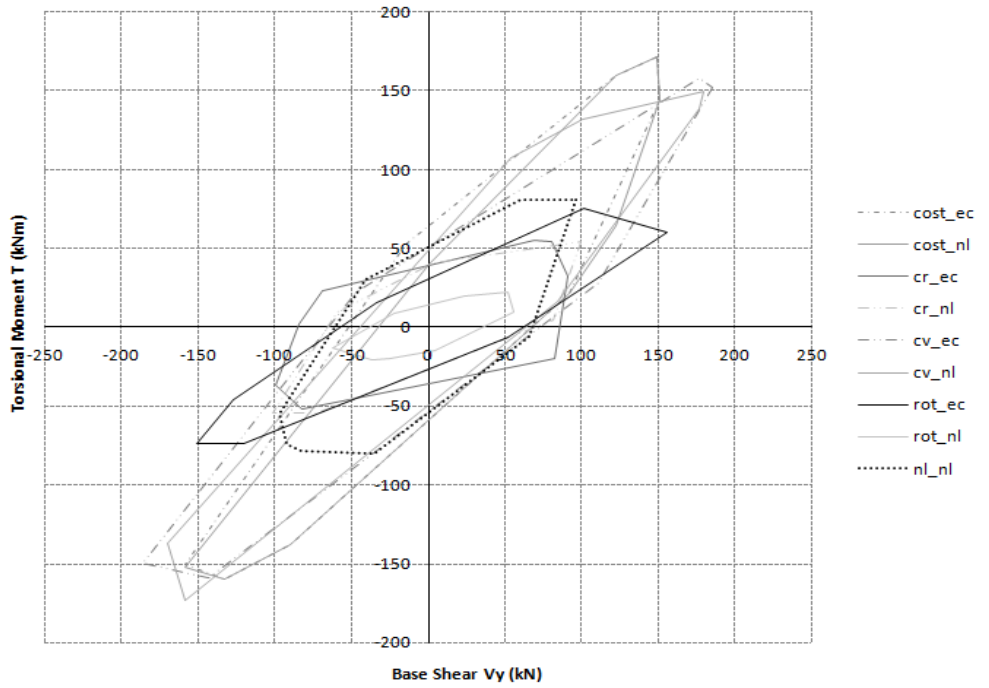

Figure 8.26 *The envelope of the BST time histories for the occasional earthquake hazard level (50in50) in x and y directions*

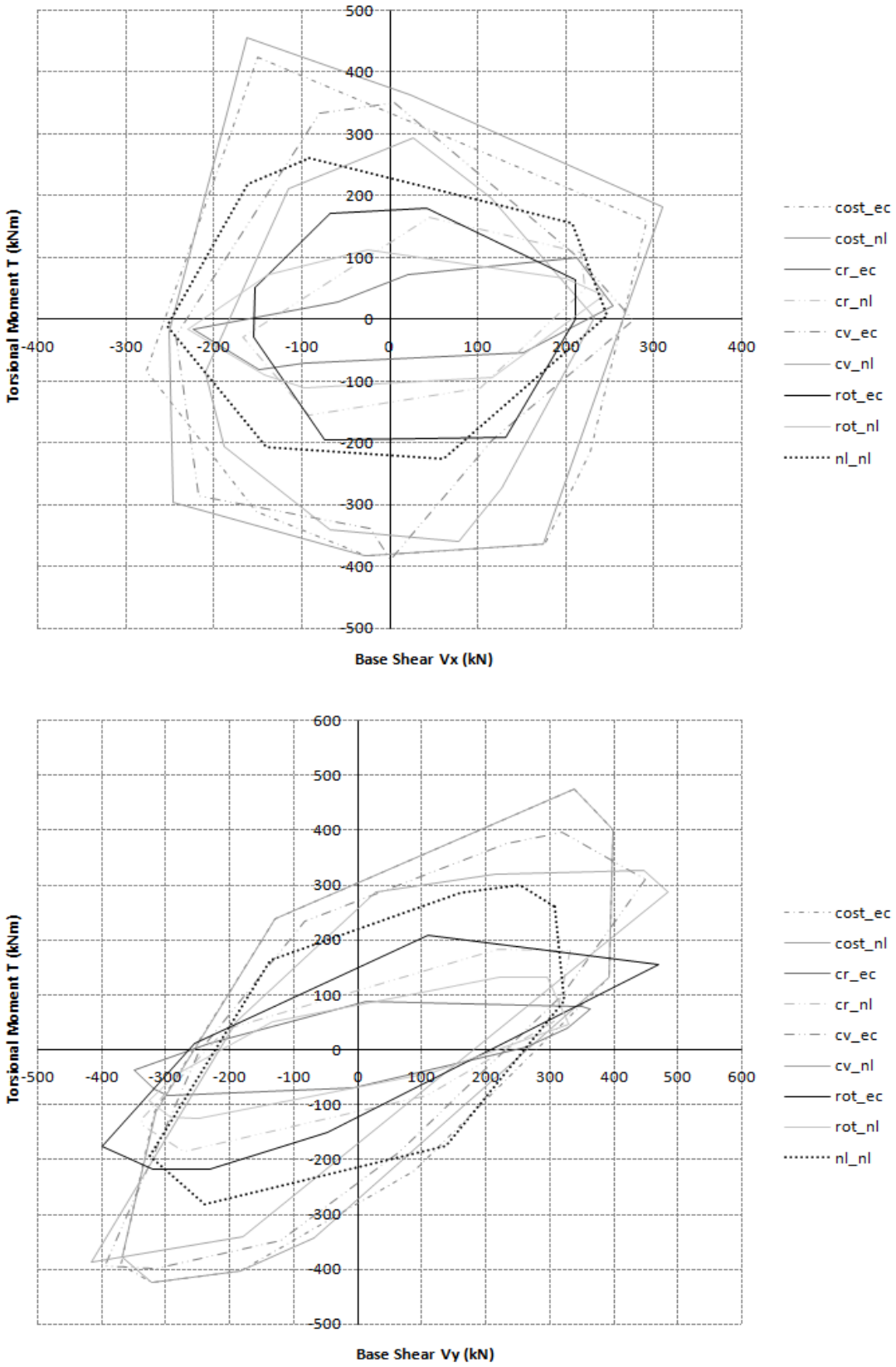

Figure 8.27 *The envelope of the BST time histories for the rare earthquake hazard level (10in50) in x and y directions*

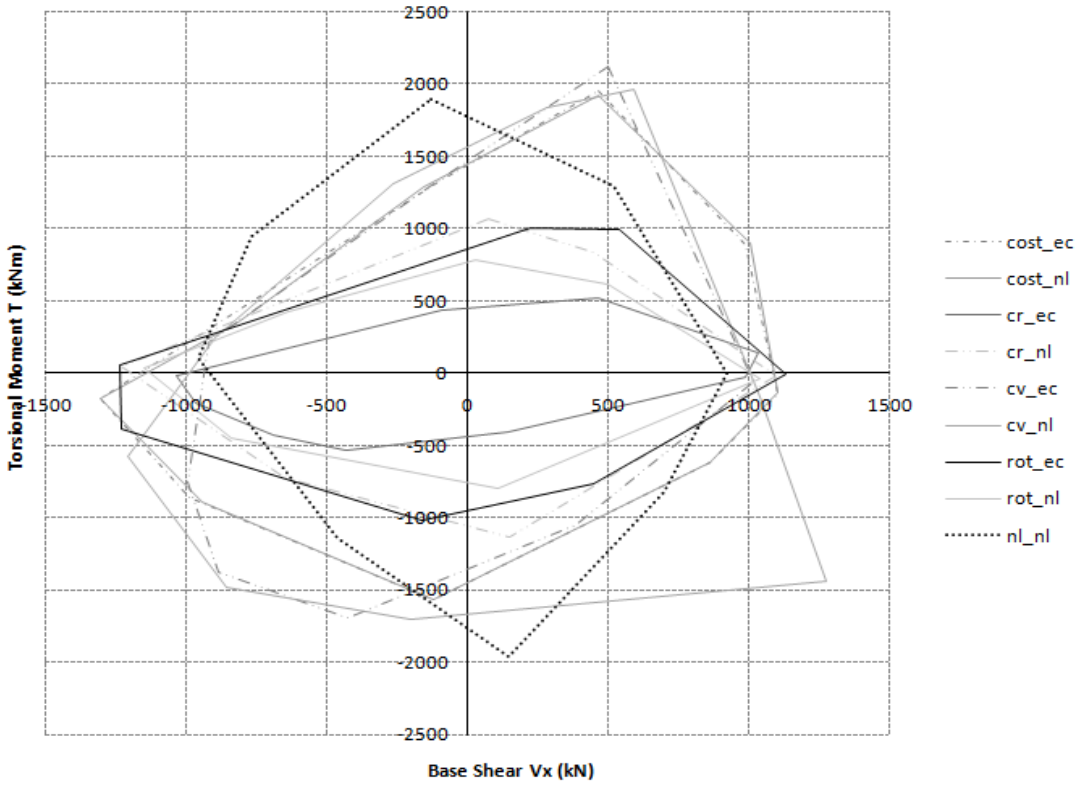

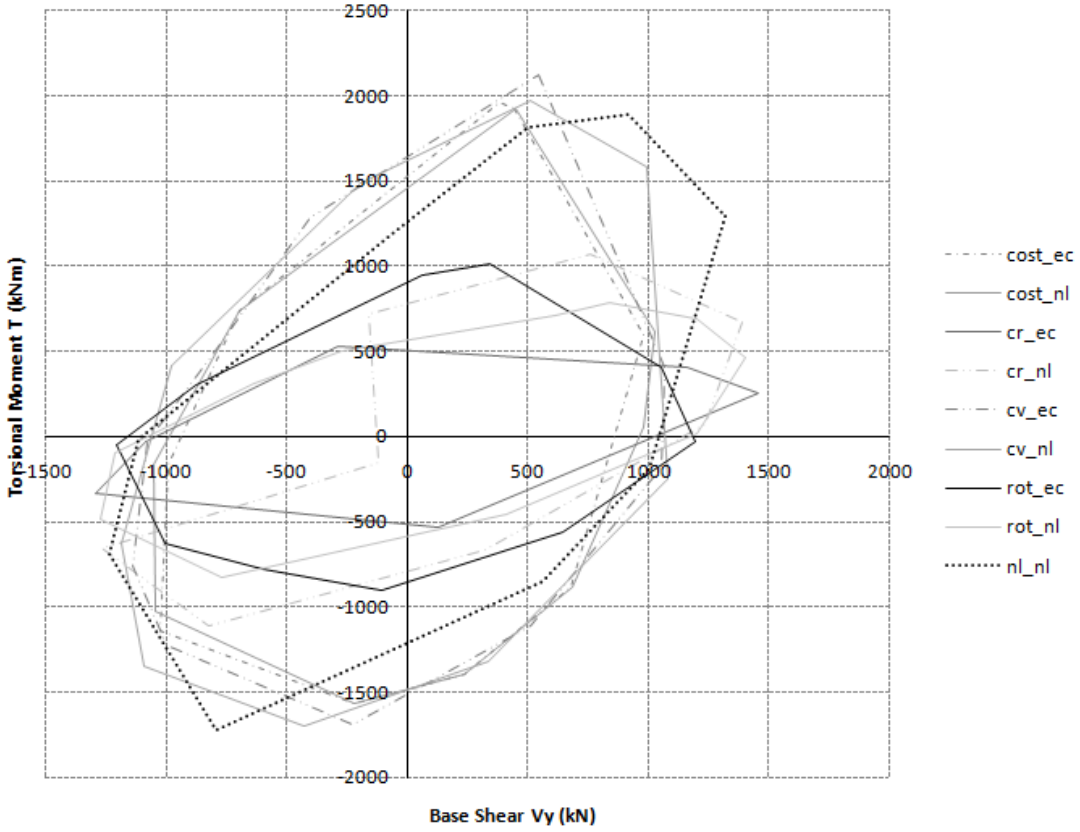

Figure 8.28 *The envelope of the BST time histories for the maximum considered event earthquake hazard level (2in50) in x and y directions*

In the occasional earthquake hazard level (50in50-Figure 8.27) in both x and y directions the design models rot_nl and cr_ec appear to perform better than the other design procedures. In particular cr_ec is increased by 136% in comparison with rot_nl. The design models cost_nl and cv_ec performed worst with their deviation from rot-nl reaching to almost 600% (638% for cost_nl, 582% for cv_ec).

As far as the rare earthquake hazard level (10in50-Figure 8.28) is concerned, the design models cr_ec and rot_nl behave better than other design procedures. Especially, rot_nl appears to have increased by 11% in the x direction and 50% in the y direction. The worst performance was observed by cost_nl and cost_ec, which burden the structure more by almost 350% in the x direction and 435% in the y direction.

Last in the maximum considered event (2in50-Figure 8.29) hazard level, the design model cr_ec again behaves better than rot_nl by 50% in both x and y directions, but are still the most well-performed design procedures. With a percentage increase of 300% and 270% from cr_ec respectively, cv_ec and cv_nl performed worst of all design models.

9.2.2 Description of Model 2

A one-storey RC building is used for the study. The layout of the second model is shown in Figure 8.29, while the south and the east views are shown in Figure 8.30, 8.31, and the 1-1 Section in Figure 8.32.

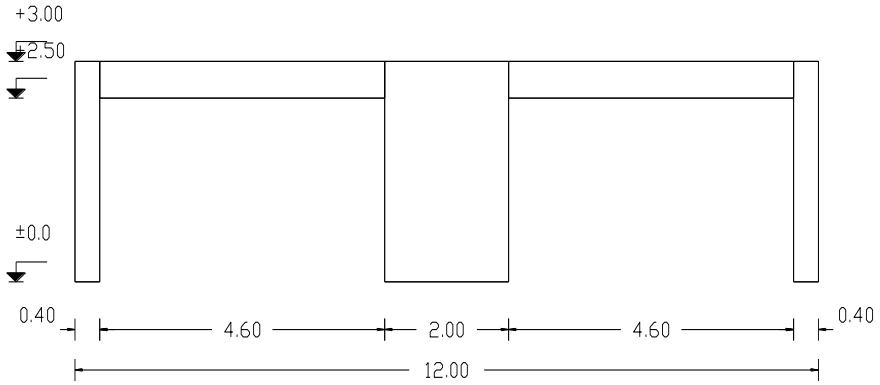

Figure 8.30 *The South view of Model2*

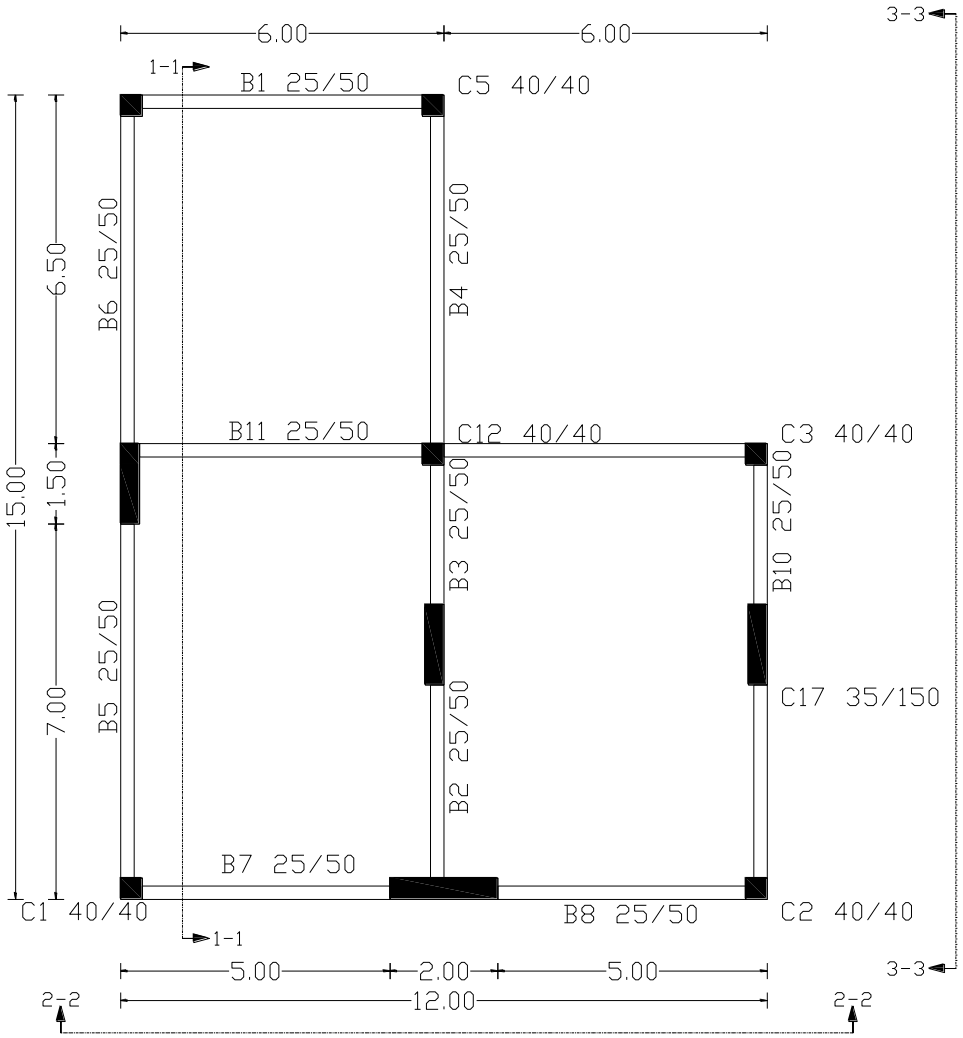

Figure 8.29 *Model2 layout*

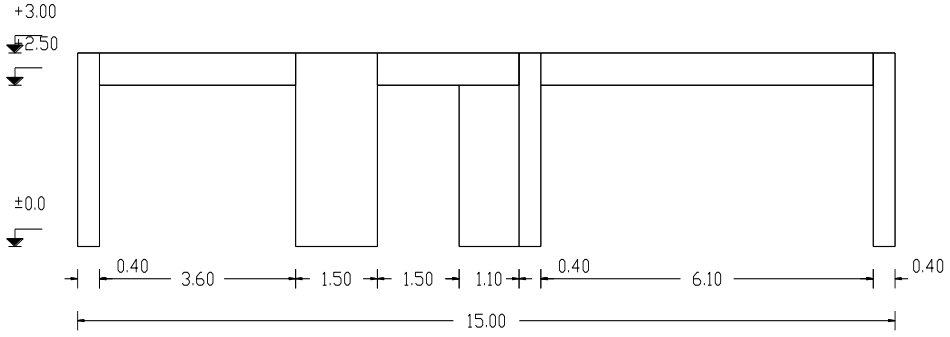

Figure 8.31 *The East view of Model2*

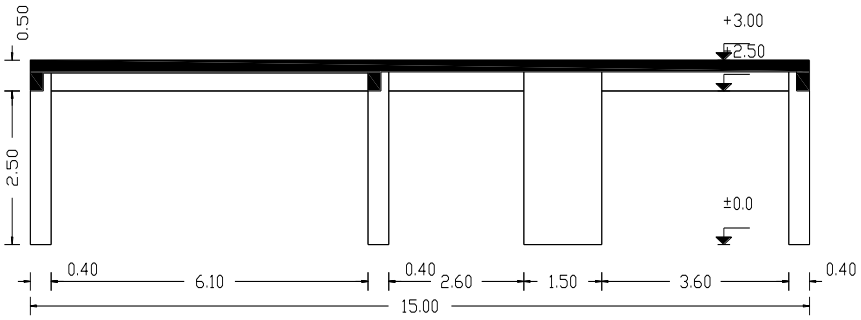

Figure 8.32 *The 1-1 Section of Model2*

In all test cases the following material properties have been considered:

Concrete:

Concrete modulus of elasticity: E_c=27.5 GPa

Concrete compressive strength at 28 days: f_c=25000 kPa

Reinforcing steel:

Steel modulus of elasticity: E_s=210 GPa

Steel yield strength: f_y=600000 kPa

The materials above correspond to the concrete class C20/25 (nominal cylindrical strength of 20 MPa) and steel class S500 (nominal yield stress of 500 MPa), while the slab thickness is equal to 13 cm.

The optimized layouts (8.33-8.41) for the different designs procedures are presented below:

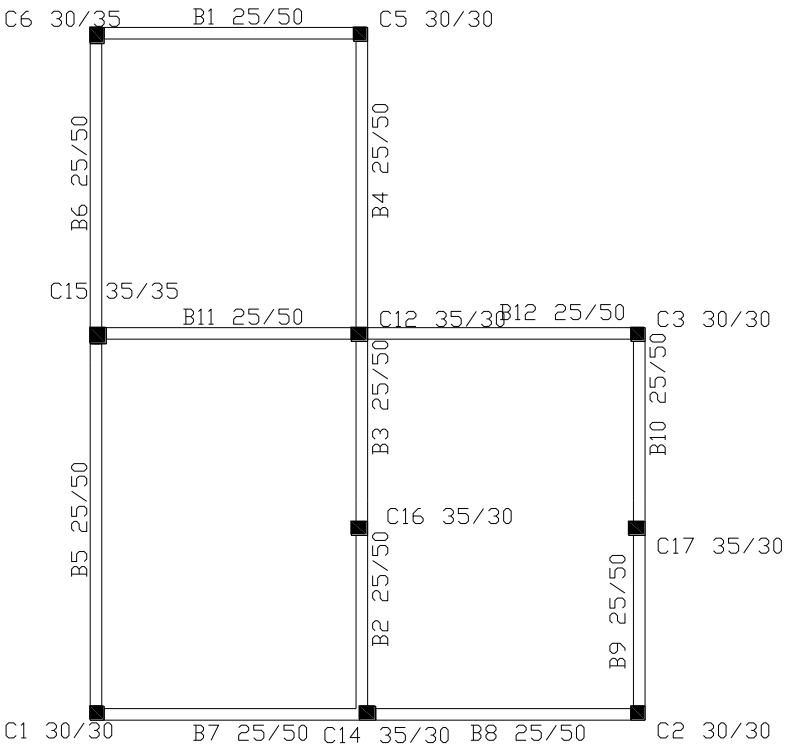

Figure 8.33 *Optimized layout through Model2_cost_ec design procedure*

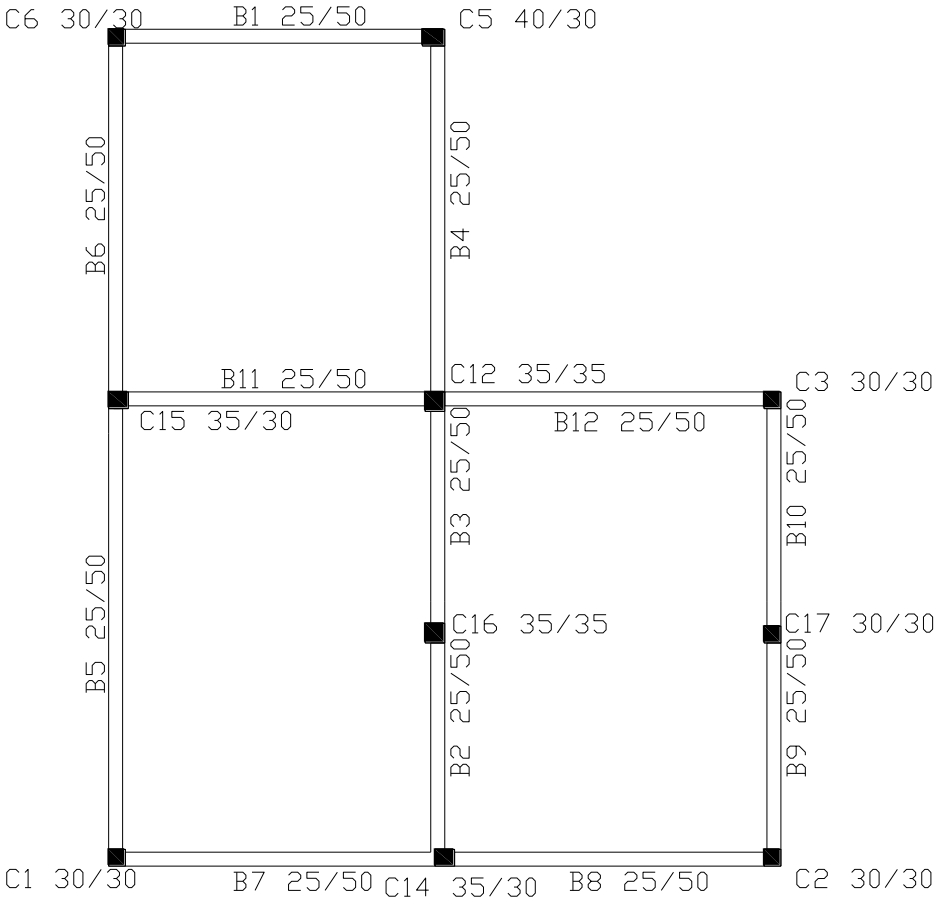

Figure 8.34 *Optimized layout through Model2_cost_nl design procedure*

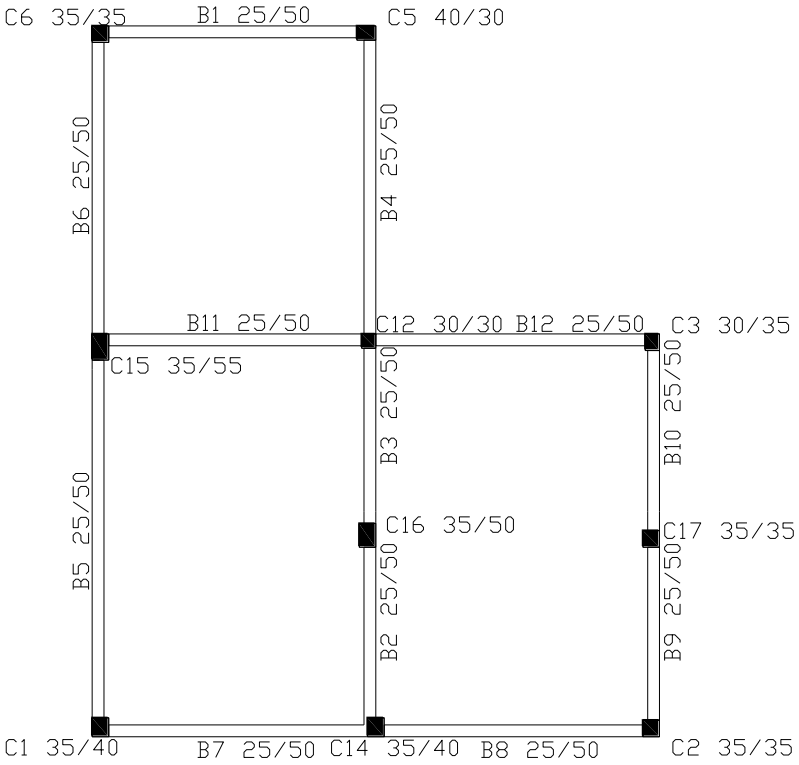

Figure 8.35 *Optimized layout through Model2_cr_ec design procedure*

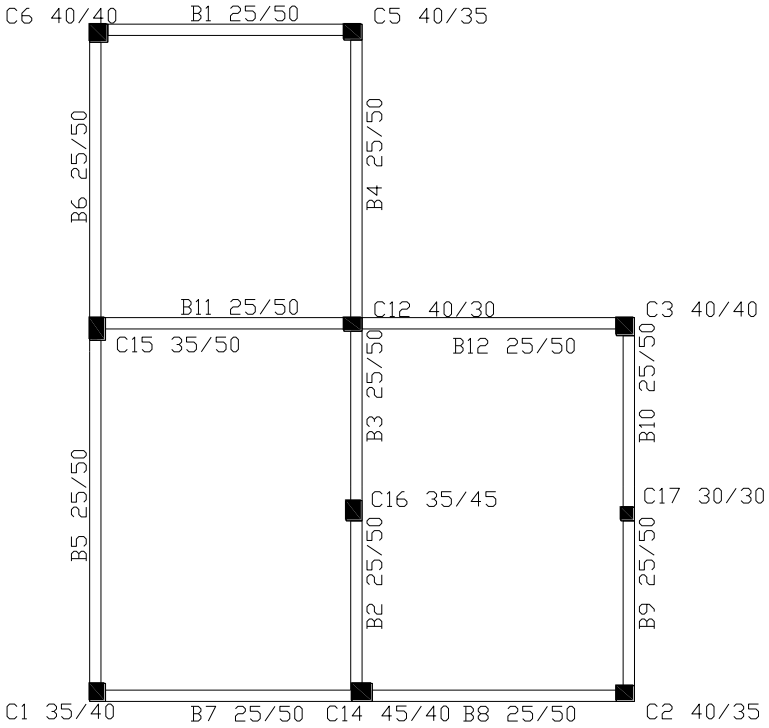

Figure 8.36 *Optimized layout through Model2_cr_nl design procedure*

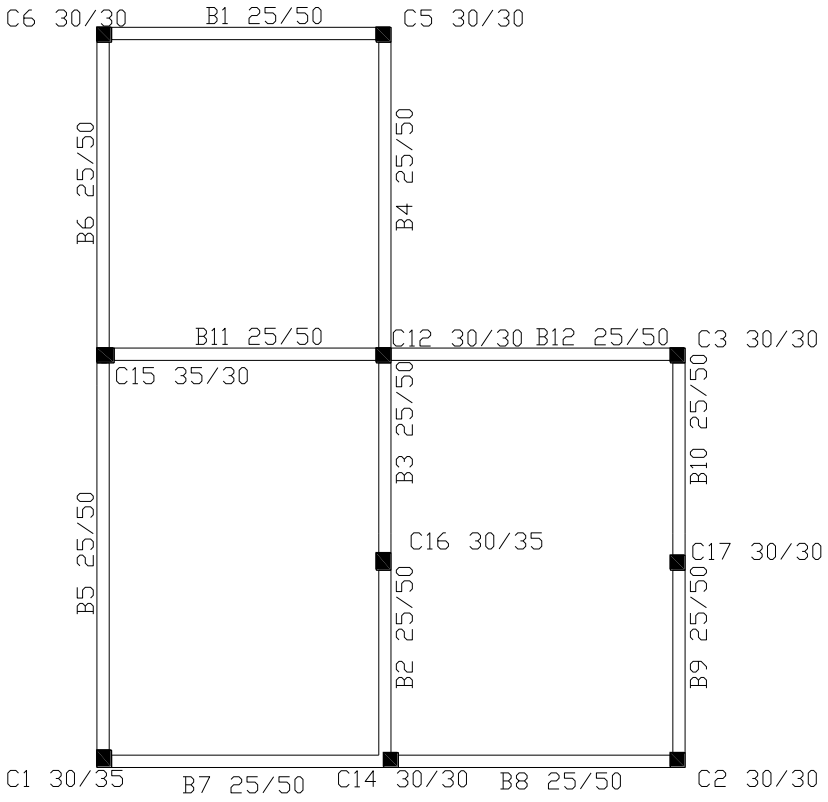

Figure 8.37 *Optimized layout through Model2_cv_ec design procedure*

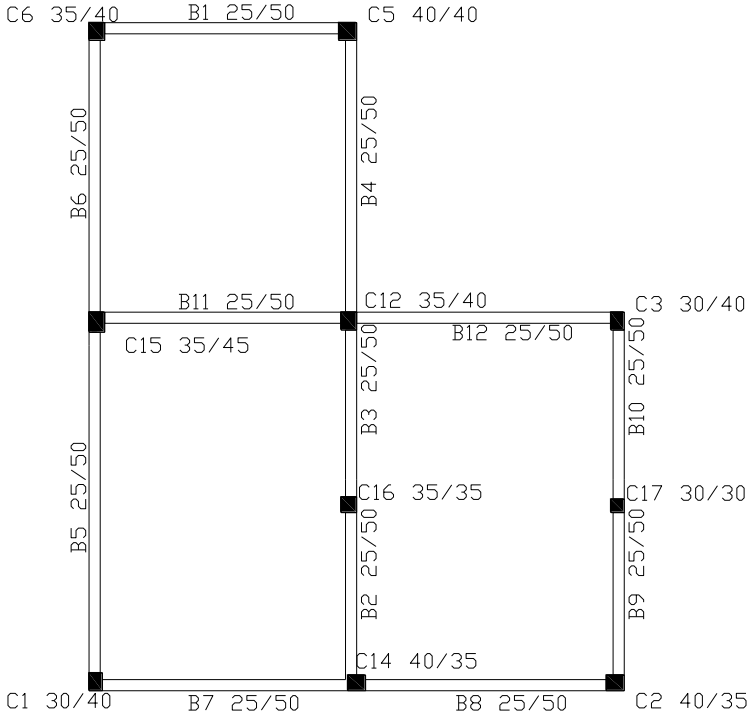

Figure 8.38 *Optimized layout through Model2_cv_nl design procedure*

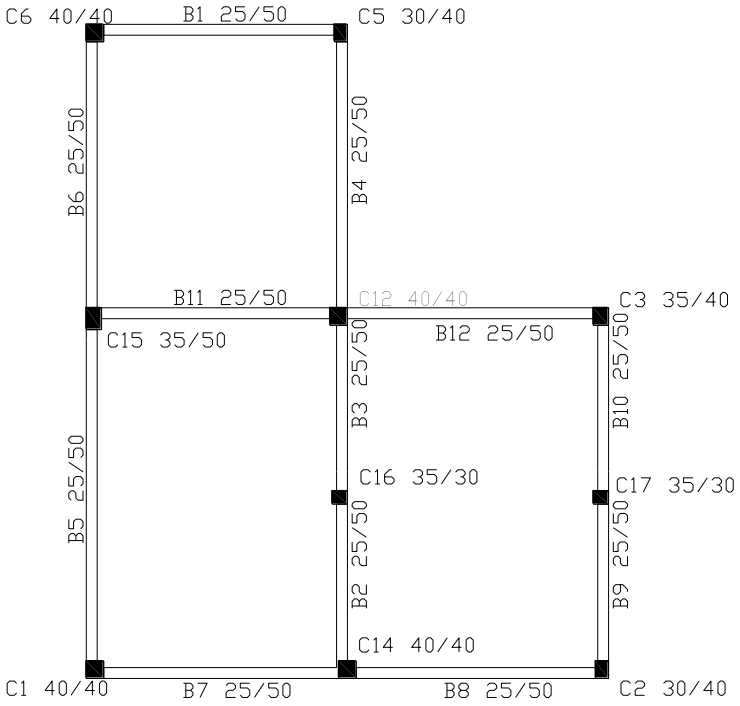

Figure 8.39 *Optimized layout through Model2_rot_ec design procedure*

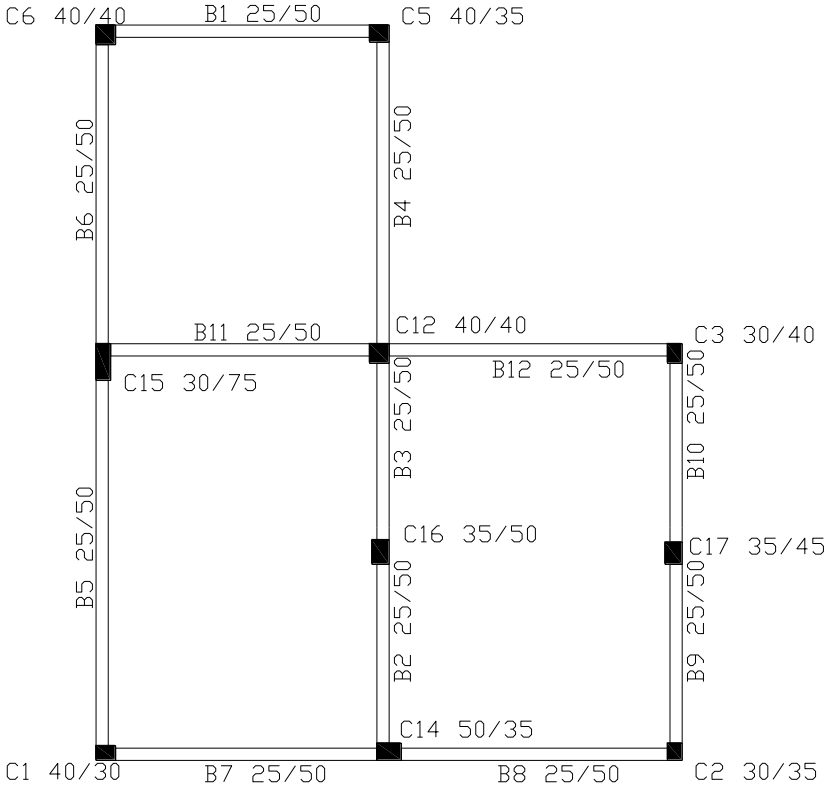

Figure 8.40 *Optimized layout through Model2_rot_nl design procedure*

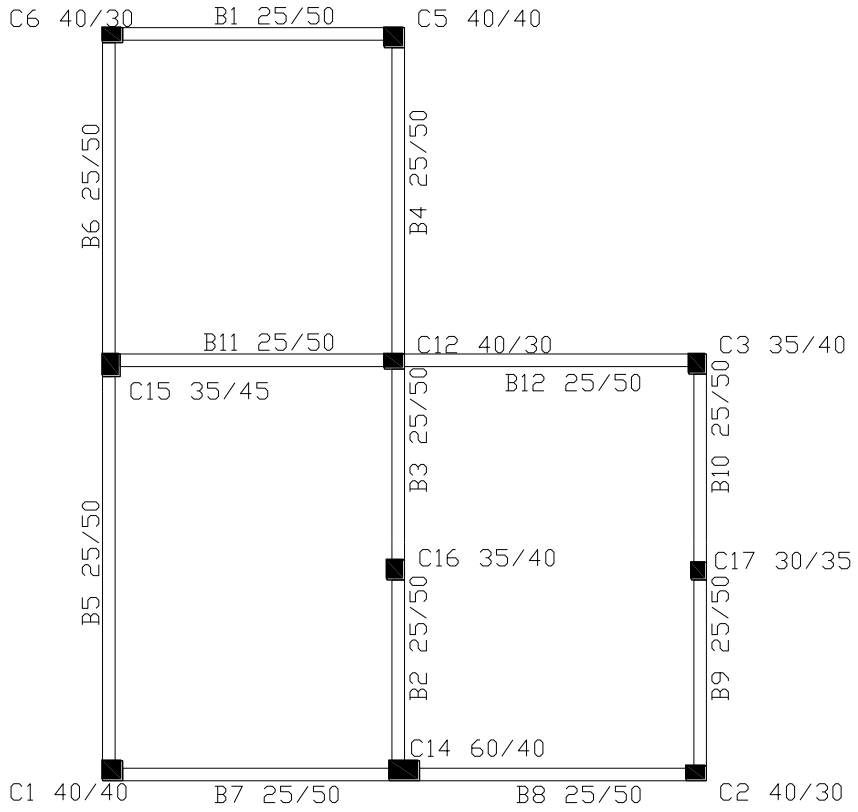

Figure 8.41 *Optimized layout through Model2_rot_nl design procedure*

Aiming at comparing various procedures in order to reduce the torsional effect, nine design procedures are compared. The model was subjected to two earthquake time historeys for every hazard level - C2_frtn and CM_riod in 50in50 level, CC_tcu101 and CC_tcu102 in 10in50 level, VL_pich and VL valu in 2in50 level.

For the first and the second design models (model_cost_ec, model_cost_nl) the objective function is the initial cost:

$$C = C_{IN} = C_{con} + C_{st} + C_{lab} \tag{8.6}$$

where $C = C_{IN}$: the initial cost of a new structure

C_{con}: the concrete cost

C_{st}: the cost of the steel of reinforcement

C_{lab}:the laboratory cost

For the third and the fourth design models (model_cr_ec, model_cr_nl) the objective function is the eccentricity of the center of rigidity:

$$e_{cr} = \sqrt{(x_{CM} - x_{CR})^2 + (y_{CM} - y_{CR})^2} \quad (8.7)$$

where x_{CM}, y_{CM}: the coordinates of the center of mass

x_{CR}, y_{CR}: the coordinates of the center of rigidity

For the fifth and the sixth design models (model_cv_ec, model_cv_nl) the objective function is the eccentricity of the center of rigidity:

$$e_{cv} = \sqrt{(x_{CM} - x_{CV})^2 + (y_{CM} - y_{CV})^2} \quad (8.8)$$

where x_{CM}, y_{CM}: the coordinates of the center of mass

x_{CV}, y_{CV}: the coordinates of the strength center

The difference between the models with the same objective function above is the behavioral constraints and the analysis procedure. The _ec design models are constrained by EAK and EKOS and analyzed with a modal analysis method. The _nl design models are designed in compliance with PBD and analyzed with a non-linear dynamic analysis.

For the seventh, eighth and the ninth design models (model_rot_ec, model_rot_nl, model_nl_nl) the objective function is the ratio of torsion:

$$ROTij = \frac{\sum_{k=1}^{n} |Vkij| - \sum_{k=1}^{n} Vkij}{\sum_{k=1}^{n} Vkij} \quad (8.9)$$

where n: the number of elements in a floor direction (x or y)

i: the corresponding shear force of the element

j: the direction of the earthquake motion

For the rot_ec and rot_nl design models the ROT is calculated for shear forces result from modal dynamic analysis but the constraints are different at _ec model EAK and EKOS are applied and at _ nl model PBD is performed. For the third design model the ROT is calculated for shear forces result from non-linear dynamic analysis and PBD process is applied.

In Table 8.16 below the results of optimization for Model1 (using 9 different design models) are depicted.

Table 8.16 *Comparison between the initial values of the objective functions and the results of the optimization procedure for all the design models*

	Initial					Final					Variation Percentage				
Design Models	**cost**	**e_cr**	**e_cv**	**rot**	**nl**	**cost**	**e_cr**	**e_cv**	**rot**	**nl**	**cost**	**e_cr**	**e_cv**	**rot**	**nl**
Model2_cost_ec	8480,88	4,93	4,63	0,99	202,06	7026,64	0,45	0,45	0,05	7026,64	-17,15	-90,85	-90,39	-95,15	3377,57
Model2_cr_ec	7477,87	0,00	2,11	0,02	215,41	7256,01	0,03	1,07	0,02	0,03	-2,97	2927,79	-49,53	-10,02	-99,99
Model2_cv_ec	9172,22	4,93	3,47	1,28	0,00	7874,58	0,10	0,02	0,03	0,00	-14,15	-97,90	-99,49	-97,42	0,00
Model2_rot_ec	8480,88	4,93	4,63	0,99	180,84	7258,07	0,04	0,67	0,02	0,02	-14,42	-99,13	-85,43	-98,05	-99,99
Model2_nl_nl	7893,57	0,00	1,83	1,28	64,47	7152,64	1,17	0,58	0,36	37,48	-9,39	0,00	-68,19	-71,74	-41,86
Model2_cost_nl	8480,88	4,93	4,63	0,99	202,06	7005,26	1,03	0,34	0,31	7005,26	-17,40	-79,11	-92,73	-68,62	3366,99
Model2_cr_nl	8480,88	4,93	4,63	0,99	202,06	7283,21	0,03	0,40	0,04	0,03	-14,12	-99,38	-91,31	-96,31	-99,98
Model2_cv_nl	9172,22	4,93	3,47	1,28	0,00	7709,23	0,33	0,03	0,10	0,00	-15,95	-93,28	-99,15	-92,56	0,00
Model2_rot_nl	8480,88	4,93	4,63	0,99	271,20	7375,14	0,02	1,26	0,02	0,02	-13,04	-99,65	-72,86	-98,04	-99,99

In Figures 8.42-8.50 below the time historeys of torsional moment and base shear in the x and y direction are presented for the three hazard levels for each design procedure.

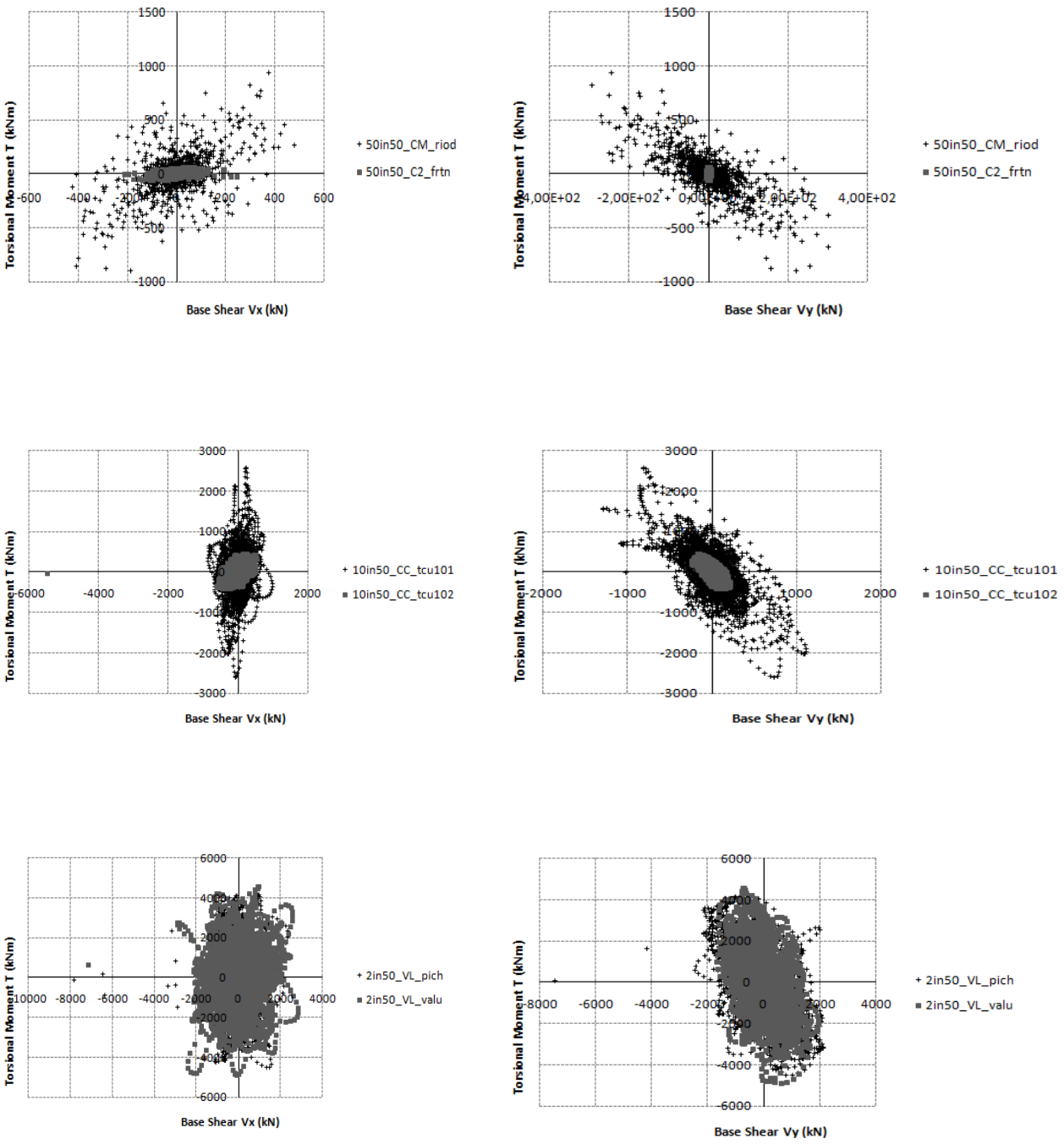

Figure 8.42 *Model2 cost ec base shear and torque time historeys for the three hazard levels in x and y directions*

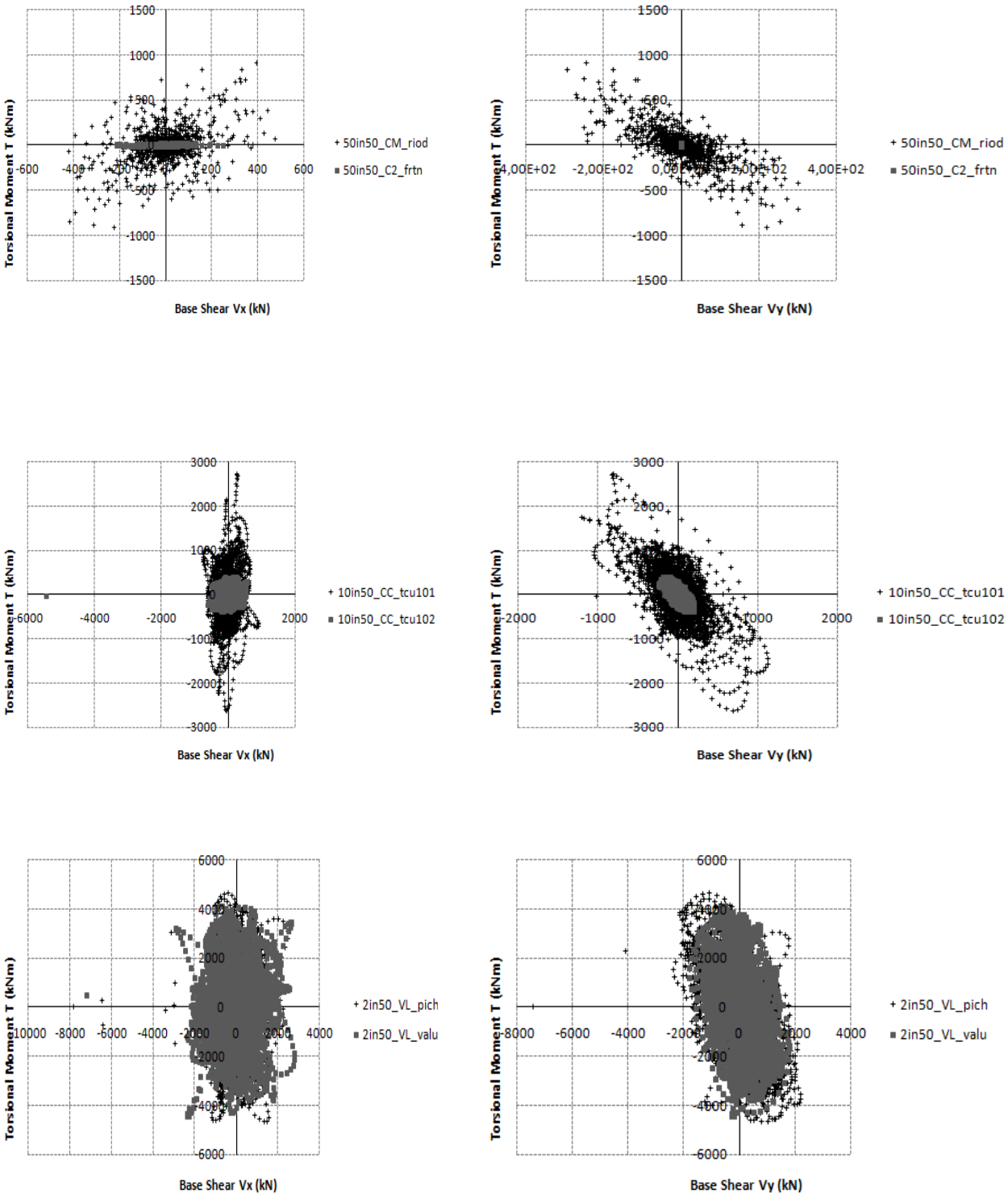

Figure 8.43 *Model2_cost_nl base shear and torque time historeys for the three hazard levels in x and y directions*

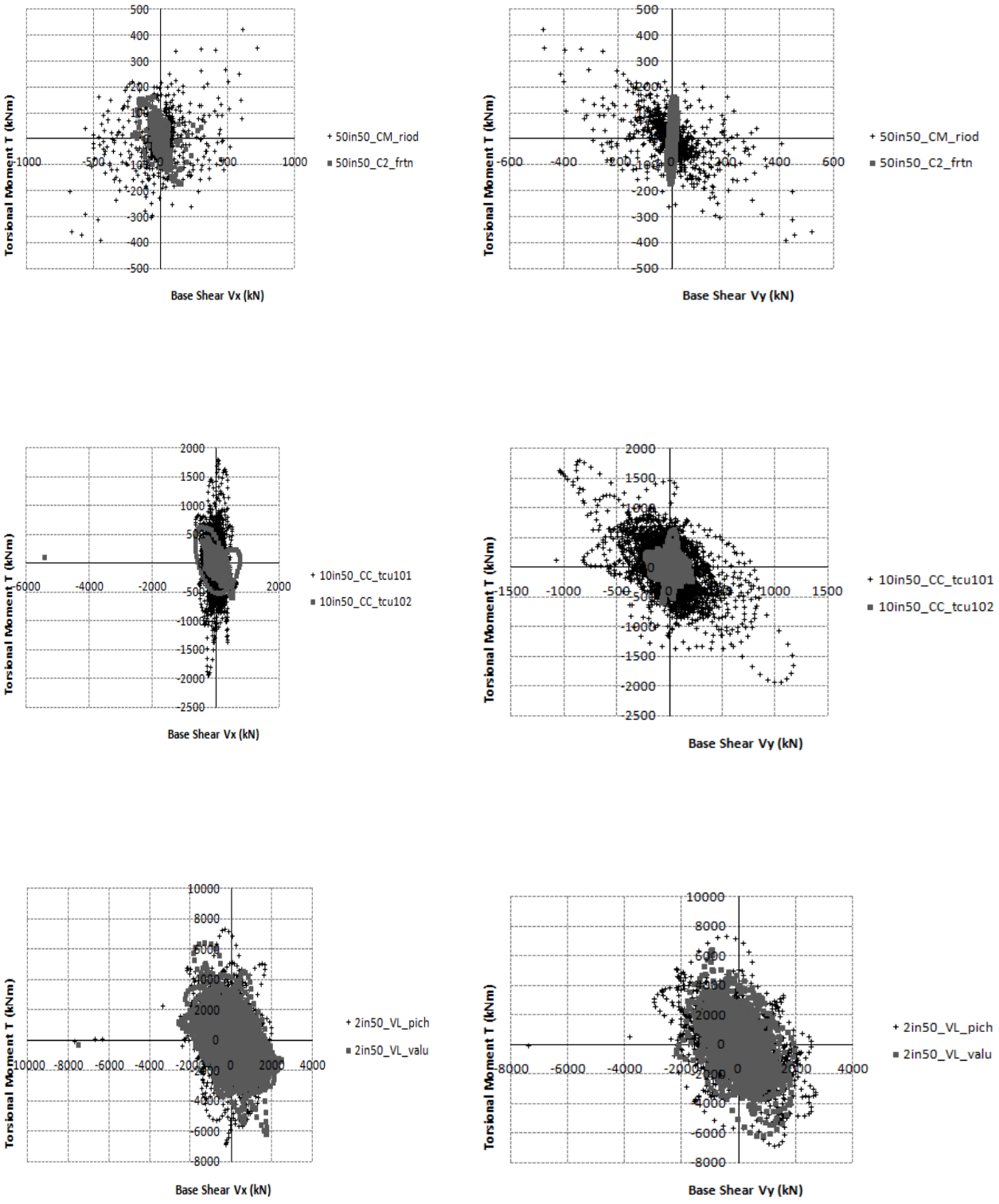

Figure 8.44 *Model2_cr_ec base shear and torque time historeys for the three hazard levels in x and y directions*

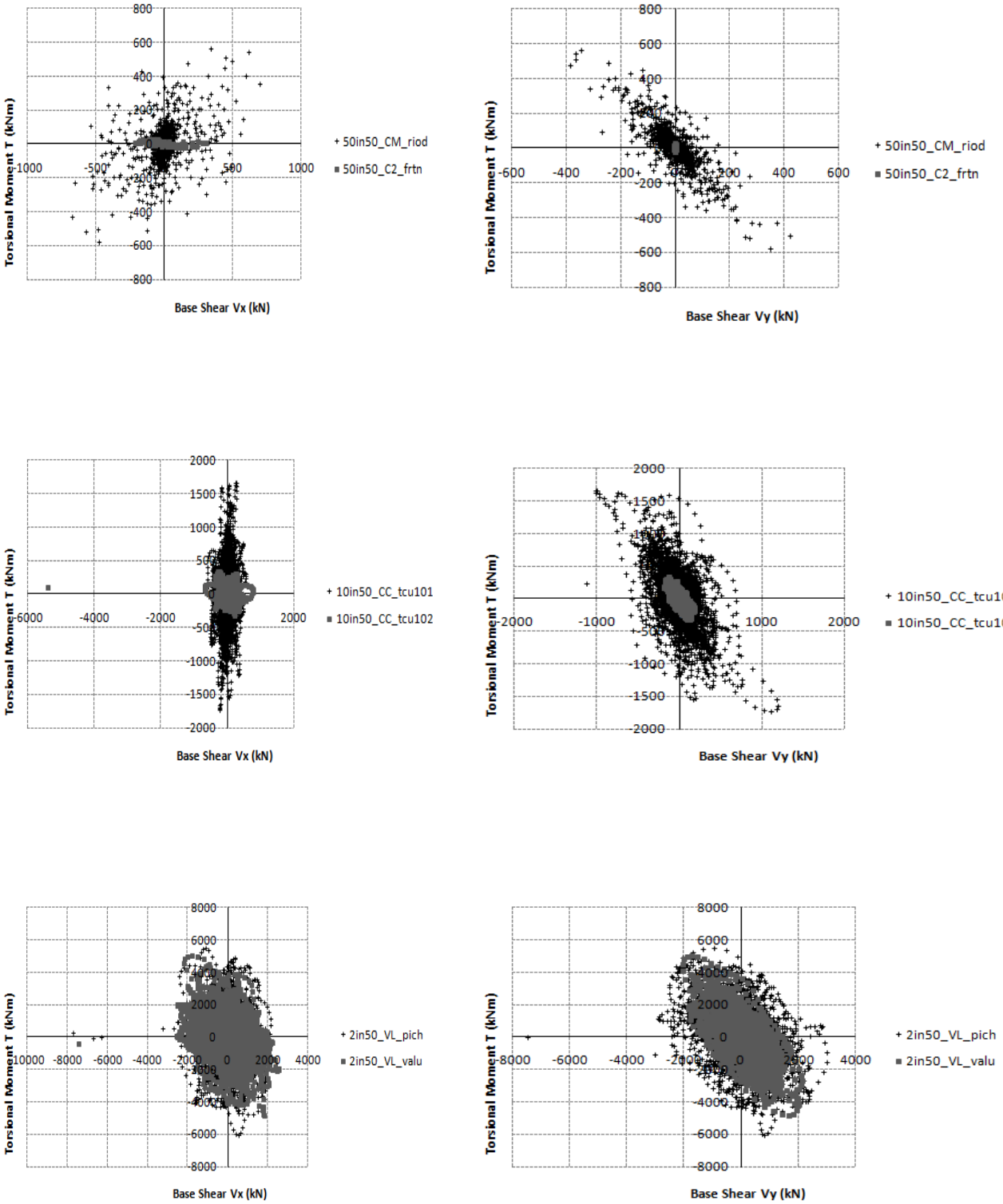

Figure 8.45 *Model2_cr_nl base shear and torque time historeys for the three hazard levels in x and y directions*

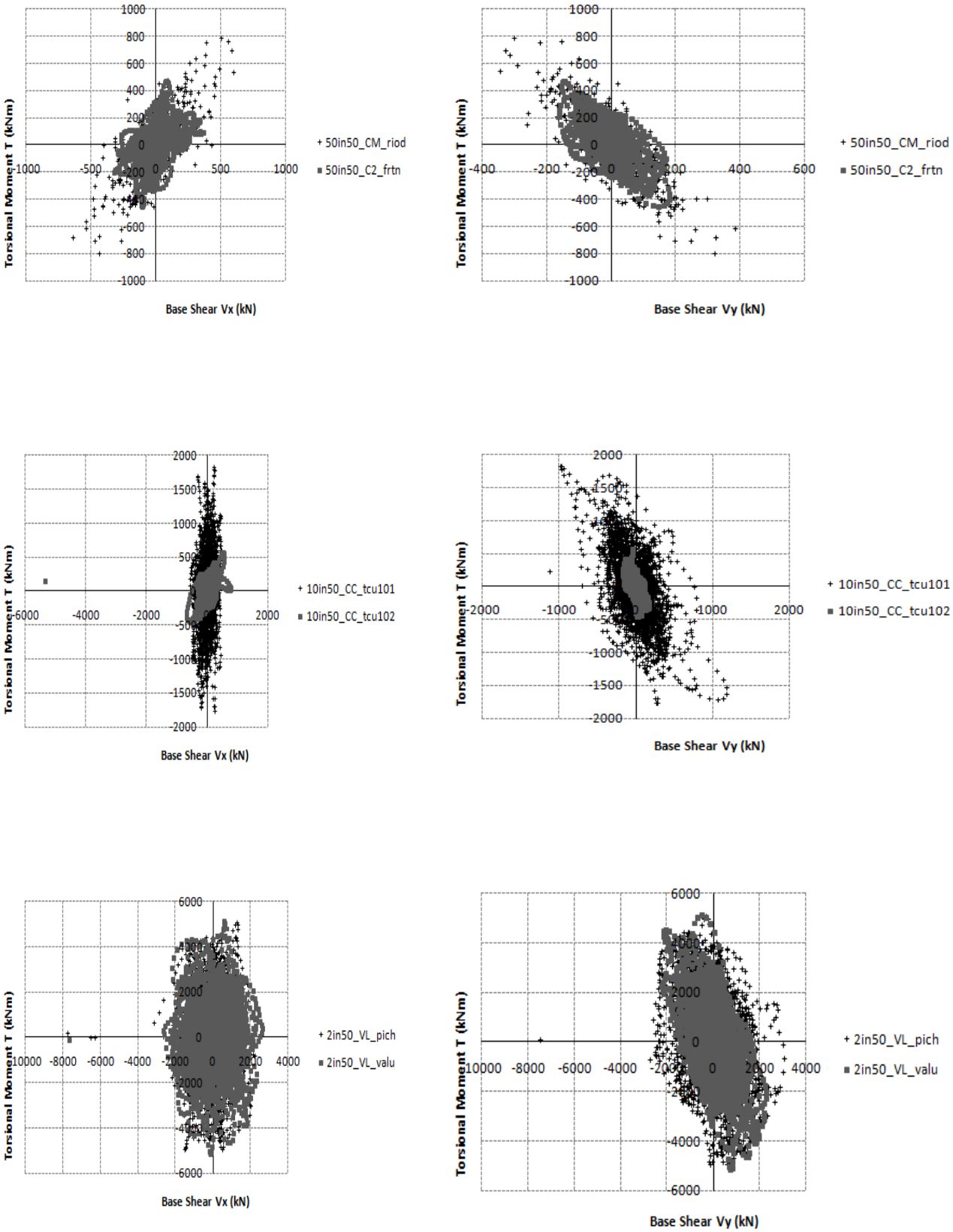

Figure 8.46 *Model2_cv_ec base shear and torque time historeys for the three hazard levels in x and y directions*

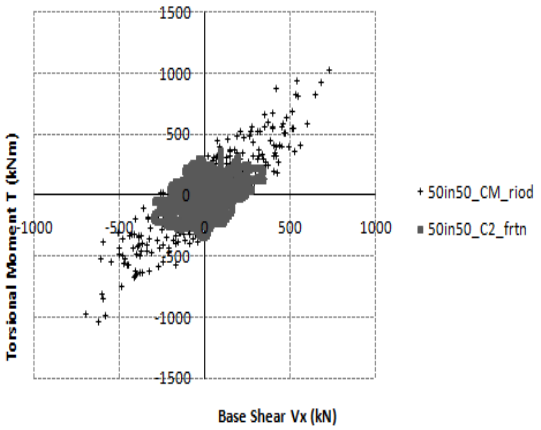

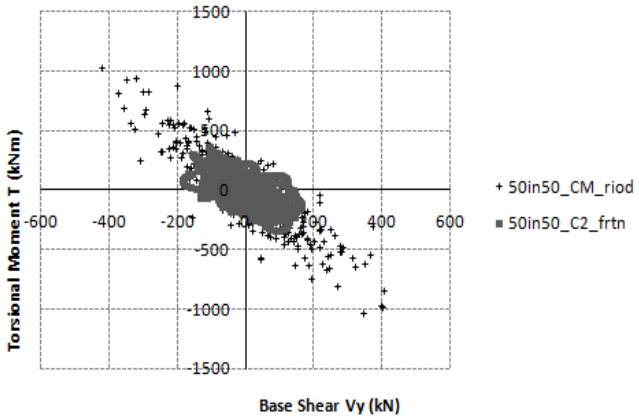

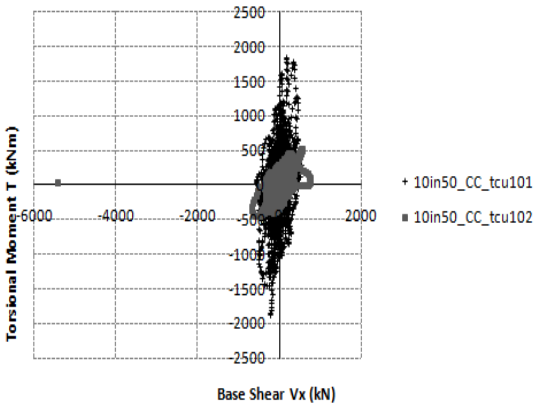

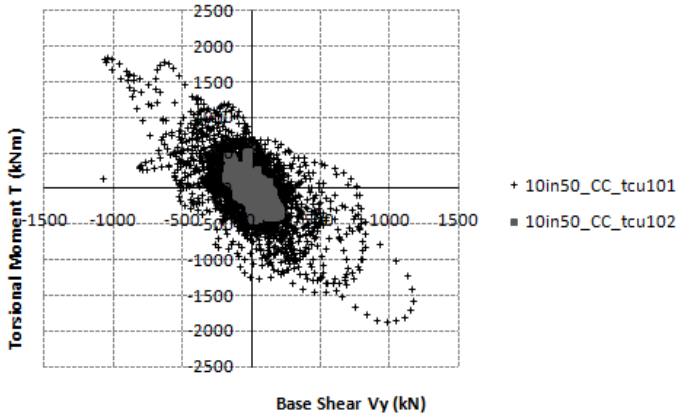

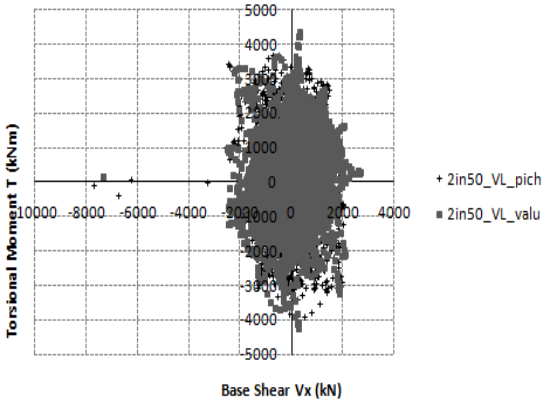

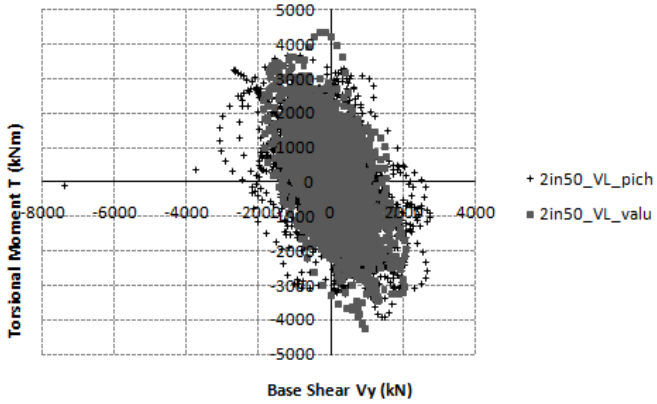

Figure 8.47 *Model2_cv_nl base shear and torque time historeys for the three hazard levels in x and y directions*

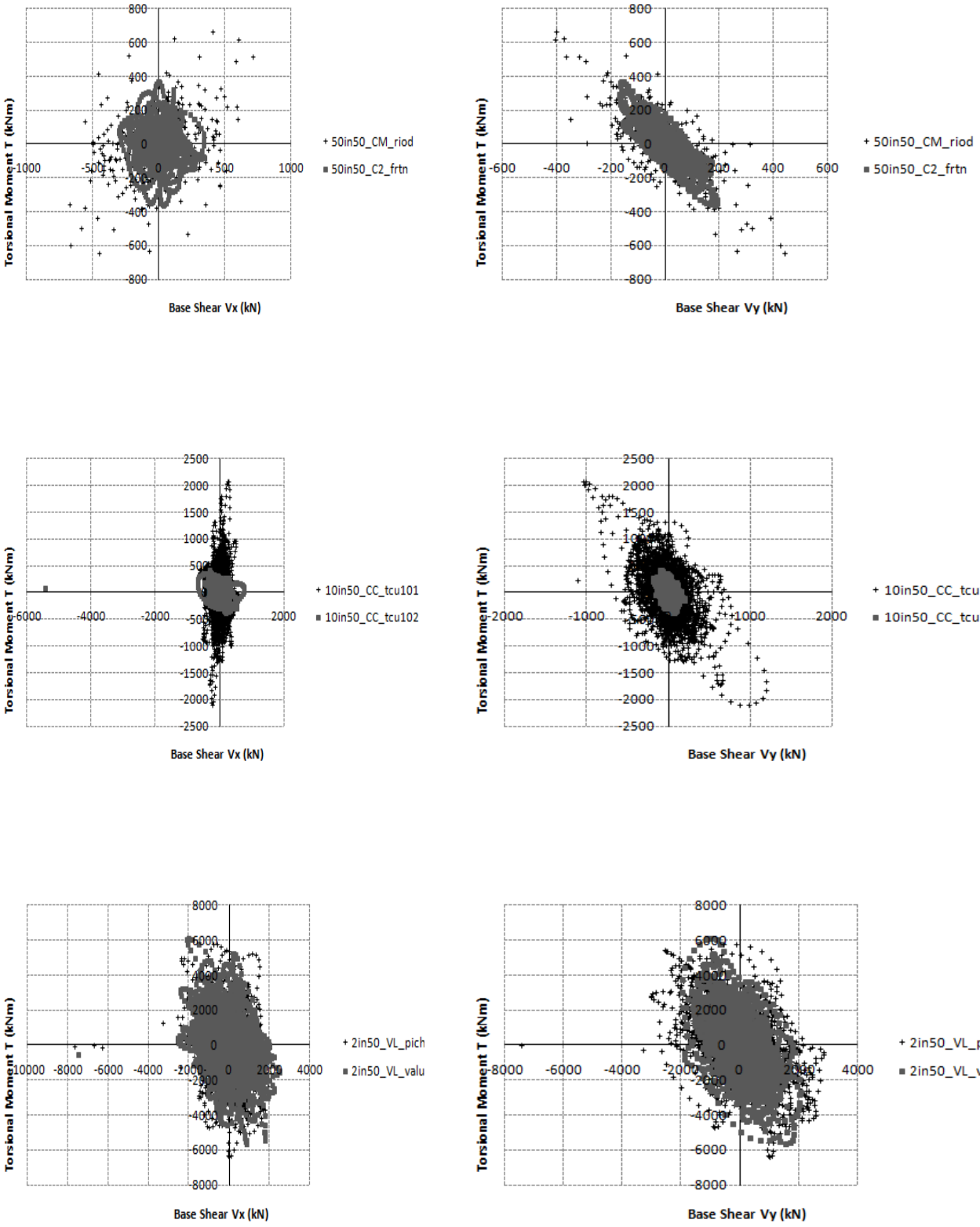

Figure 8.48 *Model2_nl_nl base shear and torque time historeys for the three hazard levels in x and y directions*

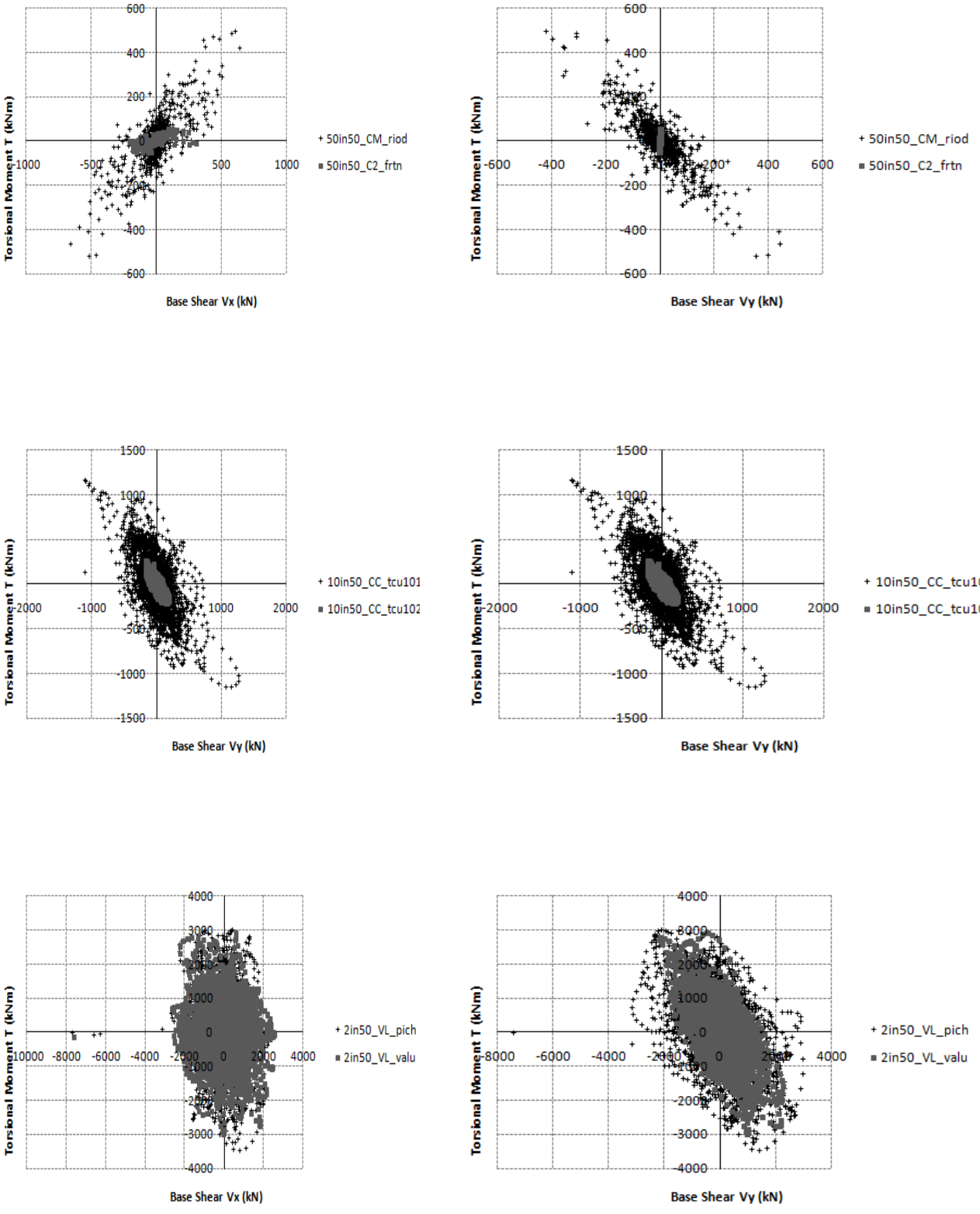

Figure 8.49 *Model2_rot_ec base shear and torque time historeys for the three hazard levels in x and y directions*

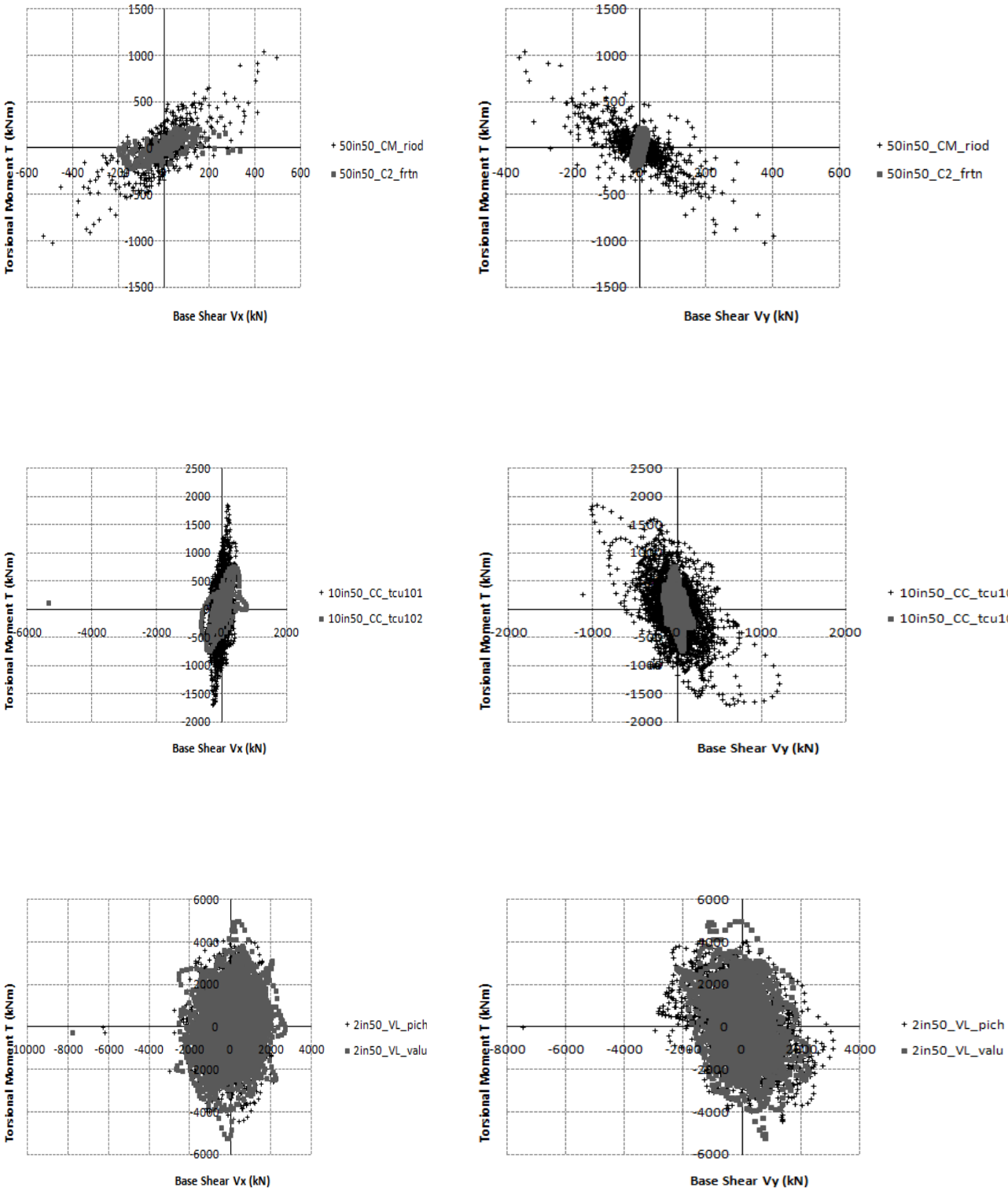

Figure 8.50 *Model2_rot_nl base shear and torque time histories for the three hazard levels in x and y directions*

In order to compare the various formulations of the optimization problem with reference to their performance against torsional effect, the envelopes of the base shear and torque time histories are developed. These envelopes are presented below so as to be able to reach any conclusions. (Figures 8.51-8.53)

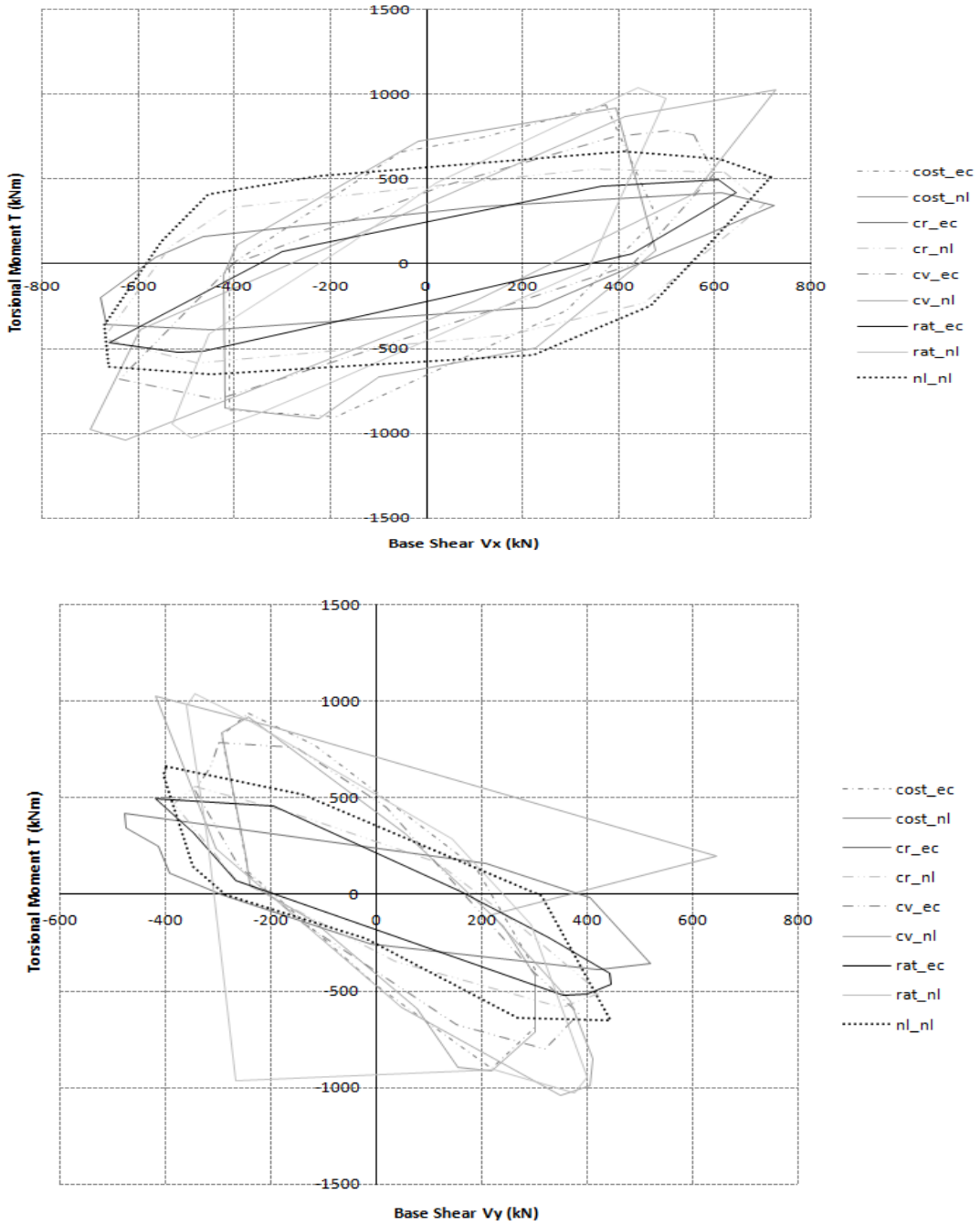

Figure 8.51 *The envelope of the BST time histories for the occasional earthquake hazard level (50in50) in x and y directions*

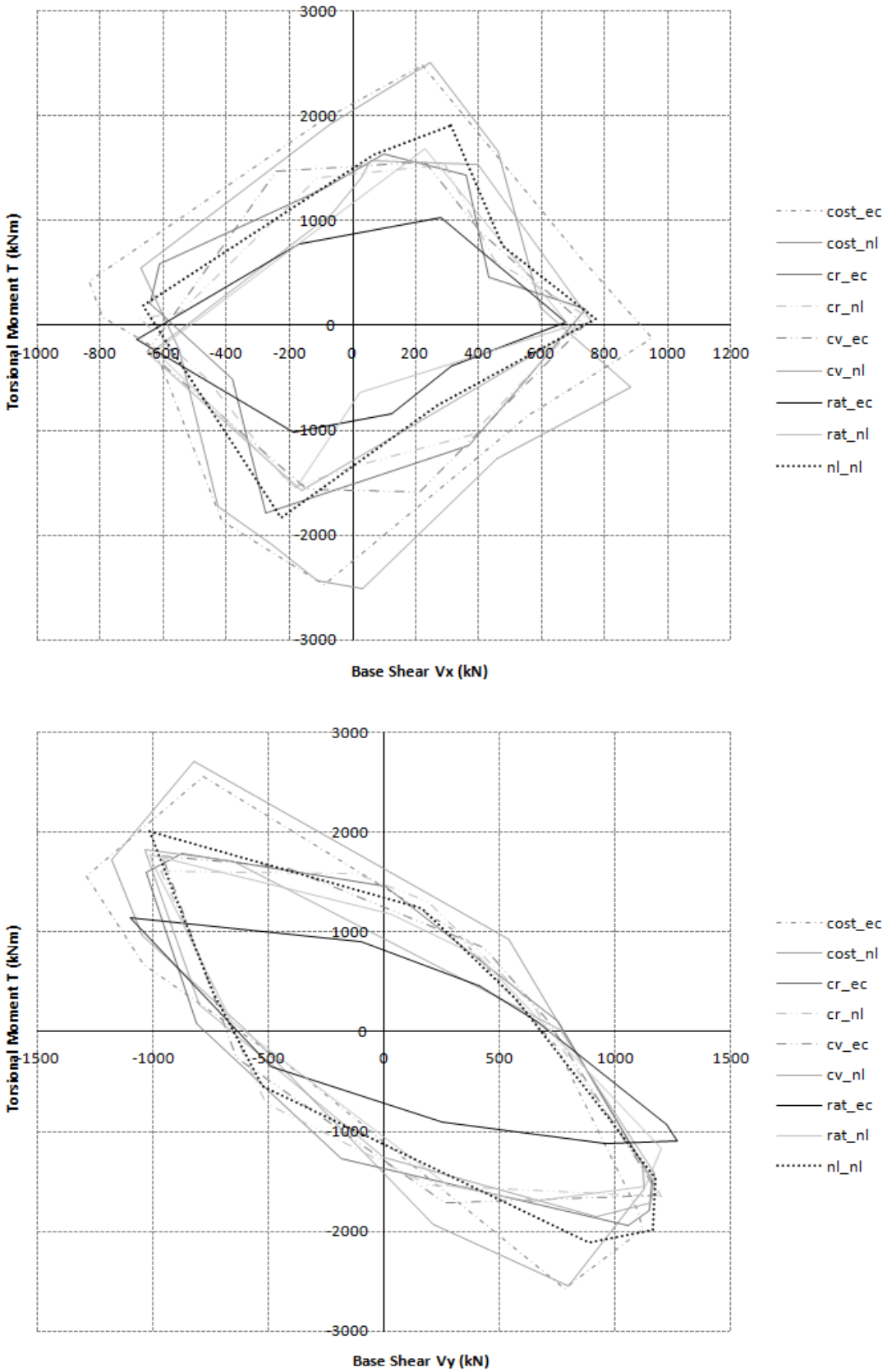

Figure 8.52 *The envelope of the BST time histories for the rare earthquake hazard level (10in50) in x and y directions*

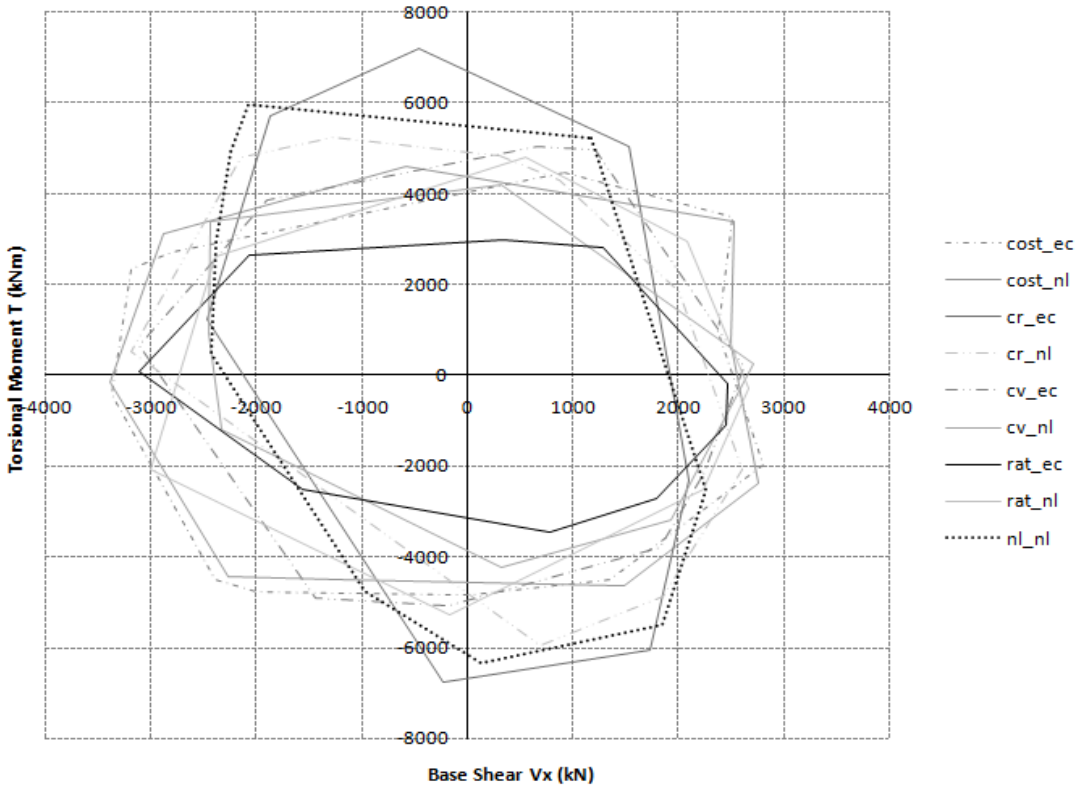

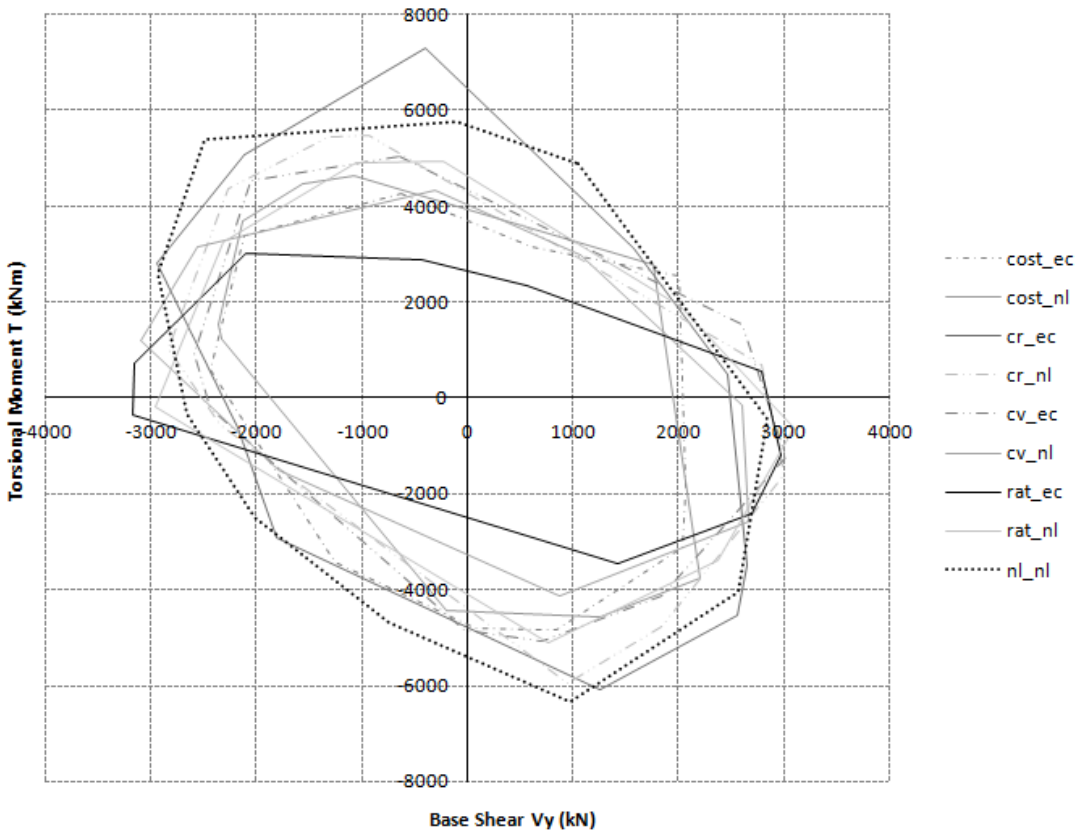

Figure 8.53 *The envelope of the BST time histories for the maximum considered event earthquake hazard level (2in50) in x and y directions*

In the occasional earthquake hazard level (50in50-Figure 8.51) in both x and y directions the design models cr_ec and rot_ec appear to perform better than the other design procedures. In particular rot_ec is increased by 18% in comparison with cr_ec. The design models cv_nl and rot_nl performed worst with their deviation from cr-ec reaching to almost 150%.

As far as the rare earthquake hazard level (10in50-Figure 8.52) is concerned, the design models rot_ec and cr_nl behave better than other design procedures. Especially, cr_nl appears to have increased by 50% in the x direction and 45% in the y direction. The worst performance was observed by cost_nl and cost_ec, which burden the structure more by almost 142% in the x direction and 125% in the y direction.

Last in the maximum considered event (2in50- Figure 8.53) hazard level, the design model rot_ec behaves better than cv_nl by 42% in the x direction and 25% in the y direction, but are still the most well-performed design procedures. With a percentage increase of 103% and 82% from rot_ec respectively, cr_ec and rot_nl performed worst of all design models.

REFERENCES

[1] K. C. Sarma & H. Adeli, "Cost optimization of concrete structures," *J. Struct. Engrg.*, vol. 124, no. 5, pp. 570–578, 1998.

[2] S. C. Ganzerli, C. P. Pantelides & L. D. Reaveley, "Performance-based design using structural optimization," *Earthquake Engrg. Struct. Dynamics 2000*, vol. 29, no. 11, pp. 1677–1690, 2000.

[3] W. M. Sebastian, "Optimisation of flexural stiffness profiles to compensate for reduced ductility in hyperstatic reinforced concrete structures," *Eng. Struct*, vol. 28, no. 6, pp. 893–902, 2006.

[4] X. K. Zou & C. M. Chan, "Optimal seismic performance-based design of reinforced concrete buildings using nonlinear pushover analysis," *Eng. Struct*, vol. 27, no. 8, pp. 1289–1302, 2005.

[5] H. K. Bachmann, "Order Number: 804.802e, Swiss Federal Office for Water and Geology, Swiss Agency for Development and Cooperation, BWG, Biel," 2002.

[6] R. D. Bertero, "Inelastic torsion for preliminary seismic design," *J. Struct. Engrg*, vol. 121, no. 8, pp. 1183–1189, 1995.

[7] C. M. Wong & W .K. Tso, "Evaluation of seismic torsional provisions in uniform building code," *J. Struct. Engrg*, vol. 121, no. 10, pp. 1436–1442, 1995.

[8] P. Fajfar, D. K. Marušić & I. Peruš, "Torsional effects in the pushover-based seismic analysis of buildings," *J. Earthquake Eng.*, vol. 9, no. 6, pp. 831–854, 2005.

[9] J. D. Pettinga, M. J. N. Priestley & S. Pampanin & C. Christopoulos, "The role of inelastic torsion in the determination of residual deformations," *J. Earthquake Eng.*, vol. 11, no. 1, pp. 133–157, 2007.

[10] C. L. Kan, A. K. Chopra "Effect of torsional coupling on earthquake forces in buildings," *J. Struct. Division Asce* , vol. 103, no. 4, pp. 805–819, 1977.

[11] S. H. Jeong & A. S. Elnashai, "New three-dimensional damage index for RC buildings with planar irregularities," *J. Structural Eng.* , vol. 132, no. 9, pp. 1482–1490, 2006.

[12] W. K. Tso, "Static eccentricity concept for torsional moment estimations," *J. Struct. Engrg*, vol. 116, no. 5, pp. 1199–1212, 1990.

[13] S. H. Jeong & A. S. Elnashai, "Analytical assessment of an irregular RC frame for full-scale 3D pseudo-dynamic testing part I: Analytical model verification," *J. Earthquake Eng.* , vol. 9, no. 1, pp. 95–128, 2005.

[14] "Eurocode 8. Design provisions for earthquake resistance of structures," *Env1998, Cen European Committee for Standardization, Brussels*, 1996.

[15] "Federal Emergency Management Agency FEMA-310," *Handbook for the Seismic Evaluation of Buildings-a Prestandard, Prepared By the American Society of Civil Engineers for the Federal Emergency Management Agency, Washington, DC*, 1998.

[16] T. Paulay, "A mechanism-based design strategy for torsional seismic response of ductile buildings," *European Earthquake Eng.* , vol. 2, p. 33–48, 1998.

[17] T. Paulay, "Some design principles relevant to torsional phenomena in ductile buildings," *J. Earthquake Eng.* , vol. 5, p. 273–308, 2001.

[18] M. García, J. C. De La Llera & J. L. Almazán, "Torsional balance of plan asymmetric structures with viscoelastic dampers," *Eng. Struct*, vol. 29, no. 6, pp. 914–932, 2007.

[19] "National Building Code of Canada. Part 4 Structural Design.," *Issued By the Canadian Commission On Building and Fire Codes, Federal Publications Inc., Toronto*, 1995.

[20] "Eurocode 2. Design of concrete structures," *Env1992, Cen European Committee for Standardization, Brussels*, 1992.

[21] Y. K. Wen & Y. J. Kang, "Minimum building life-cycle cost design criteria. I: Methodology," *J. Struct. Engrg*, vol. 127, no. 3, pp. 330–337, 2001.

[22] N. D. Lagaros, A. D. Fotis & S. A. Krikos, "Assessment of seismic design procedures based on the total cost," *Earthquake Engrg. Struct. Dynamics* , vol. 58, no. 9, pp. 1347–1380, 2006.

[23] "ATC-13. Earthquake damage evaluation data for California," *Earapplied Technology Council, Redwood City, California*, 1985.

[24] "FEMA 227: A Benefit-cost Model for the Seismic Rehabilitation of Buildings," *Federal Emergency Management Agency, Building Seismic Safety Council, Washington, DC*, 1992.

[25] "HAZUS-MH MR1, Multi-hazard Loss Estimation Methodology Earthquake Model", *Fema-national Institute of Building Sciences, Washington, DC*, 2003.

[26] Ghobarah, "On drift limits associated with different damage levels," *Int. Workshop Performance-based Seismic Design*, June 28-July 1, 2004.

[27] Y.K. Wen & Y. J. Kang, "Minimum building life-cycle cost design criteria. II: Applications," *J. Struct. Engrg*, vol. 127, no. 3, pp. 338–346, 2001.

[28] N. D. Lagaros, M. Fragiadakis & M. Papadrakakis, "Optimum design of shell structures with stiffening beams," *Aiaa J.* , vol. 42, no. 1, pp. 175–184, 2004.

[29] Somerville, P. Collins, N. Ground motion time historeys for the Humboldt Bay Bridge, Pasadena, CA, URS Corporation, 2002, www.peertestbeds.net/humboldt.htm.

[30] B. C. Papazachos, Ch. A. Papaioannou & N. P. Theodulidis, "Regionalization of seismic hazard in Greece based on seismic sources," *Natural Hazards*, vol. 8, no. 1, pp. 1–18, 1993.

[31] W. K. Tso & B. Myslimaj, "A yield displacement distribution-based approach for strength assignment to lateral force-resisting elements having strength dependent stiffness," *Earthquake Engrg. Struct. Dynamics* , vol. 32, p. 2319–2351, 2003.

10 ROT: a new design and evaluation criterion of the torsional effect on buildings

10.1 Introduction

The effect of torsion in reinforced concrete buildings was the subject of intensive investigation by many researchers. The reason is that many buildings suffer extensive damage after strong earthquake motions, due to their eccentric arrangement in the floor plan of the vertical resisting elements. Despite many attempt to propose design and/or evaluation criteria, a widely accepted criterion dealing with the effects in both the elastic and inelastic region as well as for multi-storey buildings is lacking from the corresponding literature.

In this study, we investigate the response of buildings exhibiting torsional phenomena and provide a criterion which can be a useful tool for assessing and designing a structure against torsion. The results show that structures with low values of the proposed criterion develop low values of base torque.

However, the edge displacements can increase by up to three times if the system is symmetrical [2]. Additional seismic inelastic deformation caused by structural asymmetry, Earthquake Engineering & Structural Dynamics, Vol 19, Is 2 pp. 243-258 , 1990.

Additional ductility demands on elements and additional edge displacements are taken as response parameters of interest in optimizing the strength distribution. An approximate expression to estimate the additional edge displacements due to structural asymmetry is presented. [3] Lateral strength distribution specification to limit additional inelastic deformation of torsionally unbalanced structures, Engineering Structures , Vol 14, Is 4 pp. 263-277, 1992.

10.2 Formulation

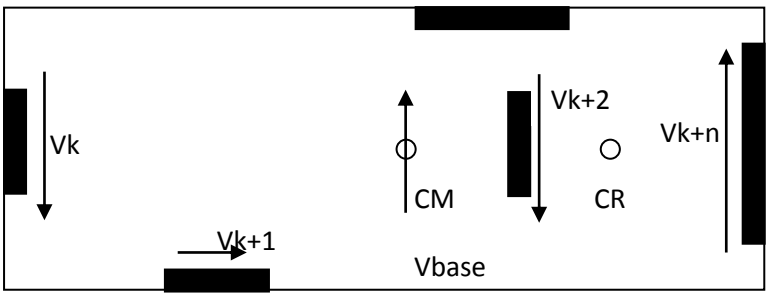

In the above figure, a generalized floor plan is shown where shear walls and the corresponding shear forces acting are depicted. The shear forces acting on the lateral resisting elements satisfy the following expression:

$$\sum_{k=1}^{n} |Vkij| \neq \sum_{k=1}^{n} Vkij$$

where:n = the number of elements in a floor direction (x or y),

i = the corresponding shear force of the element,

and j = the direction of the earthquake motion

Especially for the above floor plan with a seismic action in the y direction:

$$\sum_{k=1}^{n} |Vkxy| \neq \sum_{k=1}^{n} Vkxy = 0$$

and

$$\sum_{k=1}^{n} |Vkyy| \neq \sum_{k=1}^{n} Vkyy = Vbase$$

The floor torsion is usually computed from the elements' shear forces while the elements' torsional moments are neglected. This is a widely accepted assumption without being supported by a mathematical formulation. In this section a formulation is proposed for the torsional criterion which affects the torsional effect on the buildings. The value of the ROT can be related to the best seismic performance against torsion. This ratio has a general application in both the elastic and inelastic seismic

response of the structure. A simple example showing the computation of the Ratio Of Torsion ROT follows.

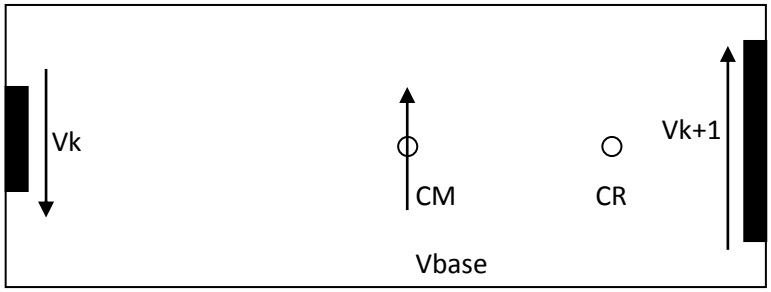

The total value of ROT for the above building is:

$$\text{ROT} = \sum_{1}^{n} \sum_{i=x, j=y}^{y, x} ROTij$$

where $ROTij = \frac{\sum_{k=1}^{n} |Vkij| - a * \sum_{k=1}^{n} Vkij}{\sum_{k=1}^{n} Vkij}$

and

n = the number of elements in a floor direction (x or y)

i = the corresponding shear force of the element

j = the direction of the earthquake motion

and α = 0 if i≠j or α = 1 if i=j

Furthermore, the single storey building of Figure 9.1 is selected for demonstrating the ROT computation in an elastic and inelastic region following the non-linear time historey procedure.

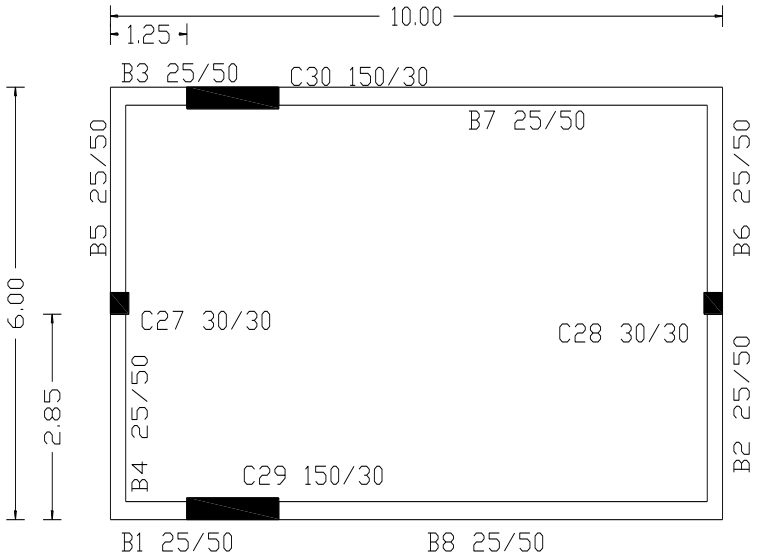

***Figure 9.1**: Geometry of the floor plan*

As we can see from the following, we can calculate the: ROTxy = 33.4*2/82 = 0,81 = 81%. That means for this simple structure the effect of the Y-Y seismic force (perpendicular to the floor eccentricity) is an 81% amplification of the floor's base shear force. So, if the ROT is minimum the structure has the minimum shear forces and thus the minimum resistance demands. If we perform a more accurate non-linear time historey analysis for this structure the ROT is very different. For six seismic records (three in each performance level: 50/50, 10/50, 2/50) the maximum ROT is 2.87. That means that the structure's shear demands is increased by 287% because of torsion. In this way, we believe that ROT is a very clear and accurate measure of a structure's torsional effect on the lateral resisting elements.

10.3 Numerical Examples

In this study three test examples are examined. In all test examples the following material properties have been considered: concrete C20/25 with modulus of elasticity E_c=30GPa and characteristic compressive cylinder strength f_{ck}= 20MPa, longitudinal and transverse steel reinforcement B500C with modulus of elasticity E_s=210GPa and characteristic yield strength $f_{yk,s}$=500MPa. The earthquake spectrum that has been used in the numerical study has the following characteristics: A=0.16g, ground type B and behavior factor q=3.0 according to EC8 [14]. The cross section

of the beams is 25x50 cm^2, while the cross section of the columns varies in each example. For all test examples, a number of different designs have been considered. The designs vary with reference to the cross sections and the longitudinal reinforcement of the columns but all have the same beams and plan layout.

In the description of the test examples the following terminology has been adopted. Symmetric stands for the structure that has symmetric stiffness and strength along the vertical elements for the x and y axis. "cv_A", "cv_B", "cv_C" stands for designs that are symmetric with reference to the stiffness but not symmetric with respect to the strength. Design "A" has the largest strength eccentricity, while design "C" has the lowest one. Furthermore, "ecc_cr" stands for the design with stiffness eccentricity and "ecc_cr_cv" stands for the design that has the center of strength and center of resistance at opposite sides of the center of mass as suggested by Tso [2]. The performance of the various designs is assessed for different seismic hazard levels with reference to their structural behavior, associated with storey drifts, shear forces of the columns, base shear and roof diaphragm rotation. For this purpose a number of nonlinear analyses have been carried out employing artificial earthquake motions that belong to the 2%, 10% and 50% hazard levels.

10.3.1 Test example 9.1

The first test example, shown in Figure 9.2, is a one-storey 3D building. For this test example, six designs are studied. The symmetric with respect to both x and y directions, three designs having strength eccentricity, one symmetric design (with stiffness and strength eccentricity equal to zero) and one design with strength and stiffness eccentricity having the center of rigidity and the center of strength at opposite sides corresponding to the center of mass. The symmetric and the strength eccentricity designs have the same column cross sections.

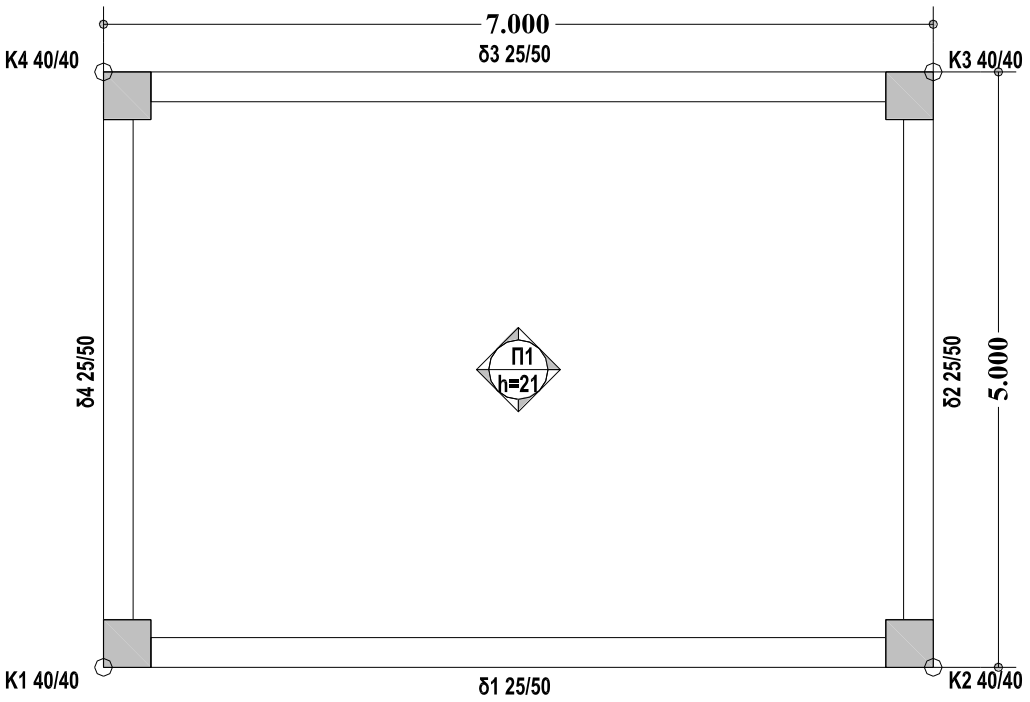

***Figure 9.2**: Plan layout of the first floor*

The results show that although, all six designs have the same total elastic stiffness, the column's drifts are not the same especially for the 2/50 hazard level. This is more evident along the x direction, where the structures are not symmetric and rotational displacements and shear forces are developed to the columns in y and x directions. This phenomenon has been described also by Llera and Chopra [1]. It is important to underline that although the designs have the same stiffness, the structure's drifts differ significantly. Furthermore, despite the fact that seismic motion is applied only in the y direction, the vertical elements develop drifts in both x and y directions (see Figure 9.3, 9.4 for all hazard levels).

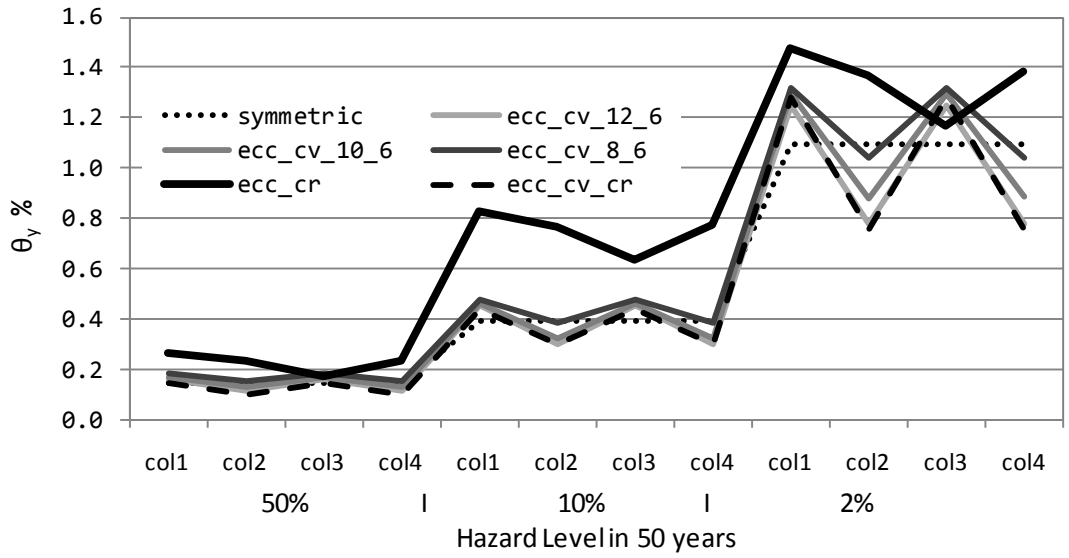

***Figure 9.3**: Column drifts of each design in y direction, for each hazard level*

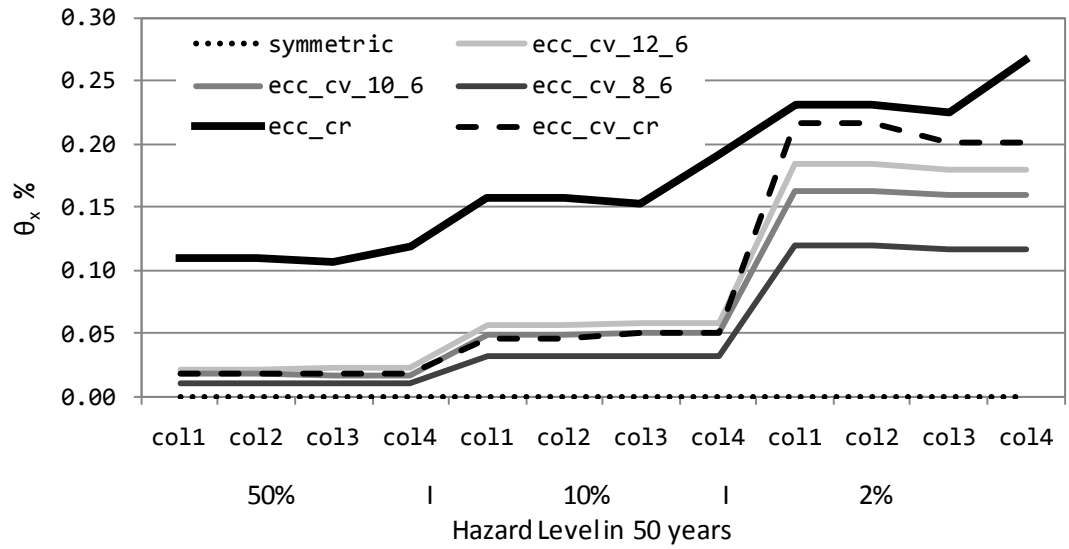

***Figure 9.4**: Column drifts of each design in x direction, for each hazard level*

Figure 9.3 depicts the interstorey drifts in the y direction at the top of all columns for the three hazard levels considered. As expected the response of all four designs with the same stiffness coincide for the low hazard level (50/50) while for the higher hazard levels a variation of the drifts' values are encountered due to the change of the columns' capacity. It should be noted that the larger the strength eccentricity is, the larger the induced drifts compared to the symmetric designs.

Figure 9.4 depicts the interstorey drift values along the x direction which is perpendicular to the direction of the seismic excitation. Although the seismic excitation is applied only along the y direction significant drift values are encountered in the x direction for almost all the designs except for the symmetric one. This is due to the fact that the other designs are not symmetric in terms of stiffness and eccentricity with reference to both directions.

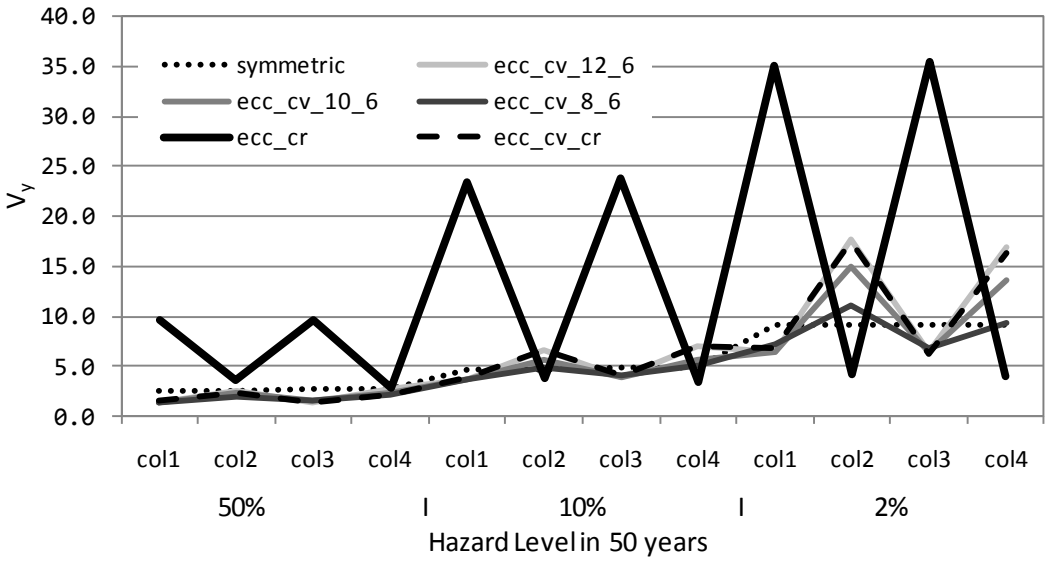

***Figure 9.5**: Column Local Y Shear Forces of each design for each hazard level*

The same conclusion can be drawn for columns shear forces. As observed in Figures 9.5 and 9.6, the internal shear forces for each column varies, especially for the 2/50 hazard level although the total forces and the structure's stiffness are the same. Furthermore, the columns develop shear forces along the x direction, while the seismic excitation is applied along the y direction. The worst design is the one with a stiffness eccentricity that develops three to five times larger shear forces from the symmetric one especially in the elastic range (i.e. 50/50 and 10/50 hazard levels).

For the 10% hazard level of Figures 9.5 and 9.6 the column shear forces are depicted for each hazard level by the two directions. Although it was expected that no shear forces would develop along the x direction, significant shear forces are encountered for all designs for the 2/50 hazard

level, while the ecc_cr design has the worst performance developing shear forces almost one order of magnitude larger than the other designs.

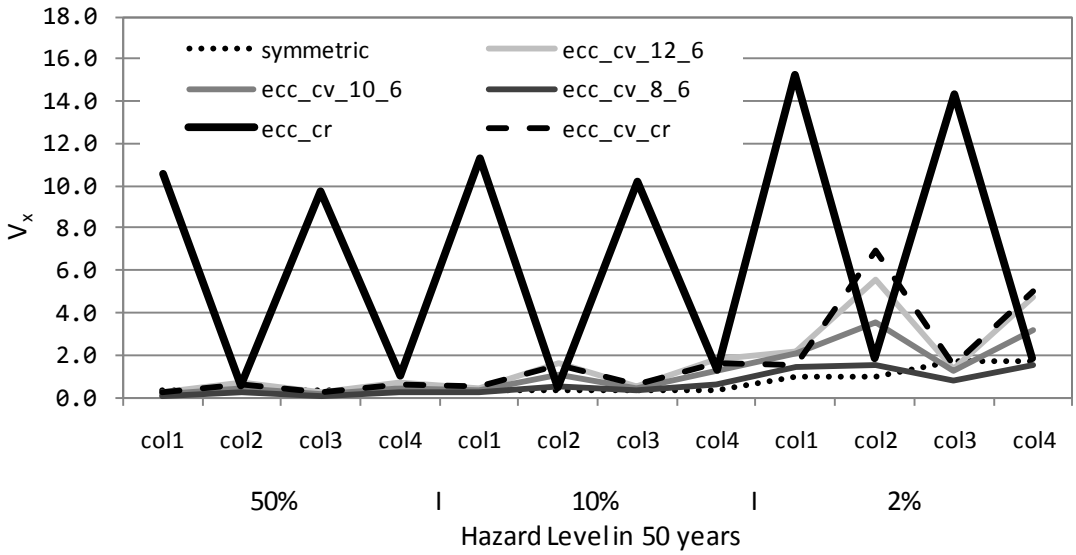

***Figure 9.6**: Column Local X Shear Forces of each design for each hazard level*

Examining the three designs with strength eccentricity, it can be seen that in the elastic range (hazard level 50%), they have almost the same internal shear forces as the symmetric design. In the inelastic range however (hazard level 10% and 2 %), a considerable increase of shear forces in x and y directions is observed. This is because the concrete starts to behave inelastically and the strength eccentricity plays a more significant role. This occurrence has been predicted by ROT as that the maximum shear forces are encountered for the design with the maximum eccentricity (see Figure 9.11).

It is very important to understand that for this simple structure none of the five torsional optimum designs – according to the three basic design philosophies against torsion – can predict minimum vales for each hazard level. Especially, as seen in Figures 9.5 and 9.6 for the three designs with center of strength eccentricity, in the elastic range the columns shear forces are almost equal to the symmetric design, but for the 2/50 hazard level, the shear forces become bigger relatively to the strength eccentricity. Similarly for the design with stiffness eccentricity, and especially for the columns that are in the stiff edge, the shear forces in x

and y direction are significant, although the structure is symmetric with reference to strength.

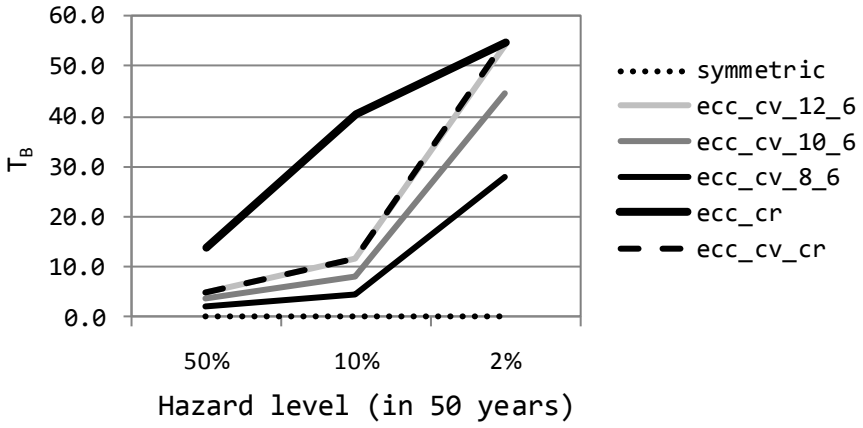

***Figure 9.7**: Structure's Base Torque of each design for each hazard level*

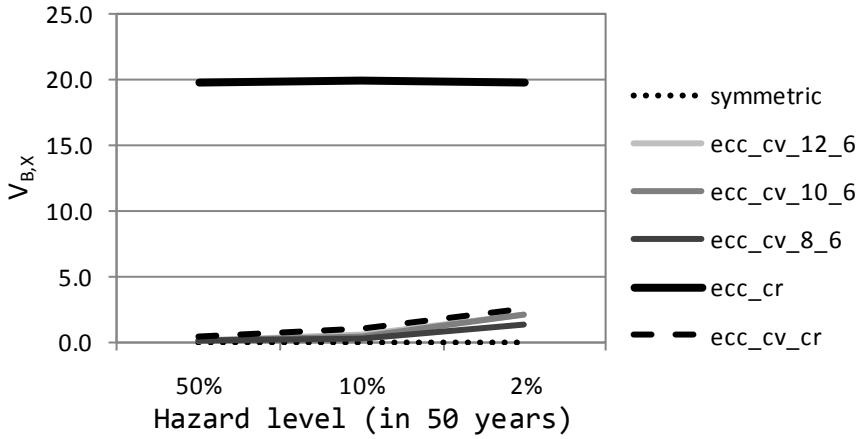

***Figure 9.8**: Structure's Base Shear X of each design for each hazard level*

Similar conclusions can be drawn for Figures 9.8-9.10 where the base shear and roof diaphragm rotation for all three hazard levels are depicted. From Figures 9.7-9.10 in conjunction with Figures 9.5, 9.6 important findings can be extracted. The base shear in the x and y direction, the base torque and the θ_{roof} follow the rule of the eccentricity concept in the elastic and inelastic range. This means that, with respect to strength eccentricity, these quantities are bigger for the collapse prevention hazard level. On the other hand, the corresponding quantities, with respect to the design with the stiffness eccentricity, are bigger in the elastic range. The resulting shear forces do not follow this rule, because we can see very big shear forces in ecc_cr for all hazard levels with an important increase for

the 10/50 hazard level of the ecc_cv design. On the contrary the proposed ROT criterion has predicted satisfactorily the structural behavior. Finally, it will be observed that the design according to [2] gives the worse results in terms of all quantities measuring the structural response.

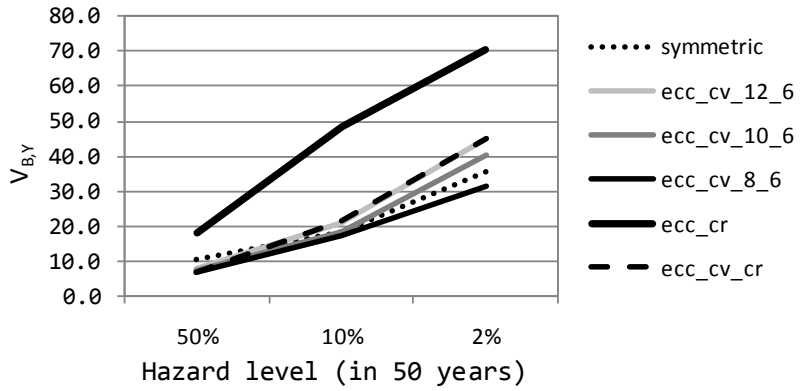

***Figure 9.9**: Structure's Base Shear Y of each design for each hazard level*

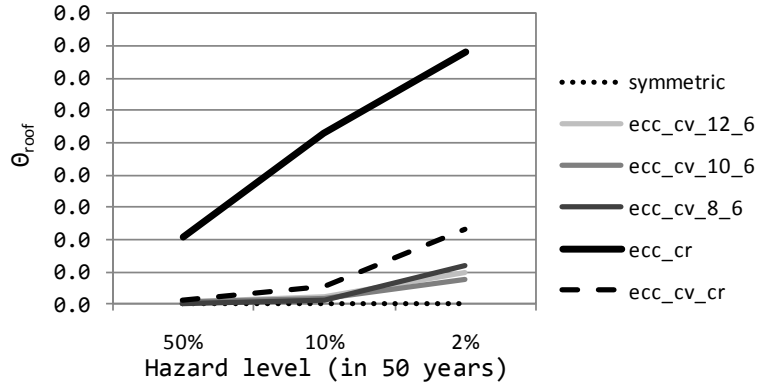

***Figure 9.10**: Roof diaphragm rotation of each design for each hazard level*

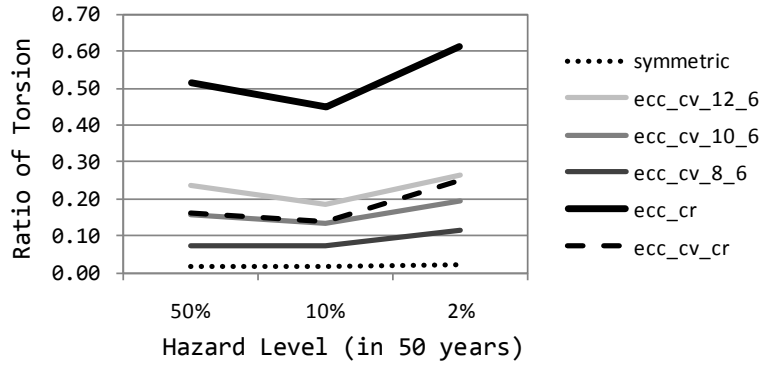

***Figure 9.11**: Ratio of torsion of each design for each hazard level*

As we can see in Figure 9.11, the ratio of torsion varies between almost zero (for the symmetric design) to 0.62 (for the design with stiffness eccentricity for the 2/50 hazard level). In this figure, the performance of the six designs is evaluated using the proposed criterion, ratio of torsion. ROT formulation is based on internal shear forces for each hazard level. It can be observed that the designs with high values of ROT correspond to high values of the elements' internal shear forces in the elastic and inelastic stage (see Figures 9.5 and 9.6). On the contrary, no other criterion proposed in the literature, can predict the performance of structures with torsional rotations. This is a proof that ROT is a general criterion for the design and the evaluation of the torsional behavior of irregular structures. This finding will be applied to the following examples.

10.3.2 Test example 2

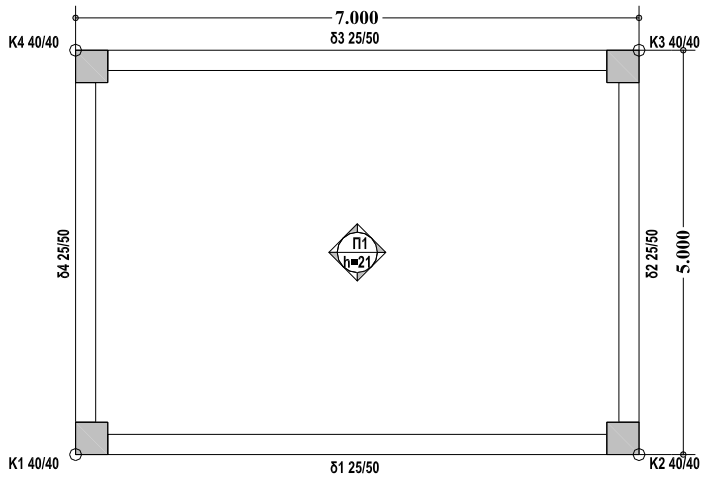

***Figure 9.12**: Plan layout of the first floor*

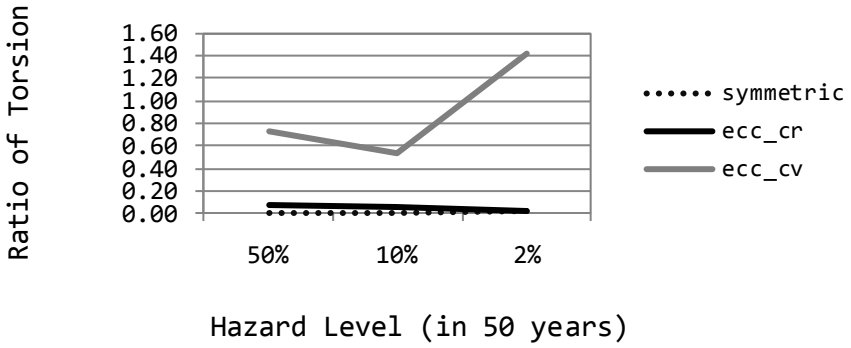

***Figure 9.13**: Ratio of Torsion of each design for each hazard level*

In this test example, we have three designs. The first is the symmetric, the second the one with stiffness eccentricity and the last with strength eccentricity but stiffness symmetric. We can see that the symmetric and ecc_cr designs have about zero rot and the ecc_cv design very bigger in the class of unit which means that we will have about 100% increase in the internal shear forces of the columns.

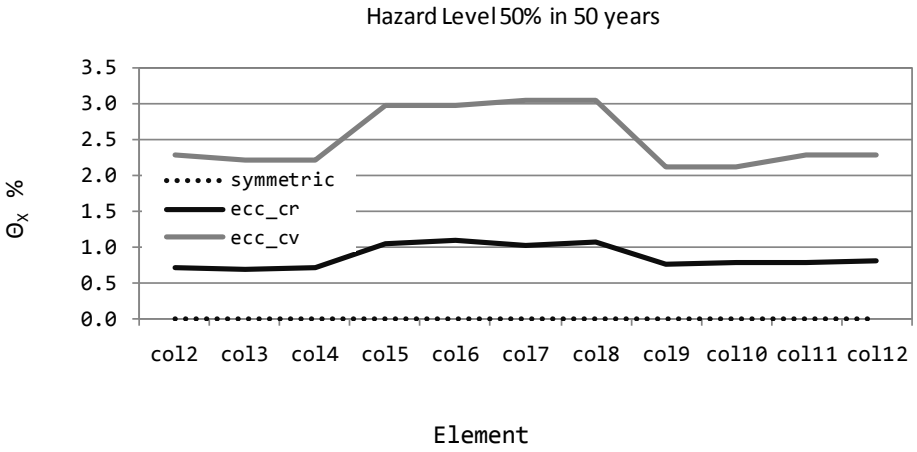

***Figure 9.14**: Column drifts of each design in x direction, for operational hazard level*

In Figure 9.14 an important difference between the structure's drifts although the stiffness is the same can be seen. This has been predicted by rot and its correspondence between the three designs and the symmetric and ecc_cv ones. The same can be seen in Figure 9.15 for the shear forces of the structure.

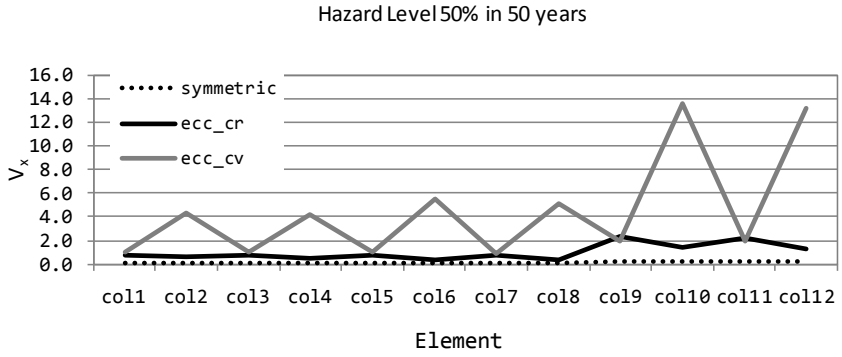

***Figure 9.15**: Column Shears of each design in x direction, for operational hazard level*

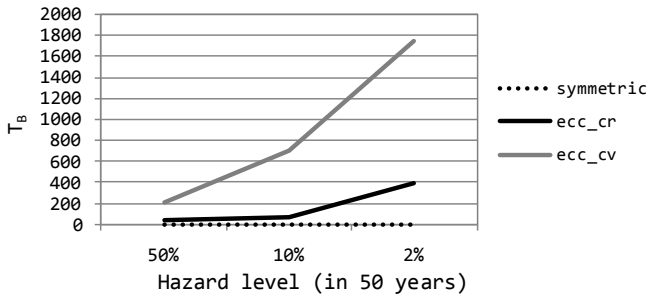

***Figure 9.16**: Column Shears of each design in x direction, for operational hazard level*

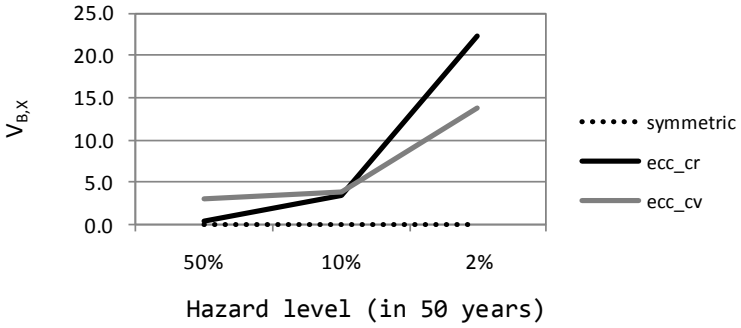

***Figure 9.17**: Column Shears of each design in x direction, for operational hazard level*

From Figures 9.16 to 9.19 it can be seen that the ecc_cv design has a very big base torque in the elastic and inelastic stage. So, the minimum ecc_cv criterion is not reliable. The same can be said for the ecc_cr design. This design has a much larger base torque in the 2% stage although it is strength symmetric. On the other hand, rot had predicted these conclusions as we can see from Figure 9.13.

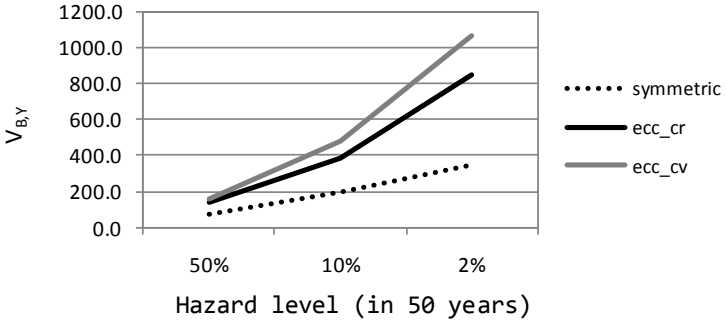

***Figure 9.18**: Column Shears of each design in x direction, for operational hazard level*

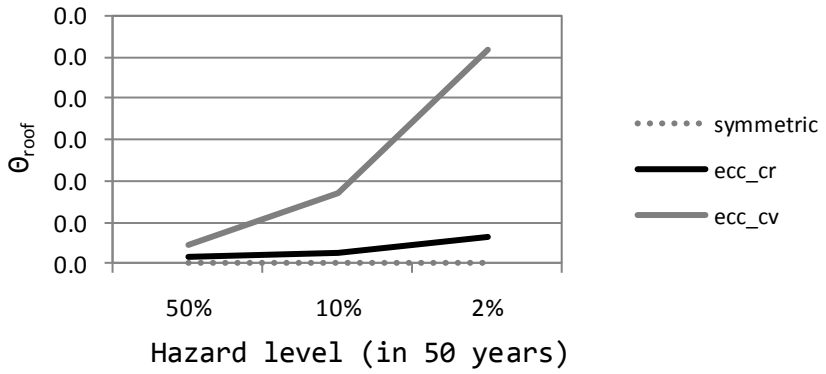

***Figure 9.19**: Column Shears of each design in x direction, for operational hazard level*

*10.3.3*Test example 3

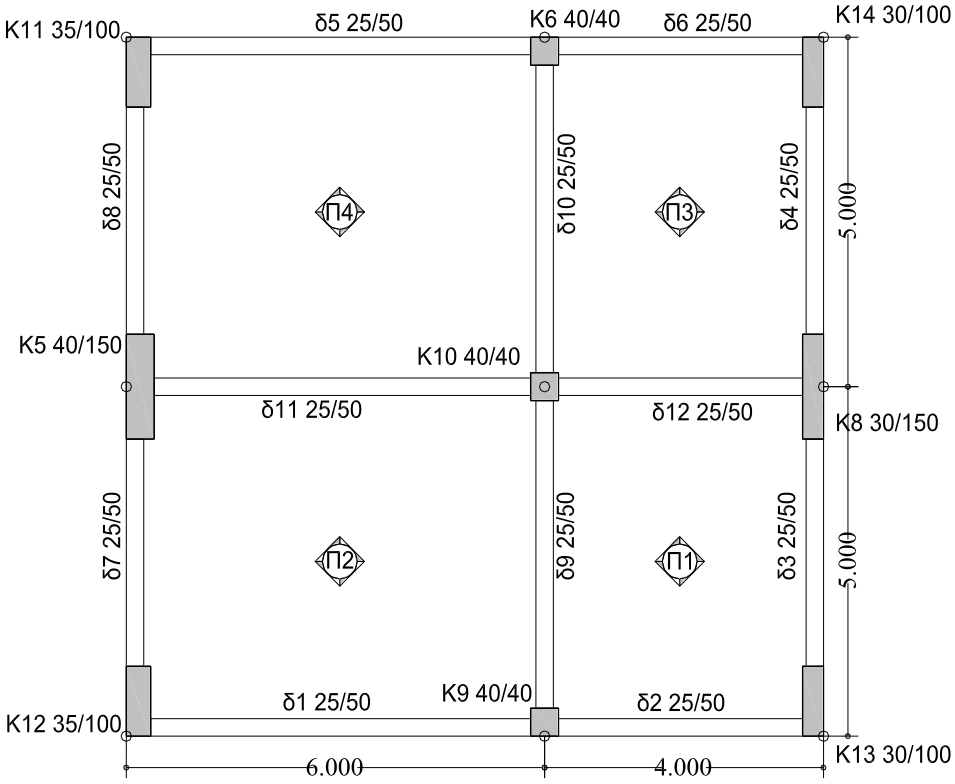

***Figure 9.20**: Plan layout of the first floor*

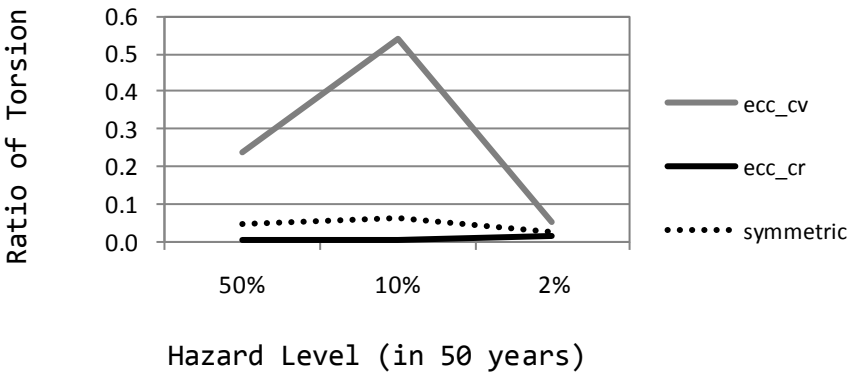

***Figure 9.21**: Ratio of torsion of each design for each hazard level*

In this test example, we have three designs for the same structure, (i) the strength eccentricity one named ecc_cv with zero stiffness eccentricity, (ii) the stiffness eccentricity named ecc_cr with zero strength eccentricity and (iii) the symmetric one. As seen in Figure 9.21, the ecc_cr design gives a better ratio of torsion than the symmetric one. Figure 9.22 shows the internal forces of the center column in all floors. It is obvious that ratio of torsion had predicted that the bigger shears will be at the ecc_cv design, followed by the symmetric and last the ecc_cr design.

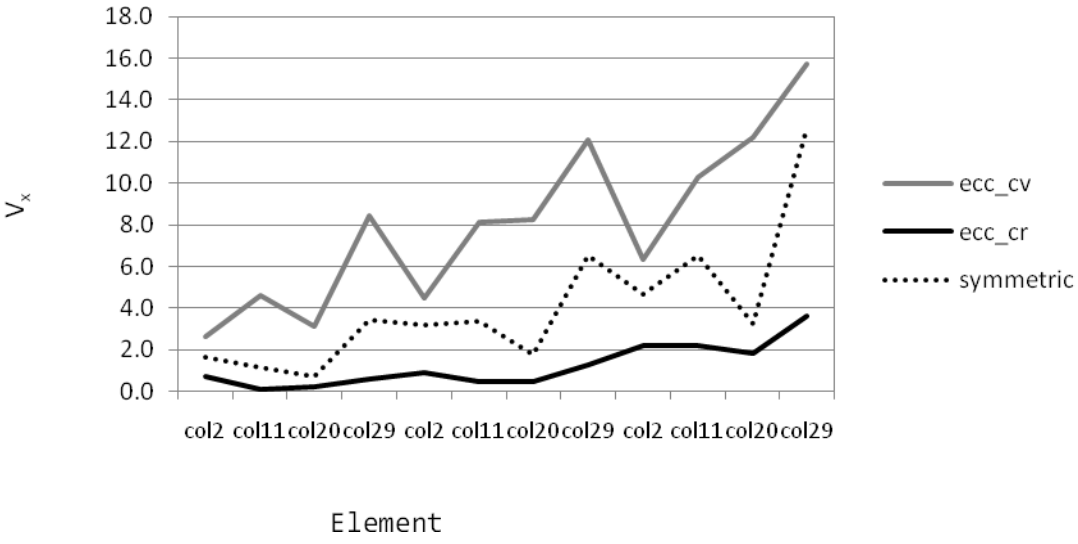

***Figure 9.22**: Column Shears of each design in x direction, for operational hazard level*

This is another case where neither the minimum cr eccentricity nor the minimum cv eccentricity and both minimum can predict the design with the less structure's internal forces due to torsion.

10.3.4 Conclusions

The first principal conclusion that all design engineers must have in mind is that although the seismic force is applied in the YY direction, the elements' internal shear forces are also in the x and y direction. This means that in the x direction the elements must have substantial shear strength such that in the case of zero or minimum rot can be about zero. This is in accordance with a false belief of many designers that the structure's base torsion causes torsional moments in the vertical resisting elements. On the contrary, base torque in eccentric structures induces additional shear forces meaning additional ductility and strength demands for the structure and of course additional cost.

In this study the test structures are designed according to the major design criteria for eccentric buildings in the current literature: i.e. mimimum rigidity eccentricity, minimum strength eccentricity and opposite location between center of rigidity and center of strength according to the mass center. As depicted previously, no criterion can be conducted to designs with optimum torsional behavior meaning low element shear forces. This is taken in consideration in simple and more complex structures too.

On the contrary, rot can predict torsional damage and additional shear forces of the element and if the stiffness's are constant it can predict drifts and also ductility demands. This applies to all test examples and many more that we have analyzed. We believe that rot describes with great accuracy the problem of torsion in a simple mathematical formula that can be used from the design engineer and for research purposes as well. The contribution of this study is that rot consists a general design and evaluation criterion for irregular buildings that can be used for linear and non-linear analyses, for one storey and several storey buildings and for simple and real structures as well. So, it can be said that rot is a more general index for structural behavior.

REFERENCES

[1] Juan C. De La Llera & Anil K. Chopra, "A SIMPLIFIED MODEL FOR ANALYSIS AND DESIGN OF ASYMMETRIC-PLAN BUILDING," *Earthquake Eng. Structural Dynamics*, vol. 24, p. 573-594, 1995.

[2] B. C. Myslimaj & W. K. Tso, "A strength distribution criterion for minimizing torsional response of asymmetric wall-type systems," *Earthquake Eng. Structural Dynamics* , vol. 31, p. 99-120, 2002.

[3] Wai K. Tso "Static Eccentricity Concept for Torsional Moment Estimations," *J. Structural Eng.*, vol. 116, pp. 1199–1212, 1990.

[4] Nikolaos D. Lagaros, Manolis Papadrakakis & Nikolaos Bakas, "Automatic Minimization of the Rigidity Eccentricity of 3D Reinforced Concrete Buildings," *J. Earthquake Eng.* , vol. 10, pp. 533–565, 2006.

[5] Juan C. De La Llera, Anil K. Chopra "Understanding the inelastic seismic behaviour of asymmetric plan buildings," *Earthquake Eng. Structural Dynamics*, vol. 24, pp. 549–572, 1995.

[6] R. D. Bertero, "Inelastic torsion for preliminary seismic design," *Earthquake Eng. Structural Dynamics*, vol. 121, no. 8, pp. 1183–1189, 1995.

[7] C .M. Wong & W. K. Tso, "Evaluation of seismic torsional provisions in uniform building code," *Earthquake Eng. Structural Dynamics*, vol. 121, no. 10, pp. 1436–1442, 1995.

[8] P. Fajfar, D.K. Marušić & I. Peruš, "Torsional effects in the pushover-based seismic analysis of buildings," *J. Earthquake Eng.*, vol. 9, no. 6, pp. 831–854, 2005.

[9] J. D. Pettinga, M. J. Priestley & S. Pampanin & C. Christopoulos, "The role of inelastic torsion in the determination of residual deformations," *J. Earthquake Eng.*, vol. 11, no. 1, pp. 133–157, 2007.

[10] C. L. Kan, A. K. Chopra "Effect of torsional coupling on earthquake forces in buildings," *J. Struct. Division Asce* , vol. 103, no. 4, pp. 805–819, 2007.

[11] S. H. Jeong & A. S. Elnashai, "New three-dimensional damage index for RC buildings with planar irregularities," *J. Structural Eng.* , vol. 132, no. 9, pp. 1482–1490, 2006.

[12] W. K. Tso, "Static eccentricity concept for torsional moment estimations," *J. Struct. Engrg.* , vol. 116, no. 5, pp. 1199–1212, 1990.

[13] S. H. Jeong & A. S. Elnashai, "Analytical assessment of an irregular RC frame for full-scale 3D pseudo-dynamic testing part I: Analytical model verification," *J. Earthquake Eng.* , vol. 9, no. 1, pp. 95–128, 2005.

[14] T. Paulay, "A mechanism-based design strategy for torsional seismic response of ductile buildings," *European Earthquake Eng.* , vol. 2, p. 33–48, 1998.

[15] T. Paulay, "Some design principles relevant to torsional phenomena in ductile buildings," *J. Earthquake Eng.* , vol. 5, p. 273–308, 2001.

[16] M. García, J.C. De La Llera & J. L. Almazán, "Torsional balance of plan asymmetric structures with viscoelastic dampers," *Eng. Struct*, vol. 29, no. 6, pp. 914–932, 2007.

11 Contribution of the thesis and future work

In this study, various structural optimum design formulations are assessed, with respect to the minimum torsional seismic response of RC buildings, for three hazard levels (frequent, occasional and rare) as well as through life-cycle cost and fragility analyses. An optimizer based on evolutionary algorithms has been implemented for the solution of the design optimization problems. From the present study the following conclusions can be drawn:

It was verified for multi-storey buildings with irregularity in plan that the rigidity center eccentricity is important mainly when the structural system behaves linearly, while for nonlinear behavior the strength's center eccentricity becomes more important. The conclusion is based on a more rigorous and generalized framework provided by structural optimization procedures where a number of recommendations for designing RC buildings are incorporated. The results are in accordance with the works of Paulay [16,17], Tso and Myslimaj [31], which were based on observations of the performance of one-storey buildings.

The second finding is related to the most appropriate design criterion for reducing the torsional response. The proposed combined formulation, where both e_{CM-CR} and e_{CM-CV} eccentricities are minimized, leads to optimum designs having an equally well response, in terms of rotation of the top diaphragm, for frequent, occasional and rare hazard levels. Moreover this design formulation exhibits the better performance with respect to the total life-cycle cost and limit state probabilities of exceedance.

The influence of a large eccentricity of the rigidity center in relation to the mass center is very important for the seismic response of buildings. In this study Evolution Strategies have been implemented for the

minimization of the distance between the mass center and the rigidity center of each floor layout of the building's vertical structural elements. The proposed design methodology is a two-stage procedure leading to the coincidence of the mass and rigidity centers for each storey layout and achieving the fulfilment of the EC2 and EC8 requirements. The minimization of the distance between the mass center and the rigidity center leads to a significant reduction of the torsional strain on the vertical elements of the structure and thus, implicitly leading to a cost-effective design of these elements. The beneficial effect of this kind of optimized layout arrangements of the columns and shear walls is directly observed on the cross sectional and transverse reinforcement requirements for the vertical elements of the structural systems. Evolution Strategies have proved to be a robust and efficient tool for an economically design optimization of seismic resistant reinforced concrete 3D frames.

The first principal conclusion that all design engineers must have in mind is that although the seismic force is applied in the YY direction, the elements' internal shear forces are also in the x and y direction. This means that in the x direction the elements must have substantial shear strength such that in the case of zero or minimum rot can be about zero. This is in accordance with a false belief of many designers that the structure's base torsion causes torsional moments in the vertical resisting elements. On the contrary, base torque in eccentric structures induces additional shear forces meaning additional ductility and strength demands for the structure and of course additional cost.

In this study the test structures are designed according to the major design criteria for eccentric buildings in the current literature: i.e. mimimum rigidity eccentricity, minimum strength eccentricity and opposite location between center of rigidity and center of strength according to the mass center. As depicted previously, no criterion can be conducted to designs with optimum torsional behavior meaning low element shear forces. This is taken into consideration in simple and more complex structures too.

On the contrary, rot can predict torsional damage and additional shear forces of the element and if the stiffness's are constant it can predict drifts and also ductility demands. This applies to all test examples and many more that we have analyzed. We believe that rot describes with great accuracy the problem of torsion in a simple mathematical formula that can be used from the design engineer and for research purposes as well. The contribution of this study is that rot consists a general design and evaluation criterion for irregular buildings that can be used for linear and non-linear analyses, for one-storey and several storey buildings and for simple and real structures as well. So, we can say that rot is a more general index for structural behavior.

These conclusions can be extended in many research fields. First of all we could perform more test examples in order to verify the results in one-storey and especially in multi-storey buildings. Also, we can enhance the constitutive model of the materials in order to have more accurate analyses as well as more accurate conclusions. Another addition to the method could be the implementation of the foundation's influence on the system's response and the structure's behavior. And last we can perform the ROT method on buildings damaged by strength earthquakes and for the retrofit procedure.